

**UNIVERSIDADE FEDERAL DE SANTA MARIA  
CENTRO DE TECNOLOGIA  
COURSE OF THE ELECTRICAL ENGINEERING GRADUATE  
PROGRAM**

**ANALYSIS OF THE LUMINOUS EFFICACY  
OF LIGHTING SYSTEMS WITH  
INTEGRATED COMMUNICATION**

**THESIS**

**Lucas Teixeira**

**Santa Maria, RS, Brazil**

**2020**

# **ANALYSIS OF THE LUMINOUS EFFICACY OF LIGHTING SYSTEMS WITH INTEGRATED COMMUNICATION**

**Lucas Teixeira**

Thesis presented to the Doctoral Course of the Graduate Program in Electrical Engineering, in the Energy Processing Area, of the Federal University of Santa Maria (UFSM-RS), in partial fulfillment of the requirements for the degree of **Doctor in Electrical Engineering**

**Advisor: Prof. Dr. Marco Antônio Dalla Costa**

**Coadvisor: Prof. Dr. Vitalio Alfonso Reguera**

**Santa Maria, RS, Brazil**

**2020**

**PPGEE/UFSM, RS TEIXEIRA, Lucas Doutor 2020**

This study was financed in part by the Coordenação de Aperfeiçoamento de Pessoal de Nível Superior - Brasil (CAPES) - Finance Code 001

Teixeira, Lucas  
Análise da eficácia luminosa de sistemas de iluminação  
com comunicação agregada / Lucas Teixeira.- 2020.  
152 p.; 30 cm

Orientador: Marco Antônio Dalla Costa  
Coorientador: Vitalio Alfonso Reguera  
Tese (doutorado) - Universidade Federal de Santa  
Maria, Centro de Tecnologia, Programa de Pós-Graduação em  
Engenharia Elétrica, RS, 2020

1. Conversão de energia 2. Comunicação por luz visível  
3. Diodo emissor de luz 4. Eficácia luminosa 5.  
Iluminação artificial I. Dalla Costa, Marco Antônio II.  
Reguera, Vitalio Alfonso III. Título.

Sistema de geração automática de ficha catalográfica da UFSM. Dados fornecidos pelo autor(a). Sob supervisão da Direção da Divisão de Processos Técnicos da Biblioteca Central. Bibliotecária responsável Paula Schoenfeldt Patta CRB 10/1728.

Declaro, LUCAS TEIXEIRA, para os devidos fins e sob as penas da lei, que a pesquisa constante neste trabalho de conclusão de curso (Tese) foi por mim elaborada e que as informações necessárias objeto de consulta em literatura e outras fontes estão devidamente referenciadas. Declaro, ainda, que este trabalho ou parte dele não foi apresentado anteriormente para obtenção de qualquer outro grau acadêmico, estando ciente de que a inveracidade da presente declaração poderá resultar na anulação da titulação pela Universidade, entre outras consequências legais.



LUCAS TEIXEIRA

**ANÁLISE DA EFICÁCIA LUMINOSA DE SISTEMAS DE ILUMINAÇÃO  
COM COMUNICAÇÃO AGREGADA**

Tese de doutorado apresentado ao Programa de Pós-Graduação em Engenharia Elétrica da Universidade Federal de Santa Maria (UFSM), como requisito parcial para a obtenção do título de **Doutor em Engenharia Elétrica**.

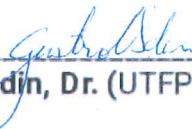
**Aprovado em 9 de outubro de 2020:**



\_\_\_\_\_  
**Marco Antônio Dalla Costa, Dr. (UFSM) – Videoconferência**  
(Presidente/Orientador)



\_\_\_\_\_  
**Vitalio Alfonso Reguera, Dr. (UFSM) – Videoconferência**  
(Coorientador)



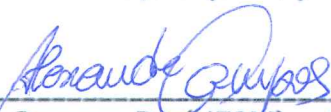
\_\_\_\_\_  
**Gustavo Weber Denardin, Dr. (UTFPR) – Videoconferência**



\_\_\_\_\_  
**Guilherme Márcio Soares, Dr. (UFJF) – Videoconferência**



\_\_\_\_\_  
**Alysson Raniero Seidel, Dr. (UFSM) – Videoconferência**



\_\_\_\_\_  
**Alexandre Campos, Dr. (UFSM) – Videoconferência**



## AGRADECIMENTOS

O autor presta aqui sua gratidão às pessoas e às entidades que lhe deram suporte e inspiração, nos mais diversos aspectos, durante sua formação e elaboração dessa tese.

À minha esposa, aos meus pais e à irmã, agradeço pela paciência e pela compreensão na minha ausência em muitos momentos durante essa jornada. Mais do que isso, agradeço pelo constante incentivo e pelo apoio que me encorajou na tomada de decisões importantes. Obrigado, Patrícia Turra, Neusa Regina Teixeira, Airton Teixeira, Laura Teixeira.

Agradeço pela disponibilidade, pelo envolvimento e pelo suporte diretamente no desenvolvimento dessa tese. Obrigado, Carlos Henrique Barriquello, Christian Barth, Felipe Loose, João Paulo Brum, José Marcos Alonso Álvarez, Rafael Beltrame. Agradeço aos meus orientadores pelo acolhimento, pelo incentivo, pela compreensão e pela confiança em mim depositada. Muito obrigado, Marco Antônio Dalla Costa, Vitalio Alfonso Reguera.

Agradeço aos mestres dos diferentes momentos da minha vida, os quais admiro por diferentes razões, sem prejuízo a aqueles não citados aqui, e cuja influência está marcada nessa tese. Obrigado, Cassiano Rech, Cesar Augusto Prior, Cesar Ramos Rodrigues, Humberto Pinheiro, João Baptista dos Santos Martins, João Batista Gomes, Junior Bohn, Marco Antônio Dalla Costa, Rafael Beltrame, Vitalio Alfonso Reguera.

Agradeço aos colegas, aos amigos e aos profissionais que são fontes de inspiração e/ou apoio durante o desenvolvimento dessa tese e em diferentes momentos de minha formação, muitas vezes sem saber, mas pelos quais tenho especial admiração. Obrigado, Airton Teixeira, Andressa Rocha Da Cas, Fernando Luis Herrmann, Gustavo Chiapinotto, Lucas Vizzotto Bellinaso, Maikel Fernando Menke, Renan Duarte, Ricardo César do Amaral, Taimur Rabuske.

Pelo suporte financeiro, pela infraestrutura e pelo apoio à ciência que tornaram possível o desenvolvimento dessa tese, a minha formação e a formação de tantos outros profissionais. Obrigado, Universidade Federal de Santa Maria (UFSM), grupo GEDRE, equipe do Programa de Pós-Graduação em Engenharia Elétrica da UFSM (PPGEE-UFSM), Colégio Técnico Industrial de Santa Maria (CTISM), Centro de Tecnologia da UFSM, Coordenação de Aperfeiçoamento de Pessoal de Nível Superior (CAPES), Conselho Nacional de Desenvolvimento Científico e Tecnológico (CNPq), Fundação de Amparo à Pesquisa do Estado do Rio Grande do Sul (FAPERGS), Instituto Nacional de Ciência e Tecnologia em Geração Distribuída de Energia Elétrica (INCT-GD).





## RESUMO

Tese Programa de Pós-Graduação em Engenharia Elétrica  
Universidade Federal de Santa Maria

### ANÁLISE DA EFICÁCIA LUMINOSA DE SISTEMAS DE ILUMINAÇÃO COM COMUNICAÇÃO AGREGADA

AUTOR: LUCAS TEIXEIRA

ORIENTADOR: MARCO ANTÔNIO DALLA COSTA

CO-ORIENTADOR: VITALIO ALFONSO REGUERA

Local e data: Santa Maria, Outubro, 2020.

A comunicação por luz visível (VLC) atualmente recebe atenção na mídia de eletrônicos de consumo principalmente por causa do potencial de melhorar a taxa de dados de acesso à Internet em comunicações móveis de curto alcance, mas várias outras novas aplicações podem ser viabilizadas usando esta tecnologia emergente. O VLC usa modulação de luz não perceptível à visão humana, mais frequentemente implementada com diodos emissores de luz (LED), para transmitir informações e, simultaneamente, fornecer iluminação útil. No entanto, apesar da intensa atividade de pesquisa sobre o assunto, do lado técnico há algumas questões em aberto e uma clara desconexão entre as soluções publicadas e a fundamentação para o reaproveitamento da luz visível para comunicação. O consumo de energia é um aspecto fundamental e preocupante considerando a finalidade da iluminação e também se reflete nas características de comunicação, uma vez que agregar tal funcionalidade a qualquer luminária pode exigir alterações de design e afetar as condições operacionais dos LEDs. Portanto, nesta tese é apresentado um estudo abrangente abordando as preocupações sobre o design de um transmissor VLC, que leva em conta os aspectos de iluminação e comunicação, focando principalmente no consumo de energia extra causado pela agregação do propósito de comunicação. A sistematização da literatura publicada permitiu apontar as tendências no desenvolvimento dessa tecnologia. Além disso, a visão geral de um dispositivo transmissor permitiu apontar as melhores opções de design na seleção de esquemas de modulação e circuito de driver de LED para VLC. A discussão sobre a largura de banda e potência do sinal também é considerada ao longo do desenvolvimento da análise com o objetivo de reduzir o consumo de energia e aumentar a taxa de dados de transmissão. Este trabalho apresenta resultados que apontam moduladores comutados como adequados para aplicações de largura de banda mais estreita, embora recentemente tenham recebido atenção significativa em pesquisas visando aumentar a largura de banda de modulação. O balanço de potência de sinal no enlace de comunicação leva à conclusão de que amplificadores de potência lineares usados como moduladores para VLC requerem energia extra menor para implementar aplicações que requerem maior largura de banda de sinal, embora estes circuitos operem com base em um princípio dissipativo.

**Palavras-chave:** Conversão de energia. Comunicação por luz visível. Diodo emissor de luz. Eficácia luminosa. Iluminação artificial.



# ABSTRACT

Doctoral Thesis  
Course of the Electrical Engineering Graduate Program  
Federal University of Santa Maria

## ANALYSIS OF THE LUMINOUS EFFICACY OF LIGHTING SYSTEMS WITH INTEGRATED COMMUNICATION

AUTHOR: LUCAS TEIXEIRA  
ADVISOR: MARCO ANTÔNIO DALLA COSTA  
COADVISOR: VITALIO ALFONSO REGUERA  
Defense Place and Date: Santa Maria, October 2020.

Visible light communication (VLC) currently receives attention in the consumer electronics media mainly because of the potential to improve the data rate of Internet access in short range mobile communications, yet several other new applications can be made feasible using this emerging technology. VLC uses modulation of light unperceptible to the human sight, most frequently implemented with light emitting diodes (LED), for transmitting information and simultaneously useful illumination is provided. However, despite the intense research activity on this subject, on the technical side there are open questions and a clear disconnection among the published solutions and the actual ground for reusing the visible light for communication. The energy consumption is a key aspect that is a concern considering the illumination purpose and also is reflected in the communication features, since aggregating such functionality to any light fixture may require design changes and affects LED's operational conditions. Therefore, in this thesis a comprehensive study is presented approaching the concerns on the design of a VLC transmitter, which accounts for illumination and communication aspects, focusing mainly on the extra energy consumption caused by aggregating the communication purpose. The systematization of the published literature allowed for understanding the trends in the development of this technology. Also, the overview of a transmitter device allowed for pointing out the best design choices in selecting modulation schemes and LED driver circuits for VLC. The discussion about the signal power and bandwidth is also considered throughout the development of the analysis aiming at reducing the energy consumption and increasing transmission data rates. This work presents results that indicate switching mode modulators as adequate for narrower bandwidth applications, although these recently received significant research attention for improving modulation bandwidth capability. The link power budget analysis leads to the conclusion that linear power amplifiers used as modulators for VLC require much lower extra energy for implementing wider bandwidth signaling, even though they work based on a dissipative principle.

**Keywords:** Energy conversion. Visible Light Communication. Light-emitting diode. Luminous efficacy. Artificial lighting.



# Contents

<b>1</b>	<b>PRESENTATION</b> .....	<b>9</b>
1.1	CHARACTERISTICS OF THE CHANNEL AND OPPORTUNITIES OF VLC ....	10
1.2	APPLICATION OF VLC .....	11
1.3	IMPLEMENTATION OF VLC .....	12
1.3.1	LED device.....	13
1.3.2	Driver circuit.....	14
1.3.3	Data modulator .....	15
1.4	RELATED WORK .....	16
1.5	PROPOSAL .....	18
1.5.1	General objective .....	18
1.5.2	Specific objectives .....	18
1.6	ORGANIZATION OF THIS THESIS .....	19
1.6.1	Comprehensive view of LED driving in Visible Light Communication.....	20
1.6.2	A Review of Visible Light Communication LED Drivers .....	20
1.6.3	On the LED Illumination and Communication Design Space for Visible Light Communication .....	21
1.6.4	Pre-Emphasis Control in Switched Mode Power Converter for Energy Efficient Wide Bandwidth Visible Light Communication.....	21
1.6.5	On Energy Efficiency of Visible Light Communication Systems .....	23
1.6.6	An overview of the structure of this thesis .....	24
<b>2</b>	<b>MANUSCRIPT 1 - COMPREHENSIVE VIEW OF LED DRIVING IN VISIBLE LIGHT COMMUNICATION</b> .....	<b>25</b>
<b>3</b>	<b>MANUSCRIPT 2 - A REVIEW OF VISIBLE LIGHT COMMUNICATION LED DRIVERS</b> .....	<b>49</b>
<b>4</b>	<b>MANUSCRIPT 3 - ON THE LED ILLUMINATION AND COMMUNICATION DESIGN SPACE FOR VISIBLE LIGHT COMMUNICATION</b> .....	<b>95</b>
<b>5</b>	<b>MANUSCRIPT 4 - PRE-EMPHASIS CONTROL IN SWITCHED MODE POWER CONVERTER FOR ENERGY EFFICIENT WIDE BANDWIDTH VISIBLE LIGHT COMMUNICATION</b> .....	<b>107</b>
<b>6</b>	<b>MANUSCRIPT 5 - ON ENERGY EFFICIENCY OF VISIBLE LIGHT COMMUNICATION SYSTEMS</b> .....	<b>121</b>
<b>7</b>	<b>DISCUSSION</b> .....	<b>133</b>
7.1	MODULATION SCHEMES .....	133
7.2	MODULATOR CIRCUIT .....	134
7.3	REVISITING THE RELATION BETWEEN VLC AND RF COMMUNICATIONS	136
<b>8</b>	<b>CONCLUSIONS</b> .....	<b>139</b>
8.1	CONTRIBUTIONS OF THIS THESIS .....	139
8.2	PUBLICATIONS .....	140
8.2.1	Published contributions of the thesis .....	140
8.2.2	Published contributions indirectly related to this thesis.....	140

8.3 FUTURE WORK ..... 141  
**REFERENCES ..... 143**

# 1 PRESENTATION

This thesis was written aiming at evaluating and pointing out the best practices for the conception of a energy-aware Visible Light Communication (VLC) lighting fixture. First of all, the artificial lighting consumes a substantial amount of energy in several applications in all sort of human-built environments. As an example, street lighting in Brazil already corresponded to 7% of the national energy demand (MARCHESAN, 2007) and in 2013 lighting technologies were responsible for 17% of total U.S. electricity consumption (INC, 2014). When considering the technology behind the light sources, Solid State Lighting (SSL) has potential for great savings of energy (U.S. Department of Energy, 2020a; International Energy Agency, 2020), having the cost-effective Light Emitting Diode (LED) technology as the state-of-the-art for energy efficiency. In United States of America the projected energy savings with adoption of LED-based lighting is estimated to correspond to 5% in the total primary energy budget by 2035 (U.S. Department of Energy, 2020b). In this sense, LED efficacy has improved considerably since 2010, the average efficacy of LEDs has improved by 6 to 8 lm/W each year in this period (International Energy Agency, 2020). These facts corroborate the perceived pressure on the illumination efficiency and on rising even further its performance by lowering the energy consumption.

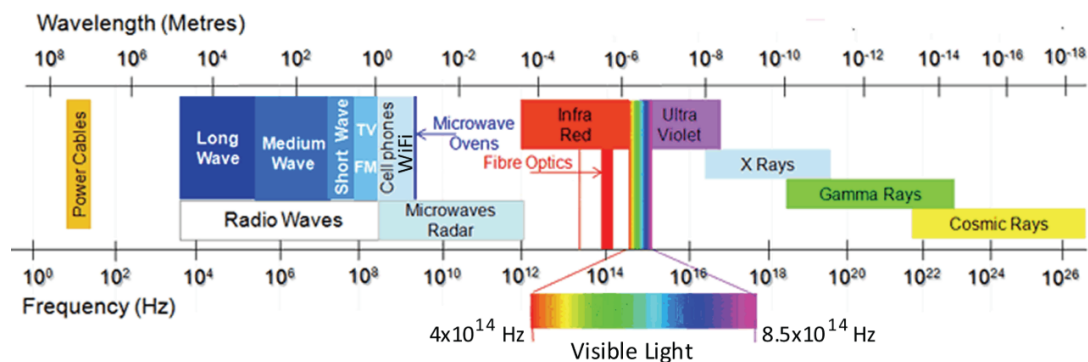
Together with the current semiconductor's inexpensive technology, the fall on the LED's cost (SCHOLAND, 2016) stimulates the wider adoption and the proposal of new applications using this light source. VLC is supported by SSL, most frequently by LED (ELGALA; MESLEH; HAAS, 2011) or by Light Amplification by the Stimulated Emission of Radiation (LASER) devices (ZAFAR; BAKAUL; PARTHIBAN, 2017; YEH; CHOW; WEI, 2019), because these light emitters allow for fast light intensity modulation. The intentional modulation of light is imperceptible to human sight and the average irradiated light is still useful for room illumination. The Joint Illumination and Communication (JIC) systems can be considered a green technology (TSIATMAS et al., 2014, 2015; SAADI et al., 2013) referring to its low energy consumption. However, the excursion of light intensity is achieved with changes in the devices's instantaneous forward current that reduces its energy conversion efficacy and requires additional concern in the design of the electronic driver circuit. Given these reasons, the energy consumption is at the focus of this thesis when evaluating the possible solutions for designing a VLC capable light fixture.



## 1.1 CHARACTERISTICS OF THE CHANNEL AND OPPORTUNITIES OF VLC

The VLC is a Free Space Optical (FSO) communication technology that uses the visible light wavelength range, from approximately 380 nm to 750 nm of the electromagnetic spectrum, as is depicted in Fig. 1.1. The exact limits of such range are dependent on the light intensity, which results in different vision regimes, and have been historically revisited and standardized (International Commission on Illumination, 2019). This application differs from optical fiber systems, because of the open medium. It is also known as Optical Wireless Communication (OWC), which allows for user mobility. VLC can be directly compared to the well-known FSO communications based on infrared light (IR) that has no visual perception in humans and it exhibits similar propagation behavior. However, the emission of IR light is constrained because of human eye hazardous effect on absorbing energy in this wavelength range (KOURKOUDELIS; TZAPHLIDOU, 2011). The spectrum range with wavelengths shorter than visible, starting in the ultraviolet (UV), has natural potential for biological tissue damage, therefore, it is not explored in open medium for communication purpose.

Figure 1.1: Electromagnetic spectrum with highlight in visible light range.



Source: (SEVINCER et al., 2013) adapted from (ELECTROPAEDIA, 2019)

The Radio Frequency (RF) uses longer wavelengths than the visible light, in the millimeters to kilometers wavelength range, therefore exhibiting different propagation behavior. The RF electromagnetic waves suffer specially of lower attenuation when crossing non-electro conductive barriers and stronger diffraction, which allows for circumventing obstacles. Moreover, the widespread adoption and long range of RF communications lead to the regulation of the use of the electromagnetic spectrum worldwide. The importance of such regulations is expressed by International Telecommunication Union (ITU):

A key component of international frequency management is the radio regulations, the binding international treaty that determines how the radio frequency spectrum is shared between different services, including space services. Covering fixed and mobile radio services, satellite systems, radio and TV broadcasting, radionavigation, meteorological monitoring, space research and Earth exploration, as well as amateur radio, the RR encompass over 2300 pages of texts and charts that prescribe how equipment and systems must operate to ensure peaceful cohabitation in today's increasingly crowded airwaves. (International Telecommunication Union, 2019).

Few free-to-use RF wavelength ranges accommodate most of the unlicensed applications of RF such as Wi-fi, Bluetooth, cordless telephones and wide variety of non-Line-of-Sight (LOS) remote controlled equipment. Hence, the applications are error tolerant because all such devices are subject to mutual interference when using these bands. Given the compact style of recent buildings and densely habited cities, these RF bands became crowded. In this context, the VLC is an alternative to this crowded electromagnetic spectrum (KARUNATILAKA et al., 2015), which can be used to substitute or complement the RF-based short range data transport services.

The visible light range of the spectrum is not regulated by ITU. Additionally, the easy confinement of light, which is already implemented given the concern on privacy, allows for higher security of VLC wireless networks and simultaneous reuse of the spectrum in adjacent rooms (SEVINCER et al., 2013). This channel suffers from very small diffraction, given the wavelengths and communication distance, which determines the directionality of the communication and the existence of shadows in the signal coverage (PATHAK et al., 2015). In a well designed illumination setup, the shadows can be avoided with the aid of reflections, minimizing dark spots. These allow for receiving the VLC signal even when the LOS is obstructed. However, reflections limit the channel frequency response that ultimately can cause the inter symbol interference due to multipath propagation (PATHAK et al., 2015).

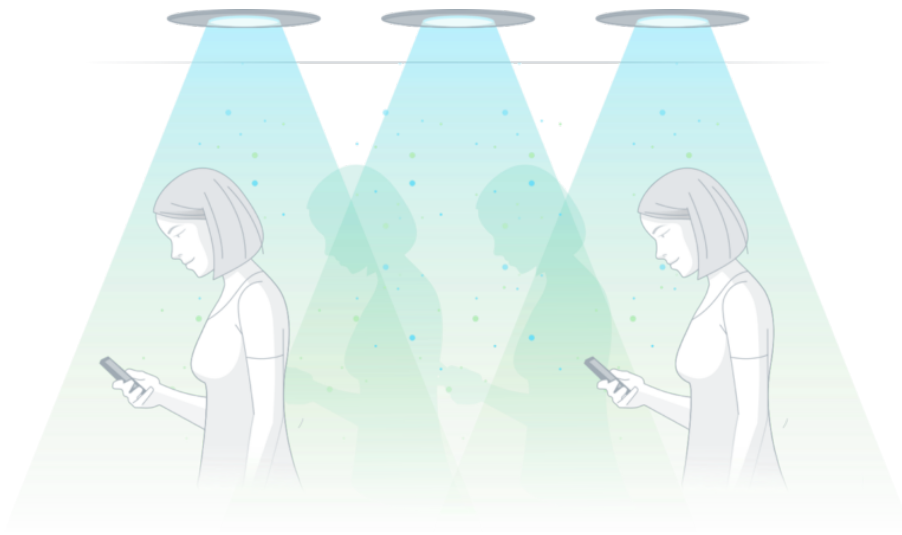
## 1.2 APPLICATION OF VLC

VLC takes advantage of a spectrum range that is easy to confine and is unregulated. Some examples of potential applications of VLC are

- Internet access, known as Light Fidelity (Li-Fi) (HAAS et al., 2016; NAVIN; NUNO, 2010), illustrated in Fig. 1.2,
- support for Internet of Things (IoT) (DEMIRKOL et al., 2019),
- indoor localization (ZHUANG et al., 2018; PANDEY; SHARAN; HEGDE, 2017),

- gesture recognition (PATHAK et al., 2015),
- screen-camera communication (PATHAK et al., 2015),
- vehicular networking (PATHAK et al., 2015),
- wireless communication in RF-sensible environments (ELGALA; MESLEH; HAAS, 2011),
- toys and entertainment (SCHMID et al., 2015),
- virtual and augmented reality (CHUN et al., 2019).

Figure 1.2: Imperceptible light modulations allows for fast and mobile Internet access



Source: (Pure Lifi, 2020)

Among the most attractive applications of VLC is Li-Fi, however, not only high data rate applications of VLC are include in this list of potential applications. Also low data rate applications, as real world interactive systems, IoT and indoor localization, are made feasible by using VLC.

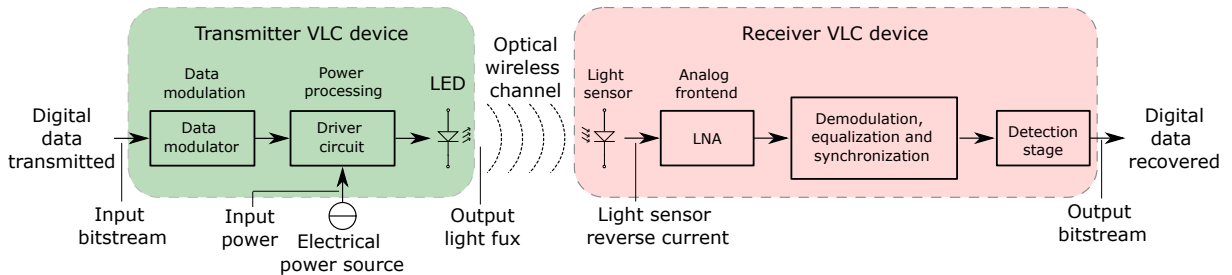
### 1.3 IMPLEMENTATION OF VLC

To begin the study of the implementation of VLC, a model of the system is presented. This model, shown in the Fig. 1.3, includes the transmitter device, the optical channel and the receiver device. The optical channel model encompasses how the output light flux of the transmitter reaches the receiver light sensor and had its geometry and complexity omitted in

this figure. The receiver device is illuminated and it processes the light intensity variations for recovering the transmitted data. It is usually the mobile part in a VLC application. In this thesis an optimal receiver is assumed. Moreover, the implementation and in-depth analysis of the receiver is out of the scope of this work, except for the aspects relevant for the computation of the link budget. A detailed analysis of the optical receivers can be found here (WANG et al., 2015; CHEN; ZHONG, 2017; BAI et al., 2017; BISPO, 2015; MARTÍNEZ-CIRO et al., 2019; LIU et al., 2016).

The VLC transmitter device is the main target of this study. This component handles the requirement to comply with the communication aspects and simultaneously ensuring the specified average light level for illumination, both keeping the highest possible energy efficiency. The contributions of this thesis are focused on the transmitting side of the VLC system. Therefore, each of the blocks of the transmitter are described in the following.

Figure 1.3: Model of VLC system including transmitter, channel and receiver blocks.



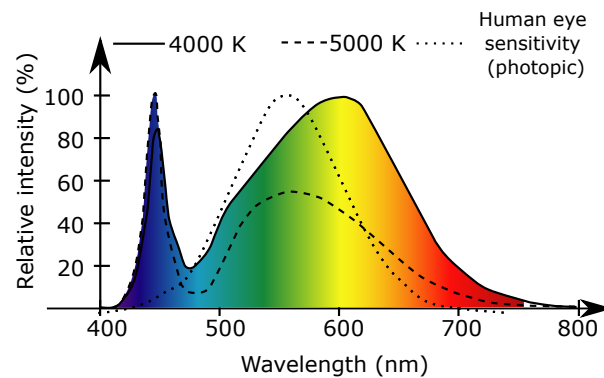
Source: Author

### 1.3.1 LED device

The LEDs are the most popular light emitters used nowadays, given their high efficacy of energy conversion, lifespan and cost. The operation of this device is based on spontaneous emission of photons, therefore, it presents a much wider power spread in comparison with LASERS. Moreover, for VLC the light average power is modulated (intensity modulation and direct detection) because these devices do not allow for the control of the phase of irradiated light components. The state-of-the-art modeling of the LED uses the photo-electro-thermal theory (PET) (HUI; QIN, 2009) that allows for analyzing the four most important aspects (photometric, electrical, thermal, and colorimetric characteristics) and foreseeing the device's performance.

Phosphor-coated white LEDs (PC-LED) are the most economic for general purpose lighting because these devices are able to generate white light and require a single regulated current source. Moreover, the dimming is achieved by simply proportionally reducing the LED's forward current, without worrying about startup, as it would be required for discharge lamps. Fig. 1.4 presents the distribution of power irradiated light of a PC-LED. In this figure, the peak in the blue wavelength range is the light produced by the semiconductor, whereas the rest of the spectrum results from the phosphor emission of longer wavelengths when stimulated by the blue light. For this type of LED, the lesser is the fraction of blue light converted, the higher is the irradiated light color temperature, as shown for 4000K and 5000K in Fig. 1.4.

Figure 1.4: PC-LED typical irradiating spectral density for 4000K and 5000K color temperatures and human eye photopic sensitivity.



Source: Author

When driving an LED, it is important to keep in mind the restrictions of any modulation (intentional or unintentional) in the light irradiated and its possible effects to the viewer's eyes. Safe limits for the light modulation in the visible spectrum range are suggested in (IEEE Power Electronics Society, 2015). In this sense, in the frequency range exceeding 2 kHz it is tolerable 100% of modulation in light intensity with low probability of effects for human exposition. It is worth noting that the LED's impedance falls when biased over the threshold voltage, given the non-linear V-I curve behavior. This leads to wide range of current modulation with small voltage changes.

### 1.3.2 Driver circuit

The LED driver circuit is one key block of the transmitter concerning its energy efficiency. The VLC dual purpose driver circuit is designed to process the average LED light

required for illumination and simultaneously generate the necessary modulation for communication purpose (SEVINCER et al., 2013). Driver circuits shall be capable of regulating the current because of LED variable threshold voltage. Moreover, the input requirement may include specification of power factor and harmonic distortion of the current drained from the mains.

The requirements of dual-purpose LED drivers differ from illumination-only drivers in the modulation capability. Frequency response bandwidth and modulation depth are the main metrics of this modulator circuit. In the literature, typical VLC's signal bandwidth is in the range from few kilohertz up to the hundreds of megahertz. The modulation depth required is explored in a smaller number of publications and have no typical values because it depends on channel attenuation caused by several geometrical factors and the required signal variance at the receiver.

A wide sort of different circuit solutions were already proposed in the VLC's literature. Owing to the LED's low impedance when forward biased, a combination of low amplitude ac voltage signal and a high dc voltage bias is a very common solution to avoid processing high voltages with very fast devices, process which would face a technological barrier. Most of these were derived from circuits typically used in RF and share common structures like bias-T for injecting ac modulated signal into a dc-biased LED (MINH et al., 2008a; DENG et al., 2019).

### **1.3.3 Data modulator**

The modulation schemes selected for any communication simultaneously affects the Bit Error Ratio (BER) at the receiver side, the complexity of signal processing involved and the shape and Probability Density Function (PDF) of the signal values. The resulting bandwidth occupied by the signal is defined according to the adopted symbol rate.

A general approach can be implemented with most of the modulation schemes by using dc-offset (DCO), i.e. adding a dc component to a communication signal built using any known modulation scheme. This can either be implemented to adjust the target illumination level, aiming at dimming support, or to avoid negative signal values, since light intensity modulation does not allow for negative signal.

The PDF plays an important role on the analysis of the behavior either of the LED device and of the driver circuit. For this work, the main aspect to be considered is regarding the PDF

and the extreme values it achieves. Both LED and circuit have limiting operating range for the current levels processed. However, especially the design of a modulator circuit usually results in lower efficiency for higher Peak-to-Average Power Ratio (PAPR) of the communication signal.

In spite of this simple introduction, the LED device, the driver circuit and the data modulator have an intrinsic interdependence when considering the multidisciplinary aspect of a VLC application. Any attempt of to oversimplify or isolate the blocks will certainly affect the energy efficiency of the lighting fixture and will not lead to a globally acceptable solution. Hence, these three blocks of the VLC system are explored in depth and holistically in this thesis to point out the best choices for implementing a VLC transmitter.

#### 1.4 RELATED WORK

Extensive literature on VLC has been published, specially from 2006 to the present. Much of the VLC channel analysis and characterization in the literature recasts previous studies on the use of IR in OWC which are prior to 2000 (AL-KINANI et al., 2018). However, many of the publications on driver circuitry are recent. Moreover, the works that match with the proposal of this thesis were published in the period starting in 2008. This fact is also related to the current electronic device's technology and the recent development of LED technology.

During the period of development of this thesis at least four other theses were under development following an energy-aware VLC system design approach. Those are (DENG, 2018; BIAN, 2019; MÉNDEZ, 2018; SALMENTO, 2019) from which several ideas were inspiring and to which the current thesis aims to contribute to further developing the understanding on the design of VLC transmitters.

Among these theses, the notorious collection that built the work of DENG (2018) approached either the effects of VLC in the LED and in the driver circuit. The author analyzed the effect of VLC on the LED (DENG et al., 2017), explored how to overcome linear and non-linear LED distortion (DENG et al., 2018), the use of average current control with a switching mode power converter as modulator (DENG et al., 2015, 2014, 2018) and also class A and AB linear modulators (DENG et al., 2019), from which the energy penalties were analyzed. The author described the thesis as:

[...] addressing the challenges in VLC physical layer with reusing the illumination systems. It shows that the data throughput can be extended by novel DSP

techniques; the power penalty for communication can be minimized by dedicated circuits and system designs; and the interference could be quantified or reduced once its effect was predicted. (DENG, 2018)

The thesis of BIAN (2019) presented several practical implementations of the multiple-input multiple-output (MIMO) VLC systems. The author used generalized space shift keying and micro-LEDs and presented wavelength division multiplexing implementation using up to 4 different LED colors, which achieved 15 Gbit/s in a MIMO configuration. Additionally, in (BIAN, 2019) the author applied solar cells for simultaneous energy harvesting and data communication, achieving up to 146 Mbit/s. Even though the focus of this complete work had the energy efficiency of the systems as one of the advantageous aspects cited by the author, it was barely treated, meanwhile the main target was demonstrating the effectiveness of modulation schemes using MIMO.

The thesis of MÉNDEZ (2018) presented numerous contributions on the use of high efficiency switching mode power converters for VLC. The work collection resulting from his thesis explored the average current control (RODRÍGUEZ et al., 2018), the ripple modulation (RODRÍGUEZ et al., 2018) and buck-derived circuit topologies (RODRÍGUEZ et al., 2019) considering practical implementation aspects for VLC LED drivers.

The thesis of SALMENTO (2019) has not been fully published because of industrial and commercial secrecy, however, the derived work (SALMENTO et al., 2019) was the closest match to the focus of the current thesis. In (SALMENTO et al., 2019), the authors present an offline VLC LED driver with an additional series switch for modulation. This performed OOK-M-FSK and was shown in experimental tests that achieved 0.99 power factor and 92% efficiency.

The most frequent focus of the theses of DENG (2018) and BIAN (2019) is on the analysis of the resulting signal, including its distortions and statistical behavior aiming at communication performance and achievable data throughput. The work of DENG (2018) also presents mathematical analysis of the energy performance of VLC modulator circuits according to the modulation index, it is, however, limited due to the LED's simplistic model and the lack of a target application to contextualize the presented performance metrics. The current thesis includes an in-depth analysis of the energy expense and resulting efficacy of intentional modulation of current either in the LED device, using the photo-electro-thermal model of a high-power PC-



LED, and in several modulator circuit types. Moreover, the current thesis includes the context of VLC application, which directly impacts the transmitter performance.

The work collection of MÉNDEZ (2018) only presented results of switching mode modulators, which limits its analysis and gives no fair base for comparison among other circuit types. The current thesis included linear mode circuits together with the switching mode modulators in the comparison among different modulator solutions. Moreover, the current thesis also explores the maximum communication bandwidth that can be achieved using switching mode modulator circuits, this aspect was not explored by MÉNDEZ (2018).

The analysis of (SALMENTO et al., 2019) presents a single modulator circuit and did not account for LED behavior in the experimental measurements. The authors present a full communication setup, including transmitter and receiver; however the energy expense of the VLC is only evaluated for a single modulation scheme. In this sense, the current thesis analyzed the models of different modulator circuits and the effects in the LED simultaneously for several modulation schemes. This showed that the effects of current modulation in the LED device is as important and may also predominate in the global efficacy analysis of the VLC transmitter.

Considering the works described above, the most relevant and similar found in the state-of-the-art on VLC, the current thesis have its proposal presented following.

## 1.5 PROPOSAL

This thesis aims at developing knowledge and solutions on the best design practices considering the energy efficiency in an LED-based VLC light fixture.

### 1.5.1 General objective

The general objective of this thesis is to evaluate and to present the most energy efficient choices for the implementation of VLC transmitters considering the use of high-power PC-LEDs and current technology electronic devices.

### 1.5.2 Specific objectives

Considering the VLC application, the expected contributions are:

- Compile and systematize the state-of-the-art literature for building a more comprehensive understanding about VLC.
- Describe how the modulation scheme, signal variance and dc dimming range are related when defining the stimuli for a high-power PC-LED.
- Describe contributions on the use of switching mode power converters as VLC LED drivers simultaneously performing average current control and intentional current modulation.
- Describe guidelines on the selection of modulation scheme and driver circuit type for an energy-efficient VLC light fixture considering its application.
- Present a comparison among several LED driver and modulator circuits solutions considering their expected energy efficiency and the applications in which they best fit.
- Analyze the actually required modulation intensity for better energy consumption-driven VLC design choices.

## 1.6 ORGANIZATION OF THIS THESIS

The rest of the thesis is presented with five self-contained Chapters from 2 to 6. Those are organized in a chronological sequence and follow a bottom-up approach, the first ones support the following, each of which is an independent manuscript.

The VLC technology joins aspects from lighting, power electronics and communication fields, which are usually fragmented in the published literature. Regardless of the numerous VLC literature using the survey and review approaches (NAVIN; NUNO, 2010; EL-GALA; MESLEH; HAAS, 2011; SEVINCER et al., 2013; KHALIGHI et al., 2014; PATHAK et al., 2015; KOMINE; NAKAGAWA, 2004), during initial development phase of this thesis it was detected that two main approaches were followed by most of the authors. Those lead to, in one hand, neglecting most communication aspects (JENQ; LIU; LEU, 2011; TANAKA; UMEDA; TAKYU, 2011; MIRVAKILI; KOOMSON, 2012; ZONG; WU; HE, 2012; ZHAO; XU; TRESCASES, 2013, 2014; SEBASTIÁN et al., 2014; HUSSAIN et al., 2015; MODEPALLI; PARSA, 2015; GONG et al., 2016; MODEPALLI; PARSA, 2017), or, in the other hand, no concern on power efficiency (SCHMID et al., 2015; KOSMAN et al., 2016; LI et al.,

2015; KISHI et al., 2014; DONG et al., 2014; CHE et al., 2014; MCKENDRY et al., 2013; FUJIMOTO; MOCHIZUKI, 2013; MINH et al., 2008a,b; VUCIC et al., 2009, 2010; FUJIMOTO; MOCHIZUKI, 2013; BAY; CITY, 2019; LI et al., 2015; MINH et al., 2008a; JALAJAKUMARI et al., 2015; KISHI et al., 2014; AGARWAL; SAINI, 2014), with very few exceptions approaching both aspects simultaneously (HUSSAIN et al., 2015; TSIATMAS et al., 2015, 2014; DENG et al., 2014; JALAJAKUMARI et al., 2015; SEVINCER et al., 2013).

Hence, in order to link these aspects that are required in a dual-purpose VLC LED driver, i. e. communication capability and efficient lighting performance, two studies resulting from literature survey and systematization were developed. The two separated manuscripts, written during the development of this thesis, are described in Section 1.6.1 and Section 1.6.2.

After the review of literature described above, follow other three contributions of this thesis concerning the LED behavior, the use of switching mode circuits as modulators and a complete analysis of the extra energy required for VLC. Those are described in Section 1.6.3, Section 1.6.4 and Section 1.6.5, respectively.

### **1.6.1 Comprehensive view of LED driving in Visible Light Communication**

The manuscript presented in Chapter 2 contains an initial review of VLC technology and related electronic circuits and LED technology over which the rest of the thesis was planned. It approaches all the engineering aspects of a dual purpose LED driver performance and, at a high abstraction level, also the aspects of the LED device that impact its performance for VLC.

### **1.6.2 A Review of Visible Light Communication LED Drivers**

The study presented in Chapter 3 is a survey of literature about LED drivers specifically aimed at VLC application. It was firstly presented with the title *Review of LED drivers for Visible Light Communication* in IECON 2019 - 45th Annual Conference of the IEEE Industrial Electronics Society (TEIXEIRA et al., 2019). After discussion and improvements, the complete manuscript presented in this thesis was written including more aspects, such as modulation schemes, circuit topologies and amplitude of modulation.

### **1.6.3 On the LED Illumination and Communication Design Space for Visible Light Communication**

After the initial review of LED device behavior under intentional light modulation, already presented, it was shown that there was no literature that included photo-electro-thermal effects of VLC in a high-power PC-LED. The electrical and optical parameters of this class of LED differs significantly from the classical theoretical LED models. In fact, at that time the published literature on VLC was limited to experimental results (HUSSAIN et al., 2015; JALAJAKUMARI et al., 2015), based on simplistic LED models (TSIATMAS et al., 2014), or did not include thermal effects (TSIATMAS et al., 2015). Moreover, at that time, the most complete work available (DENG et al., 2017) did not account for the maximum instantaneous forward current. The maximum instantaneous LED forward current is an important parameter that affects the devices reliability besides harming the irradiating efficacy. Concurrently to the development of this part of the thesis, other authors considered the LEDs PET model in a publication focused on VLC observing the resulting signal-to-noise ratio (CHEN et al., 2019). Therefore, the proposed experimentally-based study accounted for all these factors in a commercial high-power device, excluding the frequency-dependent dynamic behavior of the LED, which was already well described in the literature (MINH et al., 2008a; LEE et al., 2015) and addressed in Chapter 2.

The study contained in Chapter 4 was firstly presented with the title *On the LED Efficacy and Modulation Design Space for Visible Light Communication* in the conference 2018 IEEE Industry Applications Society Annual Meeting (IAS) (TEIXEIRA; LOOSE, 2018). Later, after improvements, the final version of this manuscript, as shown in this thesis, was published in the journal IEEE Transactions on Industry Applications (Volume: 55 , Issue: 3 , May-June 2019) with the title *On the LED Illumination and Communication Design Space for Visible Light Communication* (TEIXEIRA et al., 2019).

### **1.6.4 Pre-Emphasis Control in Switched Mode Power Converter for Energy Efficient Wide Bandwidth Visible Light Communication**

In a first active effort of this thesis to propose energy efficient solutions for VLC LED drivers, the application of typical LED drivers designed for illumination was investigated. A preliminary analysis of these driver circuits lead to the summarized relevant facts:

- Most of the general purpose LED drivers commercially available are based on switching mode power converters and the majority use pulse-width-modulation (LI et al., 2016). This sort of power converters have the advantage of high efficiency that is achieved with the use of modern fast-switching semiconductor devices and reactive passive filters.
- When forward-biased, the high-power LED's small-signal impedance is fairly low. The non-linear diode curve characteristic may be different according to the device model and power level; however, for most high power LEDs the voltage required to reach device's threshold is most of the voltage applied to forward bias it at nominal current. Therefore, the intentional modulation of the current requires only small changes to the converter's output voltage.
- Because of the LED's variable threshold voltage, which is strongly dependent on the device's temperature and also on the manufacturing variability, the majority of the driver circuit solutions implement some sort of current control. This current control requires margins for operation, the intentional modulation of current can be performed using such margins. Therefore, there is room for implementation of VLC on well-know switching mode LED drivers for illumination when low modulation index is required.
- Switching mode power converters have the dynamic of its output voltage characterized by the passive components whose main target is attenuating the switching frequency and its higher harmonics. The residual harmonic content results in a constant ripple in driver's output voltage. Minimizing this effect helps on keeping the LED's operating current as close to dc as possible and maximizing its efficacy.
- Two strategies to implement intentional modulation for VLC using switching mode power converters are reported in literature:

**Ripple modulation** This strategy is based on controlling the generation of the residual ripple components of the drivers output current or voltage to convey information in the LED's irradiated light (MÉNDEZ, 2018; ZONG; WU; HE, 2012; LOOSE et al., 2017; RODRIGUEZ et al., 2017; LOOSE et al., 2018; Rodriguez Mendez et al., 2020). This is achieved by either controlling the amplitude, phase or frequency of residual components acting on the Pulse Width Modulation (PWM) pulse character-

istics. Therefore, the signal resides in the sidebands of the switching frequency and the maximum symbol change rate is equal to the Switching Frequency ( $F_S$ ).

**Average current modulation** In this strategy the average output current is controlled by the average pulse width (DENG et al., 2014; SEBASTIÁN et al., 2014; SEBASTIAN et al., 2018; DENG et al., 2018). In this case, the modulated signal is limited to a maximum modulation bandwidth, given of the converter's commuted nature, to  $F_S/2$ , however in the literature it is very commonly sub-utilized limiting the modulation bandwidth to  $F_S/10$  or less.

The ripple modulation was investigated in other studies developed in the GEDRE research group (LOOSE et al., 2017, 2018), which received contributions from this author. However, those works are not directly the main focus of this thesis. Thus, the modulation bandwidth was identified as a bottleneck for improving the data rate for VLC when exploring the switching mode modulators using average current control. In this sense, the preemphasis control strategy was used to cope with the slow passive filter to improve the converter's modulation bandwidth.

The use of preemphasis in the control of a switching mode power converter was explored in order to demonstrate its advantages and limitations with average current control in LED-based VLC. A circuit was prototyped demonstrating the experimental performance of such strategy without any need of hardware redesign. The manuscript presented in Chapter 5 was published with the title *Pre-Emphasis Control in Switched Mode Power Converter for Energy Efficient Wide Bandwidth Visible Light Communication* in IEEE Journal of Emerging and Selected Topics in Power Electronics in December 2019 (TEIXEIRA et al., 2020).

### 1.6.5 On Energy Efficiency of Visible Light Communication Systems

The previously described analysis investigated the role of LED's behavior and the driver circuit in VLC. However, these studies do not completely clarify the real energetic performance since the required modulation depth have not been accounted. Hence, the complete communication link is considered to give a full answer to the required modulation depth given the channel attenuation, which rely on the geometrical parameters, and the noise that is implicit at the receiver. These are key factors to define the transmitted signal power for reliable communication. Whereas the transmitter shall provide enough light modulation intensity for a given set

of channel geometric parameters, data rate and receiver configuration, which differ depending on the target application.

The study of a complete VLC link, considering the Li-fi application scenario and its signal power budget, was performed and resulted in a manuscript presented with the title *An Analysis of Visible Light Communication Energy Cost* in the conference 2020 IEEE Industry Applications Society Annual Meeting (IAS) (TEIXEIRA et al., 2020). Based on this initial manuscript, after improvements, expanding the number of applications and modulations, the manuscript presented in Chapter 6 contains an in deep comparison among solutions for an energy-aware VLC design.

### 1.6.6 An overview of the structure of this thesis

This thesis is organized following a bottom-up method that explores the basic blocks of the VLC system leading to the full system analysis used in Chapter 6. This structure is summarized in Table 1.1.

	<b>Parts of a VLC communication system</b>				
	<b>Modulation</b>	<b>LED device</b>	<b>Driver circuit</b>	<b>OWC channel</b>	<b>Receiver</b>
Chapter 2		X	X		
Chapter 3	X		X		
Chapter 4	X	X			
Chapter 5	X		X		
Chapter 6	X	X	X	X	X

Table 1.1: Summary of the parts of a VLC link included in the study in each chapter.

## **2 MANUSCRIPT 1 - COMPREHENSIVE VIEW OF LED DRIVING IN VISIBLE LIGHT COMMUNICATION**



# Comprehensive view of LED driving in Visible Light Communication

L. Teixeira, *Member, IEEE*, F. Loose, *Member, IEEE*, R. R. Duarte, *Member, IEEE*, C. H. Barriquello, *Member, IEEE*, and M. A. Dalla Costa, *Member, IEEE*,

**Abstract**—A trend in short range wireless network access is the Visible Light Communication (VLC), which comes as a promise breakthrough for the industry and system designers, but the adoption of this technology still faces challenges on the technical side. Light Emitting Diode (LED) semiconductor efficacy, price and lighting aspects experienced a huge improvement within the last few years making it the reason to become a major technology for lighting applications. However, a possible barrier to the wider adoption of VLC is efficacy: lighting rise efficacy of LED devices and industrial standards may be harmed by intentional power modulation. It has been shown that the modulation of light intensity brings unavoidable extra power spent. But little information has been presented on how to deal with the LED limited efficacy and power conversion efficiency in a practicable VLC illumination device. In this sense, this paper brings a summary of LED power driving circuits and efforts reported in the literature to deal with power conversion efficiency limitations in VLC systems. We present LED efficacy and dynamic aspects, all of them pertinent to designing an illumination with joint communication feasible device. Moreover, it presents a discussion regarding modulation of light intensity using common classes of power converters in the view of LED driving. Furthermore, this paper is thought as a guide that fills the gap between data communication and LED driving areas concomitantly existing in VLC technology.

**Keywords**—Visible Light Communication, VLC, LED, Free-Space Optical Communication, Illumination.

## I. INTRODUCTION

LED technology is taking a great part in the illumination market [1] as it has already surpassed Compact Fluorescent Lamps (CFL) power efficiency and it will match its cost in the future [2], even not considering other aspects like implications of CFL expected lifetime, discard and its environment impact. The lowering prices of LED lamps is clear, [3] identified average reduction of 50% in 60W equivalent LED lamps from 2012 to 2016 (global average selling price), in some European countries they became 80% cheaper in same period. It is time to explore other opportunities that arise from

solid state lighting, and therefore allow a new class of applications for lighting systems. The media, enthusiasts and specialized people praise VLC as promising application that is foreseen to be used in short-range communication channels and can be the relief for the crowded Radio Frequency (RF) electromagnetic spectrum[4].

Even though prior references exist about the use of visible light in communication history, it is from [5] the first attempts to bringing Light Emitting Diodes (LEDs) into Free-Space Optical Communication (FSOC). In VLC, the fast modulation of LED instantaneous irradiated light, imperceptible to human eyes, is detected by the receiver electronic device without harm to illumination [6]. More than using the optical channel to signal propagation, VLC is worth because all the transmitted signaling is useful for room illumination. Use of visible spectrum of light to communication at imperceptible power level (dark room "visible light" communication) is also possible [7], but it is not focus of this paper.

The LED device is considered as part of the communications channel in a VLC system (like a conventional antenna), but also environment geometrical and propagation constraints impose bandwidth limitations, which are targets of ongoing research [8][9]. Due to power summing in optical domain of several frequencies, VLC FSOC experiences no destructive interference, except additive interference that takes place in this scenario. Multipath imposes a performance limitation of channel bandwidth due to infinite (reflected) delayed replicas of signal that are summed at the receiver and cannot be separated in detection of instantaneous power.

In order to follow expected efficiency and lamp cost [10] to achieve commercial feasibility, VLC LED drivers shall reach a balance among efficiency and functionality [11]. In consonance with highly efficiency lighting systems standards, such as Energy Star[12], electronic drivers are expected to keep the

good wall plug lumen per watt (lm/W) ratio. Energy Star imposes minimum omnidirectional lamp efficacy as 80 lm/W if Color Rendering Index (CRI) is less than 90[12].

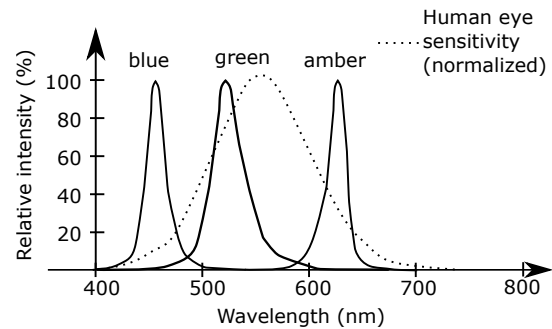
Thus, the main focus of this paper is to deal with important aspects involving energy conversion, LED limitations and driving in VLC application. We synthesize some important considerations focused on the semiconductor device, efficacy and commonly VLC-oriented technologies approaching LED drives.

In order to bring a better view of LED as part of the VLC channel, Section II introduces it as a transmitter device. Section III focuses on lighting outlook in this technology as well as efficient power conversion in LED driving. Section IV approaches aspects concerning LED dynamic behavior. Finally, Section V presents common circuits for power driving of LEDs, performance requirements and the authors' suggestion on suitable combinations of converters for best performance and efficiency.

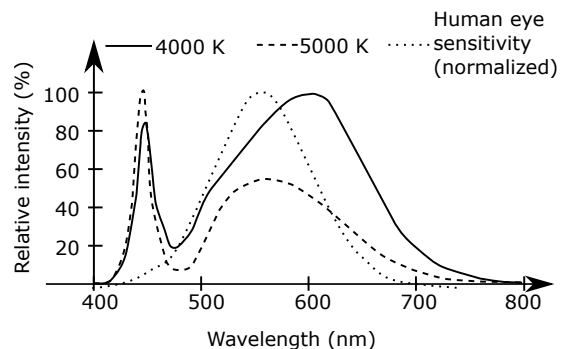
## II. LED AS TRANSMITTER DEVICE

The LED is a passive device that performs conversion of electrical energy into light according to its physical semiconductor properties, resulting in a characteristic electromagnetic spectrum. While in other optical communications, such as fiber optics (FO), infrared or laser applications, the Power Spectral Density (PSD) is well-defined and used to convey information inside the most efficient bandwidth in that physical medium, this is not the case for VLC, nor the same devices can be used in general illumination. In FSOC, using laser or infrared, there is no concern about user visual perception of that signal (those signals are usually situated outside of visible spectrum), although user's health security aspects shall be taken into account [13][14]. Illumination LEDs have, on the other hand, a much wider spectrum spreading. Therefore, they are optimized for good visual perception and power efficacy regarding human eye sensitivity profile.

In RF applications the transmitted signals present a well-defined wavelength, ranging from centimeters to meters. Nevertheless, in VLC the electromagnetic bandwidth is dependent on the LED optical features, and it varies from wavelengths within the range of 380 nm to 750 nm. Therefore, its PSD results in lumino-technical constraints (Chromaticity Coordinate - CC, Correlated Color Temperature - CCT).



(a) Typical PSD for a RGA commercial LED[16].



(b) Typical PSD for a commercial PC LED[17]. Two possible CCT weighting phosphor coating are shown.

Fig. 1: Comparison of PC and RGA typical PSDs.

Due to spectral characteristic of LEDs, coherent detection of light is not a suitable approach, unlike RF and other optical communication technologies. Most proposed applications use Intensity Modulation (IM) with Direct Detection (DD) of instantaneous power intensity [15]. DD may be performed in a single color sensor (responsible for the detection of part or the entire LED's power spectrum) or in separated colors (spectral ranges) irradiating simultaneously, giving the possibility of independent parallel communications channels in the optical domain.

In practical general purpose illumination applications, for good color rendering, Phosphor Coated (PC) or Color-Mixed (CM) LEDs are used. CM LEDs are widely available as Red-Green-Blue (RGB), Amber-Green-Blue (AGB) and other combinations (also bi-chromatic or quad-chromatic [9]) of light emitting dice are joined to build LED devices that fulfill a range of synthesizable colors. This procedure uses light additive principle and independent control of power provided for each die.

For VLC purposes, CM LEDs, whose PSD is

shown in Figure 1a, allow a differentiated communication approach that is Color Shift Keying (CSK). Literature [18] [19] describes extensively this method and it was implemented through control of instantaneous power of different colors irradiated, while keeping average color accordingly in order to achieve desired CC or CCT. Driver circuit controls individual current of each die in order to allow the definition of the power emitted in each range of light spectrum. Sensors sensitive to narrow ranges of light spectrum can detect individual transmitted components.

PC LEDs are semiconductors that emit light in the blue range (shorter wavelengths) in which a phosphor cover converts part of the light into longer wavelength range. This blend leads to a white light visual perception, with PSD as depicted in Figure 1b. These devices have almost the same PSD characteristic over an entire driving range. Although temperature and current intensity cause some minor PSD shift in a quasi static condition, modulation in driving current will mostly affect instantaneous light intensity.

Even though it was foreseen that CM LEDs can reach higher power conversion efficacy (lm/W) [20], PC LEDs are dominating the market in applications in which change in color characteristics is not needed. This is due to luminary (includes driving circuit) building simplicity and higher wall plug power to light conversion efficacy. This could be the explanation for the findings that most of VLC literature explores IM in PC LEDs. Although these devices have some specific limitation in bandwidth due to phosphor coating, the wide set of commercially available devices and good acceptance of this growing technology in lighting pushes us to agree that VLC should be analyzed in this technology background.

The LED PSD is not absolutely constant at all operation conditions, but in comparison to wavelength control performed in FO Wavelength Division Multiplexing (WDM), it can be assumed constant (with insignificant changes in profile) for communication purposes. This find comes from the following analysis: the LED PSD can be modified by temperature effect and by instantaneous current value [21]. At first, the LED PSD shift due to temperature effect occurs in a slower fashion comparing to communication dynamics, due to thermal inertia, it happens in a time base in order of seconds to minutes. So that

PSD shift due to temperature effect can be negligible during a communication round that mostly happens in a milliseconds window. And the second, the color shift in chromaticity coordinates, observed by [21] in a Phosphor Coated (PC) white LED for different dimming techniques, was shown to be less than 3,3% if instantaneous current was changed from 100mA to 1000mA (10:1 current ratio) at same temperature. This indicates that a small change in spectral emission profile, like shown in Figure 1, is expected due to driving current. Because Intensity Modulation with Direct Detection is used this will cause weak effect to the sensed signal in the receiver.

Although visible light spectrum is a free terahertz-range of frequencies available as communication media, it is clear that some limitations in LED devices play a significant role in weakening this technology, at least with current available devices.

### III. LIGHTING ASPECTS AND EFFICIENT POWER CONVERSION

Prior to the analysis of a VLC system as a communication device, it is of adamant importance the concern on efficient energy consumption. Proposing VLC as a technological step forward as a new concept of data transmission and as environment friendly, from the point that is feasible the reuse of energy resource and infrastructure, it will just make sense if the power efficiency of such device is comparable to a conventional general purpose luminaire.

Currently lighting industry intends to produce LEDs with lm/W efficacy crossing the 200 lm/W milestone at competitive prices, as foreseen in [20], and good CCR in order to achieve consumers' expectation and regulation [22]. While lamps and luminaries efficacy are lower, but expected to reach 200 lm/W[23][24] in the short term, the economy of such effort is still questionable.

Despite the intense race presented in scientific literature on high speed VLC systems, most of them ignore strict constraints of illumination functionality [10] or power conversion. In this sense, this work aims to provide a broad view of efficient LED driving in feasible lighting devices.

In most of the foreseen applications for VLC systems power is drained from fixed power network. This provides energy at higher voltage level, compared to single LEDs requirement, and AC

sinusoidal voltage (85 to 280Vac, peak from 119 V to 395 V, worldwide scenario) with power pulsing at 100 Hz to 120 Hz. Rectification and filtering may be the driver action at a first glance, but due to voltage source characteristic of LED device, power control is a mandatory driver function. Light intensity average control (dimming feature) is the next item to be thought of on a practical LED driver circuit targeting energy saving among its advantages [11].

Commercial LED drivers may require more than one stage for processing the conversion when power factor in input is concerned and LED light intensity ripple is to be minimized [25]. This trend to reduce global efficiency and increase costs, but not all systems will require several stages. In some cases, an extra stage will allow reduction in the capacitance per Watt ( $\mu F/W$ ), a common metric for evaluating LED driver circuits cost and lifespan. Section V approaches power processing aiming at LED driving.

A large set of commercial solutions are available [25] in order to LED ripple minimization with the manufacturing of ready proven circuits. Non intentional IM caused by power pulsing, besides low frequency ripple, is the concern for most applications, in frequency ranging from DC up to 1 kHz [26] since hazardous effects may occur affecting human health[27]. This range of light flicker can cause headache, excessive eye beat and photosensitive epilepsy attacks[26]. This is another limit to VLC IM, for it bounds the lower acceptable frequency of modulation. This range is further discussed in Section IV.

In frequencies above 2 kHz up to 100% of modulation index is acceptable with very low risk of harmful effects to the user [26]. Higher frequency ripples are safe regarding human health, since in this range VLC meets a useful band to IM in data transmission.

It is important to establish the definition of three ripple components observed at instantaneous light power: firstly, the result of intentional IM; secondly, the fixed power network AC frequency power pulsing (100-120Hz), and thirdly, the ripple present from Switched Mode Power Supply (SMPS) output. These ideas are further developed in Section V-B. The last can be filtered, but it is a result from limited switching frequency of circuits, together with passive filter characteristics.

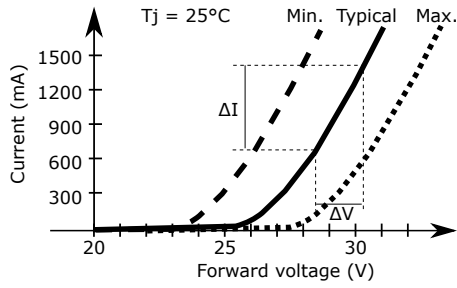
#### A. LED power control

Understanding the load's unique behavior is highly relevant to efficient power driving, Figure 2 presents LED basic electric and optic characteristics. The LED device electric characteristic impedance is strongly dependent on operating temperature and semiconductor production variability. Due to LED's sharp voltage to current transfer (low impedance after threshold voltage is achieved, see Figure 2a), it is normally driven with current mode or with current controlled voltage sources. Additionally any small voltage ripple in power supplying may be amplified in the resulting current level, thus in LED application may be especially important the attention to voltage ripple.

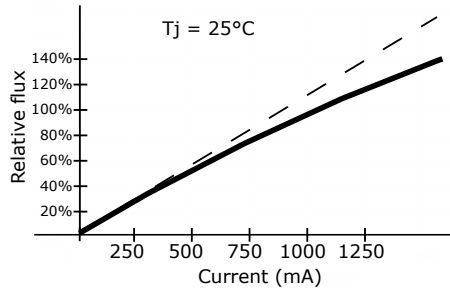
Another fundamental LED aspect seen in Figure 2b is the one concerning global light emission efficiency. The flux is not linear with current (nor with power) applied to the device. This known non-linear behavior is called Droop Effect (DE) and, together with semiconductor operating temperature, reduces the total irradiated light, decreasing power to light conversion efficacy in material higher levels of current density. Some early studies claimed that DE was possibly caused by increase in internal semiconductor temperature, but now the consensus is that reduced efficiency is caused by a phenomenon called Auger recombination that reduces the emission of light [28][29] even at constant semiconductor temperature.

There is a trade-off between the expected power to light conversion efficacy in a sample LED device: reducing the current intensity (thus also density) increases efficacy (lm/W) to the disadvantage of lower total light flux. When a not constant current is applied, the higher peak-to-average (PTA) current level, the lower will be the average conversion efficacy.

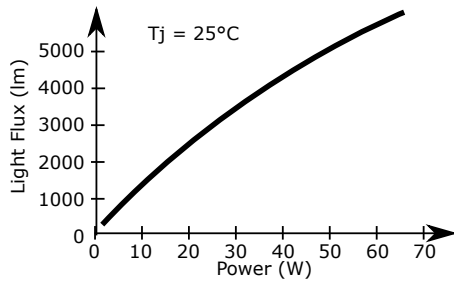
Even though the actual voltage developed across LED when current flowing is not constant, because of the small impedance when threshold is exceeded, we usually perform computation of total irradiated flux according to applied current to analyze LED efficacy. This is a simplification in the representation, commonly found in literature [30]. Actual light flux produced accordingly to LED power can be seen in Figure 2c. But it should be clear that the measurement of device efficacy actually uses lumen per watt metric (lm/W), the decay of this characteristic with



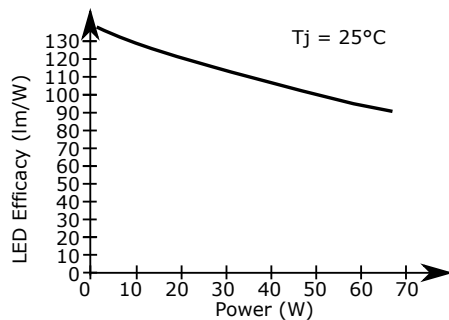
(a) Applied voltage and resulting LED current. Production variability effects shown in minimum, typical and maximum limits.



(b) Relative light flux irradiated by LED when stimulated by current (solid line). Projected relative flux with initial flux-to-current rate (dashed line).



(c) Light flux accordingly to the supplied power.



(d) Light efficacy accordingly to the device's power.

Fig. 2: Commercial LED [17] characteristic curves.

increased device power (at constant temperature) is shown in Figure 2d.

Some previous works, as [30], already explored

deeply the consequences of DE and stated the best method to drive an LED is a constant current, regarding power to light conversion efficacy. Literature reported several methods of driving an LED device in order to keep good efficiency or to reduce color shift caused by dimming. When control of power is concerned we can suggest classification in three groups, which are: Pulse Modulation (PM), Direct Current (DC) and Bi-level. Their characteristics are summarized in Figure 3 and further explored below. DC may also be called Amplitude Modulation (AM) in illumination scope, although this refers to the constant current level kept in LED device, and shall not be mistaken for communication AM of a carrier signal. Any of these methods may be also used to control lamp light intensity (dimming), however specific circuit types are used to implement each one.

These control methods concern general illumination, for VLC purpose data shall be conveyed into the power signal using one suitable modulation strategy. This may be superimposing other signals to these control methods or manipulating their usual characteristics (phase, intensity, frequency, etc.).

1) *Pulse Modulation method*: PM method uses a single current intensity level ( $I_{max}$ , point P1) that is kept in LED for a defined portion (duty cycle,  $D$ ) of stimulation period (see Figure 3a, period  $T_p$ ), the rest time the LED is off (point P2). Average current intensity in period  $T_p$  is given by Equation 1.

$$I = \frac{T_{P1}}{T_p} I_{max} = D \cdot I_{max} \quad (1)$$

This method has the advantage of almost linear average light intensity with  $D$  as control variable, but the irradiating efficacy is reduced due to operation at a high PTA (point P1 and zero) reducing efficacy due to DE. This represents modulations like Pulse Width Modulation (PWM), Pulse Density Modulation (PDM), Pulse Position Modulation (PPM), Pulse Frequency Modulation (PFM) and similar analysis apply to all of them.

2) *Direct current method*: Another common driving method is the DC (depicted in Figure 3b). This provides a well-regulated constant current level to the LED device. The challenge of implementing such strategy is keeping good voltage regulation at driver output for any level of expected current, but superior efficacy is ensured due to reduced operating current at the point (P3) and minimal possible PTA

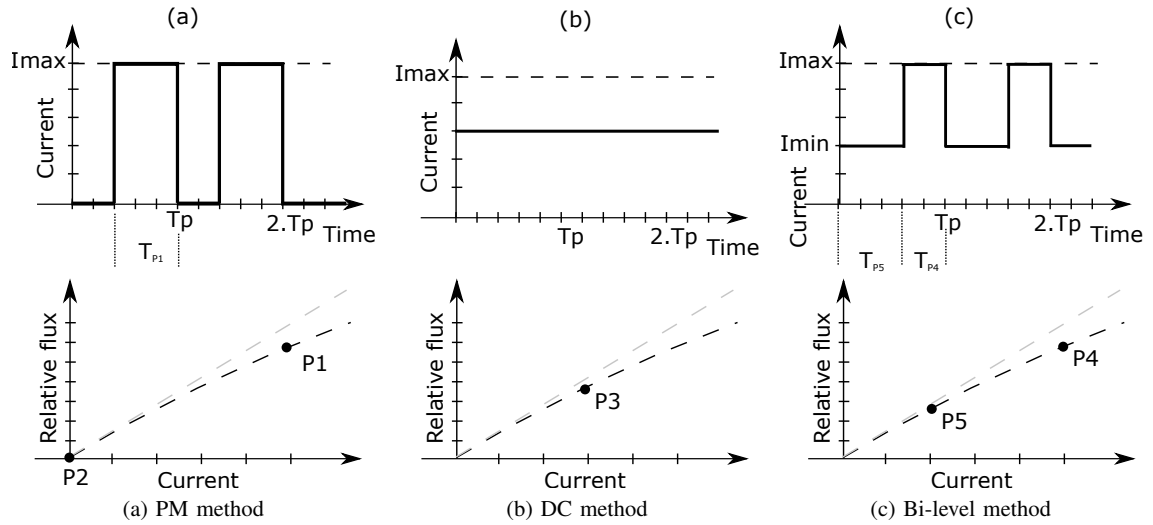


Fig. 3: LED driving methods

ratio. Even best chromatic characteristics of light in driving using DC are expected [21], the thermo-optical relation reduces color shift along a wide DC current range according to this analysis.

3) *Bi-level method*: A blend of PM and DC methods is called Bi-level [30]. It allows simpler average level control by definition of  $D$  of switching from two non-zero current levels (shown in Figure 3c, points P4 and P5). With average current level calculated accordingly to equation 2, this method has the advantage of higher efficacy when compared to PM and same dimming mechanism.

$$\mathbf{I} = \frac{T_{P4}I_{max} + T_{P5}I_{min}}{T_p} = D \cdot I_{max} + (1 - D) \cdot I_{min} \quad (2)$$

One may assert that a very high or low  $D$  of Bi-level driving approximate to DC performance, also selecting P5 current level as zero transforms it to PM method, those can be thought as a single method. A further generalization in the approach proposes any number of levels ( $n$ -level) for current targeting maximization of efficacy within any dimming range [31].

4) *Comparison*: Concerning VLC and the efficiency drop due to DE, it is desirable to keep always maximum LED current as close as possible to average, which leads to operating at higher efficacy point. DC level ensures maximum equals to average current, however DC driving generates no change

in LED instantaneous current, leaving no room for signal transmission on irradiated power intensity. Bi-level driving incorporates a level of modulated digital data in power signal, keeping a DC level and average irradiation for illumination purpose.

Bi-level method has more degrees of freedom (P4, P5 and  $D$  definition) that may be used to perform data modulation in VLC and concurrent dimming. DC and PM methods do not offer many alternatives. As a generalization, Bi-level may be the best approach to be followed among these illumination driven methods. Although those are of simple implementation (because single switch converters can implement such strategies efficiently), there are limitations due to frequency and depth of modulation. Section V further explores these aspects.

Performing any sort of intentional modulation in LED light intensity leads to lower global efficacy [32]. However, power consumption penalty is addressed when communication with illumination is implemented. But additionally to this, there arises the expectation that signal losses may occur due to LED modulation frequency limitations, which will be further presented.

#### IV. LED AS A DYNAMIC DEVICE

LEDs are mostly referred to as static devices for illumination purpose, disregarding temperature effects and long term threshold shift. But when VLC feature is designed it is important to keep in mind

that, even though it is normally not a concern on the part of the LED manufacturer and little technical information is available, LEDs have their own higher frequency dynamics.

A general approach to evaluate communication channel is to define its limitation in the frequency domain, and it is usually referred to by the cutoff frequency. This is measured as the limit after which most of the signal power provided is lost or not irradiated. This limit is the frequency in which the output of the channel has half of the observed power (-3 dB) compared to value in the passband. In the case of LED device, the cutoff frequency is defined accordingly to the decrease of light power amplitude (AC part), when compared to DC instantaneous power, sweeping stimulation current frequency.

When modulation speed of LED devices is addressed, there are some high frequency limitations, which occur due to semiconductor characteristics (this may be referred as electrical domain) or due to optical characteristic (optical domain). Reference [33] indicates the electrical domain to be always dominant in bandwidth limitation, but literature disagrees with that when PC LEDs and general illumination devices are studied rather than communication specific LEDs.

PC LEDs have an additional limitation, when compared to CM LEDs, in modulation speed due to the phosphor cover slow dynamic, limiting fast modulation in the optical domain, phosphor spontaneous emission lifetime is longer[34]. Measurements from [35] show that -3dB frequency decay occurs near 2 to 3MHz range, limiting region A in Figure 4. It is possible in the range of region B the detection of blue only spectrum without any frequency related attenuation by using an optical filter[35], because this passes through phosphor coating. This blue filter may not increase communication capability because of great attenuation and other parasitic effects due to non-ideality of the filter, which may reduce global receiver effectiveness [34].

Besides phosphor slowness limitation, the semiconductor characteristic for the same LED has cut-off frequency dependent on radioactive recombination lifetime or electrical carriers charge/charge discharge. It may also be referred as junction bandwidth. The radioactive recombination lifetime imposes a limit in the light power rise and fall time in low injection LEDs (injected carrier density less than the doping concentration). There is a direct

dependency on either carriers lifetime or light emitting efficiency of the device: highly doped devices and density of deep traps ensure shorter carriers' lifetime (allowing faster modulation rates), but they also reduce the quantum efficiency of light emission (reducing device efficacy)[36][37].

Communication dedicated LEDs are devices designed according to a much wider passband in order to reach modulation rates exceeding 1 GHz (in cost of lower efficacy). On the other hand, as the great effort of illumination is the increase of LED efficacy, it is in the opposite direction and may be a disadvantage for communication purposes using high frequencies.

However, in high injection LED devices (in which the injected carrier density exceeds the doping concentration) the injected carrier concentration dominates the recombination lifetime, thus the light bandwidth can be wider [38].

The LED junction associated charges (somewhere referred according to the equivalent capacitance) increase with semiconductor device junction area or perimeter, and also depend on the material and doping levels. One cause of this frequency limitation is the slow charge and discharge of LED junction (capacitance -  $C_j$ ) and other parasitic electrical parameters like resistance (R) of wires [39], [40], [41], [37]. This can be called RC effect or LED semiconductor bandwidth, in opposition to junction bandwidth.

The LED high frequency model [42] is built according to Figure 5c when it is forward biased,  $V_f$  represents diode threshold voltage in a linear approximation of LED forward voltage droop. This is a circuit representing LED electrical behavior. Optional model from [37], shown in Figure 5d can be used to analyze light instantaneous power: voltage applied to model terminals is analogous to LED actual current and the voltage read between  $C_j$  terminals is proportional to light power. In Figure 6 the smooth light power dynamic is shown when a square pulse of current is provided according to modeling by [37], the rise and fall ramps are exponential.

In [35] experiments, the LED semiconductor bandwidth reached 20 MHz. This range is shown as region B in Figure 4. [43] found a 35MHz bandwidth in a commercial 250 lm (at 700 mA) white LED and blue filter in receiver. Using Micro-LEDs [44] achieved cutoff frequencies exceeding

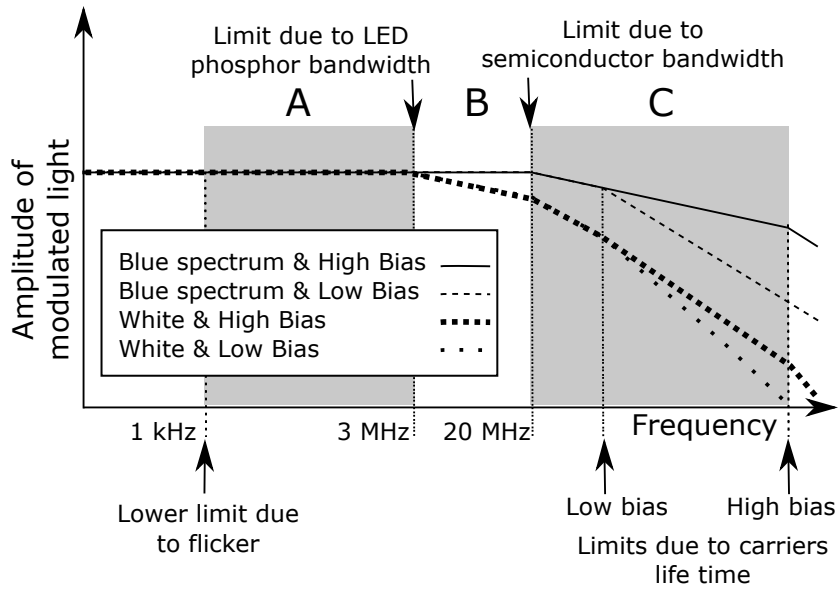


Fig. 4: LED's transfer function for power IM

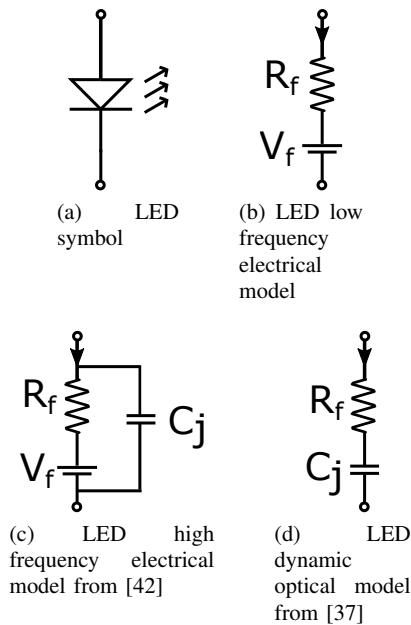


Fig. 5: Different LED models according to use.

400MHz. The observed limitation was related to the device size, smaller devices are faster.

The limitation imposed by this junction charge may change according to DC bias point applied to the LED current [41][44], since higher levels of bias lead to wider bandwidth, explained as fol-

lows. Reference [44] shows that in micro-LEDs the modulation bandwidth is approximately linear with current density in LED active region ( $mA/\mu m^2$ ).

Near the zero bias point the LED is dominated by depletion capacitance that is proportional to LED area. On the other hand, as the voltage bias is increased, the diffusion capacitance is dominating, as this is only dependent on the region injected with diode current [37]. A commercial High Bright LED (HB-LED) has high frequency model capacitance in the range of 0.5 to 1 nF[42], for a 7400 lm Organic LED (OLED) this can be in the order of magnitude in range of 200 to 400 pF/mm<sup>2</sup> and area of about 1000 mm<sup>2</sup> [45]. OLEDs have even a different capacitance variation according to polarization voltage, several studies present analysis and simulation regarding the modeling of this complex behavior [46][45][47][48][49][50].

In addition, references [41] and [44] show that forward biased inorganic LEDs have larger bandwidth that agrees with [39] and [38] when they refer to frequency response of an LED dependent on the injected current. Reference [33] states that if a small bias is provided to the LED, the limitation in bandwidth would be only the carriers' life time, because the delay in charge injection in the junction would be negligible. Analysis and modeling from [38] show that high active layer doping concentra-



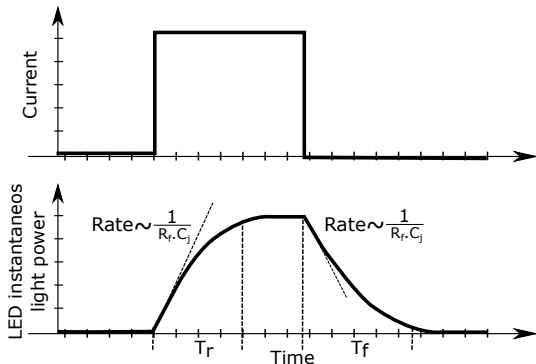


Fig. 6: LED instantaneous power

tion in a forward biased LED have double bandwidth in small signal when compared with the same device large-signal modulation.

These analyzes and literature review show that there is a great variability of devices size and characteristics, also the identified cause of performance limitation on those is not always the same. Therefore, the position of limits imposed by junction bandwidth (caused by carriers lifetime) or semiconductor bandwidth (due to RC effect), illustrated in Figure 4, may be exchanged inside region C.

#### A. Estimating cutoff frequency

A straightforward way to estimate the LED bandwidth based on instantaneous light (10% to 90% value) rise ( $T_r$ ) and fall ( $T_f$ ) times is provided by [37]:

$$f_{3dB} = \frac{1.2}{T_r + T_f} \text{Hz} \quad (3)$$

Even though bandwidth limitation exists, exceeding that cutoff frequency it is still possible to achieve higher light modulation rates in these devices, as region C shows in Figure 4. This can be done in cost of extra stimuli strength to LED, tolerating great attenuation or distortion of the produced signal. The amount of extra energy spent will be dependent on the driving electronic circuit, that will be further elaborated in the next section. Figure 4 is illustrative, not formally calculated nor measured, because amplitude decay may be different according to LED characteristic and for each phenomenon that outline the regions shown.

#### B. Overcoming limitations

Some authors that identified this remaining charge between LED terminals as a problem to high frequency modulation of LEDs propose a solution capable of dissipating remaining energy stored in the junction to extinguish light quickly [51][37]. This aids overcoming carriers life time problem, by removing residual carriers faster (carriers sweep-out), and also reducing RC limit effect by speeding up residual charge removal, in an effort to reduce fall time. But a non dissipative approach like [52] evaluated, a bidirectional buck-boost converter, would best fit to an efficiency driven design. Some solutions and consequences related to this will be discussed in Section V.

Current shaping is another method that aims the reduction of rise time of light emitted in LEDs [40], it increases LED driving frequency bandwidth. For faster start-up additional current pulse is provided to the LED in order to reach steady-state carrier concentration in the active region in less time. This is suitable to application in communication LEDs, with little concern about efficacy, because the trivial implementation of such strategy lacks of good efficiency in power conversion [37]. Reference [53] uses it together with OOK (On-Off-Keying) to show effective data transmission at data rates up to 125Mbits/s and [54] using OOK-NRZ (On-Off-Keying Non-Return to Zero) reached 456 Mbit/s with similar configuration.

Another possible approach to increase the driver and LED system bandwidth is the method of pre-emphasis of control signal (equalization), which explores the selective gain in frequency components that are in the LED or in the converter's attenuated band[55]. That leads to experiencing an almost flat gain characteristic of the system up to higher frequencies. This relies on additional dynamic range in converter control.

## V. LED POWER DRIVING

Not only LED efficacy is determinant on a VLC illumination system, but the way the energy is processed and transformed to drive LEDs is a main concern to global efficiency. It is of superior importance the modulation or codification process and how it is applied to the LED, since this is the conversion step that integrates information into the power stimuli. At this point, VLC technology differs

from conventional illumination process, literature already presents a couple of solutions, while other studies ignore the efficiency of this stage.

We show that this energy processing step may have different efficiency according to DC component parameters as well as LED dynamic behavior. First of all, it is important to differ among modulation or direct codification (encoding) of light intensity. Modulation is usually referred to as the process of changing a signal property (digital or analog data to an analog signal), whereas encoding is about representing a signal digitally (digital or analog data to digital signal or symbol).

The simple switching of a power device may generate either codification or modulation of power and current, that is referred to as a codification if that is to integrate digital information directly into instantaneous power. But from the point of view that any power level may be measured as an analog quantity, then it is possible to define it as a modulation process as well. From this point on, any data processing that aims to incorporate information into the LED device directly, in order to use it as part of communication system, may be called modulation process.

#### A. Defining time domain power signal

We can use a sort of different temporal intensity patterns (symbols) to convey information into light signals. Figure 7 shows three examples of different temporal patterns, which have intentional DC level and superimposed information built-in. Pattern Pa is a digitally switched current pulse sequence, that alternates between current level ( $I_{max}$ ) and zero. That generates an average light intensity defined by D and peak current, just like PM driving method. A very simple digital current switching modulator generates this pattern, when choosing the simpler topology, as analyzed in section V-C. The generated squared waveform signal contains a fundamental frequency and all its odd multiple frequencies due to the high slew steps, that is usually not efficient in a spectral analysis (of instantaneous light power), other patterns may fit better to communication spectral efficiency.

Pattern Pb follows another scheme, it does not completely extinguish the current, but a DC level is superimposed to define the average value, which is similar to Bi-level driving method. In a direct

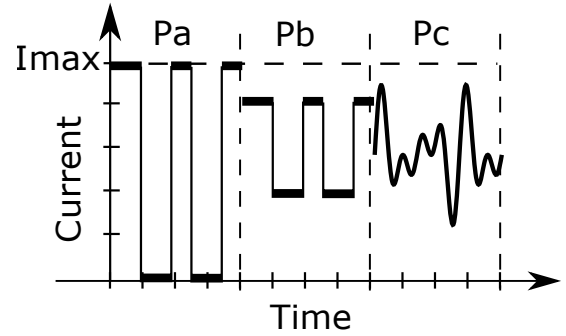


Fig. 7: Different power patterns illustrating instantaneous stimuli provided to LED device.

comparison with Pa, this scheme generates a smaller signal (AC part) proportionally to average power delivered to LED device. This implies reduced communication effectiveness, but allows a higher light emission efficacy according to the Bi-level driving method. There is a trade-off to be considered when defining signal to average levels. A digital modulator is also suitable to drive an LED device with such formatted current levels, but an advanced set of power sources or switches should be built.

Performing the actual efficacy calculation ( $\text{lm/W}$ ), for example we use power LED [17] with data provided by manufacturer at  $25^\circ\text{C}$ , in a comparison: DC stimuli provided with nominal current irradiates nominal light flux. In case Pa is used with D set to 0.5 and hence double instantaneous current level is applied (keeping average current provided to the device), total light flux is 82.8% of nominal while power provided is 6.3% increased. Therefore, efficacy ( $\text{lm/W}$ ) is decreased by 22.1%. That is a static analysis, neglecting any dynamic effect explained in Section IV, and no increase in temperature of LED junction is considered.

Either Pa or Pb schemes can be used to modulate digital data to light intensity in a quite straightforward way, that is expected to be implemented with simple hardware resources and high energy conversion efficiency. However few discrete power levels are not enough to implement some common and more efficient data modulation techniques, for example, Pulse Amplitude Modulation (PAM), Orthogonal Frequency Division (OFDM) or Frequency Division Multiple Access (FDMA), wanted in high capacity and robust communications.

It is possible the implementation of OFDM with

discrete power levels in VLC. In a study performed by [56], the author showed that pronounced signal penalties occur in signal quality when a low number of levels is used. According to [57] PAM can also be implemented using discrete power levels following the spatial summing principle, but it suffers from distortion among power steps (resulting from mismatch in LED array elements) that may be mitigated by using specialized modulation techniques.

Using a combination of parallel binary switches, reference [58] shows a methodology to equalize average current better at all branches despite the mismatch between LED devices, which can be a problem with small number of LEDs in each branch. Though [59] shows that passive self equalization of parallel branches with higher number of LEDs allows a good match without the need for extra current-balancing circuitry.

Pattern Pc in Figure 7 is a more sophisticated example, that is a typical OFDM signal sample. It is characterized by an analog power signal produced by the modulator as a continuous waveform and well defined bandwidth. This modulator should be capable of synthesizing a signal with any current level inside a defined range without high slew steps (those would cause higher frequency harmonics).

It should be clarified that beyond the AC pattern, there is a non-negative constraint in LED driving current, because light has always a positive value in LED device. Enough DC value should be ensured, so that signal clipping is prevented. If this condition is not met, strong degradation of signal may occur [60]. The high PTA characteristic of such modulation schemes like OFDM may be overcome by using different LED arrangements or modified modulation schemes [61][62][63][64]. However, neither of them is able to reduce PTA to an irrelevant level.

Fortunately the Gaussian distribution of instantaneous values around average level in an OFDM encoded signal, valid for number of frequencies components (carriers) higher than 64 [62], results in a lesser efficacy droop if compared to pattern Pa. For example, using the LED presented in Figure 2, with OFDM and 21 carriers, the signal standard deviation is 27% related to the nominal LED current. This results in an LED efficacy decrease of 8.1%. The definition of these parameters was done accordingly to reduce signal clipping probability in the example, but no direct comparison among communication merits is fair.

Best spectrum efficiency can be achieved using patterns like Pc (see Figure 7), due to the well confined spectrum of the generated signal (finite spectrum of frequencies is synthesized due to absence of high slew steps). The bandwidth of light instantaneous power is controlled accordingly to the shape of this pattern, so in a communication shared medium this is better viewed and is an advantage over previous exemplified patterns.

In order to generate such flexible signal, the modulator should have a power topology like a SMPS or Linear Power Amplifiers (LPA, for instance A, B or AB class amplifiers). One may object that a single A class amplifier is able to deal with non-negative signaling generation, but as it is stated in section IV, due to LED dynamic behavior the converter needs to sink current from output to allow faster light fall time when frequencies near semiconductor limitations need to be synthesized.

From the aforementioned modulator classes, some may be suitable for only a specific application, depending on the chosen data transmission technique, or can be applicable to different frequency ranges. Due to narrow bandwidth or low efficiency in power conversion, the choice of power converters' configurations can admit more nonlinearity due to the cost of global efficacy in illumination [65]. There follows a short review of some common and possible circuit classes to be used as LED power modulator, as well as specific considerations about conversion efficiency are addressed.

### *B. Switched mode power supplies*

Switched mode power supplies are a great contribution that power electronics brought to a wide set of consumer devices. Higher efficiency and low volume power converters are feasible using mid-to high-frequency switches. Usually LED drivers take advantage of this characteristics to achieve a compact and cheap design. Very high efficiency in DC-DC power conversion is possible due to the operating principle, non dissipative power handling is done by reactive elements. This conversion rate follows the switching frequency ( $F_s$ ), compassing energy convey.

As good energy conversion efficiency is possible, this class of converters are suitable to be used in stepping up or down the voltage level from an AC rectified source. Simultaneously it can perform

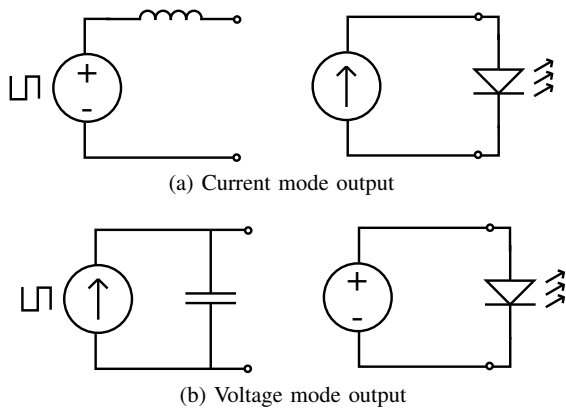


Fig. 8: Output characteristic of a switched mode power supply

power control, to ensure rejection of low frequency components, and modulation for VLC propose at higher frequency band.

The operation principle of SMPS implies that the energy absorbed from the input and also delivered to the output is not constant in time, but a pulsating component is present. This pulsating power effect is reduced by the use of an output filter that absorbs and releases energy during each cycle. Depending on the characteristic of the converter's output, the filter may be an inductor, a capacitor, as depicted in Figure 8, or an arrangement of both.

Current source characteristic output converters use an inductor as filter, a simple output filter is shown in Figure 8a, the voltage applied to the filter plus load set is a rectangular or triangular pulsed voltage. On the other hand, voltage source characteristic output converters use a capacitor as filter, a simple output filter is shown in Figure 8b, pulsating current is applied to the set. Some amount of this pulsed current is absorbed by the capacitor reducing voltage ripple. Even though good filter design is possible, the filter should be capable of reducing the effect of the switching frequency and keeping the constant DC component. The more output filter is capable of reducing unwanted current or voltage ripple, ensuring a low cutoff frequency, the slower will be the output node dynamics when this dynamic is required for intentional modulation.

Each square wave source shown in Figure 8 is characterized by pulse intensity, frequency and duty cycle. Pulse intensity is defined by converter's input voltage or current, and frequency is a design param-

eter. The average control of output is possible by definition of the duty cycle. However, this imposes a frequency synthesis limitation in output. The discrete time switching is responsible for limiting the capability of changing output instantaneous value, even though excess of power may be available to allow a wide range of control action. Reactive elements in the converters circuit represent inertia to be overcome by the device during modulation.

Figure 9 illustrates actual SMPS output voltages in two common converter circuit topologies, together with average value operating in open loop (no control is applied). It presents the moment in which a simple step is applied to switches driving D parameter ( $T_a$  instant). It is clear to see the high frequency components in output voltage signal of these converters, this is already result of first order filtering based on an inductor, and represents a clear limitation in signal efficient modulation in this class of converters.

A straightforward way to deal with this limitation was validated by [66]. The authors use this constructive limitation in a buck converter to modulate data in current ripple produced in converter's output. This is possible changing PWM phase at each cycle accordingly to the data bit to be transmitted. Also [67] explored this implementing Quadrature Amplitude Modulation(QAM) using two-phase synchronous buck converters that worked together to transmit several bits at each symbol of ripple in its output.

If the ripple is not used in order to provide useful signaling, that may harm the communication signal, for instance increasing bit error rate, like [68] and [69] analyzed in buck topology SMPSs.

The synthesized frequencies are usually said to be limited to  $1/5$  of the converter switching frequency ( $F_S$ ) in SMPS. Further research is required in this direction until drivers are designed to operate at both high modulation speeds and high efficiency levels[10].

Power converters with boost operation principle (which are boost, buck-boost, flyback and derived topologies) operating in Continuous Conduction Mode (CCM) have another limitation in output dynamics when the frequency domain transfer function of the whole circuit is analyzed. The transfer function of these circuits has a positive zero in complex plane, also called Right Half Plane Zero (RHPZ), the result of such dynamics is that for abrupt changes

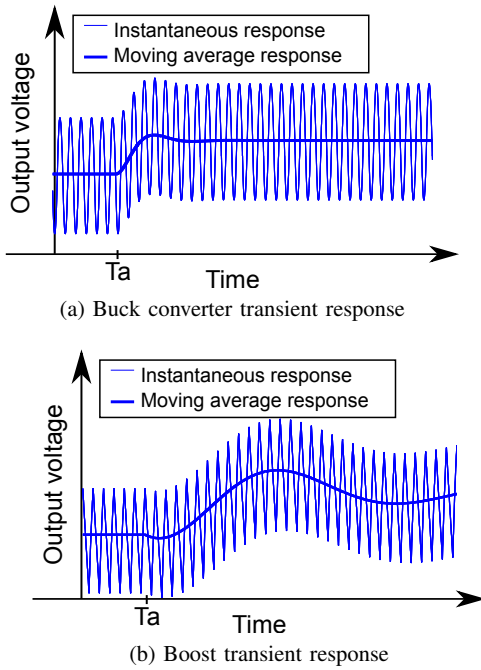


Fig. 9: Common SMPS output transient responses to small step in  $D$  at instant  $T_a$

in  $D$  will cause the output signal to first change in opposite direction than final value will stabilize[70]. For example, when a positive step in  $D$  may cause a negative transient in output voltage for a short time, after that a positive step is accomplished, as illustrated in Figure 9b just after  $T_a$ . In any close loop control including this plant, an instability may be triggered if control speed is set high.

The output of a SMPS may be controlled to follow a defined reference of output voltage or current (in average). This is interesting to the VLC that this class or amplifier can draw either of the time patterns shown in Figure 7 thus limiting the dynamic range of reference that can be tracked by the converter.

Considering that the LED plus converter filter represents a large time constant, the output fall time will limit severely the bandwidth of the synthesized signal. A solution to this can be, as proposed by [52], the use of a bidirectional power supply able to sink current from output node without additional energy loss.

Addressing the global efficiency of the SMPS, it is necessary to assess losses in each component of the circuit, that may be of major importance

determining other efficacy bottleneck. A model to losses in a buck converter is presented in [71], which includes switches (diode and MOSFET), inductor and capacitor static losses, considering low frequency modulation. A complete implementation of a single stage buck LED driver plus binary switching modulator has been demonstrated by [42] with peak efficiency of 88.6% for a 5.8 W driver.

### C. LED binary switching

From constant voltage or current source it is possible the realization of a VLC modulator by deviating or interrupting the instantaneous LED current. The power control method described here is not suitable for adjusting current or voltage levels, but only the average level is subjected to control.

The term Binary switching of LED power is used due to the discrete switching of a power supply (or a group of sources). It is usually implemented in an arrangement of semiconductor devices so that at least two levels of current can be applied according to modulation stimuli. Some options of simple two level binary switching modulators are shown in Figure 10.

A couple of advantages arise from the use of these structures, mainly the simplicity of implementation. With full control of switch state and current direct feed to LED (no reactive elements in the path) they can reach good efficiency in energy processing. Fast modulation of current stimuli is possible[42][72]. Modulation circuits of this kind realized with largely available commercial (and cheap) semiconductor switches can easily reach frequencies exceeding those LED limitations described in Section IV.

Moreover, with the degrees of freedom in LED actuation in VLC, it is possible to implement dimming directly selecting  $D$  ratio (average control) and simultaneously applying a modulation like VPPM using data to be transmitted[19][72][42][73]. But that is limited to the described in power control methods PM or Bi-level. The definition of voltage and current levels applied to LED depend on the source or on a previous power processing stage, as well as operation points, affecting LED efficacy due to DE. If voltage supply is used, according to the current-to-voltage sensibility of LED, any regulation will impact strongly on current and instantaneous power intensity. On the other hand, current-source-type converters are immune to this effect.

Analysis of LED current switching and light power considering only effect of bandwidth limitation due to RC effect in the circuit is possible by using dynamic models presented in Figure 5. This allows comparison among different binary switch modulators performance.

Binary switch modulators may perform faster than the LED due to this device's characteristics, a very simple PM using a semiconductor switch presented in Figure 10a is feed in voltage mode. During turn on stimuli a sharp light step is expected (effect identified  $P_{Sa}$ ), as only  $S_a$  and the LED itself resistances will affect the light power slew rate. On the other hand, as the switch is turned off, a longer transition time is expected as the LED will slowly discharge itself, see shadowed area. Figure 10b shows a 2-switches modulator of same type, eliminating the longer transition by operating  $S_b$  in complementary phase. Using this circuit the RC discharge of LED is faster, depending more on  $S_b$  and less on LED RC constant.

A current fed PM is shown in Figure 10c. This modulator is expected to have a slower transition (shadowed area) only at  $S_a$  turn off, that is when LED is turned on, due to LED capacitance charge with  $I_1$ , due to current mode supply. At light turn off transition ( $S_a$  switches on) a faster transition is ensured depending on  $S_a$  to discharge the LED only.

The circuits presented in Figures 10d and 10e are Bi-level modulators and require two sources each (voltage mode or current mode) and switches to be implemented. Both circuits provide a DC current level at the LED and modulates an extra step according to data.

The voltage mode Bi-level modulator (Figure 10d) is expected to have fast transitions in both light rise and fall, more limited by switches resistance and less constraint to LED RC. On the other hand, current mode Bi-level modulator (Figure 10e) shows slow transitions in light rise and fall transitions limited by LED capacitance charge time with  $I_2$  and LED RC discharge, respectively. These limitations may be overcome following circuit techniques to speed up LED charge and discharge, as in [40] already proposed to laser devices. But another class of circuits may also be suitable as modulators, the LPA, which are analyzed next.

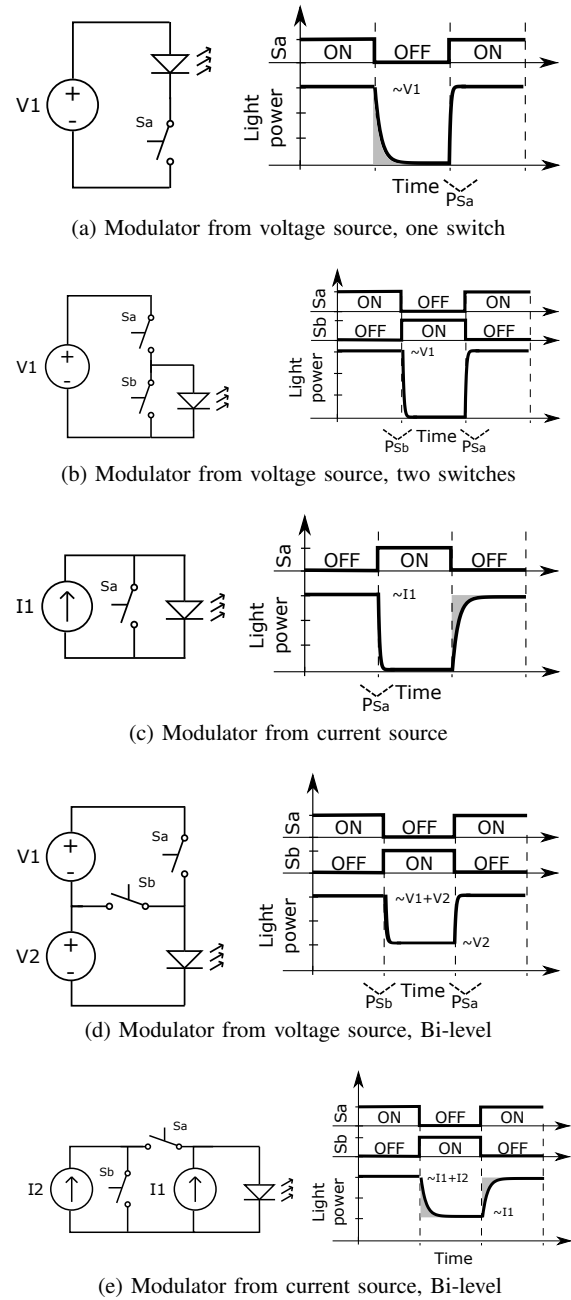


Fig. 10: Switches arranged as simple PM or Bi-level modulators

#### D. Linear power amplifiers

Linear power amplifiers are commonly used in RF or audio applications, in which the synthesized signal has high frequency. In power conversion, LPA are known to have low efficiency[74], when compared to SMPS, and are mostly used in wide bandwidth power regulators or low cost circuits.

In classical RF applications LPAs operate with a DC bias current, over which is modulated an AC signal to be amplified. This DC current presupposes a low efficiency because it is not useful, only high frequency is irradiated. In a VLC system, the same DC current that is provided to the LED with superimposed signal generates useful light[32]. Thus this class of converter can be seen from another perspective.

In the circuits presented below, the modulator can also be understood as a controlled current source, because load (LED) is directly connected to MOSFET drain terminals. On the other hand, in voltage mode (traditional) LPAs, the conversion from current to voltage would be done by an impedance (typically a resistor), that leads to a large power loss in this case.

LPA continuous waveform generation, without the restrictions of discrete power levels, or high frequency ripple, is an interesting characteristic that differs from other types of converters. Any sort of modulation can be implemented with these current levels that can be generated if enough bandwidth is provided. All power patterns presented in Figure 7 can be synthesized. The bandwidth of LPA is limited only by semiconductors and the control loop dynamics, no reactive elements are necessary. However, it is common to be used in LPA output a sort of filter (as a capacitor or inductor arrangement) to reject high frequency load variation, reducing the room of power needed to react or to ensure control loop phase margin for any load condition. This is not mandatory and the stability can be guaranteed by the controller itself.

LPA does not suffer from frequency synthesis limitation like SMPS due to the switching frequency. Therefore, modulation may be implemented in a separated frequency range from the control of output DC level. This will not limit modulation frequency to the control loop bandwidth since it will extend the modulation frequency until close to semiconductors' limit.

A simple class A LPA is schematized in Figure 11a. This is composed by a single MOSFET (M1) that controls the current drained from the constant voltage source (V1). The bias of M1 gate voltage ( $V_{GS}$ ) modulates the channel resistance. According to the LED and M1 resistance, the voltage of V1 is divided. Any other controlled semiconductor may be used in place of the MOSFET chosen.

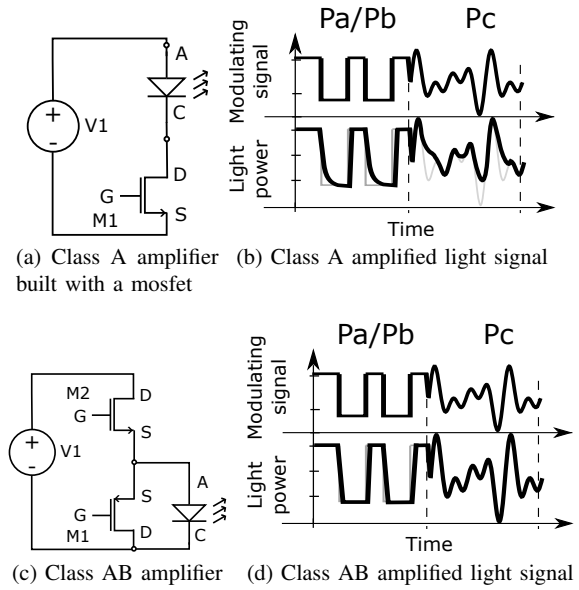


Fig. 11: Linear Power Amplifiers in simple configurations

In usual LPA, M1 is biased with a constant current kept even at no signal in output. When modulation is applied, the output current at D terminal will change to a higher value (sinking current from output node) or lower one (sourcing current to output node), providing RF or audio signals as AC part, which leads to low efficiency. In a VLC application, as stated previously, this current is useful to provide light enabling efficiency of power converter to be seen from another perspective.

The efficiency in power conversion in a class A amplifier is mainly defined by two associated factors: voltage headroom and load V-I characteristic. The voltage headroom refers to the minimum  $V_{DS}$  necessary in M1 (between terminals D and S) to keep it acting as a current source (approximated as a transconductance between  $V_{GS}$  and  $I_D$  for small signal). The total loss in MOSFET operation is given by  $V_{DS} \times I_D$  power dissipation (W).

The LED load V-I characteristic (depicted as  $\Delta V$  and  $\Delta I$  in Figure 2a) defines the amount of necessary voltage headroom that allows the expected excursion of current ( $\Delta I$ ) in the modulated current without significant signal distortion due to non-linear behavior. The possible operating points in a class A LPA are depicted with circles in Figure 12. In this figure, LED current is shown in dashed line

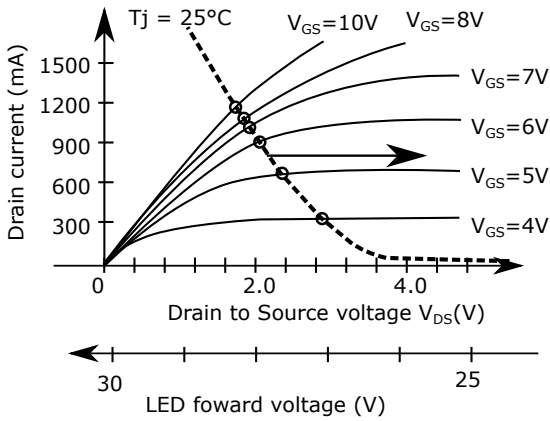


Fig. 12: Biasing configuration of a LPA driving an LED, LED forward voltage horizontally mirrored from Figure 2a in dashed line.

and MOSFET current according to  $V_{GS}$  biasing levels is shown in solid line. It is clear from these curves that for  $V_{GS}$  greater than 10V strong non-linearity in current occurs, which is not the case when  $V_{GS}$  is in the range from 4V to 6V. An increase in voltage headroom would shift LED current curve to the right, as pointed by the arrow.

High power MOSFET devices can usually operate at lower  $V_{DS}$  voltages (lower  $R_{DS}$  in on state) thus allowing lower  $V_{DS} \times I_D$  losses. But this does not ensure a more linear behavior and these devices even suffer from larger parasitic capacitances that lead to narrower converter's bandwidth. It is important to notice that the more inclined the slope of LED  $I \times V$  curve is (the lesser the LED equivalent  $R_{ON}$  is) the smaller the voltage headroom (needed for safe MOSFET operation for same  $\Delta I$ ) will be, leading to smaller  $V_{DS} \times I_D$  losses. It is known that power LEDs, single chip or Parallel Chip on Board (COB) arrangements, have lower  $R_{ON}$  characteristic, which is an advantage increasing class A converters' efficiency. Reference [32] illustrates the extra power necessary for LED driving using a class A LPA. They found that power efficiency of the JIC (Joint Illumination and visible-light Communication) driver can be above 90%.

Due to the concern on voltage headroom, which causes lower efficiency, the implementation of dimming using DC in LPA may not be the most interesting approach. On the other hand, the use of PM for dimming can be realized and allows the definition of suitable point P1 and D to achieve good

efficiency. This limits the time the modulation of useful data can be generated (during P1 only, on time) and generates unwanted modulation of light while no data transmission (that would be avoided in DC dimming).

A class AB amplifier has additional components and functionality compared to class A because it is able to sink current from output node according to the provided modulation signal, Figure 11c shows a sample circuit. In RF and audio application, it has a higher efficiency in power conversion because it can avoid a great constant current necessary in the semiconductor device even with no signal at load. MOSFET M2 sources and M1 sinks current from the load, which depends directly on correct definition of gates biasing.

In VLC application, current will be provided to the load at most times (even during no modulation) to provide average illumination. This is why the gain of efficiency is not so relevant. But it is important to define an advantage possible due to M1, when fast switching is needed. As a consequence, the excess of charge in LED junction can be quickly removed.

Commonly class AB amplifiers show a 'zero cross' distortion in output when modulation signal approaches zero and is applied directly to M1 and M2 gate terminals simultaneously. To avoid this effect, a special scheme of gate control may be used biasing M1 and M2 with  $V_{GS}$  close to its threshold or a control loop observing output voltage or current can overcome the distortion band.

Dynamic behavior of instantaneous light power for class A and AB LPAs respectively is shown in Figures 11b and 11d. Both samples of power pattern are provided as modulation signals. In Figure 11b it is clear that the light power will not follow well the modulation signal due to long fall time (defined by LED RC fall time). In case of class AB amplifier, Figure 11d, the light instantaneous power may not be so well followed when extremely high harmonic components exist in modulation signal (patterns Pa/Pb) but for a finite bandwidth signal (pattern Pc) it is suitable, no long fall time is experienced.

Less common, but also possible and feasible, would be a current feed LPA with current mode output. This approach would require the main switch to be positioned in parallel with LED (shunting an amount of current from LED branch), leaving always a current headroom for correct operation. This



would be the antagonistic to the voltage feed LPAs shown in Figure 11, but it was left out intentionally of discussion due to LED constant voltage behavior. Thus the shunt current passing through the switch at LED nominal voltage would cause an even higher power loss and lower efficiency when compared to voltage mode.

In Table I, a comparison summary is presented among circuit classes for LED driving in main aspects.

### E. Multiple stages

A known practice on power conversion, in lighting and other applications, is the use of multiple power processing stage for good adjustment of resulting energy parameters. That allows relaxing specification of each stage and further provides degrees of freedom for the circuit designer to define components (even components reuse is possible in integrated stages)[75][76][77]. This enables the reduction of the global price or volume of the converter and may allow higher efficiency. This section describes some configurations of conversion stages that the authors found relevant and useful in the scope of VLC for data modulation concerning power conversion efficiency on LED driving. The modulator stages already presented can also be applied targeting normal power processing.

Series or parallel power processing can be performed: the first may cause lower efficiency due to double power processing and the second can present advantages in this sense. Figure 13 shows both structures. In the case of series arrangement, the whole power passing through the circuit is processed by the first stage to adjust some parameters and is also reprocessed by the following stages to fulfill specifications.

To avoid the reprocessing (targeting to reduce components stress and losses), it may be useful to reprocess only a small part of the power from former stages. That is also known as reduced redundant power processing ( $R^2P^2$ ) principle [78]. The fine adjustment of parameters can be done with a circuit parallel to the load, as depicted in Figure 13b. This circuit may have smaller components (due to reduced stress), possibly an additional power supply, and can perform with wider bandwidth to correct parameters in generated current to completely fulfill modulation purpose in VLC. That approach was

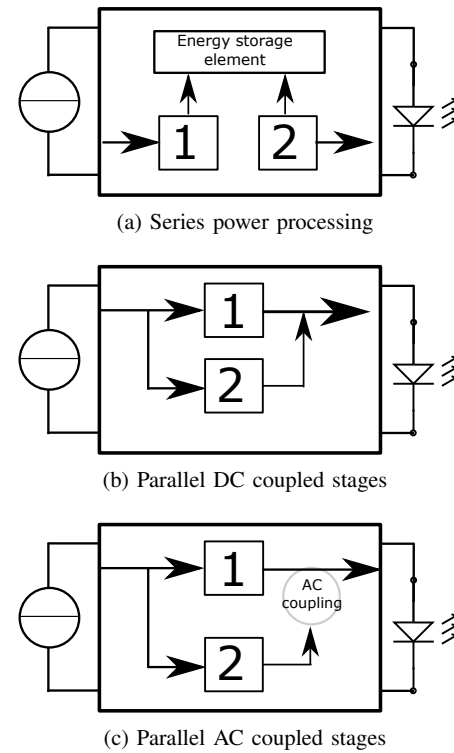


Fig. 13: Converter stage arrangements

proven to be effective by [79] using two SMPS, the efficiency of 90% was achieved in a 10 W LED load.

Parallel arrangement may either have converters DC coupled (both contribute to load DC current) or AC coupled, as depicted in Figure 13c. In this case, one of the stages (1) has full control of load average current or power while the other (2) has only AC contribution, being able to superimpose modulation or a fast varying signal to reject unwanted ripple residual of the first stage. This strategy is widely adopted in RF circuits when one pursues better efficiency in power conversion.

Recent research of [80] with same objectives, pointing solutions for better efficiency in VLC power conversion, brings a set of circuits that join parallel and series stages. Similar findings about requirements of bandwidth and components stress for each stage are also pointed out in our work, presenting more general solutions.

The following sections bring considerations about arrangements of power converters with two processing stages, and analysis are focused on better fit to VLC application.

Circuit class	Binary switching	SMPS	LPA
Power processing efficiency	High	High	Depends on the LED $R_f$ and voltage headroom
Voltage/current level adjust range	No	High	Small, compromises efficiency
LED driving method	PM or Binary, discrete steps	Any method	Any method
Spectrum efficiency	Low	Good	Best
Modulation frequency	High	Limited by converter $F_S$	High
Implementation	Simple	Requires reactive elements	May require heat sink

TABLE I: Comparison among circuit classes used as LED power modulator

1) *Binary switching and LPA*: The circuit similarity between a class A LPA and a simple binary switch modulator from voltage source (one switch) leads to the following analysis. As the same circuit can have the switch controlled in alternating periods as LPA or a binary switch better advantages of both classes can be achieved. Dimming requires minimum frequency of power signal in kHz range and data modulation can be performed in a much higher frequency, this may be one degree of freedom to be explored. This approach does not require several redundant components, but the correct definition of operation mode according to the power control and modulation requirements.

Modulation of data during on time of switch (using driving method PM) can be realized integrating binary switching and LPA. Section V-D describes this when dimming approaches. Furthermore, this allows an extra degree of freedom on the definition of P1 and D in order to maximize signal intensity during transmission, while keeping the time off just enough to ensure average light level. Figure 14 shows an example of alternated PM compared to DC, both with superimposed modulation (at higher frequency). Either of the pattern has equal average light power and AC amplitude, therefore same voltage headroom necessary to correct LPA operation. An LPA spends more energy to drive the LED with pattern modulated over DC format. On the other hand, in PM, less time slot to data modulation is available and is dependent of D (average light level is defined by DC level only).

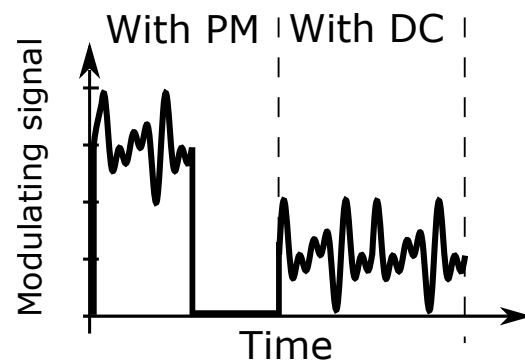


Fig. 14: PM or DC power control and simultaneous modulation superimposed.

2) *SMPS and binary switching modulator*: One major disadvantage of binary switching is exactly the leak of instantaneous voltage or current level adjustment. This will always be dependent directly on the supply, which is susceptible to LED current-to-voltage sensitivity. It great impacts in DE loss of efficacy and allows the dimming of average light level only changing D (even at no data modulation periods). The present authors suggest that integrating a SMPS regulating voltage/current level and a binary switching modulator would allow the simultaneous control of D, instantaneous voltage/current level and a gain in efficiency can be achieved. Furthermore, the binary switch modulator would reach higher modulation frequency not possible with only SMPS, while this would control average light

level only.

A previous work from [42] proved the integration concept implementing a step-down SMPS followed by a binary switch modulator. Reference [81] showed a similar approach implementing a step-down voltage converter with explicit control of dimming and data modulation with separated switches. A very similar approach that [82] implements the SMPS with an LLC resonant DC–DC converter. But we suggest that exploring further the space of possible combination of light power, D ratio controlled via SMPS output voltage level and binary switch modulator, it would be possible the maximization of AC signaling amplitude and also the minimization of DC current level at the LED to reduce DE loss (performing a dynamic choice), leading to an optimum light efficacy.

A known circuit type used in RF is an Envelope Tracking slow SMPS [83][80] that supplies the necessary voltage control according to modulated signal. It is followed by a switching or linear stage to perform base band modulation. This was proven to be more energy efficient than other solutions using only LPAs.

3) *SMPS and LPA*: The SMPS has limitations in frequency of modulation due to its operation principle and reactive elements. On the other hand, great modulation flexibility is possible in LPA application, which is similar to the RF approach extensively presented in the literature[83][84]. These authors suggest that a modulator built with a hybrid approach can be suitable to VLC application. This composition of converters, a SMPS supplying adjusted energy to an LPA, may handle better the waveform synthesis task allowing a very fast modulation as an LPA keeping a good global power efficiency comparable to SMPS.

This would handle a great range of voltage adjustment, which is not feasible with an LPA only due to efficiency compromise. Furthermore, minimizing the voltage headroom for correct operation of LPA switch, with a dynamic adjustment of provided voltage/current level to LPA, would reduce the average loss and benefit the converter efficiency. The reduction of reactive elements in SMPS and the rejection of its output inherited ripple would be another possible benefit of LPA application. Reference [32] presented a similar approach and suggested a global efficiency of 90% for LPA and 96 to 98% for SMPS can be reached considering only the losses in

the LPA during communication as originated from VLC. Otherwise, the power control of LEDs would be enabled in SMPS anyway. That is similar to the efficiency demonstrated by [80] in a 20 W LED drive with integrated VLC feature.

## VI. DISCUSSION

From the presented analysis we find relevant to highlight some aspects, specially to fill the gap between energy conversion efficiency and LED efficacy. Both have same weight on the resulting luminary lm/W efficacy, but few works found joining these approaches.

This section also brings some considerations joining knowledge from different parts of this work that the authors found relevant. Those can be contributions to define the drivers circuit more appropriated in a VLC application.

### A. Droop Effect in modulation process

Although binary switching modulation is known to be energy efficient in LED driver implementation (very simple). In case the when low duty cycle with pulse modulation (or Pa pattern) is used the Droop Effect compromises severely global efficacy for illumination purpose. The decrease of efficacy can be higher than the loss in the driver circuit. We realize that by comparing example in Section V-A(decrease of about 22.1% in efficacy) to measured loss of LED drivers reported by several references (losses around 10% or less).

On the other hand, sophisticated time domain patterns resulting from modulation, like Pc, may harm driver circuit efficiency, due to requirements applied in design. However, the resulting droop of LED efficacy is expected to be much smaller, as discussed in OFDM pattern example in Section V-A.

### B. Low data rate VLC

Current SMPS have already mature design methodologies and reach good price-to-efficiency. Indeed, they dominate LED commercial illumination devices. This type of converters may be the gateway to bring VLC to commercial applications. Only minor design changes in the circuit are needed, and good efficiency is kept. However, the limitations in driver dynamics may be the bottleneck in system bandwidth.

The LED efficacy can be a concern to this class of illumination devices. Ensuring average illumination at high efficacy levels can be accomplished by either reducing modulation index (Pb patten for example) or transmitting in short rounds (using only a small fraction of time to send data, keeping DC in rest of time). These circuits are suitable to low data rate applications, for example: indoor localization or vehicle-to-vehicle signaling.

### C. High data rate VLC

According to the presented analysis, LPA circuits are strong candidates to compose cheap and high efficient VLC modulators. Voltage headroom is a flexible parameter and its wider bandwidth is suitable for high speed communications. This class of converters is already explored in literature, but the space of solutions may allow the maximization of global energy to light efficacy on LED driving.

This work focused on circuits and LED driving from the power electronics point of view. Further exploring HF specific power circuits may provide a wider spectrum of possible solutions to VLC driving, even though the proposed classification of modulators include most of other circuits according to specific characteristics of each one.

### D. High frequency components generated by SMPS

In signal modulation using SMPS, the switching frequency components are unavoidable and cannot be completely filtered out. Those lead to higher PTA current level. However, LED transfer function can be used to impose additional attenuation to those components, due to optical or electrical domain effects, like those shown in Figure 4 inside regions B and C.

The unavoidable high frequency components can be made orthogonal to interest components. Then, they can be efficiently removed by signal processing. Orthogonality is already explored in OFDM to avoid carriers interference. However, as SMPS Fs shall be at least 5 times the frequency of the higher signal component (due to limited frequency synthesis capability of these converters), the right choice of that relationship can lead to minimum impact to signal integrity.

## VII. CONCLUSION

According to the proposed explanation to LED driving methods and review of VLC related literature, it is clear that light conversion efficacy is not a concern in most works currently available in the literature. But it is a consensus that extra energy is spent when VLC is implemented in a lighting device (driver losses and LED efficacy impact directly). Furthermore, the design of LED drivers targeting illumination is already challenging due to technology limitations and even more complex when integrating VLC feature.

The main concern, and constant focus of the present work, was the LED driving. This was thought as an easy summary of a wide literature about application of VLC in this context. But it is important to remember that the literature is much wider and solutions dealing with other aspects like minimization of capacitances, thermal management, longer life time or high power factor for LED drivers are available, and may be significant aspects to be considered in a full VLC solution.

The presented classes of converters have particular characteristics that may or not be suitable in specific VLC applications, but the integration of more conversion stages brings numerous degrees of freedom in circuit and system design. When efficiency was taken into account dealing with circuit design, we presented a couple of considerations and analyses that may provide a safe way to define system topology and initial parameters.

## REFERENCES

- [1] K. Gray, "A new way to see the light," *IEEE Industry Applications Magazine*, no. May, pp. 55–62, 2016.
- [2] I. Prepared by Navigant Consulting, "Energy Savings Forecast of Solid-State Lighting in General Illumination Applications," U.S. Department of Energy, Tech. Rep. August, 2014.
- [3] M. Scholand, "Fast Learning Curves – LED Lighting's Rapid Reduction in Price," CLASP Europe, Tech. Rep. August, 2016. [Online]. Available: <http://clasp.ngo/en/Resources/Resources/PublicationLibrary/2016/Study-retail-prices-of-LED-lamps-dropping-rapidly>
- [4] S. Shao, A. Khreishah, M. Ayyash, M. B. Rahaim, H. Elgala, V. Jungnickel, D. Schulz, and T. D. C. Little, "Design of a visible-light-communication enhanced WiFi system," *CoRR*, vol. 7, no. 10, pp. 960–973, 2015. [Online]. Available: <http://arxiv.org/abs/1503.02367>
- [5] G. Pang, T. Kwan, C.-h. Chan, H. Liu, E. Engineering, P. Road, and H. Kong, "LED Traffic Light as a Communications Device," in *Intelligent Transportation Systems, 1999*, 1999, pp. 0–5.

- [6] W. O. Popoola, "Impact of VLC on Light Emission Quality of White LEDs," *Journal of Lightwave Technology*, vol. 34, no. 10, pp. 2526–2532, 2016.
- [7] T. Borogovac, M. B. Rahaim, M. Tuganbayeva, and T. D. C. Little, "“ Lights-off ” Visible Light Communications," in *2nd IEEE Workshop on Optical Wireless Communications*, 2011, pp. 797–801.
- [8] T. C. Bui, S. Kiravittaya, N. H. Nguyen, N. T. Nguyen, and K. Spirinmanwat, "LEDs configuration method for supporting handover in visible light communication," *IEEE Region 10 Annual International Conference, Proceedings/TENCON*, vol. 2015-Janua, no. Vlc, pp. 0–5, 2015.
- [9] A. Sevincer, A. Bhattarai, M. Bilgi, M. Yuksel, and N. Pala, "LIGHTNETs: Smart lighting and mobile optical wireless networks - A survey," *IEEE Communications Surveys and Tutorials*, vol. 15, no. 4, pp. 1620–1641, 2013.
- [10] A. Tsiatmas, C. P. M. J. Baggen, F. M. J. Willems, J. P. M. G. Linnartz, and J. W. M. Bergmans, "An illumination perspective on visible light communications," *IEEE Communications Magazine*, vol. 52, no. 7, pp. 64–71, 2014.
- [11] J. Gancarz, H. Elgala, and T. D. C. Little, "Impact of lighting requirements on VLC systems," *IEEE Communications Magazine*, vol. 51, no. 12, pp. 34–41, 2013.
- [12] ENERGY STAR, "ENERGY STAR ® Program Requirements for Computers Partner Commitments," p. 35, 2016. [Online]. Available: <https://www.energystar.gov/sites/default/files/specs/Version61ComputersFinalProgramRequirements.pdf>
- [13] S. Harnilovic, "Wireless optical communication systems," *PhD Proposal*, 2005.
- [14] ANSI, "American National Standard for Safe Use of Lasers," American National Standards Institute, Tech. Rep., 2014.
- [15] L. Wu, Z. Zhang, J. Dang, and H. Liu, "Adaptive modulation schemes for visible light communications," *Journal of Lightwave Technology*, vol. 33, no. 1, pp. 117–125, 2015.
- [16] B. Merkmale, "OSRAM OSTAR Projection Compact Datasheet Version 2 . 1 ( not for new design ) LE ATB N7WM window on top , RoHS compliant Features technology with glass window on top Besondere Merkmale • Gehäusetyp : Kompakte Lichtquelle in SMT Technologie mit Glasabdecku," OSRAM, Tech. Rep., 2015.
- [17] Bridgelux, "Bridgelux Vero 18 array series," Bridgelux, Tech. Rep., 2013. [Online]. Available: <https://www.bridgelux.com/resources/ds32-bridgelux-vero-18-data-sheet-gen-6>
- [18] J. Kosman, O. Almer, A. V. N. Jalajakumari, S. Videv, and H. Haas, "60 Mb / s , 2 meters Visible Light Communications in 1 klx Ambient using an Unlensed CMOS SPAD Receiver," *Photonics Society Summer Topical Meeting Series (SUM)*, 2016 *IEEE*, vol. 1, pp. 171–172, 2016.
- [19] IEEE Computer Society, "IEEE Standard for Local and metropolitan area networks - Part 15.7: Short-Range Wireless Optical Communication Using Visible Light," *IEEE Std 802.15.7-2011*, vol. 1, no. September, pp. 1–286, 2011.
- [20] U. D. of Energy, "Multi-Year Program Plan," U.S. Department of Energy, Tech. Rep. April, 2014.
- [21] K. H. Loo, Y. M. Lai, S. C. Tan, and C. K. Tse, "On the color stability of phosphor-converted white LEDs under DC, PWM, and bilevel drive," *IEEE Transactions on Power Electronics*, vol. 27, no. 2, pp. 974–984, 2012.
- [22] B. Maury, W. Editor, L. Magazine, T. California, and E. Commission, "California tightens color performance of LED based lamps," pp. 2–4, 2016.
- [23] A.-E. Marcu, R.-A. Dobre, and M. Vlădescu, "Investigation on Available Bandwidth in Visible- Light Communications," 2016.
- [24] I. Orion Energy Systems, "ISON™ HIGH BAY," 2017. [Online]. Available: <http://files.orionlighting.com/resources/PRODUCT/ISON/datasheets/170124{ }ISONHighBay{ }HBIF3.pdf>
- [25] S. Li, S. C. Tan, C. K. Lee, E. Waffenschmidt, S. Y. R. Hui, and C. K. Tse, "A Survey, Classification, and Critical Review of Light-Emitting Diode Drivers," *IEEE Transactions on Power Electronics*, vol. 31, no. 2, pp. 1503–1516, 2016.
- [26] IEEE Power Electronics Society, "IEEE Recommended Practices for Modulating Current in High-Brightness LEDs for Mitigating Health Risks to Viewers," *IEEE Std 1789-2015*, pp. 1–80, 2015.
- [27] S. M. Berman, D. S. GreenHouse, R. D. Clear, and W. R. Thomas, "Human electroretinogram responses to video displays, fluorescent lighting, and other high frequency sources," *Optometry and Vision Science*, vol. 68, pp. 645–662, 1991.
- [28] N. F. Gardner, G. O. Müller, Y. C. Shen, G. Chen, S. Watanabe, W. Götz, and M. R. Krames, "Blue-emitting InGaN-GaN double-heterostructure light-emitting diodes reaching maximum quantum efficiency above 200 A cm<sup>2</sup>," *Applied Physics Letters*, vol. 91, no. 24, pp. 12–15, 2007.
- [29] J. Iveland, L. Martinelli, J. Peretti, J. S. Speck, and C. Weisbuch, "Direct measurement of auger electrons emitted from a semiconductor light-emitting diode under electrical injection: Identification of the dominant mechanism for efficiency droop," *Physical Review Letters*, vol. 110, no. 17, pp. 1–5, 2013.
- [30] W. K. Lun, K. H. Loo, S. C. Tan, Y. M. Lai, and C. K. Tse, "Bilevel current driving technique for LEDs," *IEEE Transactions on Power Electronics*, vol. 24, no. 12, pp. 2920–2932, 2009.
- [31] S.-c. Tan, "General n -Level Driving Approach for Improving of Fast-Response Saturable Lighting Devices," *IEEE Transactions on Industrial Electronics*, vol. 57, no. 4, pp. 1342–1353, 2010.
- [32] A. Tsiatmas, F. M. J. Willems, J. P. M. G. Linnartz, S. Baggen, and J. W. M. Bergmans, "Joint illumination and visible-Light Communication systems: Data rates and extra power consumption," *2015 IEEE International Conference on Communication Workshop, ICCW 2015*, pp. 1380–1386, 2015.
- [33] G. Keiser, *Optical Fiber Communications*, 3rd ed. McGraw-Hill, 2000.
- [34] Y.-C. Chi, D.-H. Hsieh, C.-Y. Lin, H.-Y. Chen, C.-Y. Huang, J.-H. He, B. Ooi, S. P. DenBaars, S. Nakamura, H.-C. Kuo, and G.-R. Lin, "Phosphorous Diffuser Diverged Blue Laser Diode for Indoor Lighting and Communication," *Scientific Reports*, vol. 5, no. 1, p. 18690, 2016. [Online]. Available: <http://www.nature.com/articles/srep18690>
- [35] J. Grubor, S. Randel, K.-d. Langer, and J. W. Walewski, "Broadband Information Broadcasting Using LED-Based Interior Lighting," *Journal of Lightwave Technology*, vol. 26, no. 24, pp. 3883–3892, 2008.
- [36] R. H. Saul, T. P. Lee, and C. A. Burrus, "Light-Emitting-Diode Device Design," in *Semiconductors and Semimetals*, 1985, vol. 22, pp. 193–237.
- [37] E. F. Schubert, *Light-Emitting Diodes*. Cambridge, 2006.
- [38] R. Windisch, A. Knobloch, M. Kuijk, C. Rooman, B. Dutta, P. Kiesel, G. Borghs, G. H. D?hler, and P. Heremans, "Large-signal-modulation of high-efficiency light-emitting diodes for

- optical communication," *IEEE Journal of Quantum Electronics*, vol. 36, no. 12, pp. 1445–1453, 2000.
- [39] Z. Ghassemlooy, W. Popoola, and S. Rajbhandari, *Optical wireless communications: system and channel modelling with Matlab®*. CRC Press, 2012. [Online]. Available: <https://goo.gl/5o47ii>
- [40] T. P. Lee, "Effect of Junction Capacitance on the Rise Time of LEDs and on the Turn-on Delay of Injection Lasers," *Bell System Technical Journal*, vol. 54, no. 1, pp. 53–68, 1975.
- [41] Y. Pei, S. Zhu, H. Yang, L. Zhao, X. Yi, J. Wang, and J. Li, "LED Modulation Characteristics in a Visible-Light Communication System \*," *Optics and Photonics Journal*, vol. 2013, no. 2011, pp. 139–142, 2013.
- [42] K. Modepalli and L. Parsa, "Dual-purpose offline LED driver for illumination and visible light communication," *IEEE Transactions on Industry Applications*, vol. 51, no. 1, pp. 406–419, 2015.
- [43] J. Vucic, C. Kottke, S. Nerreter, K. D. Langer, and J. W. Walewski, "513 Mbit/s visible light communications link based on DMT-modulation of a white LED," *Journal of Lightwave Technology*, vol. 28, no. 24, pp. 3512–3518, 2010.
- [44] J. J. D. McKendry, D. Massoubre, S. Zhang, B. R. Rae, R. P. Green, E. Gu, R. K. Henderson, A. E. Kelly, and M. D. Dawson, "Visible-Light Communications Using a CMOS-Controlled Micro-Light-Emitting-Diode Array," *Journal of Lightwave Technology*, vol. 30, no. 1, pp. 61–67, 2012. [Online]. Available: <http://ieeexplore.ieee.org/lpdocs/epic03/wrapper.htm?arnumber=6072221>
- [45] J. Jacobs, D. Hente, and E. Waffenschmidt, "Drivers for OLEDs," *Conference Record - IAS Annual Meeting (IEEE Industry Applications Society)*, pp. 1147–1152, 2007.
- [46] V. C. Bender, T. B. Marchesan, and J. M. Alonso, "Solid-State Lighting: A Concise Review of the State of the Art on LED and OLED Modeling," *IEEE Industrial Electronics Magazine*, vol. 9, no. 2, pp. 6–16, 2015.
- [47] R.-L. Lin, J.-Y. Tsai, D. Buso, and G. Zissis, "OLED Equivalent Circuit Model With Temperature Coefficient and Intrinsic Capacitor," *IEEE Transactions on Industry Applications*, vol. 52, no. 1, pp. 493–501, 2016. [Online]. Available: <http://ieeexplore.ieee.org/document/7175001/>
- [48] I. H. Campbell, D. L. Smith, and J. P. Ferraris, "Electrical impedance measurements of polymer light-emitting diodes," *Applied Physics Letters*, vol. 66, no. 22, pp. 3030–3032, 1995.
- [49] D. Buso, S. Bhosle, Y. Liu, M. Ternisien, C. Renaud, and Y. Chen, "OLED electrical equivalent device for driver topology design," *IEEE Transactions on Industry Applications*, vol. 50, no. 2, pp. 1459–1468, 2014.
- [50] V. Shrotriya and Y. Yang, "Capacitance-voltage characterization of polymer light-emitting diodes," *Journal of Applied Physics*, vol. 97, no. 5, 2005.
- [51] T. Kishi, H. Tanaka, Y. Umeda, and O. Takyu, "A high-speed LED driver that sweeps out the remaining carriers for visible light communications," *Journal of Lightwave Technology*, vol. 32, no. 2, pp. 239–249, 2014.
- [52] R.-l. Lin and G. Zissis, "Bidirectional OLED Buck Driver Jhong-Yan Tsai David Buso," in *IEEE Industry Applications Society Annual Meeting*, no. Ccm, 2015, pp. 1–10.
- [53] J. Vucic, C. Kottke, S. Nerreter, K. Habel, a. Buttner, K.-D. Langer, and J. Walewski, "125 Mbit/s over 5 m wireless distance by use of OOK-Modulated phosphorescent white LEDs," *2009 35th European Conference on Optical Communication*, no. 1, pp. 9–10, 2009.
- [54] N. Fujimoto and H. Mochizuki, "477 Mbit/s visible light transmission based on OOK-NRZ modulation using a single commercially available visible LED and a practical LED driver with a pre-emphasis circuit," *Optical Fiber Communication Conference and Exposition and the National Fiber Optic Engineers Conference (OFC/NFOEC)*, 2013, pp. 1–3, 2013. [Online]. Available: <http://www.opticsinfobase.org/abstract.cfm?URI=NFOEC-2013-JTh2A.73>
- [55] X. Chen, H. Li, C. Min, and H. Chen, "Real Time Transmission Technology of 610Mbps Visible Light Communication Utilizing Phosphor-based LED," pp. 7–9, 2017.
- [56] T. Fath, C. Heller, and H. Haas, "Power Level Stepping," *Journal of Lightwave*, vol. 31, no. 11, pp. 1734–1743, 2013.
- [57] J. Du, W. Xu, H. Zhang, and C. Zhao, "Visible Light Communications Using Spatial Summing PAM with LED Array," *IEEE Wireless Communications and Networking Conference*, 2017.
- [58] X. Qu, S. C. Wong, and C. K. Tse, "A current balancing scheme with high luminous efficacy for high-power LED lighting," *IEEE Transactions on Power Electronics*, vol. 29, no. 6, pp. 2649–2654, 2014.
- [59] D. Gacio, "Study on Passive Self-equalization of Parallel-connected LED Strings," *IEEE Transactions on Industry Applications*, 2013.
- [60] M. Shi, C. Wang, H. Guo, Y. Wang, X. Li, and N. Chi, "A High-Speed Visible Light Communication System based on DFT-S OFDM," *IEEE International Conference on Communication Systems*, no. 2015, pp. 0–4, 2016.
- [61] S. Han and J. Lee, "An overview of peak-to-average power ratio reduction techniques for multicarrier transmission," *Wireless Communications, IEEE*, no. April, pp. 56–65, 2005. [Online]. Available: [http://ieeexplore.ieee.org/xpls/abs/\\_all.jsp?arnumber=1421929](http://ieeexplore.ieee.org/xpls/abs/_all.jsp?arnumber=1421929)
- [62] J. Armstrong and A. Lowery, "Power efficient optical OFDM," *Electronics Letters*, vol. 42, no. 6, 2006.
- [63] H. Zhang, Y. Yuan, and W. Xu, "PAPR Reduction for DCO-OFDM Visible Light Communications via Semidefinite Relaxation," *IEEE Photonics Technology Letters*, vol. 26, no. 17, pp. 1718–1721, 2014.
- [64] M. S. A. Mossaad, S. Hranilovic, and L. Lampe, "Visible Light Communications Using OFDM and Multiple LEDs," *IEEE Trans. Commun.*, vol. 63, no. 11, pp. 4304–4313, 2015.
- [65] A. Jovicic, J. Li, and T. Richardson, "Visible light communication: Opportunities, challenges and the path to market," *IEEE Communications Magazine*, vol. 51, no. 12, pp. 26–32, 2013.
- [66] F. Loose, R. R. Duarte, C. H. Barriquello, M. A. D. Costa, L. Teixeira, and A. Campos, "0 Ripple-based Visible Light Communication Technique for Switched LED Drivers." Cincinnati: IEEE Industry Applications Society, 2017.
- [67] J. Rodriguez, D. G. Lamar, J. Sebastian, and P. F. Miaja, "Taking Advantage of the Output Voltage Ripple of a Two-Phase Buck Converter to Perform Quadrature Amplitude Modulation for Visible Light Communication," *2017 IEEE Applied Power Electronics Conference and Exposition (APEC)*, no. Vlc, pp. 2116–2123, 2017.
- [68] X. Deng, J. P. M. G. Linnartz, K. Arulandu, G. Zhou, and Y. Wu, "Effect of buck driver ripple on BER performance in visible light communication using LED," *2015 IEEE International Conference on Communication Workshop, ICCW 2015*, no. 2, pp. 1368–1373, 2015.
- [69] X. Deng, Y. Wu, K. Arulandu, G. Zhou, and J.-p. M. G. Linnartz, "Performance comparison for illumination and

- visible light communication system using buck converters,” *2014 IEEE Globecom Workshops (GC Wkshps)*, pp. 547–552, 2014. [Online]. Available: <http://ieeexplore.ieee.org/lpdocs/epic03/wrapper.htm?arnumber=7063489>
- [70] C. Basso, “The Right Half Plane Zero, a Two-Way Control Path,” 2008.
- [71] J.-p. M. G. Linnartz, “Wireless optical communication in illumination systems,” in *2016 IEEE Photonics Society Summer Topical Meeting Series (SUM)*, vol. 1. IEEE, jul 2016, pp. 104–107. [Online]. Available: <http://ieeexplore.ieee.org/lpdocs/epic03/wrapper.htm?arnumber=7548764>
- [72] B. Hussain, F. Che, F. Zhang, T. S. Yim, L. Cheng, W.-h. Ki, C. P. Yue, and L. Wu, “A Fully Integrated IEEE 802 . 15 . 7 Visible Light Communication Transmitter with On-Chip 8-W 85 % Efficiency Boost LED Driver C216 C217,” in *2015 Symposium on VLSI Circuits Digest of Technical Papers*, 2015, pp. 216–217.
- [73] S. Zhao, “A Dimmable LED Driver For Visible Light Communication based on the LLC Resonant Converter,” *2013 Twenty-Eighth Annual IEEE Applied Power Electronics Conference and Exposition*, no. VIc, 2013.
- [74] A. Jovicic, J. Li, and T. Richardson, “Visible light communication: Opportunities, challenges and the path to market,” *IEEE Communications Magazine*, vol. 51, no. 12, pp. 26–32, 2013.
- [75] G. G. Pereira, M. A. Dalla Costa, J. M. Alonso, M. F. De Melo, and C. H. Barriquello, “LED Driver Based on Input Current Shaper Without Electrolytic Capacitor,” *IEEE Transactions on Industrial Electronics*, vol. 64, no. 6, pp. 4520–4529, 2017.
- [76] P. S. Almeida, H. A. C. Braga, M. A. Dalla Costa, and J. M. Alonso, “Offline soft-switched LED driver based on an integrated bridgeless boost-asymmetrical half-bridge converter,” *IEEE Transactions on Industry Applications*, vol. 51, no. 1, pp. 761–769, 2015.
- [77] P. S. Almeida, D. Camponogara, H. A. Braga, M. A. Dalla Costa, and J. M. Alonso, “Matching LED and Driver Life Spans: A Review of Different Techniques,” *IEEE Industrial Electronics Magazine*, vol. 9, no. 2, pp. 36–47, 2015.
- [78] D. Camponogara, G. F. Ferreira, A. Campos, M. A. Dalla Costa, and J. Garcia, “Offline LED driver for street lighting with an optimized cascade structure,” *IEEE Transactions on Industry Applications*, vol. 49, no. 6, pp. 2437–2443, 2013.
- [79] J. Rodriguez, D. G. Aller, D. G. Lamar, and J. Sebastian, “Energy Efficient Visible Light Communication Transmitter Based on the Split of the Power,” pp. 2420–2427, 2017.
- [80] J. Sebastian, D. Aller, J. Rodriguez, D. Lamar, and P. Miaja, “On the role of the power electronics on visible light communication,” *Conference Proceedings - IEEE Applied Power Electronics Conference and Exposition - APEC*, pp. 2420–2427, 2017.
- [81] A. Mirvakili and V. J. Koomson, “High efficiency LED driver design for concurrent data transmission and PWM dimming control for indoor visible light communication,” *2012 IEEE Photonics Society Summer Topical Meeting Series, PSST 2012*, vol. 2, pp. 132–133, 2012.
- [82] S. Zhao, J. Xu, and O. Trescases, “Burst-mode resonant LLC converter for an LED luminaire with integrated visible light communication for smart buildings,” *IEEE Transactions on Power Electronics*, vol. 29, no. 8, pp. 4392–4402, 2014.
- [83] F. H. Raab, P. Asbeck, S. Cripps, P. B. Kenington, Z. B. Popovic, N. Potheary, J. F. Sevic, and N. O. Sokal, “Power amplifiers and transmitters for RF and microwave,” *IEEE Transactions on Microwave Theory and Techniques*, vol. 50, no. 3, pp. 814–826, 2002.
- [84] R. C. Beltrame, M. L. da Silva Martins, C. Rech, and H. L. Hey, “Hybrid power amplifiers - a review,” *XI Brazilian Power Electronics Conference*, pp. 189–195, 2011.

### **3 MANUSCRIPT 2 - A REVIEW OF VISIBLE LIGHT COMMUNICATION LED DRIVERS**



# A Review of Visible Light Communication LED Drivers

L. Teixeira, F. Loose, J. M. Alonso,

C. H. Barriquello, V. Alfonso Reguera, and M. A. Dalla Costa

## Abstract

Visible light communication (VLC) has been a research trend topic for nearly the last ten years. Some recent studies have highlighted the energy-communication trade-off that a VLC LED driver must face in order to assure good energy efficiency and suitable information transmission to keep the status of a *green technology*. Besides the limitations of the current LED technology, the selection and design of the energy processing and modulation stage pose a major challenge to the implementation of these systems. This paper presents a survey of VLC LED drivers by making a classification of the most relevant published research existing in the literature from 2006 to 2019, including a detailed analysis of most relevant implementation aspects. Among the different modulation schemes reviewed in this paper, it was found that binary modulation schemes are the most common ones employed in these systems. Additionally, switching converters stand out among the different converter topologies because they can provide a good overall efficiency at high power levels, even though they cannot achieve as high data rate as VLC drivers based on linear mode modulator.

## Index Terms

Visible light communication (VLC), LED Drivers, Efficiency, Illumination, Data Rate, Digital Communication.

## I. INTRODUCTION

Visible light communication (VLC) can be considered as a green technology [1] because it can save energy by using the light for both lighting and communication purposes. To achieve this goal, it must be assured that the communication functionality does not significantly degrade the system efficacy compared to conventional LED luminaries. Energy focused solutions that simultaneously address illumination aspects and communication concerns are called VLC LED drivers [2]. The LED efficacy under VLC modulation and the selected electronic driver circuitry are critical aspects for the system global efficiency [3], [4] .

A great number of different approaches of VLC LED drivers have been presented in the literature, which will be reviewed and classified in this paper. Previous works have only presented short reviews or summaries of solutions for VLC drivers. For example, smart solutions were reviewed in [1], [5]–[10]. However, neither of these papers presented a comprehensive classification of the existing literature. There are several investigation approaches that concern the implementation of a VLC LED driver, Fig. 1a systematises research in four distinct wide areas, namely: i) channel and applications [48], [49], ii) codes and methods [50], iii) communication stack and integration [51]–[53], and iv) hardware and methods. Among these, the hardware and methods concern circuits, physical devices and its technologies. In this context, this paper aims at reviewing the current solutions for energy conversion and data transmission in VLC applications.

The features concerning energy conversion and data transmission in a VLC LED driver are in the physical layer in a communication stack using visible light as the media, these relations are systematised in Fig. 1b. The implementation of light modulation depends on the LED current control capability. Hence, in the figure, this function can be seen in the data transmission path in which the studied circuits perform current modulation. This study includes also a general view of the most relevant types of LED drivers used as power converters and as modulators. The main focus is on organizing the available information to guide future works, identifying opportunities

and exposing advantages and limitations of the presented solutions.

The references included in this survey were selected according to the following criteria:

1) *Inclusion Criteria*: Published works aiming at VLC applications that present circuits or test electronic drivers in which the modulator type was clearly specified [2], [3], [5], [6], [8]–[47].

2) *Exclusion Criteria*: i) References focused only on LED characterization [54]–[59], VLC channel analysis [48], [60]–[66], receiver design [67]–[72] or modulation schemes [50], [71], [73]–[77], without driver specification, and ii) proposed topologies without mathematical support or without simulation or experimental results.

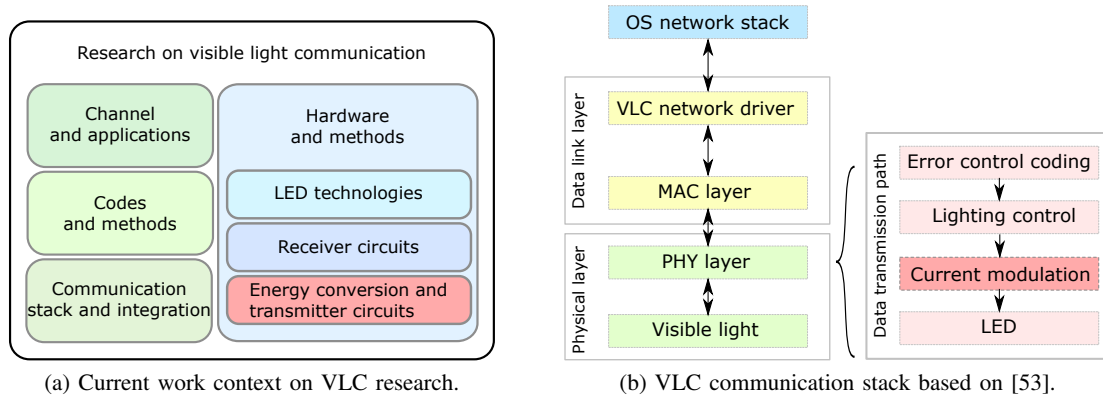


Fig. 1. Research context and application in a communication stack.

There are some previous papers in the literature that have presented short reviews and summaries about VLC LED drivers. In [1] two approaches for high efficient VLC drivers are highlighted: i) narrowband modulation, in the range of tens of kHz, applied to switching power converters, which is costless in terms of component count, but only suitable for data rates of hundreds of kbps, ii) wide band modulation, in the range of several MHz, which is costly due to the necessity of additional circuitry, but which can achieve data rates of tens of Mbps. In [5], 11 implementation methods for modulation bandwidth (BW) improvement for LED drivers are compared. Even though not all of them aim at VLC applications, the strategies which can be highlighted are carrier sweep out, pre-equalization, and post-equalization. Contemporaneously,

[6] compares two different strategies applied to a buck converter used as an LED driver: average current control and binary current shunting. The paper concludes that the former strategy is preferable from the efficiency point-of-view. Additionally, [7] presents a short introduction concerning the ac-dc stage and current regulation roles in VLC LED drivers.

A more recently published paper [8] presents an extensive review of possible solutions for VLC drivers, most of them based on the split of the power, or on hybrid topologies using both linear and switching converters. In [10], [37] several solutions based on the split of the power are presented, which use two circuits in order to achieve a wide modulation BW while keeping good energy efficiency. For this purpose, the two converters are connected so that each of them provides a part of the output voltage. Another reference introduces 4 solutions to implement a full ac-dc VLC LED driver [9]: i) average current control, ii) LED series switch, iii) constant dc bias plus ac-coupled power amplifier, and iv) a novel inductorless topology, which is the solution proposed in the paper. Finally, another review on VLC drivers is presented in [39]. However, the main focus of this paper is on losses evaluation of series and linear modulators operating under different modulation strategies.

This is an improved version of a previous work [78] in which new information related to modulation schemes, circuit topologies, full converter drivers, application specific integrated circuits, modulation factor and modulation amplitude have been included. Furthermore, this survey was updated with the most recently published works.

This work is organized as follows. First, an overview of modulation strategies commonly used for VLC is presented in Section II. Second, the structure of a VLC LED driver is presented in Section III. Third, the proposed topology classification is described in Section IV. Fourth, the state of the art of VLC LED drivers including the most relevant performance figures is presented in Section V. Finally, Section VI summarizes the conclusions of this review.

## II. MODULATION STRATEGIES FOR VLC APPLICATIONS

In a VLC application, the communication signal is carried by the LED irradiated light. It is unipolar because the light is modulated in intensity, therefore the common passband modulation schemes can only be used with a superimposed dc level. Most literature assumes that the light intensity of an LED is proportional to its current, both of them keeping the same waveform because of the quasi-linear relationship between them [79]. For VLC, the average light level is used to provide the visual perception, in which the communication signal must not take part. For this purpose, the communication signal must be allocated in a band free of harmful flicker effects, known as flicker-safe band [80], [81]. In this review, from a communication perspective, bandwidth, bit load (number of bits transmitted per symbol) and spectral efficiency will be addressed. The selection of the modulation strategy represents a very important aspect of the VLC system since it defines the features and possible topologies of the modulator. Fig. 2 illustrates the waveforms of the most common VLC modulation schemes, which can be classified as follows:

1) *Baseband Modulation*: it is based on using predefined sets of pulse shapes, usually rectangular pulses, which are also known as line codes. Examples include binary pulse modulation schemes as on-off keying (OOK), variable pulse-position modulation (VPPM), 2-level pulse amplitude modulation (PAM), and multiple level PAM, as for example 4-level PAM and 8-level PAM. Manchester is a line code that in VLC has no components at low frequencies other than the dc; it ensures no flicker if a high enough carrier frequency is thus selected. However, the other line codes, since the corresponding spectrum of the signal is dependent on the pulse harmonic components and symbol change rate, cannot ensure a flicker-safe communication in VLC. Hence, to avoid harmful flicker, an encoding method before the line code generation must be implemented, e. g., 4B6B, 8B10B or other run-length limited codes [50]. Other strategies to compensate the average light level and avoid flicker can be implemented in the time interval

between frames (inter-frame) [82]. However, these line codes and inter-frame strategies also affect the bandwidth to data rate trade-off, harming the overall communication performance.

2) *Passband Modulation*: this modulation scheme is generated by shifting the frequency of a baseband signal into a higher band. In VLC, common passband schemes shall be modified for unipolar signaling or shall be biased with enough dc level to avoid negative signal value. One or more carriers can be used in the modulated signal, known as single carrier modulation scheme (SCM) or multiple carrier modulation scheme (MCM), respectively. Examples of SCM are phase-shift keying (PSK), frequency-shift keying (FSK) and quadrature amplitude modulation (QAM). Examples of MCM are discrete multitone (DMT) and orthogonal frequency-division multiplexing (OFDM). Several different OFDM schemes are used in VLC because of the non-negative signal restriction, for example, Direct Current-Offset OFDM (DCO-OFDM) [83], Asymmetrically Clipped Optical OFDM (ACO-OFDM) [84], Flip-OFDM [85] and Unipolar OFDM (U-OFDM) [86].

Binary pulse modulation schemes can be implemented by simply interrupting or shunting the LED current. They produce baseband signals, which can be generated by very simple circuits. Therefore, their frequency spectrum includes less signal power inside the essential bandwidth when compared to other more complex modulation schemes. Particularly, phosphor-covered white LEDs exhibit a characteristic cutoff frequency around 3 MHz, which limits signal bandwidth and data rate in VLC applications [11] if no equalization or pre-emphasis is applied. In this sense, modulation schemes with a narrower spectral power distribution take more advantage of this technology.

In Fig. 2, the prefix of the modulation names ( $M$ ) represents the number of the different symbols provided by the scheme. Therefore, the bit load of this modulation can be calculated as  $\log_2(M)$  bit/symbol. Another important parameter is the modulation spectral efficiency, measured in bps/Hz, which is defined as the quotient between the modulation data rate and its bandwidth.

Further VLC modulation schemes, including dimming strategies and other multi-carrier modulation schemes can be found in [49], [50], [87].

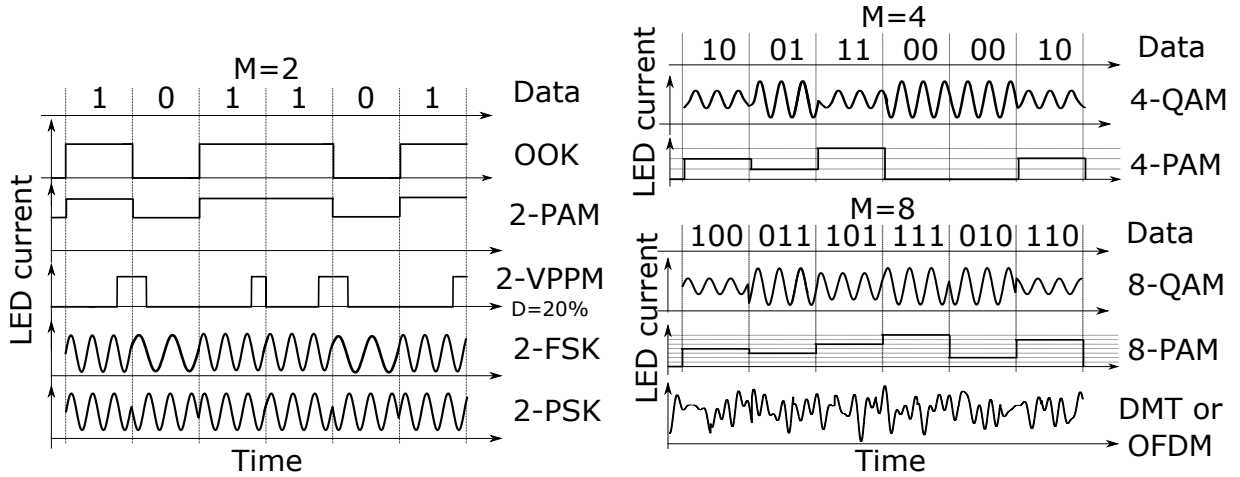


Fig. 2. VLC modulation waveforms.

The modulation factor ( $\gamma$ ) is used in order to compare the solutions of the literature considering the LED current modulation capability. In this case, the LED ac rms current ( $i_{LED\_rms}^{AC}$ ), that is equal to the current standard deviation for a great number of samples, is used to represent the amplitude of the communication signal in a more general fashion than only peak or peak-to-peak measurement. Therefore, using the average LED current ( $I_{LED}$ ), the modulation factor is calculated according to  $\gamma = i_{LED\_rms}^{AC}/I_{LED}$  for all the modulation schemes. Because the light is considered reasonably proportional to LED current, the modulation factor is the ratio between useful communication signal intensity and average light irradiated by an LED used for VLC.

The analysis using the modulation factor allows for a fair comparison among the communication capability of the published works focusing on the signal amplitude owing to its simplicity, although aspects like LED impedance and average output power are not considered. Also, this performance can be extrapolated to estimate the possible operating distance through channel models [48] and the achievable data rate through specific modulation models [88], [89].

### III. VLC DRIVER STRUCTURE

The block diagram of a VLC LED driver is illustrated in Fig. 3. As can be seen, it is made up by the three following stages:

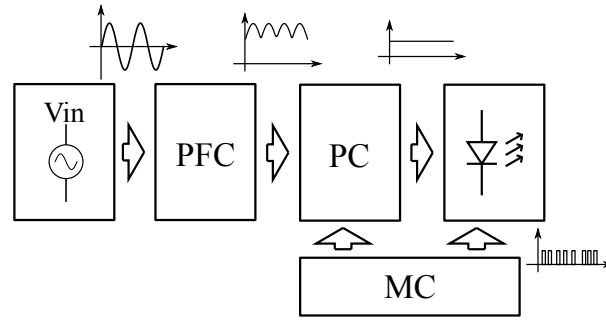


Fig. 3. VLC LED driver structure.

1) *Power Factor Correction (PFC) Stage*: This first block rectifies the ac grid voltage while assuring a low distortion of the current drained from the grid in order to satisfy energy quality standards. This requirement is very restrictive in illumination devices with power above 5 W [90], [91].

2) *Power Control (PC)*: This block is used to generate a regulated dc voltage or current to supply the LED at its nominal operating point. Moreover, dimming may be accomplished by this block. This converter must be able to regulate the output voltage of the PFC stage, filtering any residual low frequency ripple.

3) *Modulator for Communication (MC)*: This is the extra block that adds the VLC functionality to a conventional LED driver. It is dedicated to generate the VLC LED stimuli, which can be obtained by a voltage or current shaping process. The circuit topology of this block is defined according to the type of modulation and bandwidth requirements, among other aspects like cost, circuit complexity, efficiency, etc.

However, not all these blocks are required in every VLC system. For example, a battery-operated LED driver will omit the PFC stage. Likewise, the separation among circuit blocks



is not mandatory, e.g. integrated power stages may perform two functions simultaneously in a single stage [92].

The following solutions can be found in the literature: i) full converter (FC), which is the solution including all features corresponding to the three power processing blocks, as illustrated in Fig. 3, ii) dc-supplied converter (DCS), which includes only the PC and MC stages, iii) simple modulator (SM) driver, which implements only the MC stage.

FCs are very relevant in VLC applications because they include all stages to supply the LED from the ac grid, which usually ranges from 85 to 240  $V_{\text{rms}}$ . They can be applied as stand-alone solutions powered from the mains. Moreover, due to the requirements of the drivers, additional complexity and lower efficacy compared to DCS or SM are to be expected. Therefore, because of their relevance, FCs will be more specifically addressed in Section V-G.

Finally, each of the VLC driver building blocks shown in this section can be implemented using a wide sort of different circuit topologies. Next section presents the proposed classification of these circuit topologies.

#### IV. MODULATOR TYPES

In this section, a classification of the different modulators is presented. This classification will be used in Section V to sort the works published in the literature and to explore their most relevant features. Four types of circuits are defined according to their operating principles:

##### A. *Linear Mode Modulator (LMM)*

These topologies are based on transistors operating within their linear region. Common types are class A, B, AB and C amplifiers [93]. Particularly, class C amplifiers can also be used as narrowband amplifiers. Thus, they operate based on a dissipative principle because there is a considerable voltage across the transistors power terminals simultaneously to the main current flow in order to keep the expected operating point. Therefore, the energy efficiency of this class

of modulator is usually lower than the efficiency achieved by other modulator types. This type of circuit is also used as radio frequency (RF) amplifiers in wide bandwidth applications.

### B. Switching Mode Modulator (SMM)

These converters are based on transistors operating in saturation or cut-off regions to generate a square waveform that is afterward applied to an LC band-pass filter [93] or low-pass filter [94]. The band-pass-filter based modulators, class C circuits for example, are mostly employed as modulator in radio frequency communications owing to their high energy efficiency. However, those are not common in VLC applications because the LED requires a constant bias current. In this sense, the low-pass filter-based modulator fits better for this application because it provides the constant bias current together with the current modulation capability. The low-pass-filter based modulator is designed so that it allows the communication signal to be applied to the LED while attenuating the higher switching frequency harmonics. Its operating principle provides higher efficiency because both conduction and switching losses are low.

The switching frequency ( $F_S$ ), together with the amount of ripple allowed in the output current, defines the filter characteristics. Usually, most common filter choices are first [30] or second-order [2], but higher orders are also possible by increasing the number of passive elements [10]. Thus, the choice of  $F_S$  directly affects the filter passband bandwidth while the dc level is employed to provide the average illumination. SMMs can be operated in two different ways:

1) *Average Current Control*: It consists of shaping the LED average current by modulating the duty cycle ( $D$ ) [6], [8], [24], [38] to track a low-frequency reference whose harmonic content remains within the filter passband.

2) *Ripple Modulation (RM)*: It takes advantage of the converter inherent residual frequency content that remains after filtering [2], [18], [36], [41], [47]. This can be implemented either by controlling the frequency [18] or the phase ( $\phi$ ) [2], [36], [41], [47] of the switching signal according to the information to be transmitted. Hence, this scheme allows the signal band to

exceed the filter bandwidth. However, in this case, the resulting signal shape is directly dependent on the filter parameters.

### *C. Series Switch Modulator (SSM)*

This modulator is based on turning on and off the LED by using a series switch. This circuit cannot control the instantaneous current level, which is generated by the previous dc-dc conversion stage. As an actuator, a single transistor, e.g. a BJT or MOSFET, is usually employed. This type of modulator differs from LMM in that there is no transistor bias current to operate the transistor in linear region. On the contrary, the transistor is operated in cut-off and saturation regions, as an open and closed switch respectively. Therefore, this circuit is only able to generate rectangular pulses, which reduces the possible signal modulation space. An alternative implementation of this circuit consists of using one additional switch to sweep out the remaining electrical carriers from the LED P-N junction during the turn-off process. This decreases the turn-off time and helps in enlarging the modulation bandwidth [5], [16].

### *D. Parallel Switch Modulator (PSM)*

This modulator is based on supplying the LED by a constant current source, which can be shunted by a switch connected in parallel with the LED. When the switch is turned on, the current through the LED is interrupted. Therefore, it can reproduce binary pulse modulation schemes that require only on and off levels. Therefore, similar modulation schemes as in the case of the SSM can be implemented. However, this solution presents lower efficiency due to the power losses in the switch during shunting [6].

### *E. Possible modulation schemes*

The previously presented modulator types have specific limitations regarding the modulation schemes that can be generated. Table I depicts the modulator types with the corresponding possible modulation schemes.

TABLE I  
MODULATOR TYPES WITH POSSIBLE MODULATION SCHEMES.

Modulator type	Modulation scheme			
	Baseband		Passband	
	Binary pulse based <sup>a</sup>	Multiple-level pulse based <sup>b</sup>	Single carrier <sup>c</sup>	Multiple carrier <sup>d</sup>
LMM	X	X	X	X
SMM	X	X	X	X
SSM	X <sup>e</sup>			
PSM	X <sup>e</sup>			

<sup>a</sup> Examples: OOK, VPPM, PWM.

<sup>b</sup> Example: M-PAM.

<sup>c</sup> Examples: dc-biased ASK, PSK and QAM.

<sup>d</sup> Examples: DCO-OFDM, ACO-OFDM, Flip-OFDM, U-OFDM, dc-biased DMT.

<sup>e</sup> One of the light levels is zero, therefore the signal amplitude is associated with the average signal value.

#### F. Typical converter types behavior

A summary containing circuit examples, time domain waveforms and spectrum of generated signals for each modulator type is presented in Table II. In this table, the same modulation strategy was illustrated for all modulator types. In this representations, symbol frequency ( $F_{SYM}$ ), symbol period ( $T_{SYM}$ ), switching frequency ( $F_S$ ) and switching period ( $T_S$ ) have the only purpose of correlating time and frequency domain representations. This is meant as a general view of the modulators behavior and resulting signal, a deeper analyze concerning other aspects is presented in next section.

TABLE II  
TYPICAL BEHAVIOR OF MODULATOR CIRCUITS ACCORDING TO MODULATOR TYPE.

Modulator type	Example of circuit	Example of typical waveform	Example of typical spectrum
LMM			
SMM			
SSM			
PSM			

## V. REVIEW OF VLC LED DRIVERS

In order to compare the performance of the different solutions investigated in this review, commercial performance metrics used for conventional lighting are used as reference levels [95]. These levels are employed when comparing power and efficiency ratings. Similarly, the data rate used in common applications for audio and video streaming are also used as reference [96]. However, some of the publications do not provide information on these specific metrics and therefore they could not be included in the comparison.

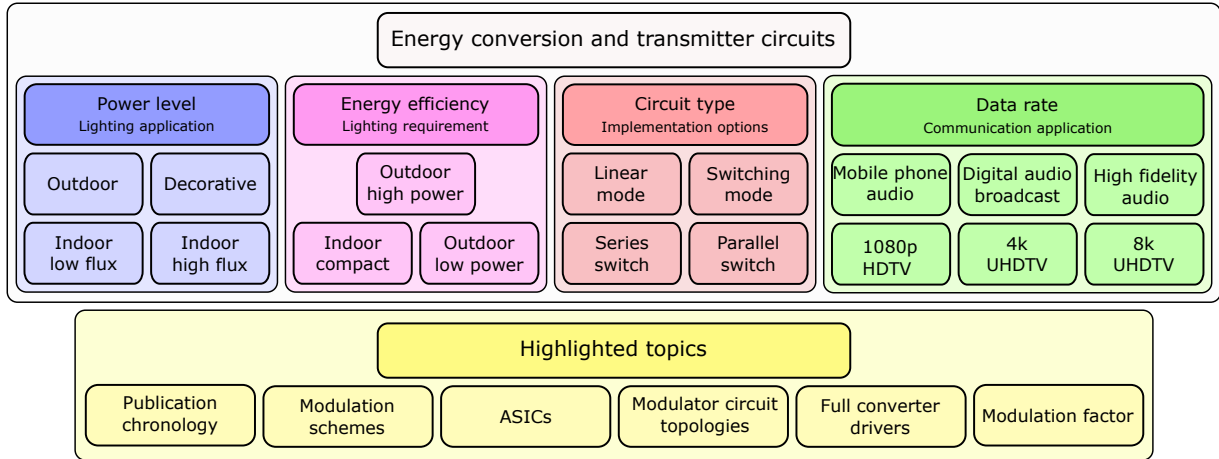


Fig. 4. Key aspects of the review on energy conversion and transmitter circuits.

In this review, the VLC drivers are classified following 4 key aspects that are present in any analyses, namely: i) power level, ii) energy efficiency, iii) data rate and iv) circuit type, as is summarized in Fig. 4. Those aspects comprehend the lighting, the application in communications and the implementation of the modulators for VLC. Also, Fig. 4 lists some highlighted topics focused on specific sections. The structure of the review can be summarized as follows:

1) *Chronology of Publications*: Section V-A explores the VLC LED drivers that have been proposed in the last 13 years classified by modulator types.

2) *Modulation Schemes*: The modulation plays an important role in the VLC system design because the choice of the driver topology is directly determined by the modulation to be

implemented. The types of modulations reported in the surveyed literature are analyzed in Section V-B.

3) *Monolithic Integrated Circuit Solutions*: Many authors have proposed to implement VLC LED drivers into application specific integrated circuits (ASICs). This represents an interesting trend nowadays and therefore it will be studied in Section V-C.

4) *Power Rating*: The power rating is a key feature of the VLC LED driver taking into account that their main objective is to provide lighting. Thus, this aspect is analyzed in Section V-D.

5) *Energy efficiency*: Even though luminous efficacy is a key feature of any LED driver, most of the publications found in the literature do not provide this information. Therefore, electrical efficiency has been considered in this study, as will be presented in Section V-E.

6) *Circuit Topologies*: One of the most relevant objectives of this work is to explore the different circuit topologies proposed in the literature, which will be classified and studied in Section V-F.

7) *Full Converters*: FCs are very relevant because they include all the necessary stages to implement the VLC LED driver from the grid. Also, since they all share similar features and requirements, they will be specifically analyzed in Section V-G.

8) *Modulation factor*: In Section V-H the modulation factor is used to compare the solutions of the reviewed literature. The amplitude of modulated current is represented, which is proportional to the communication signal amplitude, in order to provide a fair comparison regarding the modulation capability of each solution.

Finally, in Section V-I, a summary of VLC modulator types and features is provided to help on the selection of suitable circuits for VLC application.

### A. Publication Chronology

Fig. 5 depicts the accumulated number of publications of each year from 2008 to 2019 classified according to the modulator type. Those publications that presented more than one modulator type were considered multiple times. This is the reason why the total accumulated number of publication in 2019 (49) exceeds the number of references included in this review (44).

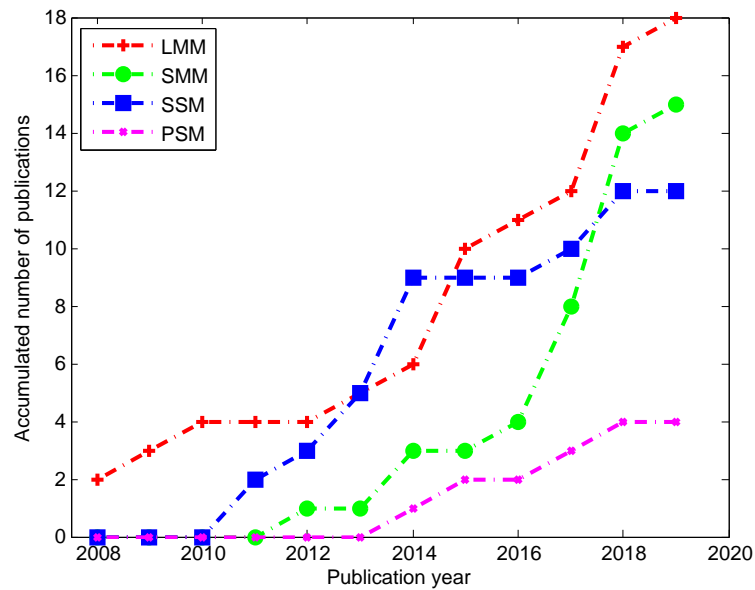


Fig. 5. Accumulated number of publications on VLC drivers.

The first conclusion based on this data is that LMM-based converters head the number of published works. However, it can be seen that SMMs have experienced a great increase since 2016, overcoming the number of published works based on SSM in 2018. A second conclusion is that the research about VLC trends to the same circuit types as used in conventional LED drivers, most of them based on SMM [97]. This suggests that such design trend is motivated by the fact that designers are pursuing higher efficiency and lower circuit complexity, both of them attainable by reducing the number of power processing stages.



TABLE III  
NUMBER OF PUBLICATIONS ACCORDING TO MODULATION BAND AND MODULATOR TYPE.

Modulation band	Circuit type				Total
	LMM	SMM	SSM	PSM	
Baseband	12	3	12	4	27
Passband	8	11	0	0	19
Both	2	0	0	0	2

### B. Modulation Schemes

Table III shows the number of publications according to modulator types and modulation band. As can be seen, the greater number of publications corresponds to baseband implementations, even though these schemes are more likely to generate harmful flicker. Table IV gathers the number of publications according to the modulation schemes and modulator type. As can be seen, the binary pulse modulation schemes are very often reported [3], [5], [6], [9], [11]–[13], [15]–[17], [19]–[23], [25], [26], [28], [30], [32], [35], [38], [43], [45]. The popularity of these modulation schemes can be explained by two main reasons:

- They can be implemented with simple solutions as SSM or PSM, but also with more complex modulators as LMM or SMM.
- Important standards such as IEEE 802.15.7 [82], JEITA CP-1221, CP-1222 and CP-1223 from Japan Electronics and Information Technology Industries Association (JEITA) [98], which are based on binary modulation schemes, are very frequently referred in the literature as a requirement of the proposed solutions.

Although multi-carrier modulations are very commonly used in wireless communications, they appear in a smaller number of publications, either under OFDM [10], [27], [29], [31], [37], [39], [39], [42], [44], [47] or under DTM [14], [40] schemes. Usually, research works less focused on VLC LED drivers address these modulation schemes, especially OFDM, as promising for VLC applications [7]. Additionally, even though LMMs are able to generate

TABLE IV  
NUMBER OF PUBLICATIONS ACCORDING TO THE MODULATION SCHEMES AND MODULATOR TYPE.

Modulation scheme		Circuit type				Total
		LMM	SMM	SSM	PSM	
Pulse based	<b>binary</b>					
	OOK	8	1	9	2	20
	VPPM	1	3	3	4	11
	Manchester	1	1	1	1	4
	<b>Multiple-level</b>					
	PAM	4	0	0	0	4
Carrier based	<b>Single-carrier</b>					
	QAM	1	3	0	0	4
	PSK	1	5	0	0	6
	FSK	0	1	0	0	1
	<b>Multi-carrier</b>					
	OFDM	6	4	0	0	10
	DMT	1	1	0	0	2

highly complex modulations, such as OFDM and DMT, most of the works in the literature do not take advantage of this capability; they usually employ these circuits to generate less spectral-efficient binary pulse modulations. In this sense, the reported LMM-based solutions could achieve a much higher data rate while keeping the same bandwidth, if more complex and more bandwidth-efficient modulation schemes were used. It is very likely that the optical communication standards IEEE 802.11bb [99] (OFDM), IEEE 802.15.13 [100] (OFDM) and IEEE 802.15.7m [101] (OFDM and DMT) that are expected to be released in the near future will include these bandwidth-efficient schemes.

Finally, it must be noted that in Table III and Table IV only those publications that clearly reported the information about modulation schemes were considered [2], [3], [5], [6], [9]–[47].

### C. ASIC-based Drivers

ASIC-based VLC LED drivers [5], [9], [17], [17], [20], [22], [23], [26], [27], [30]–[32] represent a more significant number of the solutions proposed in the surveyed literature compared

to the number of drivers implemented using discrete general purpose components. In ASIC-based solutions most of the system components are integrated in silicon, being the only external components inductors and capacitors.

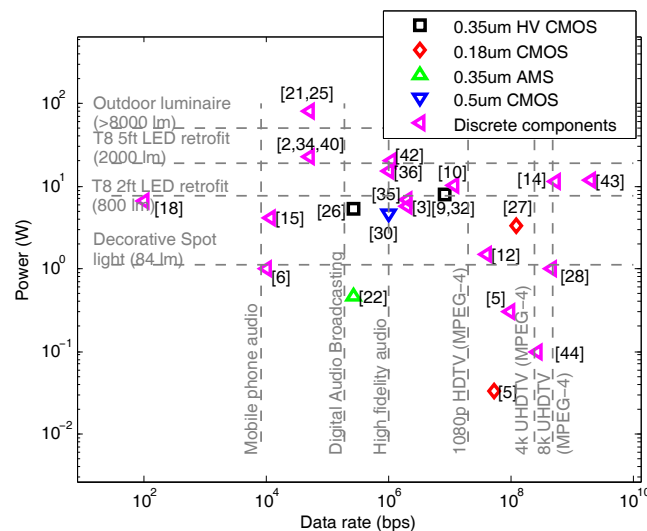


Fig. 6. Comparison of data rates and power levels of ASIC-based and discrete drivers.

Fig. 6 presents power and data rate information of the surveyed solutions classified according to ASIC technology node. Also, discrete circuit solutions are shown for comparison. As can be seen, ASIC-based VLC LED drivers have data rates from 10 kbps [23] to 120 Mbps [27]. Additionally, the maximum power rating of ASIC-based solutions is 8 W [9], [32], which is only suitable for indoor applications. The ASIC semiconductor technology nodes range from 0.18 to 0.5  $\mu\text{m}$  complementary metal-oxide-semiconductor (CMOS) processes, some of them using Bipolar-CMOS-DMOS or high-voltage (HV) CMOS technologies.

ASIC-based solutions are often designed for high performance, low power consumption and scalability for production. However, as can be seen in Fig. 6, taking into account power and data rate performances, none of the solutions implemented in ASIC differs significantly from the discrete ones. Among the ASIC-based solutions, [26] and [17] join two separated converters in

the same ASIC; they use a switching mode converter as the first stage and a dedicated modulator as the second stage.

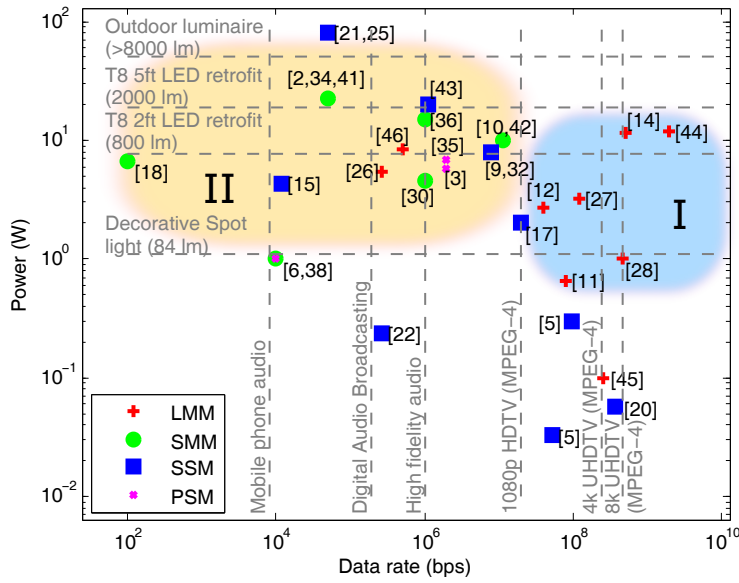
Nevertheless, ASIC-based solutions have proven to be a feasible possibility to integrate VLC LED drivers into single monolithic circuits, including all necessary stages for power conversion and signal processing. Furthermore, complex circuit topologies that would require a great number of circuit components, as in [9], can be implemented into elegant ASIC-based solutions. Additionally, it is well known that the wide adoption and price drop of digital technologies such as audio players, graphics processing units and wireless communications, only happened when ASIC-based devices reached the market. Likewise, integration into ASIC, together with standardization, should be the first steps towards VLC widespread deployment [102] [103].

#### D. Power Level

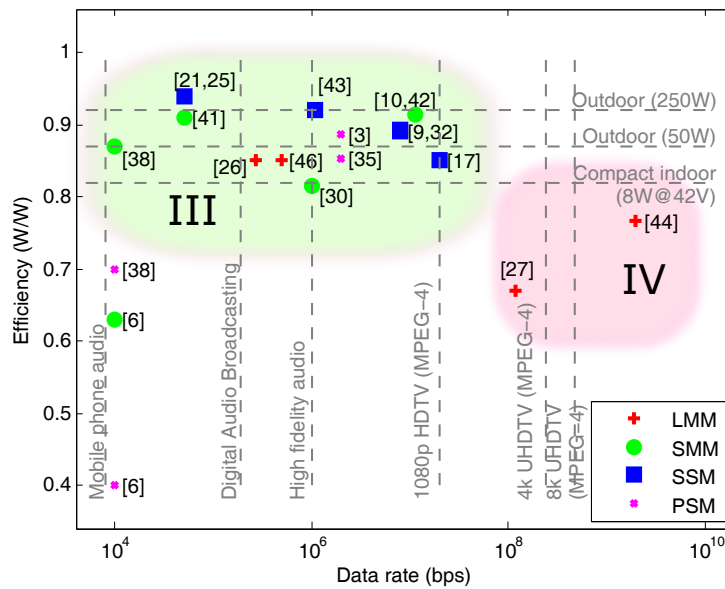
Fig. 7a depicts the output power rating ( $P_{LED}$ ) and data rate of the reviewed solutions. As can be seen, the drivers that occupy specific areas of the chart can be grouped in clusters, which indicates that they have common characteristics, as illustrated by areas I and II in Fig. 7a. Cluster I is characterized by the modulator type, while cluster II features both power rating and data rate.

The line indicating 1080p HDTV stream data rate (20 Mbps) represents an important boundary for cluster I. On its right side, the higher data rate solutions are located, for which the LMM-based drivers predominate. Additionally, in cluster I the lower power boundary is represented by the decorative spot light ( $\approx 1.0$  W), which is the minimum power reference for practical illumination. In this sense, this first cluster of solutions providing high data rates is formed only by LMM [12], [14], [27], [28], [44].

On the other hand, as can be seen in Fig. 7a, the cluster II is defined by the area of data rate lower than the 1080p HDTV stream (20 Mbps) and power rating from 4.2 W [15] up to 80 W [21], [25]. In this cluster, SMM and SSM predominate, existing solutions suitable for most power



(a) Comparison of data rate and power levels according to modulator type.



(b) Comparison of data rate and power efficiency according to modulator type.

Fig. 7. Power level and efficiency of VLC LED drivers.

rating applications. However, only a few SSM-based solutions [21], [25] can be highlighted as having enough power rating for outdoor applications. Additionally, the SMM-based drivers are the most common solutions for indoor applications in the range 800-2000 lm.

### *E. Energy Efficiency*

The energy efficiency is a key aspect in any LED driver. In this section, the energy efficiency is calculated by the ratio between the LED average power and the input power of the complete driver. Fig. 7b presents the efficiency and data rate classified accordingly to modulator types. Two clusters can be identified, which are designated as III and IV in the figure.

As can be seen in Fig. 7b, cluster III is located in the area with data rate below 20 Mbps, which corresponds to the 1080p HDTV streaming reference [3], [9], [10], [17], [21], [25], [26], [30], [32], [35], [38], [41]–[43]. The solutions that have efficiency levels compatible with commercial LED drivers, i. e. over 82%, are mostly based on SSM or SMM. All the converters in cluster III present good efficiency, yet they exhibit low data rates. It is important to highlight that in this group only [35] and [3] are FC.

Cluster IV groups the highest performance solutions in terms of data rate, which are 120 Mbps [27] and 2 Gbps [44]. However, these solutions are based on the less-efficient LMM. Therefore, compared to cluster III they present lower efficiency, which is even below the reference levels for commercial lighting applications. Nevertheless, the data rates achieved by the solutions in cluster IV are able to support HDTV and UHD TV streamings. Among the solutions included in this cluster, only [44] has all driver stages corresponding to a FC. The higher data rates achieved by LMM based solutions were verified to be possible because of wider modulation bandwidth and also owing to the use of high spectral efficient modulation schemes.

As a conclusion of this comparison, efficiency compatible to commercial LED drivers was reported mostly by solutions based on SSM and SMM. Finally, another relevant conclusion is that few PSM-based solutions are proposed, which even perform with efficiency similar or lower than solutions based on SSM and SMM.

### F. Circuit topologies

This section presents a description and comparison of circuit topologies presented in the surveyed literature. Table V shows a summary of circuit topologies classified according to modulator type, including power rating and efficiency. In the following, a complete description according to the proposed classification is carried out.

1) *SSM and PSM*: Fig. 8 illustrates the structures of these modulators together with their operating waveforms. In this type of modulators, the rise and fall times,  $T_R$  and  $T_F$  respectively, are key parameters to define the maximum modulation bandwidth. These times are directly related to the performance of the switches and the LED device. In the case of the SSM shown in Fig. 8a the switch performance affects the rise time, while the LED performance defines the fall time. Additionally, in the modulator shown in Fig. 8b both rise and fall times are only affected by the performance of the switches, having the LED performance less influence on these times [5], [16]. Therefore, owing to this improved performance, this type of modulator can operate faster than the circuit shown in Fig. 8a.

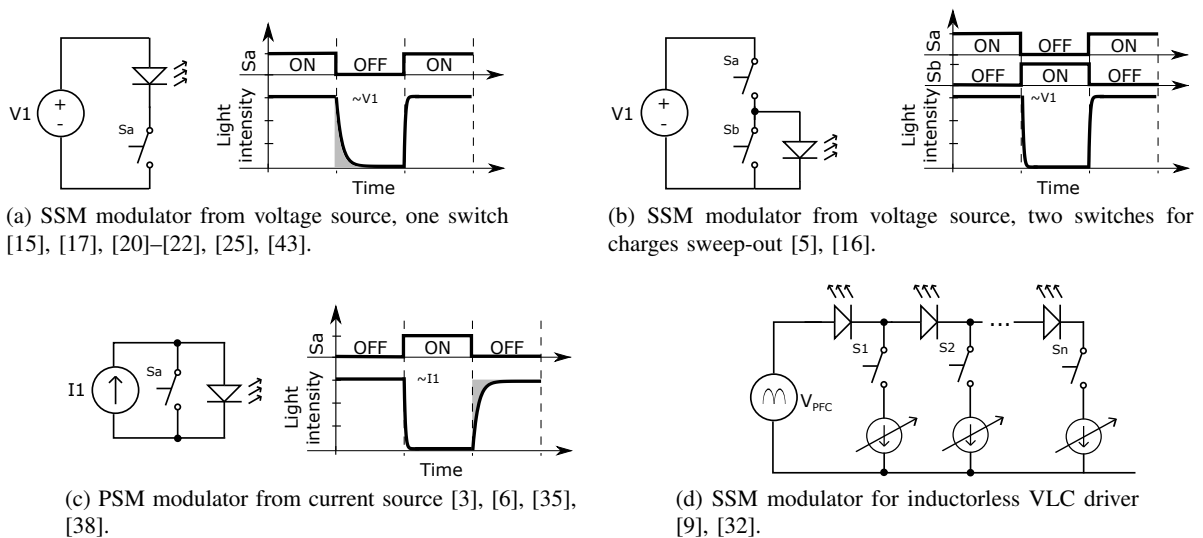


Fig. 8. Switches arranged as MC

TABLE V  
CIRCUIT TOPOLOGIES SUMMARY

Ref.	Power (W)	Efficiency (%)	Circuit or topology
<b>LMM</b>			
[11]	-	-	Multi-ressonant equalization + buffer amplifier (BUF634T) + dc T-biased
[12]	1.5	-	16-channel multi-ressonant equalization + buffer amplifiers (BUF634T) + dc T-biased
[13]	-	-	Custom-designed two-stage class-AB amplifier + dc T-biased
[14]	11.5	-	RF linear driver (ZHL-6A) + dc T-biased
[23]	-	-	Current-mode logic and pre-emphasis with extra parallel buffer
[26]	5.4	85	Boost + series biased MOSFET modulator
[27]	3.3	67	Current steering DAC, series biased MOSFETs as current sources
[28]	1.0	-	Pre-emphasis circuit + emitter flower BJT stage + series biased MOSFET circuit
[29]	-	90	Series biased BJT modulator
[31]	-	-	Custom 4-channel current mode CMOS DAC
[39]	-	-	Class A or AB + T-bias
[39]	-	-	Series biased MOSFET
[44]	12.0	77	Low frequency transf. + rectifier + SEPIC + series biased BJT modulator with equalization
[45]	0.1	-	Pre-distortion and equalization amplifiers (ZHL-6A-S+) + dc T-biased (ZFBT-4R2G+)
[46]	8.3	85	Ripple modulation with Class E amplifier assisted by linear class AB amplifier
<b>SMM</b>			
[2], [34]	22.6	-	Synchronous buck
[41]	22.6	91	
[6]	1.0	63	Buck
[38]	1.0	84	
[40]	-	-	
[8]	20.0	90	Two-phase buck
[24]	100.0	88	
[37]	10.0	90	
[10], [42]	10.1	91	
[18]	6.7	-	Boost
[30]	4.6	81	Buck (GaN FETs)
[36]	15.0	-	Two-phase synchronous buck
[47]	10.0	96	
<b>SSM</b>			
[5], [16]	0.3	-	Series FET and parallel carrier sweep-out FET (GaAs FET)
[5]	0.033	-	Series MOSFET and parallel carrier sweep-out MOSFET implemented in 0.18- $\mu\text{m}$ CMOS
[9], [32]	8.0	89	Rectifier with valley fill + switches in series with LED branches
[19]	-	-	BJT emitter follower + pre-emphasis
[15]	4.2	-	Series switch unspecified modulator
[20]	-	-	
[17]	2	85	Series MOSFET modulator
[22]	0.5	-	
[21], [25]	80.0	94	PFC rectifier + LLC switching converter + series MOSFET modulator
[43]	20.0	92	Buck-boost + series MOSFET modulator
<b>PSM</b>			
[3]	5.8	89	Rectifier with valley fill + buck + parallel MOSFET modulator
[6]	1.0	40	Buck + parallel MOSFET modulator
[38]	1.0	66	
[35]	6.9	85	Rectifier + buck-boost-buck + parallel MOSFET modulator



In the case of the PSM the fall time is affected by the switch performance and the rise time is mainly dependent on the LED characteristics.

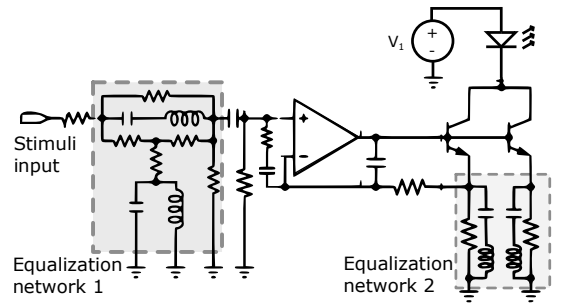
Among these modulator types, the structures depicted in Fig. 8a and Fig. 8c are more commonly found in the literature.

A slightly different approach reported in [9], [32] implements an arrangement of 12 switches and controlled current sources used as a VLC modulator, as shown in Fig. 8d. This solution uses a front-end PFC stage based on a valley fill circuit. According to the authors, the converter achieves a high PF and a smooth control of the LED currents. In addition, this solution provides low flicker and avoids the use of inductors, thus making it possible to integrate most of the circuitry in an ASIC.

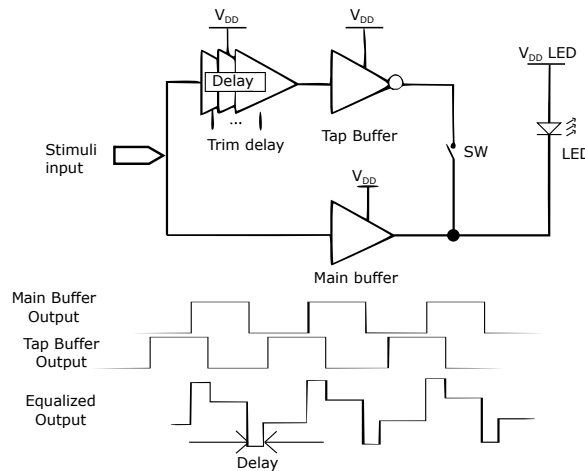
2) *LMM*: The reported solutions using LMM employ a wide sort of circuit topologies. It is clear to see in Table V that most of the solutions employ equalization [11], [12], [44], [45], pre-emphasis [19], [28] or pre-distortion [45] strategies, which compensate the well-known LED or other component dynamics to achieve a wider bandwidth. This is usually performed using passive networks aided by active components [11], [12], [19], [28], [44], as illustrated in Fig. 9a as an example. They can also be realized using a delay chain [23], as presented in Fig. 9b.

Other solutions are based on using MOSFET current sources to control the LED current [27], [31]. As an example, Fig. 9c depicts the structure that performs the digital-to-analogue conversion (DAC) in the power circuit instead of in the signal processing stage. For this purpose, transistors  $M_i$  act as binary weighted current sources. Transistors  $M_{ci}$  and  $M_i$  are cascode structures that increase the modulator output impedance. This improves signal linearity by reducing current distortion regardless of LED impedance. This circuit was implemented into an ASIC and reported as suitable for high data rates (120 Mbps) achieving a reasonable power efficiency [27].

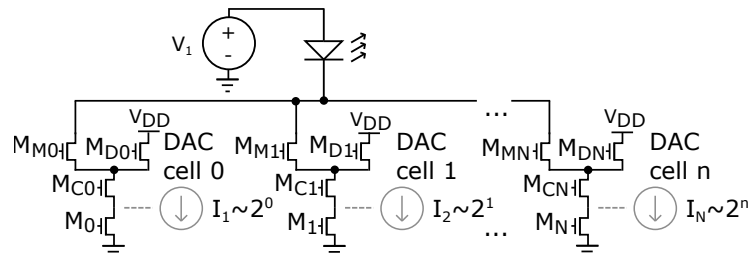
Fig. 10a shows a structure that is frequently reported as signal injector in LMM, which is the dc T-biased coupler, also known as ac-couple circuit. A modulated signal (ac input) is summed up to a dc current to build the LED stimuli current, so that the LMM does not process the dc



(a) LMM with analog pre-emphasis using series BJT modulator [44].



(b) LMM pre-emphasis using a delay chain [23].



(c) LMM using current steering DAC topology [27].

Fig. 9. LMM related circuits (part 1).

current. Thus, better overall efficiency can be achieved because the dc part can be processed by a separate converter.

Other alternative solutions to the dc T-biased coupler employ series biased BJT [29], [44] or MOSFET [26], [28], [39] to implement the modulator. Fig. 10b shows an example based

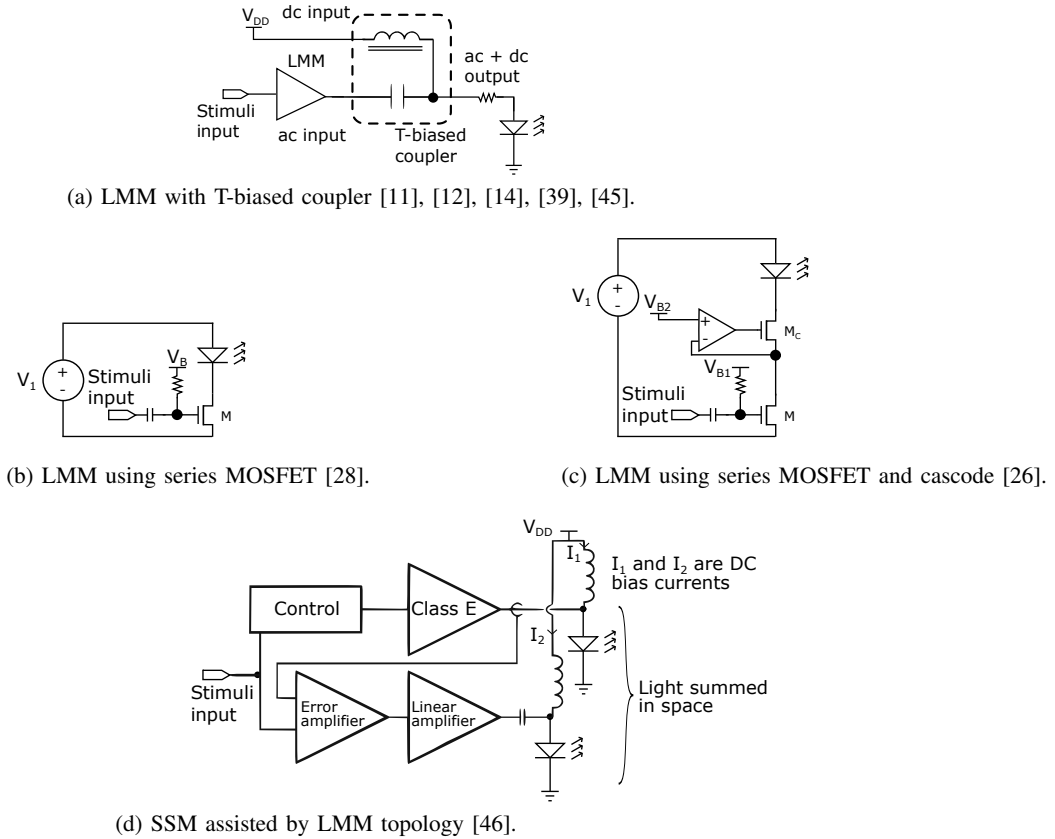


Fig. 10. LMM related circuits (part 2).

on a single series transistor, while in Fig. 10c a cascode structure is employed to increase the output impedance of the current source, as in the DAC solution. However, in these solutions the transistors have to operate in linear region processing all the dc current, which decreases the modulator efficiency.

A hybrid solution presented by [46] employs as class E narrow-band SMM that is assisted by a class AB LMM. The circuit used in this solution can be seen in Fig. 10d, it uses a T-biased coupler in which most of the current modulation is performed by a class E amplifier (85%) with some level of distortion due to the narrow band. Hence, the linear amplifier improves the modulation reproduction fidelity by means of an additional contribution to light based on a current feedback. The advantage of higher efficiency of SMM (81%) and the dc bias, which

delivers 75% of the power, prevails over the lower LMM efficiency. Therefore the final solution efficiency achieved 85% with SMM switching at 1MHz and achieved 250kHz of modulation bandwidth.

3) *SMM*: Most of the SMM-based solutions employ average current control previously presented in Section IV-B. As an example, [6] proposes a buck converter switching at 100 kHz tracking a much slower signal of 10 kHz, as shown in Fig. 11a. In this case, the current through the LED is composed of a dc component with a superposed square waveform communication signal. Similarly, [30] presents a buck converter, operating at 10 MHz that can track a 1 MHz VPPM communication signal. Additionally, this converter can achieve a reasonable good efficiency of 81 %.

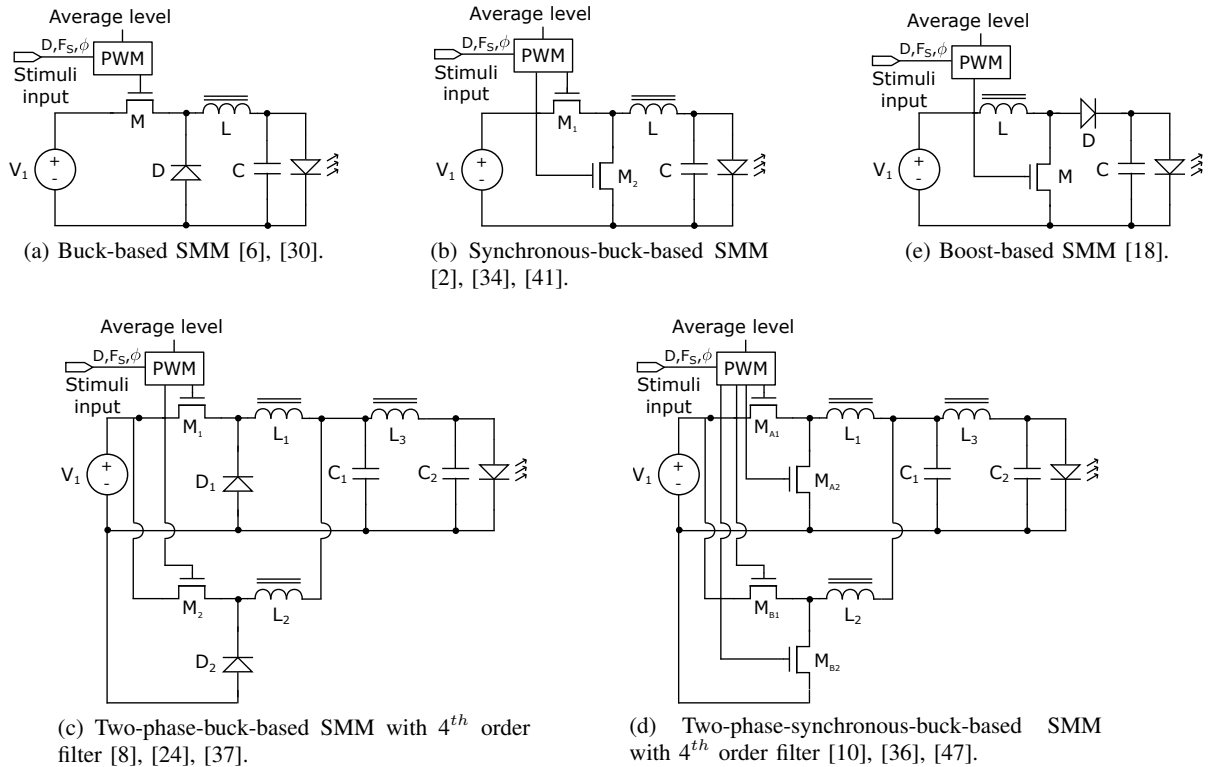


Fig. 11. Topologies of SMM VLC modulators.

A two-phase buck converter with 4<sup>th</sup> order filter is reported in [24], as illustrated in Fig. 11c. This converter operates at switching frequency of 10 MHz tracking a communication signal with a harmonic content from dc up to 3.125 MHz. The proposed converter also achieves a very high efficiency of up to 92 %. A similar converter is presented in [8].

Another solution [10] uses a structure based on a 10-MHz two-phase synchronous buck modulator, as shown in Fig. 11d, and a synchronous buck converter switching at 250 kHz (not shown in the figure). The latter processes most of the power, while the former is used to achieve a wide modulation bandwidth. In this structure both converters process the same load current, while splitting the output voltage between them, which is known as split-of-the-power strategy. Indeed, the presented prototype is able to track a communication signal with components up to 3 MHz while keeping high efficiency (up to 93.6 %).

On the other hand, strategies based on ripple modulation have also been proposed. [18] presents a boost converter, as shown in Fig. 11e, in which the switching frequency is modulated for data encoding. Two switching frequencies, 40 kHz and 80 kHz, are used to transmit the binary digits. Also, in other references the two-phase synchronous buck converter is proposed to implement ripple modulation. In [36] this converter is used to generate a QAM modulated signal, while in [47] multi-carrier modulation is implemented. Likewise, [2], [34], [41] explore the synchronous buck topology to perform ripple PSK modulation. Additionally, [41] showed that the drop of the system luminous efficacy due to VLC modulation was only 3 %.

### *G. Full Converter Drivers*

Full converters were introduced in Section III as a complete solution to implement off-line VLC LED drivers. Therefore, in this section the works that present FC solutions will be further investigated. Table VI summarizes the main characteristics and performance of these works. In this table, the number of controlled stages considers only the active ones because they greatly increase the complexity of the system. Passive solutions are used as input stage in some cases;

TABLE VI  
MAIN CHARACTERISTICS AND PERFORMANCE OF FC VLC LED DRIVERS.

Ref.	MC Type	Ctrl. stages	Power (W)	Power Factor	Efficiency (%)	Data rate (bps)	Description
[3]	PSM	2	5.8	0.88	88.6	$2 \cdot 10^6$	Rect. + valley fill + Buck + PSM
[9]	PSM	1	8	0.904	89.2	$8 \cdot 10^6$	Rect. + valley fill + 12 parallel switches
[25]	SSM	3	80	-	94	$50 \cdot 10^3$	PFC rectifier + LLC converter + SSM
[35]	PSM	2	6.9	-	85.2	$2 \cdot 10^6$	Rect. + PFC buck-boost-buck converter + PSM
[44]	LMM	2	12	-	76.6	$2 \cdot 10^9$	Line frequency transf. + rect. + SEPIC + LMM

however, they have a much lower impact on the complexity of the driver.

Most of the works present two separated controlled stages that accomplish all the required functions corresponding to rectification/PFC, power control and modulation. The exception is the solution that uses no inductors [9]. It employs a passive rectifier and valley fill PFC circuit followed by only one controlled stage that performs both PC and MC functions. Owing to the extra amount of controlled switches, 12 in this stage, extra degrees of freedom are available for the generation of different LED current patterns. This allows the driver to simultaneously control both average lighting level and shape the communication signal into the emitted light.

All the FC-based works present a power efficiency ranging from 85 % to 94 %. The only work that presents an efficiency below 80% is the one that employs LMM [44]. However, this work presents a much higher data rate compared to the others. As can be seen in the table, there is a very strong opposite behavior between efficiency and data rate. As shown in Fig. 12, when representing data rate (in logarithmic scale) versus efficiency, a clear linear relationship is found, which highlights the strong trade-off between these two parameters. According to this characteristic, every increasing point of efficiency (1%) corresponds to a decreasing of 1.75 times in data rate.

#### H. Modulation factor

For the sake of simplicity and to allow for a comparison among different test scenarios from the literature, in this section the analysis extends up to the LED driver output electrical

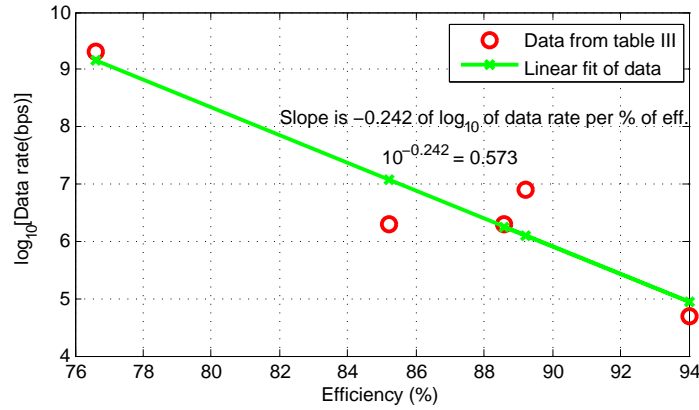
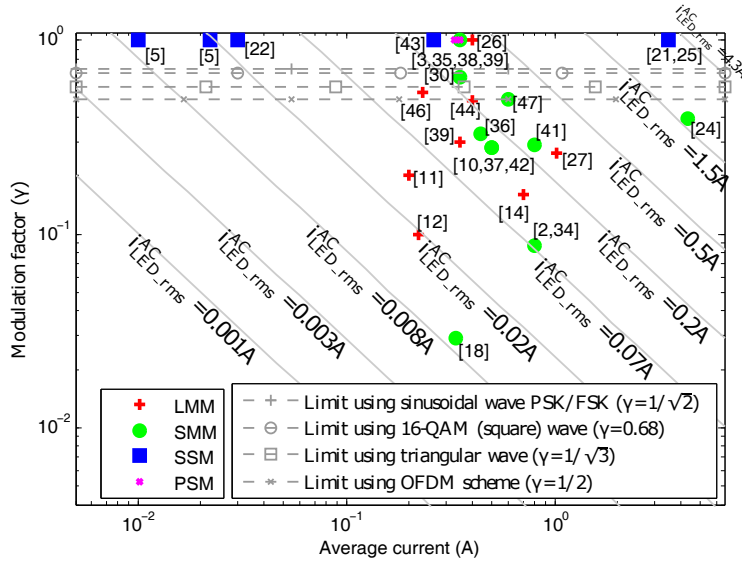


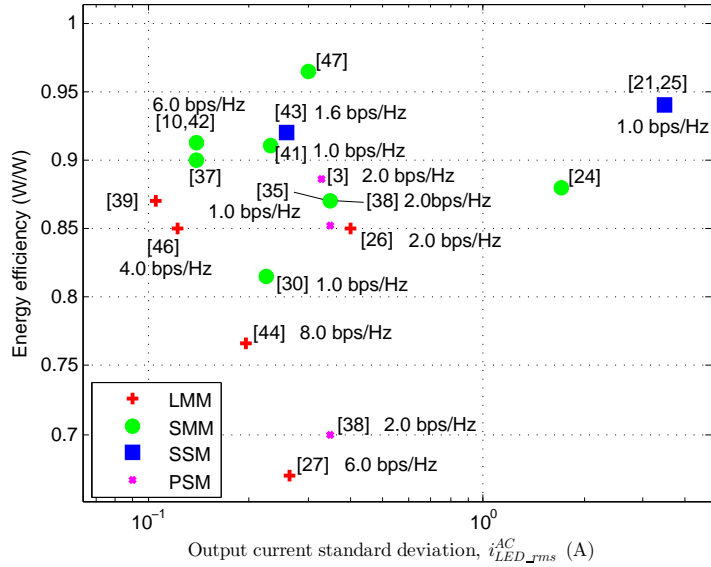
Fig. 12. Efficiency and data rate from Table VI data with its linear regression.

terminals. When signal power is addressed, it refers to an extrapolation from the electrical current provided to the LED. Therefore, it is only meant for a comparison among the reviewed solutions considering similar LED emitter and open optical channel conditions. Fig. 13a depicts the modulation factor calculated according to the average current from the literature. In the analysis presented in this figure the higher is the modulation factor, the more the light dynamic range is used for communication. Signal amplitude depends on the average light level and the modulation factor, which in turn is limited according to the implemented modulation scheme. Therefore, the achievable signal amplitude is not directly connected to the modulator topology, however it defines the possible modulation schemes.

In Fig. 13a there are lines with same communication signal amplitude, which is represented by  $i_{LED\_rms}^{AC}$ . The diagonal bands, shown in gray in the figure, represent equivalent communication signal power. For example, [5] and [12] achieved equivalent modulation capability in communication signal power because both are at the same amplitude level, in which  $i_{LED\_rms}^{AC} = 0.02A$ . Additionally, Fig. 13b presents energy efficiency according to the output current amplitude, thus same communication signal amplitude correspond to vertical lines in this figure. In this sense, [3], [26], [27], [30], [35], [38], [39], [41], [43], [47] achieved similar communication signal



(a) Modulation factor and average current of surveyed literature.



(b) Energy efficiency of solutions according to output current standard deviation.

Fig. 13. Modulation capability data of the solution.

power, with  $i_{LED\_rms}^{AC} \approx 0.3A$ , regardless of the LED average current and with a wide range of modulation indexes, which can be seen in Fig. 13a, and different modulation schemes. In the analysis of the absolute values, [21], [25] reached the highest modulation amplitude (3.5 A)



using a SSM, therefore  $\gamma=1$ , and the second higher modulation amplitude is reported in [24], which achieved 1.71A with  $\gamma=0.4$  using a SMM.

It is easy to see in Fig. 13a that all works implementing SSM or PSM based modulators achieve modulation factor equals to 1. This happens because the binary modulation schemes that can be generated by these modulators produce only zero and the peak current value. Also, this modulation factor is the maximum possible when calculated considering the positive current restriction inherit to the LED. However, not only SSM or PSM can perform these level of modulation factor, also [39] and [26] used LMM to achieve modulation factor equals to 1 by using binary pulse based modulation schemes. For other modulation schemes, their peak-to-average value also constrains the maximum modulation factor that can be performed, whose limits are depicted in Fig. 13a in horizontal dashed lines. Those are defined according to the signal shape or according to the variance of the signal for OFDM scheme [40]. In this sense, [47] and [44] used OFDM modulation schemes and reached a modulation factor close to its limit, while [24] has lower modulation factor for the same scheme. All other works presented test data using modulation factors below the maximum for the corresponding modulation scheme.

Finally, Fig. 13b clearly shows the effect of higher amplitude of output current in LMM, which leads to lower energy efficiencies. Hence, most of LMM occupy only the left-most side of this chart, which indicates lower signal amplitude levels. Owing to the different operation principles, SMM and SSM have the higher efficiencies, however the higher signal power is poorly used in low complexity modulations by SSM, see annotated corresponding spectral efficiency values in the figure. Due to these facts, the right choice of modulator topologies to reach higher signal power with higher energy efficiency is within SMMs. This result contrasts with data rate results presented in Section V-E, in which LMM have clear superior performance. In this sense, better use and exploration of higher complexity modulation schemes with SMM may bring further advances in data rate with less energy efficiency penalty.

### *I. Features summary*

Table VII presents a summary of the features and surveyed literature data for each modulator type. This contains the key aspects to select a VLC modulator type according to target lighting power level, efficiency or modulation scheme to be implemented.

## VI. CONCLUSIONS

The current study has presented an up-to-date review on the VLC LED drivers, highlighting the most relevant facts and conclusions about the state of the art of this technology. First of all, switching mode converters are identified as a trend among the VLC LED drivers. Additionally, series switch and linear mode modulator circuits are also among the most frequent solutions in the literature.

With regard to modulation, binary modulation schemes are the majority of the reported strategies. Even though they achieve lower spectral efficiency than other strategies, their simplicity of implementation make them the choice in most of the reported solutions. Another motivation of the extensive use of binary modulation schemes is that they have already been adopted by some VLC standards, as the IEEE 802.15.7 and JEITA CP-1221, CP-1222 and CP-1223. However, the research on VLC LED drivers might soon change its focus to more complex modulation schemes as new optical communication standards are expected to be released in a near future, such as IEEE 802.11bb (using OFDM), IEEE 802.15.13 (using OFDM) and IEEE 802.15.7m (using OFDM and DMT). Among the solutions integrated into ASICs, when considering power and data rates, none of them exhibit improved performance compared with discrete solutions.

The linear mode modulator solutions presented a great variety of circuit topologies, which have on average lower power levels and lower efficiencies when compared to other modulator types. On the other hand, the buck and buck-derived modulators are the most frequent topologies among switching mode modulators, which perform with high efficiencies but still with limited data rates. Also, reasonable good efficiency was reported with series switch modulator circuits.

TABLE VII  
SUMMARY OF CIRCUIT TYPES AND FEATURES.

Modulator type	Complexity	Bandwidth	Modulation types	Distortion	Efficiency	Power level and application	Main limitation
LMM	Intermediate, has a high number of components	Wide, 100's of MHz	Any scheme	Due to semiconductor non-linear behavior	Low, in average below 80 %	Low, in average 5.0 W, indoor low and medium power lighting	Voltage headroom for semiconductor biasing causes substantial dissipated power.
SMM	Complex, high switching frequency and passive components.	Narrow, few MHz	Any scheme	Non-linear converter gain and inherit current ripple <sup>a</sup>	High, in average 85.5 %	High, in average 19.4 W, indoor medium and high power lighting	Limited switching frequency, thus narrow bandwidth due to necessary filtering.
SSM	Simple	Intermediate, 10's of MHz	Only binary pulse based schemes	High order frequency harmonics are attenuated	High, in average 90 %	High, in average 14.3 W, indoor medium and high power lighting	Is only capable of generating simple modulations, the data rates is affected by average light control strategy.
PSM	Simple	Intermediate, 10's of MHz	Only binary pulse based schemes	High order frequency harmonics are attenuated	Low, in average 70 %	Low, in average 3.7 W, indoor low and medium power lighting	Is only capable of generating simple modulations and have lower efficiency than SSM.

<sup>a</sup> In cases that the ripple itself is not used for information encoding, this is outside of signal band used in average current control.

However, they present limitations on the modulation schemes that can be reproduced. Moreover, they require an intermediate stage to regulate the LED voltage, which makes the system more complex. Additionally, most of the off-line solutions have two controlled power processing stages, for which a strong trade-off between data rate and efficiency has been observed.

Finally, signal amplitude is connected to the modulator circuit type and to the energy efficiency considering current modulator circuit topologies. Moreover, the low spectral efficiency of the used modulation schemes points out that switching-mode-modulator based solutions have potential to achieve higher data rate with little energy efficiency penalty. That can be accomplished by using modulation schemes with higher spectral efficiency and taking advantage of the available signal amplitude. Also, linear-mode-modulator based solutions achieved lower signal amplitude, even so, they achieved higher data rates due to wider modulation bandwidth at the cost of lower energy efficiency.

#### ACKNOWLEDGMENT

This study was financed in part by the Coordenação de Aperfeiçoamento de Pessoal de Nível Superior - Brasil (CAPES) - Finance Code 001, PROEX program, PRPGP/UFSM, INCT-GD, CAPES proc 23038.000776/2017-54, CNPq proc 465640/2014-1, FAPERGS proc 17/2551-0000517-1.

#### REFERENCES

- [1] A. Tsiatmas, C. P. M. J. Baggen, F. M. J. Willems, J. P. M. G. Linnartz, and J. W. M. Bergmans, "An illumination perspective on visible light communications," *IEEE Communications Magazine*, vol. 52, no. 7, pp. 64–71, 2014.
- [2] F. Loose, R. R. Duarte, C. H. Barriuello, M. A. Dalla Costa, L. Teixeira, A. Campos, M. A. D. Costa, L. Teixeira, and A. Campos, "Ripple-based visible light communication technique for switched LED drivers," in *2017 IEEE Industry Applications Society Annual Meeting, IAS 2017*, vol. 2017-Janua. Cincinnati: IEEE Industry Applications Society, 2017, pp. 1–6.
- [3] K. Modepalli and L. Parsa, "Dual-purpose offline LED driver for illumination and visible light communication," *IEEE Transactions on Industry Applications*, vol. 51, no. 1, pp. 406–419, 2015.

- [4] L. Teixeira, F. Loose, J. P. Brum, C. H. Barriuello, V. A. Reguera, and M. A. Dalla Costa, "On the LED Illumination and Communication Design Space for Visible Light Communication," *IEEE Transactions on Industry Applications*, vol. 55, no. 3, pp. 3264–3273, 2019.
- [5] T. Kishi, H. Tanaka, Y. Umeda, and O. Takyu, "A high-speed LED driver that sweeps out the remaining carriers for visible light communications," *Journal of Lightwave Technology*, vol. 32, no. 2, pp. 239–249, 2014.
- [6] X. Deng, Y. Wu, K. Arulandu, G. Zhou, and J.-p. M. G. Linnartz, "Performance comparison for illumination and visible light communication system using buck converters," *2014 IEEE Globecom Workshops (GC Wkshps)*, pp. 547–552, 2014.
- [7] D. Karunatilaka, F. Zafar, V. Kalavally, and R. Parthiban, "LED Based Indoor Visible Light Communications: State of the Art," *IEEE Communications Surveys & Tutorials*, vol. 17, no. 3, pp. 1649–1678, 2015.
- [8] J. Sebastian, D. G. Lamar, D. G. Aller, J. Rodriguez, and P. F. Miaja, "On the Role of Power Electronics in Visible Light Communication," *IEEE Journal of Emerging and Selected Topics in Power Electronics*, vol. 6, no. 3, pp. 1210–1223, sep 2018.
- [9] Y. Gao, L. Li, and P. K. T. Mok, "An AC Input Inductor-Less LED Driver for Efficient Lighting and Visible Light Communication," *IEEE Journal of Solid-State Circuits*, pp. 1–13, 2018.
- [10] J. Rodríguez, D. G. Lamar, P. F. Miaja, D. G. Aller, and J. Sebastián, "Power Efficient VLC Transmitter Based on Pulse-Width Modulated DC-DC Converters and the Split of the Power," *IEEE Transactions on Power Electronics*, vol. 34, no. 2, pp. 1726 – 1743, 2019.
- [11] H. L. Minh, D. O. Brien, G. Faulkner, L. Zeng, K. Lee, D. Jung, and Y. Oh, "80 Mbit / s Visible Light Communications Using Pre-Equalized White LED," *2008 34th European Conference on Optical Communication*, vol. 5, no. September, pp. 1–2, 2008.
- [12] —, "High-Speed Visible Light Communications Using Multiple-Resonant Equalization," *IEEE Photonics Technology Letters*, vol. 20, no. 14, pp. 1243–1245, 2008.
- [13] J. Vucic, C. Kottke, S. Nerreter, K. Habel, a. Buttner, K.-D. Langer, and J. Walewski, "125 Mbit/s over 5 m wireless distance by use of OOK-Modulated phosphorescent white LEDs," *2009 35th European Conference on Optical Communication*, no. 1, pp. 9–10, 2009.
- [14] J. Vucic, C. Kottke, S. Nerreter, K.-d. D. Langer, and J. W. Walewski, "513 Mbit/s visible light communications link based on DMT-modulation of a white LED," *Journal of Lightwave Technology*, vol. 28, no. 24, pp. 3512–3518, 2010.
- [15] F. L. Jenq, T. J. Liu, and F. Y. Leu, "An AC LED smart lighting system with visible light time-division multiplexing free space optical communication," *Proceedings - 2011 5th International Conference on Innovative Mobile and Internet Services in Ubiquitous Computing, IMIS 2011*, pp. 589–593, 2011.
- [16] H. Tanaka, Y. Umeda, and O. Takyu, "High-Speed LED Driver for Visible Light Communications with Drawing-Out of Remaining Carrier," in *2011 IEEE Radio and Wireless Symposium*. IEEE, 2011, pp. 295–298.
- [17] A. Mirvakili and V. J. Koomson, "High efficiency LED driver design for concurrent data transmission and PWM dimming

- control for indoor visible light communication,” *2012 IEEE Photonics Society Summer Topical Meeting Series, PSST 2012*, vol. 2, pp. 132–133, 2012.
- [18] S. Zong, J. Wu, and X. He, “A Novel Method for Illumination and Communication Using White Led Lights,” in *6th IET International Conference on Conference: Power Electronics, Machines and Drives (PEMD 2012)*, no. 61174157, 2012.
- [19] N. Fujimoto and H. Mochizuki, “477 Mbit/s visible light transmission based on OOK-NRZ modulation using a single commercially available visible LED and a practical LED driver with a pre-emphasis circuit,” *Optical Fiber Communication Conference and Exposition and the National Fiber Optic Engineers Conference (OFC/NFOEC)*, 2013, pp. 1–3, 2013.
- [20] J. D. Mckendry, K. Henderson, E. Kelly, D. Dawson, C.-c. G.-b. Leds, S. Zhang, S. Watson, J. J. D. Mckendry, D. Massoubre, A. Cogman, R. K. Henderson, A. E. Kelly, and M. D. Dawson, “1.5 Gbit/s Multi-Channel Visible Light Communications Using CMOS-Controlled GaN-Based LEDs,” *Journal of Lightwave Technology*, 2013.
- [21] S. Zhao, J. Xu, and O. Trescases, “A dimmable LED driver for Visible Light Communication (VLC) based on LLC resonant DC-DC converter operating in burst mode,” in *2013 Twenty-Eighth Annual IEEE Applied Power Electronics Conference and Exposition*, 2013, pp. 2144–2150.
- [22] F. Che, B. Hussain, L. Wu, and C. P. Yue, “Design and implementation of IEEE 802.15.7 VLC PHY-I transceiver,” in *Proceedings - 2014 IEEE 12th International Conference on Solid-State and Integrated Circuit Technology, ICSICT 2014*, 2014, pp. 5–8.
- [23] Z. Dong, F. Lu, R. Ma, L. Wang, C. Zhang, G. Chen, A. Wang, and B. Zhao, “An integrated transmitter for LED-based visible light communication and positioning system in a 180nm BCD technology,” in *Proceedings of the IEEE Bipolar/BiCMOS Circuits and Technology Meeting*, 2014, pp. 84–87.
- [24] J. Sebastián, P. Fernández-Miaja, F. J. Ortega-González, M. Patiño, and M. Rodríguez, “Design of a Two-Phase Buck Converter With Fourth-Order Output Filter for Envelope Amplifiers of Limited Bandwidth,” *Transactions on Power Electronics*, vol. 29, no. 11, pp. 5933–5948, 2014.
- [25] S. Zhao, J. Xu, and O. Trescases, “Burst-Mode Resonant LLC Converter for an LED Luminaire With Integrated Visible Light Communication for Smart Buildings,” *IEEE Transactions on Power Electronics*, vol. 29, no. 8, pp. 4392–4402, 2014.
- [26] B. Hussain, F. Che, F. Zhang, T. S. Yim, L. Cheng, W.-h. Ki, C. P. Yue, and L. Wu, “A Fully Integrated IEEE 802.15.7 Visible Light Communication Transmitter with On-Chip 8-W 85 % Efficiency Boost LED Driver C216 C217,” *2015 Symposium on VLSI Circuits Digest of Technical Papers*, 2015.
- [27] A. V. N. Jalajakumari, K. Cameron, R. Henderson, D. Tsonev, and H. Haas, “An Energy Efficient High-Speed Digital LED Driver for Visible Light Communications,” in *IEEE ICC 2015 Conference Proceedings*, 2015, pp. 5054–5059.
- [28] H. Li, X. Chen, J. Guo, Z. Gao, and H. Chen, “An analog modulator for 460 MB/S visible light data transmission based on OOK-NRS modulation,” *IEEE Wireless Communications*, vol. 22, no. 2, pp. 68–73, 2015.
- [29] A. Tsiatmas, F. M. J. Willems, J. P. M. G. Linnartz, S. Baggen, and J. W. M. Bergmans, “Joint illumination and

- visible-Light Communication systems: Data rates and extra power consumption,” *2015 IEEE International Conference on Communication Workshop, ICCW 2015*, pp. 1380–1386, 2015.
- [30] C.-S. A. Gong, Y.-C. Lee, J.-L. Lai, C.-H. Yu, L. R. Huang, and C.-Y. Yang, “The High-efficiency LED Driver for Visible Light Communication Applications,” *Scientific Reports*, vol. 6, no. 1, p. 30991, 2016.
- [31] J. Kosman, O. Almer, A. V. N. Jalajakumari, S. Videv, and H. Haas, “60 Mb / s , 2 meters Visible Light Communications in 1 klx Ambient using an Unlensed CMOS SPAD Receiver,” *Photonics Society Summer Topical Meeting Series (SUM), 2016 IEEE*, vol. 1, pp. 171–172, 2016.
- [32] Y. Gao, L. Li, and P. K. T. Mok, “22.8 An AC-Input Inductorless LED Driver for Visible-Light-Communication Applications with 8Mb/s Data-Rate and 6.4% Low-Frequency Flicker,” in *2017 International Solid-State Circuits Conference Proceedings*, 2017, pp. 384–386.
- [33] M. Kong, Y. Chen, R. Sarwar, B. Sun, B. Cong, J. Xu, O. College, and Z. Road, “Optical Superimposition-based PAM-4 Signal Generation for Visible Light Communication,” in *2017 16th International Conference on Optical Communications and Networks (ICOON)*, 2017, pp. 16–18.
- [34] F. Loose, R. Duarte, C. H. Barriquello, M. A. D. Costa, L. Teixeira, and A. Campos, “Using the Inherent Ripple Waveform of a Synchronous Buck Converter for Visible Light Communication in LED Drivers,” in *10 Seminário de Eletrônica de Potência e Controle - SEPOC*, 2017, pp. 7–11.
- [35] K. Modepalli and L. Parsa, “Lighting Up with a Dual-Purpose Driver,” *2 IEEE Industry Applications Magazine*, no. March/April, pp. 2–12, 2017.
- [36] J. Rodriguez, D. G. Lamar, J. Sebastian, and P. F. Miaja, “Taking Advantage of the Output Voltage Ripple of a Two-Phase Buck Converter to Perform Quadrature Amplitude Modulation for Visible Light Communication,” *2017 IEEE Applied Power Electronics Conference and Exposition (APEC)*, no. Vlc, pp. 2116–2123, 2017.
- [37] J. Rodriguez, D. G. Aller, D. G. Lamar, and J. Sebastian, “Energy Efficient Visible Light Communication Transmitter Based on the Split of the Power,” *2017 IEEE Energy Conversion Congress and Exposition (ECCE)*, pp. 2420–2427, 2017.
- [38] X. Deng, Y. Wu, K. Arulandu, G. Zhou, and J.-p. M. G. Linnartz, “Performance Analysis for Joint Illumination and Visible Light Communication using Buck Driver,” *IEEE Transactions on Communications*, vol. 66, no. 5, pp. 2065–2078, 2018.
- [39] X. Deng, K. Arulandu, Y. Wu, S. Mardanikorani, G. Zhou, and J. P. M. Linnartz, “Modeling and Analysis of Transmitter Performance in Visible Light Communications,” *IEEE Transactions on Vehicular Technology*, vol. 68, no. 3, pp. 2316–2331, 2019.
- [40] A. Krohn, S. Pachnicke, and P. A. Hoeher, “Visible Light Communication with Multicarrier Modulation Utilizing a Buck-Converter Circuit as Efficient LED Driver,” in *Photonische Netze*, 2018, pp. 48–52.
- [41] F. Loose, L. Teixeira, R. R. Duarte, M. A. Dala Costa, C. H. Barriquello, M. A. Costa, and C. H. Barriquello, “On the Use of the Intrinsic Ripple of a Buck Converter for Visible Light Communication in LED Drivers,” *IEEE Journal of Emerging and Selected Topics in Power Electronics*, vol. 6, no. 3, pp. 1235–1245, 2018.
- [42] J. Rodriguez, D. G. Aller, D. G. Lamar, and J. Sebastian, “Performance evaluation of a VLC transmitter based on the

- split of the power,” in *2018 IEEE Applied Power Electronics Conference and Exposition (APEC)*. IEEE, mar 2018, pp. 1179–1186.
- [43] M. L. G. Salmento, G. M. Soares, J. M. Alonso, and H. A. C. Braga, “A Dimmable Off-line LED Driver with OOK-M-FSK Modulation for VLC Applications,” *IEEE Transactions on Industrial Electronics*, vol. 0046, no. c, pp. 1–1, 2018.
- [44] Z.-Y. Wu, Y.-L. Gao, J.-S. Wang, X.-Y. Liu, and J. Wang, “A Linear Current Driver for Efficient Illuminations and Visible Light Communications,” *Journal of Lightwave Technology*, vol. 36, no. 18, pp. 3959–3969, 2018.
- [45] M. Zhang, M. Zhang, D. Han, Z. Ghassemlooy, P. Luo, and Y. Zhang, “Real-Time 262-Mb / s Visible Light Communication With Digital Predistortion Real-Time 262-Mb / s Visible Light,” *IEEE Photonics Journal*, vol. 10, no. 3, pp. 1–10, 2018.
- [46] D. G. Aller, D. G. Lamar, P. F. Miaja, J. Rodríguez, and J. Sebastián, “Design of a Linear-Assisted VLC-LED Transmitter Based on Summing the Light,” in *Proceedings of 45th Annual Conference of the IEEE Industrial Electronics Society*, Lisbon, 2019, pp. 4128–4133.
- [47] J. Rodriguez, D. G. Lamar, D. G. Aller, P. F. Miaja, and J. Sebastian, “Reproducing Multi-Carrier Modulation Schemes for Visible Light Communication with the Ripple Modulation Technique,” *IEEE Transactions on Industrial Electronics*, no. Early access, 2019.
- [48] A. Al-Kinani, C. X. Wang, L. Zhou, and W. Zhang, “Optical wireless communication channel measurements and models,” *IEEE Communications Surveys and Tutorials*, vol. 20, no. 3, pp. 1939–1962, 2018.
- [49] L. E. M. Matheus, A. B. Vieira, L. F. M. Vieira, M. A. M. Vieira, and O. Gnawali, “Visible Light Communication: Concepts, Applications and Challenges,” *IEEE Communications Surveys & Tutorials*, vol. PP, no. c, pp. 1–1, 2019.
- [50] S. H. Lee, S.-Y. Jung, and J. K. Kwon, “Modulation and coding for dimmable visible light communication,” *Communications Magazine, IEEE*, vol. 53, no. 2, pp. 136–143, 2015.
- [51] M. Obeed, A. M. Salhab, M.-S. Alouini, and S. A. Zummo, “On Optimizing VLC Networks for Downlink Multi-User Transmission: A Survey,” *IEEE Communications Surveys & Tutorials*, vol. 21, no. 3, pp. 2947–2976, 2019.
- [52] A. Gupta, P. Garg, and N. Sharma, “Hard switching-based hybrid RF/VLC system and its performance evaluation,” *Transactions on Emerging Telecommunications Technologies*, vol. 30, no. 2, pp. 1–12, feb 2019.
- [53] S. Schmid, T. Bourchas, S. Mangold, and T. R. Gross, “Linux light bulbs: Enabling internet protocol connectivity for light bulb networks,” *VLCS 2015 - Proceedings of the 2nd International Workshop on Visible Light Communications Systems, co-located with MobiCom 2015*, pp. 3–8, 2015.
- [54] C.-I. Liao, Y.-f. Chang, C.-I. Ho, and M.-c. Wu, “High-Speed GaN-Based Blue Light-Emitting Diodes With Gallium-Doped ZnO Current Spreading Layer,” *IEEE Electron Device Letters*, vol. 34, no. 5, pp. 611–613, 2013.
- [55] C. Shen, “Visible Lasers and Emerging Color Converters for Lighting and Visible Light Communications,” in *Light, Energy and the Environment*. Washington, D.C.: OSA, 2017, p. SW3C.2.
- [56] A.-E. Marcu, R.-A. Dobre, and M. Vlădescu, “Investigation on Available Bandwidth in Visible- Light Communications,” in *IEEE 22nd International Symposium for Design and Technology in Electronic Packaging*, Oradea, 2016.



- [57] Y. Pei, S. Zhu, H. Yang, L. Zhao, X. Yi, J. Wang, and J. Li, "LED Modulation Characteristics in a Visible-Light Communication System," *Optics and Photonics Journal*, vol. 2013, no. 2011, pp. 139–142, 2013.
- [58] W. O. Popoola, "Impact of VLC on Light Emission Quality of White LEDs," *Journal of Lightwave Technology*, vol. 34, no. 10, pp. 2526–2532, 2016.
- [59] S. Mei, X. Liu, W. Zhang, R. Liu, L. Zheng, R. Guo, and P. Tian, "High-Bandwidth White-Light System Combining a Micro-LED with Perovskite Quantum Dots for Visible Light Communication," *ACS Applied Materials & Interfaces*, vol. 10, no. 6, pp. 5641–5648, feb 2018.
- [60] K. Xu, H.-Y. Yu, Y.-J. Zhu, and Y. Sun, "On the Ergodic Channel Capacity for Indoor Visible Light Communication Systems," *IEEE Access*, vol. 5, pp. 833–841, 2017.
- [61] M. S. Ab-Rahman, N. I. Shuhaimi, L. A. H. Azizan, and M. R. Hassan, "Analytical study of signal-to-noise ratio for visible light communication by using single source," *Journal of Computer Science*, vol. 8, no. 1, pp. 141–144, 2012.
- [62] A. Al-Kinani, C.-x. Wang, H. Haas, and Y. Yang, "Characterization and Modeling of Visible Light Communication Channels," in *2016 IEEE 83rd Vehicular Technology Conference (VTC Spring)*. IEEE, may 2016, pp. 1–5.
- [63] X. Ma, F. Yang, S. Liu, and J. Song, "Channel estimation for wideband underwater visible light communication: a compressive sensing perspective," *Optics Express*, vol. 26, no. 1, p. 311, 2018.
- [64] I. Stefan and H. Haas, "Analysis of Optimal Placement of LED Arrays for Visible Light Communication," *Vehicular Technology Conference (VTC Spring), 2013 IEEE 77th*, pp. 1–5, 2013.
- [65] T. Komine, S. Haruyama, and M. Nakagawa, "A study of shadowing on indoor visible-light wireless communication utilizing plural white LED lightings," *Wireless Personal Communications*, vol. 34, no. 1-2, pp. 211–225, 2005.
- [66] P. Shamsudheen, E. Sureshkumar, and J. Chunkath, "Performance Analysis of Visible Light Communication System for Free Space Optical Communication Link," *Procedia Technology*, vol. 24, pp. 827–833, 2016.
- [67] Z. Wang, D. Tsonev, S. Videv, and H. Haas, "On the Design of a Solar-Panel Receiver for Optical Wireless Communications With Simultaneous Energy Harvesting," *IEEE Journal on Selected Areas in Communications*, vol. 33, no. 8, pp. 1–12, 2015.
- [68] C. CHEN and W.-D. ZHONG, "Performance Comparison of Different Types of Receivers in Indoor MIMO-VLC Systems," in *Proceedings of the International Conference on Computer Networks and Communication Technology (CNCT 2016)*, no. February. Paris, France: Atlantis Press, 2017.
- [69] R. Bai, R. Jiang, T. Mao, W. Lei, and Z. Wang, "Iterative receiver for ADO-OFDM with near-optimal optical power allocation," *Optics Communications*, vol. 387, no. November 2016, pp. 350–356, 2017.
- [70] F. R. Bispo, "Using an LED as a Sensor and Visible Light Communication device in a Smart Illumination System," Ph.D. dissertation, Universidade Nova de Lisboa, 2015. [Online]. Available: <http://run.unl.pt//handle/10362/15627>
- [71] R. A. Martínez-Ciro, F. E. López-Giraldo, A. F. Betancur-Perez, and J. M. Luna-Rivera, "Design and Implementation of a Multi-Colour Visible Light Communication System Based on a Light-to-Frequency Receiver," *Photonics*, vol. 6, no. 2, p. 42, 2019.

- [72] Y. Liu, H.-Y. Chen, K. Liang, C.-W. Hsu, C.-W. Chow, and C.-H. Yeh, "Visible Light Communication Using Receivers of Camera Image Sensor and Solar Cell," *IEEE Photonics Journal*, vol. 8, no. 1, pp. 1–7, 2016.
- [73] K. Bandara, P. Niroopan, and Y. H. Chung, "PAPR reduced OFDM visible light communication using exponential nonlinear companding," *2013 IEEE International Conference on Microwaves, Communications, Antennas and Electronic Systems, COMCAS 2013*, no. October, pp. 21–23, 2013.
- [74] B. Bai, Z. Xu, and Y. Fan, "Joint LED dimming and high capacity visible light communication by overlapping PPM," *WOCC2010 Technical Program - The 19th Annual Wireless and Optical Communications Conference: Converging Communications Around the Pacific*, 2010.
- [75] M. S. A. Mossaad, S. Hranilovic, and L. Lampe, "Visible Light Communications Using OFDM and Multiple LEDs," *IEEE Trans. Commun.*, vol. 63, no. 11, pp. 4304–4313, 2015.
- [76] L. Kong, W. Xu, H. Zhang, C. Zhao, and X. You, "R-OFDM for RGBA-LED-Based Visible Light Communication With Illumination Constraints," *Journal of Lightwave Technology*, vol. 34, no. 23, pp. 5412–5422, 2016.
- [77] H.-C. Guo, Y.-F. Xu, X.-J. Li, L. Zhang, Y.-J. Wang, and N. Chi, "A high-speed phosphorescent LED-based visible light communication system utilizing SQGNRC precoding technique," *Photonic Network Communications*, 2017.
- [78] L. Teixeira, F. Loose, J. M. A. Álvarez, C. H. Barriquello, V. A. Reguera, and M. A. D. Costa, "Review of LED drivers for Visible Light Communication," in *Proceedings of 45th Annual Conference of the IEEE Industrial Electronics Society*, Lisbon, 2019, pp. 1–6.
- [79] E. F. Schubert, *Light-Emitting Diodes*. Cambridge, 2006.
- [80] S. M. Berman, D. S. GreenHouse, R. D. Clear, and W. R. Thomas, "Human electroretinogram responses to video displays, fluorescent lighting, and other high frequency sources." *Optometry and Vision Science*, vol. 68, pp. 645–662, 1991.
- [81] IEEE Power Electronics Society, "IEEE Recommended Practices for Modulating Current in High-Brightness LEDs for Mitigating Health Risks to Viewers," *IEEE Std 1789-2015*, pp. 1–80, 2015.
- [82] IEEE Computer Society, *IEEE Standard for Local and metropolitan area networks - Part 15.7: Short-Range Wireless Optical Communication Using Visible Light*. IEEE Computer Society, 2011, vol. 1, no. September.
- [83] Y. Hei, Y. Kou, G. Shi, W. Li, and H. Gu, "Energy-Spectral Efficiency Tradeoff in DCO-OFDM Visible Light Communication System," *IEEE Transactions on Vehicular Technology*, vol. 68, no. 10, pp. 9872–9882, oct 2019.
- [84] X. Li, R. Mardling, and J. Armstrong, "Channel Capacity of IM/DD Optical Communication Systems and of ACO-OFDM," in *2007 IEEE International Conference on Communications*. IEEE, jun 2007, pp. 2128–2133.
- [85] N. Fernando, Y. Hong, and E. Viterbo, "Flip-OFDM for unipolar communication systems," *IEEE Transactions on Communications*, vol. 60, no. 12, pp. 3726–3733, 2012.
- [86] D. Tsonev, S. Sinanovic, and H. Haas, "Novel unipolar orthogonal frequency division multiplexing (U-OFDM) for optical wireless," *IEEE Vehicular Technology Conference*, 2012.
- [87] S. K. A. Yaklaf and K. S. Tarmissi, "Multi-Carrier Modulation Techniques for Light Fidelity Technology," *2019 19th*

- International Conference on Sciences and Techniques of Automatic Control and Computer Engineering (STA)*, pp. 70–73, 2019.
- [88] A. Gupta and P. Garg, “Statistics of SNR for an Indoor VLC System and its Applications in System Performance,” *IEEE Communications Letters*, vol. PP, no. c, pp. 1–1, 2018.
- [89] I. J. Electron, C. Aeü, L. Qian, X. Chi, and L. Zhao, “Analysis of effective capacity for visible light communication systems with mobility support,” *Int. J. Electron. Commun. (AEÜ)*, vol. 88, no. September 2017, pp. 38–43, 2018.
- [90] ENERGY STAR, “ENERGY STAR Program Requirements for Computers Partner Commitments for Lamps (Light Bulbs).” p. 35, 2016. [Online]. Available: <https://www.energystar.gov/sites/default/files/specs/Version61ComputersFinalProgramRequirements.pdf>
- [91] IEC, “IEC 61000-3-2 Electromagnetic compatibility. Limits for harmonic current emissions (equipment input current lower than 16 A per phase),” 2018.
- [92] J. M. Alonso, D. Gacio, A. J. Calleja, F. Sichirollo, M. F. Da Silva, M. A. Costa, and R. N. Do Prado, “Reducing storage capacitance in off-line LED power supplies by using integrated converters,” *Conference Record - IAS Annual Meeting (IEEE Industry Applications Society)*, pp. 1–8, 2012.
- [93] F. H. Raab, P. Asbeck, S. Cripps, P. B. Kenington, Z. B. Popovic, N. Potheary, J. F. Sevic, and N. O. Sokal, “Power amplifiers and transmitters for RF and microwave,” *IEEE Transactions on Microwave Theory and Techniques*, vol. 50, no. 3, pp. 814–826, 2002.
- [94] D. Xu, “Topologies and Control Strategies of Very High Frequency Converters: A Survey,” *CPSS Transactions on Power Electronics and Applications*, vol. 2, no. 1, pp. 28–38, 2017.
- [95] O. GmbH, “OSRAM products,” 2018. [Online]. Available: [www.osram.com](http://www.osram.com)
- [96] TELECOMMUNICATION, S. SECTOR, and O. ITU, “H.264 : Advanced video coding for generic audiovisual services,” p. 812, 2017. [Online]. Available: <https://www.itu.int/rec/T-REC-H.264-201704-I>
- [97] S. Li, S. C. Tan, C. K. Lee, E. Waffenschmidt, S. Y. R. Hui, and C. K. Tse, “A Survey, Classification, and Critical Review of Light-Emitting Diode Drivers,” *IEEE Transactions on Power Electronics*, vol. 31, no. 2, pp. 1503–1516, 2016.
- [98] “JEITA Standards - Visible Light Communications,” 2019. [Online]. Available: [https://www.jeita.or.jp/cgi-bin/standard/\\_e/list.cgi?cateid=1{&}subcateid=50](https://www.jeita.or.jp/cgi-bin/standard/_e/list.cgi?cateid=1{&}subcateid=50)
- [99] N. Serafimovski, T. Baykas, and V. Jungnickel, “Status of IEEE 802 . 11 Light Communication TG,” 2019. [Online]. Available: <http://www.ieee802.org/11/Reports/tgbb{&}update.htm>
- [100] S. Title, A. M. Ofdm, D. Submitted, T. Baykas, M. Uysal, O. Narmanlioglu, R. Kizilirmak, and C. Aytac, “Project: IEEE P802.15 Working Group for Wireless Personal Area Networks (WPANs),” IEEE, Tech. Rep. July, 2019. [Online]. Available: <http://www.ieee802.org/15/pub/TG13.html>
- [101] “IEEE 802.15 WPANTM 15.7 Maintenance: Short-Range Optical Wireless Communications Task Group ( TG 7m ),” p. 2019, 2019. [Online]. Available: <http://www.ieee802.org/15/pub/IEEE802{&}15WPAN15{&}7Revision1TaskGroup.htm>
- [102] “Pure Lifi.” [Online]. Available: <https://purelifi.com/>

- [103] K. L. Bober, M. Emmelmann, V. Jungnickel, A. Corici, and D. Xiong, "LC-optimized PHY for TGbb," Fraunhofer Institute, TU Eindhoven, Tech. Rep. May, 2019. [Online]. Available: <http://www.ieee802.org/11/Reports/tgbb{#}update.htm{#}JUL19>



## **4 MANUSCRIPT 3 - ON THE LED ILLUMINATION AND COMMUNICATION DESIGN SPACE FOR VISIBLE LIGHT COMMUNICATION**

# On the LED Illumination and Communication Design Space for Visible Light Communication

Lucas Teixeira\*, Felipe Loose\*, João Paulo Brum\*

Carlos Henrique Barriquello\*, Vitalio Alfonso Reguera\*, Marco Antônio Dalla Costa\*

\*Universidade Federal de Santa Maria

Av. Roraima, 1000, Santa Maria, RS, Brazil

Email: teixeira@ieee.org

**Abstract**—Visible Light Communication (VLC) is a promising application for short-range wireless digital communications, presenting itself as a breakthrough for future lighting systems. The use of Light Emitting Diodes (LEDs) as transmitters by modulating their light intensity requires the correct design from both illumination and communication perspectives. However, in face of worldwide efforts for efficient energy consumption, the modulation of light imposes an energy cost that VLC cannot avoid. It has been shown that the modulation of light intensity brings unavoidable extra power expense. Thus, this paper brings a deeper analysis of the LED concerning its operating limits and efficacy with joint illumination and VLC intended modulations. The study uses a static photometrical, electrical and thermal model of the LEDs, in order to perform an analytical analysis regarding illumination and communication. Base modulation strategies supported by the IEEE 802.15.7 standard (PHY I and PHY II) were compared side-by-side with other classical modulation schemes, such as PAM, PSK, FSK, QAM and OFDM, from an energy conversion point of view. The results mark the design space connecting a set of possible modulation schemes with the desired average total light flux. This analysis guides the selection of the modulation technique according to the available power for a VLC system when efficacy is constrained. Moreover, the results show that the thermal effects not only reduce LED efficacy, but also constrict possible operating conditions regarding VLC in terms of communication signal power.

**Keywords**—Energy conversion, Light emitting diodes, Visible Light Communication.

## I. INTRODUCTION

In recent years the mobile applications and continuous growth of data rate has lead to a wide adoption of radio frequency (RF) as a communication medium. Hence, inside the available portion of the unlicensed spectrum, short-range technologies such as WLAN, ZigBee and Bluetooth are simultaneously disputing bandwidth among neighbor devices. Therefore, in dense urban scenarios, such effect is leading to a crowded RF spectrum, thus reducing the performance experienced by the users. In this context, Visible Light Communication (VLC) is presented as an alternative medium for wireless communications [1]. Moreover, it offers a series of advantages, such as intrinsic network security, high spatial reuse and also existing lighting infrastructure seamless adaptation [2].

The forward current of the LED modulates the instantaneous light flux ( $\phi(t)$ ), while the average perceived level of the

flux ( $\bar{\phi}$ ) is responsible for illumination intensity. In a scenario employing VLC, the fast modulation of the light emitted by the LEDs, imperceptible to human eyes, can be used to carry digital information without harming the lighting function. Furthermore, as a constraint, modulation of light shall be in a frequency range that avoids flicker effects, which may harm human health [3].

Literature shows that extra power is needed to reach the same irradiated light flux in LED devices when intentional modulation of light is performed [4][5][6]. A previous work [7] already explored, in an energy efficiency perspective, the behavior of the light-modulated LED. That study shows the space of possible stimuli shapes and ranges to satisfy communication metrics (available power for communication) and the cost to the overall efficacy of the device. The analysis of signal excursion over a typical LED shows the extra power spent for driving same LED with binary modulation (2-PAM) and continuous modulation (OFDM) [8]. Furthermore, extra power necessary to drive an LED using OFDM or 2-PAM modulation was estimated from the forward voltage curve [4], also extra power spent in the energy processing circuit was analysed. However, most of previous works were based on a linearized LED electrical model.

Different results arise from calculating extra power spent by light-modulated LEDs using more or less accurate models [6]. Nonetheless, extra attention must be given to the operating temperature of the device: the semiconductor radiating efficacy drops severely with the increase of temperature, which will also reduce lifespan and reliability [9][10]. Additionally, the maximum current stimuli provided to the LED device shall be limited for safe operating and lifespan. None of the aforementioned studies could address all those effects simultaneously. Given these reasons, there is still an open research gap when considering the space of possible modulation schemes applied to the LED light, concerning their impact on illumination aspects. Hence, based on the arguments aforementioned, this paper is focused on the analysis of the luminous efficacy of the LED ( $\eta$ , given in lumens per watt - lm/W) considering thermal conditions and intentional modulation of light for VLC. It is an extension of the previous work shown in [7].

This paper is organized as follows: Section II presents the LED electrical to optical energy conversion and related issues. Section III introduces aspects on modulation schemes for data transmission. Section IV presents the chosen metrics used in

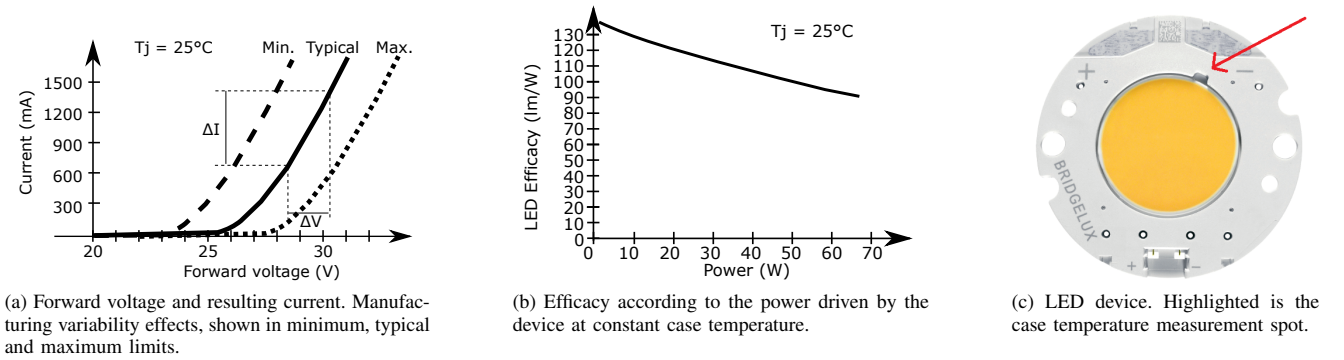


Fig. 1: Characterization of the LED .[11]

the analysis, also the experimental procedures and modeling. Section V presents simulation results and discussion. Finally, section VI closes the text with the main conclusions.

## II. ENERGY CONVERSION IN LEDs

Understanding the unique behavior of the LED load is highly relevant to its efficient power driving. Fig. 1 presents the LED basic electrical and optical characteristics. The characteristic impedance of the LED is strongly dependent on the operating temperature and semiconductor manufacturing variability. Moreover, due to its sharp voltage to current relation (low impedance after threshold is surpassed, see Fig. 1a), it is normally driven with current mode or from current controlled voltage supply.

In addition, another fundamental aspect on LEDs is seen in Fig. 1b, which is related to the global light emission efficacy. The curve flux vs. forward current is nonlinear, which is the result of the so-called Droop Effect (DE) [12]. This efficiency reduction is independent on the semiconductor temperature.

Additionally, the semiconductor operating temperature reduces the total irradiated light. As LED semiconductor temperature rises, it decreases the LED forward voltage (defined by the coefficient  $k_{VF}$ , presented in Table I), therefore reducing slightly its electrical power. However, this effect is weak when compared to the derate in the total irradiated light flux, defined by  $k_\phi$ , see Table I. Given these reasons, an LED operating at higher temperatures has lower luminous efficacy. This penalty adds up with the decrease in global efficacy when the driver performs any sort of intentional modulation of the LED current [6].

Furthermore, the two main functions of light modulation are dimming and data transmission. While the former controls the average light level, the latter includes information by changing instantaneous light flux. Dimming is a main feature required to most electronic LED based luminaires. This function allows flexible illumination conditions, increasing energy savings and also enhancing user experience. Hence, previous researches have already explored the consequences of the nonlinearities of LEDs, presenting several dimming methods to drive an LED

with a constant current source, regarding efficacy [13]. The methods can be classified into three categories: PWM Mode (PM), Amplitude Mode (AM) and Bilevel. These control methods are aimed to general illumination, but the same concerns on efficiency are also addressed later to VLC. Modulation strategies for dimming purposes were already deeply explored [13] [14][15], but for communication there are still few efforts reported. Therefore, next section describes some modulation schemes used to communication.

## III. MODULATION SCHEMES FOR COMMUNICATION

The choice of a particular modulation scheme deeply affects the performance of communications, such as data rate and power budget. The performance of the modulation depends on the Signal-to-Noise power Ratio (SNR). Therefore, it is possible to increase the data rate using extra signal power, under the same channel noise conditions. Thus, in VLC, one wants to design and maximize the level of irradiated power in the modulating signal in order to increase the SNR, therefore improving communication capacity [16][17], while keeping the  $\bar{\phi}$  constant for illumination purposes.

Moreover, modulation schemes capable of carrying several bits per transmitted symbol increase data rate, taking advantage of the available bandwidth and SNR. On the other hand, simple modulations, that carry only few bits per symbol, have less spectral efficiency, but require smaller values of SNR to reach the same Bit Error Ratio (BER) [18]. The available literature guided the selection of the modulation schemes for VLC presented in this study. First, carrierless modulations are addressed, followed by the carrier-based ones. The schemes are given in terms of a current stimulus.

*a) Pulse Amplitude Modulation (PAM):* the information is conveyed in discrete levels of the signal; 2, 4 or 8 levels are used; the rectangular pulses are generated at 100% duty cycle (D) [4][19][20]. In this sense, the On-Off Keying (OOK), used in IEEE 802.15.7 [21], is a particular case of 2-PAM.

*b) Variable Pulse Position Modulation (VPPM):* this scheme uses rectangular pulses, and information is conveyed into its position inside a symbol period [19][22]. VPPM allows



dimming by regulating the duty cycle of the pulse. IEEE 801.15.7 defines 12 discrete duty cycle steps for this function and recommends a 2-VPPM bit load.

The following carrier-based modulations are included in the study:

*c) Phase Shift Keying (PSK) and Frequency Shift Keying (FSK):* in this case both modulation schemes use sinusoidal carriers [19][23]. While using phase or frequency hops for modulating data, the amplitude of the signal remains constant for each symbol.

*d) Quadrature Amplitude Modulation (QAM):* using sinusoidal carrier, the possible combinations of phase and amplitude are used to create a set of symbols for transmission, usually displayed in the form of constellation diagrams [19][24].

*e) Orthogonal Frequency Division Multiplexing (OFDM):* it is a multi-carrier modulation technique that uses a set of orthogonal sinusoidal signals independently modulated [2][4][24]. Direct Current biased Optical OFDM (DCO-OFDM) [25] was used.. The distribution of signal intensity tends to a Gaussian shape, because of independent modulations and the simultaneous presence of several carriers. Therefore, it can be analyzed by the probability of the signal exceeding a given threshold. Hence, the Complementary Cumulative Distribution Function (CCDF) is used to calculate this threshold from the acceptable clipping probability [26]. In this sense, signal power was limited in such a way that at most 0.2% of samples are clipped.

In what follows, the analysis of further penalties in overall efficacy of a lighting system with VLC will be based on the above described.

#### A. Considerations on selecting the modulation strategy

First, the selection of the modulation scheme for VLC must avoid flicker and consider dimming possibility. Second, among the ones mentioned, PSK, FSK and 2-VPPM encoding ensure no spectral content at lower frequencies, regardless of data. Thus, they are naturally flicker free, if one correctly selects the symbol period. On the other hand, OFDM, QAM and PAM have variable amplitude excursion, which is dependent on the data content and are affected by the nonlinear relation of current to light flux. Hence, due to intermodulation, such effects may result in lower frequency content in the light intensity, which may cause flicker.

Moreover, considering dimming feature, VPPM allows the change of average illumination by means of changing the pulse width. FSK, PSK and QAM have no DC content and require a superimposed constant value to control the average light flux. PAM pulses do not have the same average value over a symbol period, since they are dependent on the amplitude of the pulse. In this case, it allows dimming by using channel encoding methods on the data transmitted. Additionally, carrier-based modulations are preferable when one wants to avoid both  $1/f$  noise and flicker effect.

#### B. Limit values for the LED current

For safety and lifespan conditions, lighting LEDs shall operate in limited conditions of instantaneous current, occasionally

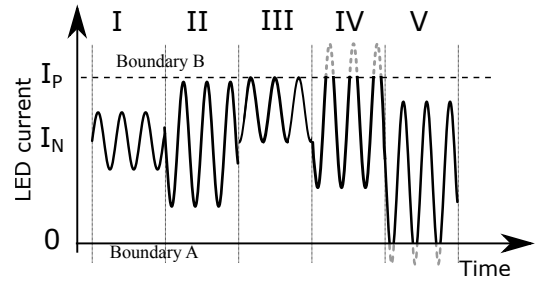


Fig. 2: Time domain  $k_{AC}$  and  $k_{DC}$  levels and clipping.

defined by a maximum value. Moreover, signal clipping may happen at zero current or at very high current levels. To avoid this effect on modulated pulses with negative values, DC biasing must be provided to the LED current. In this sense, the maximum allowed current level ( $I_P$ ) is indicated by the LED manufacturer to avoid catastrophic failure of the device.

Therefore, there is a trade-off between DC biasing and signal alternating components in order to limit the current range. To clarify this dependence, Fig. 2 depicts an example with five current patterns that can be applied to the LED. In the first and the second patterns (I and II), the same average value ( $I_N$ ) has a superimposed modulation, with different AC power, with pattern II being the double of pattern I. Patterns III and IV have also the same average current with superimposed AC amplitudes, except they are clipped. Moreover, clipping occurs in pattern IV because it exceeds  $I_P$ ; this operating limit is herein named Boundary B. In pattern V, the DC bias is not enough to avoid negative current levels and clipping also occurs at zero level. This operating limit is named Boundary A.

Both clipping effects shown in patterns IV and V generate pronounced distortion that may cause loss of information. These effects are further explored in Section IV-E. Therefore, in this study, clipping conditions are undesirable and a design space is defined by the operating points within Boundary A and Boundary B.

## IV. METHODOLOGY

The analysis performed in this study is as follows: The main goal is to depict LED actual performance towards current stimuli and operating temperature considering the boundaries and modulations aforementioned. The focus concerns the LED energy conversion efficacy. For this analysis, simulations used an LED static model with instantaneous current ( $i(t)$ ) as an input stimulus.

This study covers both electrical and optical domains. The effects caused by the geometry of the LED and the optical channel propagation impairments are not considered. A comprehensive study of these effects can be found in [2]. The thermal effects are simulated as a result from the surrounding temperature ( $T_{ENV}$ ), the heat sink thermal resistance ( $R_{CA}$ ) and the heat produced by the device. No dynamic effect is considered, hence the steady state temperature is used.

Moreover, the model is memoryless and with no bandwidth limitations. Next section presents the set of metrics chosen to analyze illumination and communication simultaneously, as well as the system model and parameters used in the study.

#### A. Metrics

The main performance metric from the LED output is light flux, measured in lumens (lm). For illumination, the useful light flux is therefore the average value ( $\overline{\phi}$ ). The power of the communication signal is only the AC part  $\phi_\sigma$  (lm) of the light flux. This power is calculated from the RMS light flux, according to (1), in which  $t_o$  and  $t_f$  stand for begin and end times of signal sample, respectively. Mathematically, one may relate (1) as the standard deviation of  $\phi(t)$ . It is known that a strong nonlinear relation exists between  $i(t)$  and  $\phi(t)$ , therefore causing distortion on the communication signal generated. In consequence, this study focuses on the light flux  $\phi_\sigma$  as the communication metric.

$$\phi_\sigma = \sqrt{\left(\frac{1}{t_f - t_o} \int_{t_o}^{t_f} [\phi(t)]^2 dt\right) - (\overline{\phi})^2} \quad (1)$$

LED efficacy is calculated from (2) and expressed in lm/W, where  $P_E$  is the averaged electric power delivered to the LED.

$$\eta = \frac{\overline{\phi}}{P_E} \quad (2)$$

Either metrics, signal power, light flux or efficacy, can also be shown in a normalized form, according to  $\phi_n$  or  $\eta_n$ , displayed in Table I.

#### B. LED complete model

The LED model follows classical electrical, photometrical and thermal concepts [27]. Electric current and voltage ( $V_F$ ) have their instantaneous value. While the electric power is given in terms of its average. For the photometrical variables, instantaneous and averaged light flux are considered. The instantaneous total light flux is here preferred, because the light intensity depends on the LED and receiver geometrical characteristics, along with the separation distance. In the thermal model the temperature increases linearly with  $P_E$  and the equilibrium operating temperature ( $T_C$ , static) is determined in the calculations. The following relations among all the physical quantities are in (3) to (7), forming the set of equations to be solved. See symbols in Table I.

$$V_F(t) = V_{FP}(i(t)) + k_{VF} \cdot (T_C - T_N) \quad (3)$$

$$\phi(t) = \phi_P(i(t)) \cdot (1 + k_\phi \cdot (T_C - T_N)) \cdot \phi_n \quad (4)$$

$$P_E = \overline{V_F(t) \cdot i(t)} \quad (5)$$

$$P_{RAD} = k_{RAD} \cdot \overline{\phi(t)} \quad (6)$$

Table I: LED parameters, after measurements and calibration.

Parameter	Value
Nominal forward voltage	29.5 V
$V_F$ temperature coefficient - $k_{VF}$	-0.15mV/ $^\circ$ C
Nominal forward current - $I_n$	1.05A
Maximum $i$ - $I_P$	2.10 A
Nominal light flux - $\phi_n$	4000lm
Proportion among $\phi$ and radiated power - $k_{RAD}$	0.0031W/lm
$\phi$ derate coefficient - $k_\phi$	-0.213%/ $^\circ$ C
Nominal efficacy - $\eta_n$	129.1lm/W
Heat sink thermal resistance - $R_{CA}$	2.25 $^\circ$ C/W
Calibration environment temperature	21.7 $^\circ$ C
Nominal case temperature - $T_N$	25.0 $^\circ$ C
Maximum case temperature	105.0 $^\circ$ C

$$T_C = R_{CA} \cdot (P_E - P_{RAD}) + T_{ENV} \quad (7)$$

$V_{FP}(i)$  stands for the polynomial regression representing forward voltage to instantaneous LED current, at constant case temperature  $T_N$ , shown in Fig. 1a. Likewise,  $\phi_P(i)$  stands for the polynomial regression of light flux in function of current (at  $T_N$ ) normalized to  $\phi_n$ . The overline notation ( $\overline{\cdot}$ ) stands for average over time. Radiated power ( $P_{RAD}$ ) is the amount of energy converted to light and radiated, calculated with (6).

This model is not a linearization in the LED electrical behavior near the operating point, as is commonly found in literature [6][22][25]. In fact, it is an accurate modeling of the actual nonlinear relations. The solution of this model is performed by finding the equilibrium operating temperature in order to calculate the aforementioned metrics.

#### C. Model calibration

In order to better match this model to the real device and heat sink, the first step was to conduct a series of experiments considering  $\phi$ ,  $T_C$  and  $V_F$ . These experiments were meant to reduce mismatch in manufacturing uncertainty of parameters and aging effects with respect to the LED datasheet [11].

The device under test was a Bridgelux Vero 18 array series COB LED, part number BXRC-50C4000-F-24, shown in Fig. 1c. Due to low thermal resistance (junction to case), the manufacturer provides data about efficacy and operation limit regarding to the case temperature. This quantity is measured in the specific spot highlighted in Fig. 1c. Table I presents all parameters obtained from the LED.

As the first step for calibration, the LED device was attached to a suitable heat sink and it was stimulated with several different modulated current waveforms. During this experiment, measurements of environment and case temperature were recorded. The inertia of the thermal quantities is much slower than the current stimuli, therefore those measurements took place after thermal operating conditions were stabilized (temperature change rate  $< 0.1^\circ$ C/min). Each operating point has a modulation shape and superimposed average level, as defined in Section IV-D; a total of 106 operating conditions were tested.

Additionally, the instantaneous light and the electrical parameters of instantaneous forward voltage and current were measured. Also, the total light flux (average) was determined

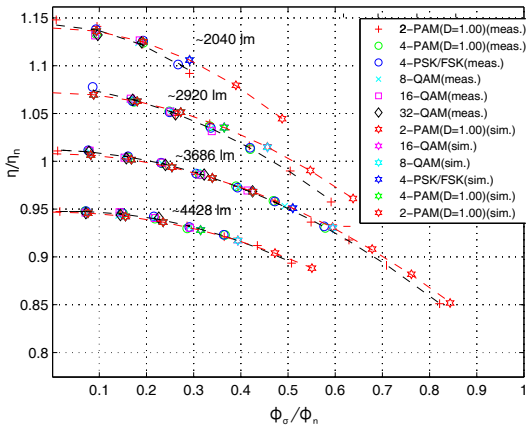


Fig. 3: Real device measurements and simulation results.

by using an integrating sphere with a calibrated spectrophotometer (model Inventifine CMS-5000).

It was also acquired the instantaneous light with a light-to-voltage sensor to analyze the resulting communication signal. The transducer used is a photodiode [28] along with a transimpedance amplifier [29]. It has the bandwidth much wider than the signals applied. The instantaneous total light flux ( $\phi(t)$ ) is estimated with the aid of the light-to-voltage measurements and the corresponding measurement of average light flux.

The forward voltage of the model (for current and temperature) was adjusted according to the measured data. In this case, the nominal light flux ( $\phi_n$ ), at case temperature of 25°C, was found to be 4000 lm. The curve  $V_F(i)$  was obtained up to the maximum allowed device DC current ( $I_P$ , Boundary B).

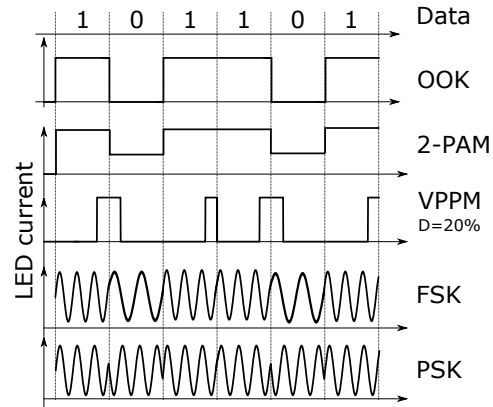
From the measured AC light signal and efficacy it was possible to compare these operating conditions. This result is shown in Fig. 3. It shows different modulation results for four average light flux measurements. Those results were based in several modulations schemes and they show a reasonable match between modeled and physical device.

#### D. Description of the generated current signal

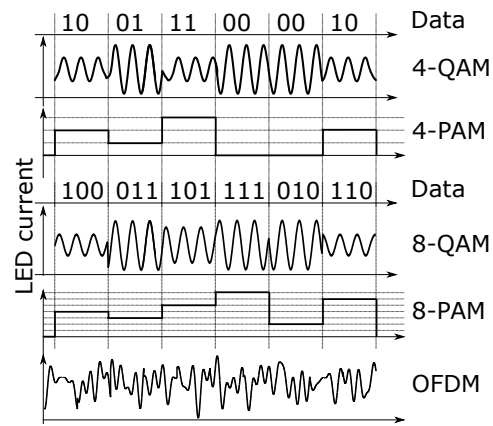
To build a set of current stimuli, first a signal intensity sample ( $sa(t)$ ) is defined for each modulation scheme. Each test signal contains all the possible symbols for a selected modulation scheme. It is assumed that the symbols are equiprobable. The pulse shapes do not have the restriction of non negative values. They only represent the communication part of the signal, as described in Section III.

Furthermore, to define different values of  $\phi_\sigma$ , the sample was scaled by a constant ( $k_{AC}$  level, unit is ampere,  $\{k_{AC} \in \mathbb{R}, k_{AC} \geq 0\}$ ). To build the complete stimulus waveforms, DC biasing ( $k_{DC}$ , also unit ampere,  $\{k_{DC} \in \mathbb{R}, k_{DC} \geq 0\}$ ) is added to the sample, according to (8).

$$i(t) = k_{AC}.sa(t) + k_{DC} \quad (8)$$



(a) Binary encoding and modulation schemes.



(b) N-level bit loaded modulation schemes.

Fig. 4: Modulated current samples.

However, not all combination of  $k_{AC}$  and  $k_{DC}$  levels are valid, because some of them exceeded the limits defined (boundaries A and B). Fig. 4 shows examples of current stimuli generated following this methodology for all the modulations. Therefore it is convenient to find the required relations among  $k_{AC}$  level,  $k_{DC}$  level, LED limits and the signal sample shape ( $sa(t)$ ). Those are explored next.

#### E. Limit operating conditions

The  $k_{AC}$  and  $k_{DC}$  levels are defined to simulate the boundary conditions of operation, aiming to outline the possible design area constrained by LED efficacy, average light flux and communication signal power. Indeed, the boundaries explained in III-B limit the possible operating area.

Maximum  $k_{AC}$  level is restricted to the range described in (9) and (10). The first is due to maximum current in LED (Boundary B), in case  $\max[sa(t)] > 0$ . The second is, for  $\min[sa(t)] < 0$ , due to zero current (Boundary A), where  $\max[\cdot]$  stands for maximum value of signal,  $\min[\cdot]$  stands for minimum.

$$k_{AC} \leq \frac{I_P - k_{DC}}{\max[sa(t)]} \quad (9)$$

$$k_{AC} \leq \frac{-k_{DC}}{\min[sa(t)]} \quad (10)$$

Moreover, there is a third limit condition regarding the LED case temperature, which refers to maximum semiconductor junction temperature ( $T_j$ ), and here it is named Boundary C. It affects operating conditions when  $\bar{\phi}$  is higher than the nominal or when  $R_{CA}$  is wrongly designed. In case this limit is slightly exceeded, it may harm LED expected lifespan and decrease energy efficiency. In the same way, at higher temperatures, it can cause device failure and permanent damage.

Finally, evaluating the three limiting factors, it is possible to define the area in which the LED device can operate and also the total light flux in each case. The next section brings a set of different results in order to provide enough basis to understand the relations among LED efficacy, total light flux and modulation.

## V. RESULTS AND DISCUSSION

The ranges of operating points are defined according to current stimuli parameters (modulation,  $k_{AC}$  and  $k_{DC}$  levels) and limited by instantaneous current level and case temperature. The following five sections are focused on showing a pertinent aspect to support the research findings.

### A. Modulation design space

This section describes the effect of modulation type 2-PAM, at a range of  $k_{DC}$  and imposing the limits described in Section IV-E. To show the possible range of solutions, the three variables are presented in different planes. Fig. 5 and Fig. 6 depict resulting signal power and LED efficacy, respectively, for  $\bar{\phi}/\phi_n$ . These plots show the interdependence of  $\eta$ ,  $\phi_\sigma$  and  $\bar{\phi}$ . As an specific case of 2-PAM, OOK has a very limited operating range, which is also shown in this figure.

Both results are over the same  $R_{CA}$  and  $T_{ENV}$  conditions in calibration condition, see Table I. For instance, if one wants to hold a defined  $\eta/\eta_n = 0.98$ , one must follow the correspondent dashed curve in Fig. 5. All the points over this curve would ensure this efficacy while changing  $\phi_\sigma$  and  $\bar{\phi}$  simultaneously. Likewise, Fig. 6 shows the efficacy in function of  $\bar{\phi}/\phi_n$ . Therefore, the choice of  $\bar{\phi}/\phi_n$  must be within the shaded area of Fig. 6 to guarantee both VLC and lighting. Moreover, in Fig. 5, boundary at  $\phi_\sigma = 0$  (no modulation) is in the bottom of this plane.

It is also clear that the case temperature (Boundary C) imposes a slight restriction to the maximum light flux ( $\bar{\phi}/\phi_n=1.43$ ). Beyond this condition efficacy would fall below 80% of  $\eta_n$ , also imposing hazardous operation to the device.

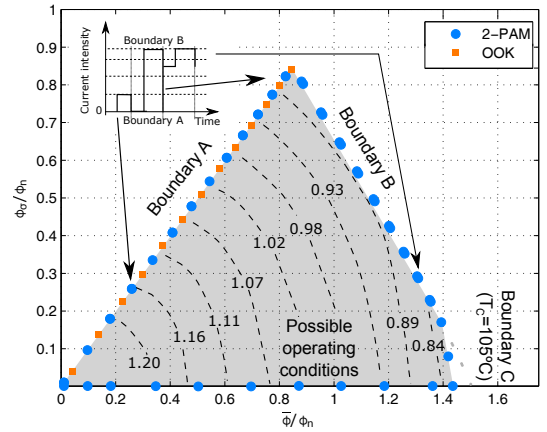


Fig. 5: Space of normalized signal intensity, according to total light flux. In detail, example of pulse shapes at three operating conditions. Dashed lines show constant efficacy curves ( $\eta/\eta_n$ ).

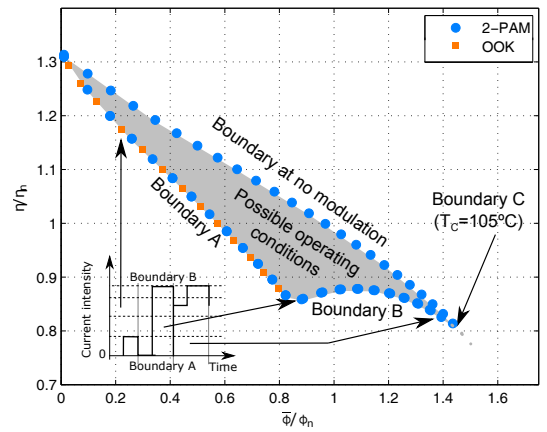


Fig. 6: LED efficacy according to total light flux. Gray dotted area depicts projection of operating points that exceeded Boundary C.

### B. Heat sink and the thermal limit

The following results are brought to show the effects of heat sink design. Fig. 7 and Fig. 8 show the change of Boundary C by varying  $R_{CA}$ . A reduction in the maximum  $\bar{\phi}/\phi_n$  from 1.15 to 0.78 with  $R_{CA}$  3 and 5 °C/W, respectively, can be observed.

There is no thermal restriction when  $R_{CA}$  is 1°C/W. In this case the heat sink is oversized and  $T_C$  would not reach its maximum value allowed. The limits due to current level still apply. However, as expected, these are the conditions to maximum signal strength and higher efficacy. Therefore, for the case when  $R_{CA} = 5$  °C/W, the model shows that maximum current could not achieve boundary B due to overheating. Additionally, Fig. 8 confirms the drop of efficacy that results from heating of the LED junction. Not only higher efficacy can

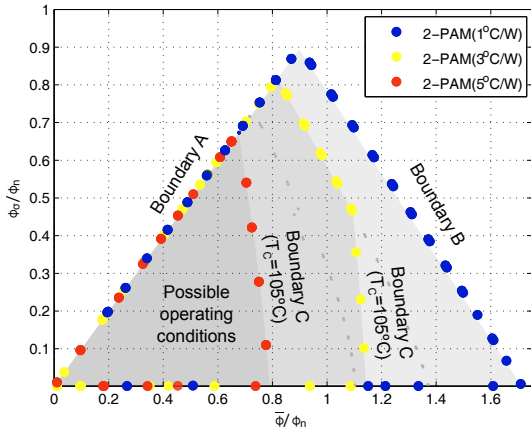


Fig. 7: Space of normalized signal intensity, according to total light flux. Effect of  $R_{CA}$  from 1 to 5  $^{\circ}C/W$  heat sink.

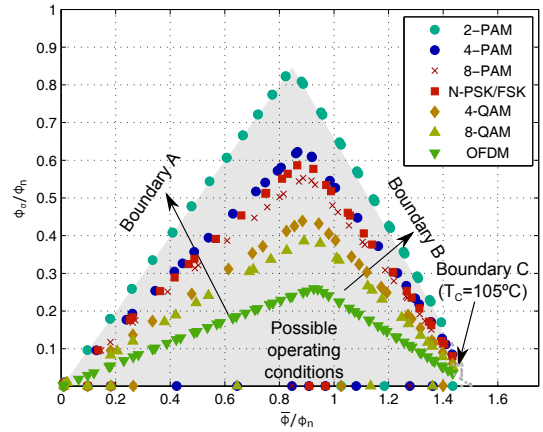


Fig. 9: Space of signal power for different modulation strategies.  $R_{CA} = 2.25^{\circ}C/W$

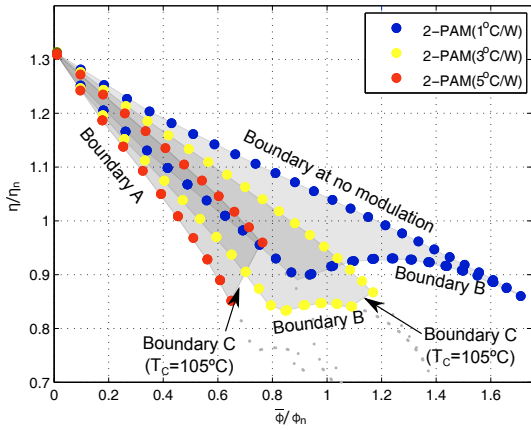


Fig. 8: LED efficacy according to total light flux. Effect of  $R_{CA}$  from 1 to 5  $^{\circ}C/W$  heat sink.

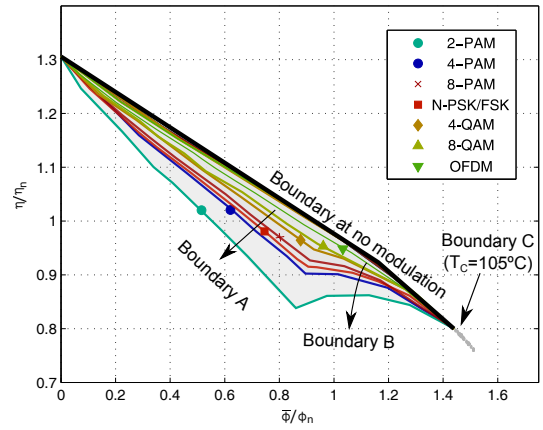


Fig. 10: LED efficacy according to total light flux for different modulation strategies.  $R_{CA} = 2.25^{\circ}C/W$

be achieved by adequate thermal design, but also dimming and range for the communication signal is enlarged. Hence, in order to expand and verify such effects for the other modulation schemes, next section presents different design spaces.

### C. Comparison among modulation strategies

The group of results in Fig. 9 and Fig. 10 show the performance of different modulation strategies and pulse shapes. In this case, 4- and 8-QAM have 2 and 4 amplitude levels, respectively. Reference [7] showed that modulation strategies with higher spectral efficiency can reach lower  $\phi_{\sigma}$ . This is consistent with the results presented here, showing that schemes with higher spectral efficiency (4- and 8-PAM, 4- and 8-QAM) have reduced  $\phi_{\sigma}$  when compared to their counterparts (2-PAM and 2-QAM). Furthermore, the 2-PAM signal can reach higher signal power compared to the other schemes.

On the other hand, the higher signal power comes along with smaller efficacy values. It is important to highlight the distances and cost of peak modulation. For instance, in the case of 2-PAM and 8-QAM, comparing the peak signal power the first has +6.4dB of  $\phi_{\sigma}$  ( $\times 2.1$ ) at the cost of extra 12.16%  $\eta$  drop. Moreover, the OFDM scheme was found to be the most affected by the Boundaries A and B, thus having the lower signal power among all, its peak performed was only 30% of maximum signal power that 2-PAM can reach.

### D. Temperature versus modulation derates

As mentioned earlier, efficacy may drop according to temperature increase and also with communication signal power increase. There is no fair way to separate completely these effects since they are interdependent, as explained in IV-B. However, starting from the analysis of (4) and simulations under the defined conditions, some comparisons were performed.

Table II: Comparison between limiting conditions at no modulation and maximum modulation strength (2-PAM),  $\phi/\phi_n = 0.64$ .

$R_{CA}$ ( $^{\circ}C/W$ )	$\Delta T_C$ ( $^{\circ}C$ )	$k_{\phi} \cdot \Delta T_C$ (%)	$\Delta \eta$ (%)
0.00	0.00	-0.00	-11.78
0.50	0.92	-0.20	-11.86
1.00	2.42	-0.52	-12.87
1.50	3.64	-0.78	-12.99
2.00	5.09	-1.09	-13.43
2.50	6.39	-1.36	-13.56
3.00	8.03	-1.71	-14.00
3.50	9.40	-2.00	-14.13
4.00	13.27	-2.83	-15.45
4.50	15.55	-3.32	-15.93
5.00	20.58	-4.39	-17.39

The factor including temperature in (4) is  $(1 + k_{\phi} \cdot (T_C - T_N))$ . Analyzing this part, it is possible to estimate the decrease caused in  $\bar{\phi}$  by the temperature ( $k_{\phi} \cdot \Delta T_C$ ), which can be used to compare operating conditions according to a difference between their temperatures ( $\Delta T_C$ ). Also, from any pair of operating points selected, it is possible to calculate the total light flux derate ( $\Delta \eta$ ) caused by current modulation and temperature from  $\eta/\eta_n$ . The difference between  $k_{\phi} \cdot \Delta T_C$  and  $\Delta \eta$  is roughly the effect of  $\phi_P(i)$  in (4), which corresponds to the losses due to modulation. Thus, the simulations were performed at  $\bar{\phi} = 0.64\phi_n$ , which is limited by maximum  $T_C$  in the worst  $R_{CA}$  case. Table II presents these results.

From Table II the isolated contribution of current modulation is depicted in the case  $R_{CA} = 0^{\circ}C/W$ . This drop concerns the nonlinearity of the LED and corresponds to  $-11.78\%$  in  $\eta$ . Moreover, the increase of only  $6.39^{\circ}C$  in  $T_C$  ( $R_{CA} = 2.5^{\circ}C/W$ ) represented a  $1.36\%$  decrease in  $\bar{\phi}$  (10% of  $\Delta \eta$ ). In this condition, there is a balance between heat sink size and operating efficacy, but leads to the conclusion that temperature contributes only to a small part of the efficacy losses. Finally, the condition when  $R_{CA} = 5.0^{\circ}C/W$  is the worst scenario, in which a severe restriction to  $\bar{\phi}$  is applied due to maximum  $T_C$ , as a result of a bad thermal design. Even in this case, the overheat caused by modulation is still producing only  $4.39\%$  decrease in  $\bar{\phi}$  and the total loss of  $\eta$  was found to be  $17.39\%$ . The decrease due to temperature represents roughly  $1/4$  (25, 2%) of the total drop of efficacy. Therefore, the effect of current modulation, due to  $\phi_P(i)$ , dominates the extra loss.

#### E. VPPM duty-cycle flexibility

The VPPM modulation has an additional degree of freedom due to the signal duty cycle (D) that changes the pulse shape, while  $k_{AC}$  and  $k_{DC}$  levels are also variables. In Fig. 11 and Fig. 12 there are results with five values for D. Those results show that boundaries A and B are flexible accordingly to D.

Finally, the thermal limit (i.e. the rightmost limit) was similar to the other schemes shown. However, the signal power can be maximized for any light flux by setting the modulation duty cycle appropriately. In contrast, the other modulation strategies do not have such flexibility, therefore the maximum signal power is achieved only at a fixed light flux. This leads

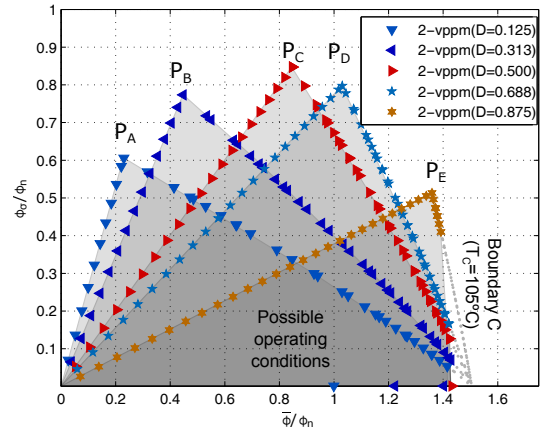


Fig. 11: Space of normalized signal power VPPM.  $R_{CA} = 2.25^{\circ}C/W$

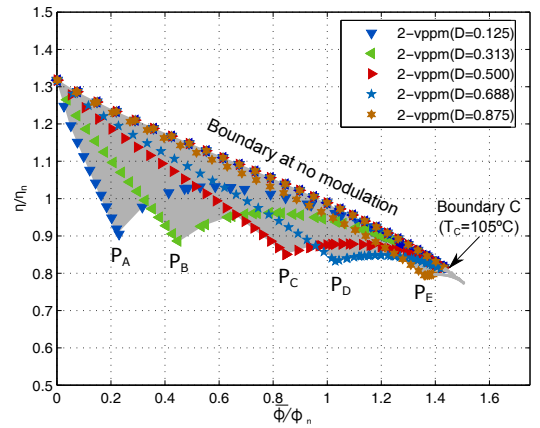


Fig. 12: LED efficacy according to total light flux.  $R_{CA} = 2.25^{\circ}C/W$

to a conclusion that VPPM is a very favorable modulation strategy to maximize communication signal strength.

On the other hand, those peak signal strength operating conditions (labeled  $P_A$ - $P_E$  in Fig. 11) are the same minimum efficacy conditions also labeled in Fig. 12. Therefore, these results again illustrate the trade-off between illumination efficacy and communication.

## VI. CONCLUSIONS

This work explored the limitations in the communication signal that can be imposed in VLC using an LED as a transmitter. In this scenario, modulation of the LED current for data transmission affects the overall efficacy of the device. The results show how the available range of instantaneous light flux is bounded by the LED current values (zero and maximum) and the semiconductor junction temperature. The design space proposed in this work relates efficacy, average light flux and

the power available for communication. The interdependence of these relations are linked with the choice of modulation schemes to be used.

Within the observed modulation schemes, the range of excursion of the LED current severely limits the light signal ( $\phi_\sigma$ ), specially at low or high average light flux ranges. Such aspect leads to bad communication performance over dimming range. However, for VPPM scheme this limitation is less pronounced, suggesting the clear advantage over others, due to the extra degree of freedom.

Furthermore, by using the thermal model of the LED, the average light flux that can be reached in VLC systems was clearly defined. The analysis shows that there is a noticeable drop in efficacy due to the nonlinear behavior of the LED when modulation is present. At the cost of few dBs of signal power ( $\phi_\sigma$ ) any modulation among the selected can be used with little drop of the efficacy (<2%). However, less spectrally efficient schemes reach greater  $\phi_\sigma$ , at the expense of a drop in LED efficacy of up to 20%. Such penalty should not be neglected, since this effect contributes to higher losses when compared to the losses caused by the temperature increase. Also, the raw temperature effect was estimated to be responsible of roughly  $\frac{1}{4}$  of the efficacy drop within the design space. Therefore, the nonlinearity of the LED light-to-current curve ( $\phi_P(i)$ ) dominates the efficacy drop observed.

Finally, the experimental results presented in this work show that when power LEDs are used for VLC, the current technology imposes significant constraints regarding illumination and communication. Therefore, real world applications of mixed VLC and lighting must account for those aspects, in order to properly develop a reliable and efficient lighting system with dual capabilities.

#### ACKNOWLEDGMENT

This work was supported by Brazilian government through PROEX program, PRPGP/UFMS, INCT-GD, CAPES proc 23038.000776/2017-54, CNPq proc 465640/2014-1, FAPERGS proc 17/2551-0000517-1. This study was financed in part by the Coordenação de Aperfeiçoamento de Pessoal de Nível Superior - Brasil (CAPES) - Finance Code 001.

#### REFERENCES

- [1] S. Shao, A. Khreishah, M. Ayyash, M. B. Rahaim, H. Elgala, V. Jungnickel, D. Schulz, and T. D. C. Little, "Design of a visible-light-communication enhanced WiFi system," *CoRR*, vol. 7, no. 10, pp. 960–973, 2015. [Online]. Available: <http://arxiv.org/abs/1503.02367>
- [2] D. Karunatilaka, F. Zafar, V. Kalavally, and R. Parthiban, "LED Based Indoor Visible Light Communications: State of the Art," *IEEE Communications Surveys & Tutorials*, vol. 17, no. 3, pp. 1649–1678, 2015. [Online]. Available: <http://ieeexplore.ieee.org/lpdocs/epic03/wrapper.htm?arnumber=7072557>
- [3] S. M. Berman, D. S. GreenHouse, R. D. Clear, and W. R. Thomas, "Human electroretinogram responses to video displays, fluorescent lighting, and other high frequency sources." *Optometry and Vision Science*, vol. 68, pp. 645–662, 1991.
- [4] X. Deng and J.-p. M. G. Linnartz, "Poster : Model of extra power in the transmitter for high-speed visible light communication," in *2016 Symposium on Communications and Vehicular Technologies (SCVT)*. Mons: IEEE, 2016.
- [5] X. Deng, Y. Wu, K. Arulandu, G. Zhou, and J.-p. M. G. Linnartz, "Performance Analysis for Joint Illumination and Visible Light Communication using Buck Driver," *IEEE Transactions on Communications*, vol. PP, no. 99, pp. 547–552, 2017.
- [6] A. Tsiatmas, F. M. J. Willems, J. P. M. G. Linnartz, S. Baggen, and J. W. M. Bergmans, "Joint illumination and visible-Light Communication systems: Data rates and extra power consumption," *2015 IEEE International Conference on Communication Workshop, ICCW 2015*, pp. 1380–1386, 2015.
- [7] L. Teixeira, F. Loose, C. H. Barriquello, and M. A. Dalla Costa, "On the LED Efficacy and Modulation Design Space for Visible Light Communication," in *2018 IEEE Industry Applications Society Annual Meeting, Portland - OR*, 2018, pp. 1–6. [Online]. Available: <https://ieeexplore.ieee.org/document/8544602>
- [8] X. Deng, Y. Wu, A. M. Khalid, X. Long, and J.-P. M. G. Linnartz, "LED power consumption in joint illumination and communication system," *Optics Express*, vol. 25, no. 16, p. 18990, 2017. [Online]. Available: <https://www.osapublishing.org/abstract.cfm?URI=oe-25-16-18990>
- [9] P. S. Almeida, D. Camponogara, H. A. Braga, M. A. Dalla Costa, and J. M. Alonso, "Matching LED and Driver Life Spans: A Review of Different Techniques," *IEEE Industrial Electronics Magazine*, vol. 9, no. 2, pp. 36–47, 2015.
- [10] M. H. Chang, D. Das, P. V. Varde, and M. Pecht, "Light emitting diodes reliability review," *Microelectronics Reliability*, vol. 52, no. 5, pp. 762–782, 2012. [Online]. Available: <http://dx.doi.org/10.1016/j.microrel.2011.07.063>
- [11] Bridgelux, "Bridgelux Vero 18 array series," Bridgelux, Tech. Rep., 2013. [Online]. Available: <https://www.bridgelux.com/resources/ds32-bridgelux-vero-18-data-sheet-gen-6>
- [12] M. Binder, A. Nirschl, R. Zeisel, T. Hager, H.-J. Lugauer, M. Sabathil, D. Bougeard, J. Wagner, and B. Galler, "Identification of nnp and npp Auger recombination as significant contributor to the efficiency droop in (GaIn)N quantum wells by visualization of hot carriers in photoluminescence," *Applied Physics Letters*, vol. 103, no. 7, 2013. [Online]. Available: <https://aip.scitation.org/doi/pdf/10.1063/1.4818761?class=pdf>
- [13] W. K. Lun, K. H. Loo, S. C. Tan, Y. M. Lai, and C. K. Tse, "Bilevel current driving technique for LEDs," *IEEE Transactions on Power Electronics*, vol. 24, no. 12, pp. 2920–2932, 2009.
- [14] K. H. Loo, Y. M. Lai, S. C. Tan, and C. K. Tse, "Stationary and adaptive color-shift reduction methods based on the bilevel driving technique for phosphor-converted white LEDs," *IEEE Transactions on Power Electronics*, vol. 26, no. 7, pp. 1943–1953, 2011.
- [15] S.-c. Tan, "General n-Level Driving Approach for Improving of Fast-Response Saturable Lighting Devices," *IEEE Transactions on Industrial Electronics*, vol. 57, no. 4, pp. 1342–1353, 2010.
- [16] K. Xu, H.-Y. Yu, Y.-J. Zhu, and Y. Sun, "On the Ergodic Channel Capacity for Indoor Visible Light Communication Systems," *IEEE Access*, vol. 5, pp. 833–841, 2017. [Online]. Available: <http://ieeexplore.ieee.org/document/7812579/>
- [17] A. Tsiatmas, C. P. M. J. Baggen, F. M. J. Willems, J. P. M. G. Linnartz, and J. W. M. Bergmans, "An illumination perspective on visible light communications," *IEEE Communications Magazine*, vol. 52, no. 7, pp. 64–71, 2014.
- [18] B. P. Lathi, *Modern Digital and Analog Communications Systems*, 3rd ed., A. S. Sedra and M. R. Lightner, Eds. Nova York: Oxford University Press, 1998.
- [19] J. Sebastian, D. Aller, J. Rodríguez, D. Lamar, and P. Miaja, "On the role of the power electronics on visible light communication," *Conference Proceedings - IEEE Applied Power Electronics Conference and Exposition - APEC*, pp. 2420–2427, 2017.
- [20] P. Deng and M. Kavehrad, "Effect of white LED DC-bias on modulation speed for visible light communications," *arXiv preprint arXiv:1612.08477*, 2016.
- [21] IEEE Computer Society, "IEEE Standard for Local and metropolitan

area networks - Part 15.7: Short-Range Wireless Optical Communication Using Visible Light." IEEE, 2011, no. September, pp. 1–286.

- [22] K. Modepalli and L. Parsa, "Dual-purpose offline LED driver for illumination and visible light communication," *IEEE Transactions on Industry Applications*, vol. 51, no. 1, pp. 406–419, 2015.
- [23] J. Rodríguez, D. G. Lamar, P. F. Miaja, D. G. Aller, and J. Sebastián, "Power Efficient VLC Transmitter Based on Pulse-Width Modulated DC-DC Converters and the Split of the Power," *Transactions on Power Electronics*, no. [accepted for publication], 2018.
- [24] A. V. N. Jalajakumari and K. Cameron, "An Energy Efficient High-Speed Digital LED Driver for Visible Light Communications," in *IEEE ICC 2015 Conference Proceedings*, 2015, pp. 5054–5059.
- [25] Y. Sun, F. Yang, and L. Cheng, "An Overview of OFDM-Based Visible Light Communication Systems from the Perspective of Energy Efficiency versus Spectral Efficiency," *IEEE Access*, vol. PP, no. c, pp. 1–1, 2018. [Online]. Available: <https://ieeexplore.ieee.org/document/8492417/>
- [26] S. Han and J. Lee, "An overview of peak-to-average power ratio reduction techniques for multicarrier transmission," *Wireless Communications, IEEE*, no. April, pp. 56–65, 2005. [Online]. Available: [http://ieeexplore.ieee.org/xpls/abs/\\_all.jsp?arnumber=1421929](http://ieeexplore.ieee.org/xpls/abs/_all.jsp?arnumber=1421929)
- [27] S. Y. Hui and Y. X. Qin, "A general photo-electro-thermal theory for light emitting diode (LED) systems," *IEEE Transactions on Power Electronics*, vol. 24, no. 8, pp. 1967–1976, 2009.
- [28] V. Semiconductors, "BPW34," Vishay Semiconductors, Tech. Rep., 2011. [Online]. Available: <https://www.vishay.com/docs/81521/bpw34.pdf>
- [29] J. Caldwell, "TI Designs – Precision : Verified Design 1 MHz , Single-Supply , Photodiode Amplifier Reference Design," Texas Instruments Incorporated, Tech. Rep. November, 2014.



**Lucas Teixeira** (S'11) was born in Venâncio Aires, Brazil, in 1989. He received the B.S. degree in Electrical Engineering in 2012 and M.Sc. degree in Computer Science (focused in Signal Processing) in 2015, both from the Federal University of Santa Maria, Brazil. From 2012 to 2016 he worked in digital and mixed signal IC design in Santa Maria Design House. He had also experience in electronic embedded devices development and as telecommunications Engineer. Since 2017 he is teacher at technological courses in the Federal University of Santa Maria,

Brazil. He is currently working towards the PhD degree in electrical engineering. His research interests include light-emitting-diode lighting systems, internet of things and visible light communication systems.



**Felipe Loose** (S'17) was born in Cruz Alta, Brazil, in 1991. He received his B.S. and M.Sc. degrees in electrical engineering by the Federal University of Santa Maria in 2016 and 2018, respectively. He is currently pursuing his Doctoral degree at the same institution. Felipe is an active member of both IEEE Industry Applications Society and Power and Energy Society, working along the IEEE Student Branch Chapter at the Federal University of Santa Maria. His research interests include power electronics applications, solid-state lighting systems, digital signal

processing and visible light communications.



**João Paulo Brum** was born in Santiago, Brazil, in 1997. He is currently pursuing the undergraduate degree in telecommunications engineering at Federal University of Santa Maria (UFSM). Since 2016, he has been a researcher with the GEDRE/UFSM - Intelligence in Lighting. His current research interests include car-to-car communication, electronic noise, transmitters and receivers for visible light communication, signal processing and system modelling.



**Carlos Henrique Barriquello** was born in Três Passos, RS, Brazil, in 1984. He received the B.Sc., M.Sc. and Ph.D. degrees in Electrical Engineering from the Federal University of Santa Maria (UFSM) in 2007, 2009 and 2012, respectively. Since 2012, he has been Adjunct Professor in the Electronics and Computing Department at the UFSM, Brazil. Also, he has been a researcher with the GEDRE/UFSM Intelligence in Lighting research group since 2008. His research interests include embedded and real time systems, wireless sensor and actuator networks,

lighting systems, visible light communications and smart grid communication networks.



**Vitalio Alfonso Reguera** received the B.Eng. degree in telecommunications and electronics engineering from the Universidad Central "Marta Abreu" de Las Villas (UCLV), Cuba. He received the M.Sc. degree in telecommunications engineering, and the Ph.D. degree in electrical engineering, from the same university in 2000 and 2007, respectively. He is currently visiting professor at the Electrical Engineering Graduate Program of the Federal University of Santa Maria (PPGEE/UFSM), Brazil. His current research interests include wireless networks, communication

protocols and IoT.



**Marco Antônio Dalla Costa** (S'03, M'09, SM'17) was born in Santa Maria, Brazil, in 1978. He received the B.S. and M.Sc. degrees in Electrical Engineering from the Federal University of Santa Maria, Brazil, in 2002 and 2004, respectively, and the Ph.D. degree (with honors) in Electrical Engineering from the University of Oviedo, Gijón, Spain, in 2008. From 2008 to 2009 he was Associate Professor at the Universidade de Caxias do Sul, Brazil. Since 2009 he is Professor at the Federal University of Santa Maria, Brazil. Dr. Dalla Costa is coauthor of more than 60

journal papers and more than 100 international conference papers, and is holder of 2 Spanish patents. He is also the Vice-Chair of the Industrial Lighting and Displays Committee (ILDC) from the IEEE Industry Applications Society and serves as reviewer for several IEEE Journal and Conferences in the field of power electronics. Dr. Dalla Costa is Associate Editor for the IEEE Transactions on Industrial Electronics and also for the IEEE Journal of Emerging and Selected Topics in Power Electronics. His research interests include dc/dc converters, power factor correction, lighting systems, high-frequency electronic ballasts, discharge-lamp modeling, light-emitting-diode systems, renewable energy systems, solid state transformers, and visible light communication systems.





**5 MANUSCRIPT 4 - PRE-EMPHASIS CONTROL IN SWITCHED MODE  
POWER CONVERTER FOR ENERGY EFFICIENT WIDE BANDWIDTH  
VISIBLE LIGHT COMMUNICATION**

# Pre-Emphasis Control in Switched Mode Power Converter for Energy Efficient Wide Bandwidth Visible Light Communication

L. Teixeira, F. Loose, J. M. Alonso, R. C. Beltrame,  
C. H. Barriuelo, V. Alfonso Reguera, and M. A. Dalla Costa

**Abstract**—Visible Light Communication (VLC) shows up as a trend for short-range wireless networks. However, from the energy point-of-view, there is still a lack of LED drivers that support considerable data rates with high efficiency. Common solutions would include Switched Mode Power Converters (SMPC), which are efficient, but they still face challenges regarding the modulation bandwidth for VLC. Thus, this paper presents an analysis of a Pre-Emphasis (PE) technique to overcome the low bandwidth constraint of SMPC. The PE filter is used to render the frequency response of the circuit to provide a wider bandwidth for communications. It operates on the duty cycle of the converter and it dictates the average output signal value over a switching period. Finally, the technique is presented in a theoretical approach with aligned experimental results in a 21.5 W buck-converter-based LED driver switched at 1 MHz, with 89% efficiency and an increased modulation bandwidth from 8.12 kHz to 450 kHz (55 times).

**Keywords**—Visible Light Communication, VLC, LED Drivers, Efficiency, Pre-Emphasis.

## I. INTRODUCTION

Visible light communication (VLC) enables a wide range of applications demanding data communication from internet of things (IoT) connected devices [1], indoor localization, up to 5G mobile network attocells [2], among many others. As an extra feature, VLC demands that illumination infrastructure also performs instantaneous light modulation at frequencies imperceptible to the human eye.

Although very promising, the realization of VLC modulation capable devices faces technical challenges concerning the bandwidth (BW) of light modulation [3]–[5], drop of efficacy of the LED [6], [7] and also electronic driver limitations [8], [9]. In order to not cause a substantial decrease in the energy efficiency of an illumination device, VLC needs to be seen as an incremental feature

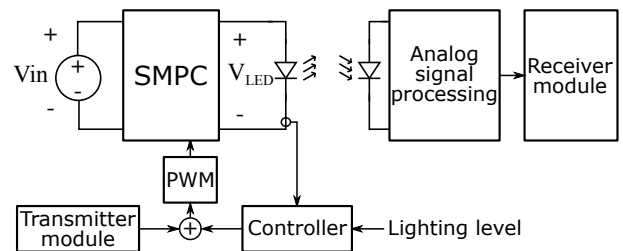


Fig. 1: Application of a SMPC as VLC LED driver.

that is subject to several restrictions. Thus, the most energy-efficient approach is to use the well-known high efficient LED driver circuit topologies. Some workaround can be implemented to overcome their limitations on implementing light modulation.

Consumer electronic LED drivers are mostly designed using Switched Mode Power Converters (SMPC). They are more efficient power sources which also present reduced circuit volume, weight and cost due to the available range of switching frequencies of their semiconductors (hundreds of kHz to dozens of MHz). For VLC, those circuits may be used as modulators at the transmitter, as showed in [10]–[13]. One example of application and block diagram of a SMPC-based VLC system is depicted in Fig. 1. This diagram shows how the communication and lighting control are connected in a single VLC LED driver used to send data from transmitter to receiver modules. However, in terms of signal dynamics at the light output, single SMPCs [8], [10]–[13] are not the fastest drivers among other solutions reported for VLC. Therefore, in order to increase the system modulation bandwidth, some solutions have been proposed in the literature [14]–[17]. Nevertheless, these solutions require extra elements as linear amplifiers [14], [15] or extra switch modulators [16], [17], which penalize the efficiency and increase circuit complexity. An alternative solu-

tion that does not require extra power components is based on using the SMPC residual ripple to convey the information [10], [11], [13], which limits the system bandwidth due to the narrow converter filter cut-off frequency. Given these reasons, this work is focused on average current control, not on ripple modulation, since it enables the system to implement baseband and passband VLC modulation schemes.

We explore a method known as pre-emphasis (PE) or pre-equalization that was already applied to VLC to increase linear drivers BW [3]–[5]. Since then, available literature was focused on compensating the LED dynamic behavior. Hence, when applied to SMPCs, this strategy is effective to increase the modulation bandwidth with small gain and phase errors in the bandwidth of the interest [18], which is a novelty in the design of VLC lighting systems.

This work is organized as follows. Section II presents the control structure with PE of an LED driver. Section III presents an analysis of the SMPC with PE along with design considerations. Section IV presents simulation results confirming the model and analysis. Follows, Section V presents experimental results as well as performance metrics. Finally, Section VI summarizes the conclusions of our work.

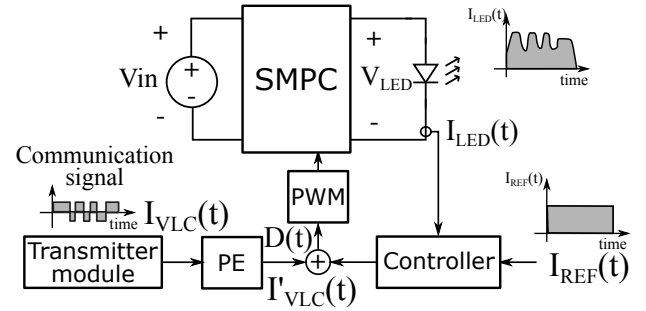
## II. PRE-EMPHASIS CONTROL OF A VLC SMPC

First, this section presents the full control structure of a power converter with VLC. Second, the PE filter is contextualized in this system to provide background to the following method.

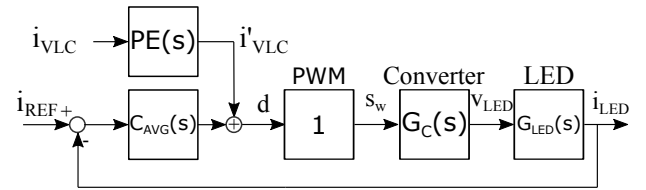
### A. LED driver control scheme including PE

In LED lighting, control is mandatory to regulate the dc output current for illumination. It can be actively performed in a closed-loop scheme tracking a provided reference ( $I_{REF}$ ). Fig. 2a presents the block diagram of a VLC LED driver as the schematic shown in Fig. 1 with additional PE filter. Fig. 2b shows the control diagram of a VLC LED driver with PE in the feedforward path. The controller  $C_{AVG}(s)$  regulates a dc reference on the output ( $I_{LED}$ ), and it operates on a bandwidth well below the one required for the VLC signal. Hence, the system transfer function (TF) from  $I_{REF}$  to  $I_{LED}$  is depicted in (1).

$$\frac{I_{LED}(s)}{I_{REF}(s)} = \frac{C_{AVG}(s) G_C(s) G_{LED}(s)}{1 + C_{AVG}(s) G_C(s) G_{LED}(s)} \quad (1)$$



(a) System block diagram including PE.



(b) Control diagram of a VLC LED driver with PE in the feedforward path.

Fig. 2: Representations of VLC LED driver with PE.

For good average light control, the gain of  $C_{AVG}(s)$  must be high. This can be accomplished at low frequencies (near dc), so that  $|C_{AVG}(s)G_C(s)G_{LED}(s)| \gg 1$  and, in this case,  $|I_{LED}(s)/I_{REF}(s)| \approx 1$ , ensuring good average reference tracking.

Regarding the PE method, it compensates for the low-pass dynamics of the converter by inserting the data signal in a feedforward path on the driver control loop. Additionally, we may design the transfer function  $PE(s)$  to overcome the low-pass characteristics of the plant seen by the communication signal. Thus, one way to analyze  $PE(s)$  is by observing the transfer function that relates the data signal  $I_{VLC}(s)$  to  $I_{LED}(s)$ , shown in (2).

$$\frac{I_{LED}(s)}{I_{VLC}(s)} = \frac{PE(s) G_C(s) G_{LED}(s)}{1 + C_{AVG}(s) G_C(s) G_{LED}(s)} \quad (2)$$

The analysis of (2) is performed considering separated frequency ranges. The first range is for average current control for lighting (near dc). The second concerns communication signal band (higher frequencies). In the lower band,  $C_{AVG}(s)$  has a high gain ( $|C_{AVG}(s)G_C(s)G_{LED}(s)| \gg 1$ ), thus rendering  $I_{LED}(s)/I_{VLC}(s) \approx PE(s)/C_{AVG}(s)$ , showing that the controller will reject any communication signal in this band. Moreover, in the communication signal band, the average controller  $C_{AVG}(s)$  does not actuate if its gain is low in such frequency. Thus

$|C_{AVG}(s)G_C(s)G_{LED}(s)| \ll 1$  and, in this case,  $I_{LED}(s)/I_{VLC}(s) \approx PE(s)G_C(s)G_{LED}(s)$ . Finally, this last is the TF that is used to design the PE filter.

In this work, we addressed the digital control design based on a DSP. This structure allows for a lower sampling rate of  $I_{LED}$ , since the bandwidth of the control loop is much lower than the bandwidth of the signal for communication (BWS). Attention is required to provide a suitable anti-aliasing filter according to the signal sampling frequency. Thus, the computation of  $C_{AVG}(s)$  can also be performed in a slower pace. Only the PE filter and the PWM modulator are required to operate at the switching frequency rate.

### B. Pre-emphasis filter

Starting from the known distortion that the duty cycle (D) signal suffers when passing through the SMPC circuit, according to TF in (2), an inverse effect can be applied to  $I_{VLC}$  stimuli to give the complete system response a constant gain and linear phase in the interest band. Some assumptions, as well as the conditions to apply this method and consequences for the system dynamics are further explored next.

In commercial LED drivers, the filter is the main dynamic limiting factor on modulating the light for VLC. In SMPC LED drivers operating with a switching frequency below 1 MHz, the bandwidth of the filter (BWF),  $G_C$  in Fig. 2b, is usually designed below 100 kHz, in order to limit the high frequency output current ripple. In this case, the intrinsic cutoff frequency of phosphor-covered LEDs, which is usually around 3 MHz, represents a secondary factor that does not limit the modulation bandwidth. Therefore, the PE method is used to cope with the frequencies in the range between BWF and  $F_S/2$ .

The PE filter can be implemented in a continuous- or discrete-time domain, and it shall be integrated to the converter into the  $D(t)$  value provided to the PWM modulator. Thus, the amplitude drop at the passive filter output will be compensated by the PE filter. The frequency response of this filter is depicted in the Bode diagram of Fig. 3. It shows a small magnitude drop as well as little distortion into the signal phase within the additional bandwidth that can be occupied by VLC signal using PE. Although it seems a narrow band of spectrum in Fig. 3, this additional bandwidth corresponds to 80% of

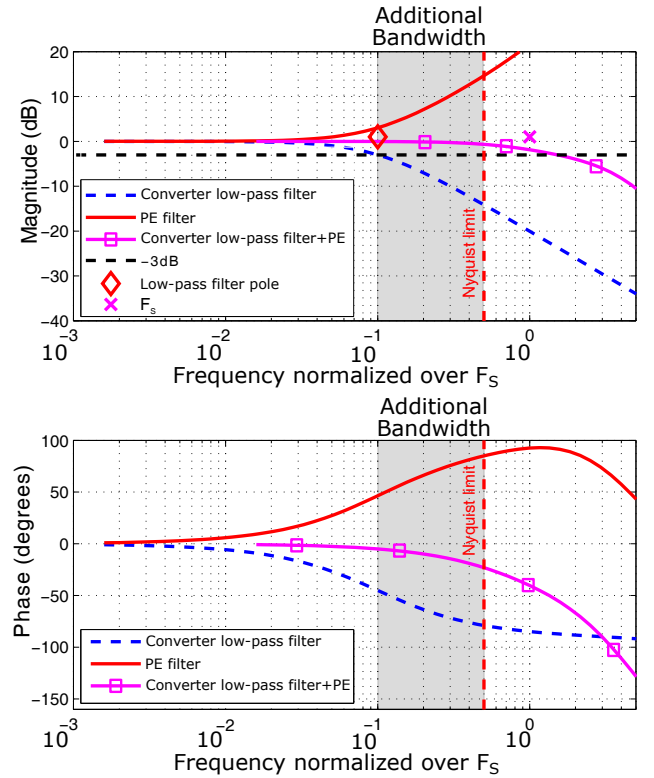


Fig. 3: Frequency response of the system parts and its expected converter with PE behavior.

the useful bandwidth below the limit imposed by Nyquist criterion.

## III. DETAILS OF PE IMPLEMENTATION TO VLC SMPC

In order to provide context, firstly we present a generic structure and model of a SMPC. Secondly, the basis and limitations of the PE method are explored. Finally, we present the design of the average controller and PE filter.

### A. Generic model of SMPCs

In VLC applications and LED lighting, the most common SMPC encountered are derived from the principles of the step-down buck converter. These SMPC circuits are responsible for filtering a digitally pulsed signal generated by the PWM in order to obtain its average value, depending on the inductance ( $L$ ) and capacitance ( $C$ ) of the filter.

The switching frequency  $F_S$  directly affects the filter BW, while dc regulation is expected for average illumination level. Therefore, Fig. 4 presents a generalization of the power structure of a SMPC, in

which the main converter power blocks are: switch arrangements and passive filter. For better visual perception the frequency of pulses in  $S$  is lower than the necessary to produce  $v_{LED}$  as smooth as shown in the figure. The switches provide a PWM voltage. The average gain over a switching period is then defined by  $D(t)$ , which is the main control variable and responsible to transfer data to the output current and also regulate the dc light level.

The method explored in this work makes it possible the generation of any VLC signal shape that may be accomplished by a time variation of the duty cycle  $D(t)$ . However, the limitations to the average current control method are the switching frequency and the dynamics given by the frequency response of the passive elements and the LED load. First,  $F_S$  dictates the pace of the PWM, and it limits the changes of  $D(t)$  by one switching period to another. Second, the BWF, which plays a major role on the output dynamic, may distort the signal in the case when  $BWS > BWF$ , if not properly compensated.

Therefore, the open-loop TF in block diagram of Fig. 4 represents the signal path for communications and lighting. A PWM with pulses aligned at the beginning of the period behaves similarly to a zero-order hold and, therefore, it causes no significant distortion to the signal in the band of interest that comes from dc to  $F_S/2$ . A linear phase lag is caused in the signal band indeed, however it represents a constant time delay. Therefore, a constant gain was adopted for the PWM frequency response in this analysis.

The converter TF  $G(S) = \hat{V}_{LED}(s)/\hat{S}(s)$  represents a filter dynamic for perturbations around the operating point. The output voltage frequency components that can be controlled by  $D(t)$  are within the limits of zero and  $F_S/2$ , due to the Nyquist criterion imposed by the PWM. For example, Fig. 4 depicts the case in which the signal ( $D$ ) occupies a bandwidth that slightly exceeds BWF, hence most of the energy outside this range is lost, stored in the passive elements, leading to a smooth signal shape in  $v_{LED}$ . Without any additional signal processing stage, if the BWS is wider than the BWF, the communication signal degrades its shape, affecting the communication capabilities.

#### B. Current residual ripple as a design constraint

The residual ripple cannot be avoided in the converter output, that is presented in Fig. 4 by

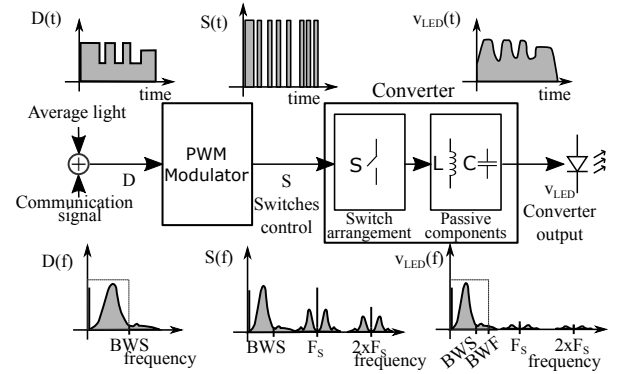


Fig. 4: Expected signal measured at each stage when  $BWF > BWS$ .

$V_{LED}$ , and corresponds to the frequency components around  $F_S$  and its harmonics. The choice of  $F_S/BWF$  ratio directly impacts ripple intensity in the converter output. In this sense, the higher the BWF, for the same  $F_S$ , the more ripple amplitude in the output.

Ripple percentage can be expressed by the ratio of ac rms value over average [7]. Alternatively, for pure sinusoidal ripple, it can be calculated as peak deviation over average [19]. A small ripple does not account for significant detriment in converter efficiency, nor in LED efficacy or visual perception, if  $F_S$  is allocated in a flicker-free band. However, more intense ripple may cause a drop in converter efficiency (due to higher component stress) and LED efficacy drop. As a reference, a small ripple factor of less than 20% applied to a power LED device causes an LED efficacy drop of less than 2% [7].

The LED linearized model is electrically represented by the threshold voltage ( $V_{th}$ ) with the series LED dynamic resistance ( $R_{LED}$ ) [19], which is valid while forward biased and around a given operating point. The current ripple factor ( $\gamma$ ) can be calculated from the LED instantaneous current ( $i_{LED}$ ) and average current ( $I_{LED}$ ), as presented in (3).

$$\gamma = \frac{i_{LED\_rms}^{AC}}{I_{LED}} \quad (3)$$

where  $i_{LED\_rms}^{AC}$  is the ac rms ripple of the LED current.

The frequency harmonic components of  $i_{LED}$  are directly defined by the filter bandwidth according to the ratio  $F_S/BWF$ . Fig. 5 presents an abacus for

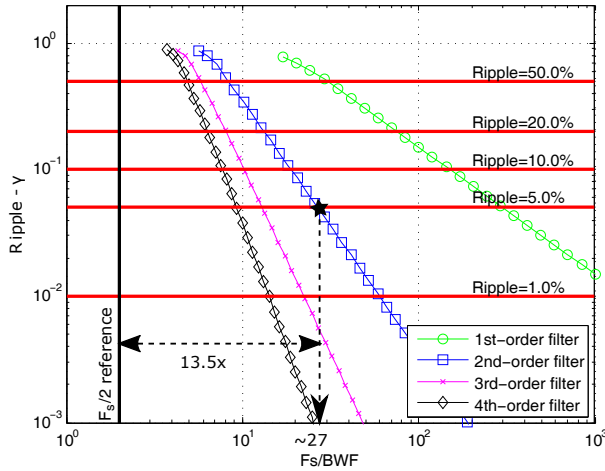


Fig. 5: Ripple factor abacus according to a range of  $F_S/BWS$  for filters up to 4<sup>th</sup> order.

this relation for filter order up to 4 using commercial high power LED parameters [20] and  $D=0.5$ .

### C. Foundation for PE method in SMPC

The application of the PE filter in SMPC PWM generation is possible due to the following identified opportunities:

1) *Excess of control energy*: It is available due to the converter TF and LED voltage to current reasonable gain,  $G_{LED}(s) = 1/R_{LED}$ , valid for perturbations at frequencies below 3 MHz in white LEDs. The fine control of the converter output during dc regulation generates regular small changes to  $D(t)$ . Therefore, there is still enough excursion on the control signal for intentional modulation. Hence, such facts allow the increase of signal power specially in components that are attenuated by the following stages of the converter.

2) *The  $F_S/BWF$  ratio*: It is limited in its minimum value by the ripple that is allowed by design, as explored in the previous section. In this sense, the less residual ripple that is allowed from the  $F_S/BWF$  ratio, the more room exists for acting with PE (see Fig. 3). As an example, a ripple level below 5% can be achieved using a second-order filter with minimum ratio of  $F_S/BWF \approx 27$ , as can be seen in the solid star marker in Fig. 5. That leaves room for a bandwidth increase of  $\approx 13.5$  times, in the  $F_S/BWF$  range from 27 to 2, as pointed by the dashed arrow in the figure.

These opportunities turned the application of the PE method possible, although the physical inertia of the filter is the key to understand why the components above BWF have a higher cost for intentional modulation. This and other limitations to the exposed method are explored in next section.

### D. Limitations of PE method

There are two main identified aspects of the PE method that are disadvantages: i) dynamic range of  $I_{VLC}$  and ii) coupling between signal frequency components inside the bandwidth of interest and switching harmonic components outside of it. These aspects are addressed in the analysis that follows.

Inductor inertia is analyzed by the current rise and fall rates ( $dI_L/dt$ ) or the slew-rate the system can perform. Hence, the inductance value ( $L$ ) and the voltage applied ( $V_L$ ) are the converter parameters that determine this performance, according to inductor branch equation  $V_L = L dI_L/dt$ . This example approaches an inductor, but a similar analysis is also valid for a capacitor or high order filters containing multiple reactive components.

Moreover, to generate any frequency component, modeled as a pure sinusoidal current signal  $A \sin(\omega t)$ , its rise and fall rates are the main concern on regarding the system dynamic. They are dependent on the signal amplitude and frequency, in this case  $d(A \sin(\omega t))/dt = A\omega \cos(\omega t)$ . As the  $\cos(\omega t)$  part is within the range  $[-1, +1]$ , to track it in the filter output the value of  $dI_L/dt$  shall match or exceed  $[-A\omega, +A\omega]$ . This analysis can be expanded to any signal that is the sum of several components, which leads to the conclusion that the higher frequencies require more rise and fall rates, thus having higher cost to be generated.

Given these facts, to generate a signal using limited rise and fall rates one can either reduce its bandwidth (decrease the  $\omega$ ) or its amplitude ( $A$ ). However, it is common that in SMPCs the  $V_L$  applied to the filter is different at each operating stages, leading to different rise and fall rates. This comes with filter requirements and it is not a design choice. Nevertheless, when it is modeled around an operating point and for small deviations in  $D(t)$ , the linear TF  $G_C(s)$  is still valid.

Furthermore, not only the slew-rate shall be considered, but also the  $D(t)$  dynamic range limits the PE method to avoid pronounced distortion to the

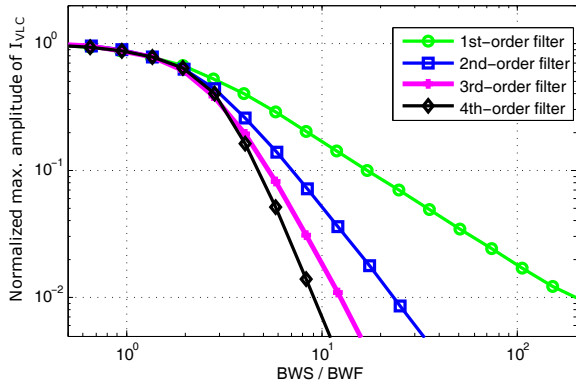


Fig. 6: Maximum amplitude of  $I_{VLC}$  according to the relationship of signal and filter bandwidths.

communication signal,  $D(t) \in [0, 1]$ . The duty cycle is generated by the addition of the control action from  $C_{AVG}$  and the VLC signal  $i'_{VLC}$ , as depicted in Fig. 2b. However, only the latter is considered in this analysis because the former is much slower than the communication signal, as explained in Section III-E. Thus, the BWS will impact directly in  $i'_{VLC}$ , which can be expressed as in (4).

$$i'_{VLC}(t) = \mathcal{L}^{-1}(I_{VLC}(s) \cdot PE(s)) = \approx \sum_i (PE_i \cdot I_{VLCi} \sin(w_i t + \phi_i)) \quad (4)$$

where  $\mathcal{L}^{-1}$  stands for inverse Laplace transformation,  $I_{VLCi}$ ,  $w_i$  and  $\phi_i$  are the amplitude, angular frequency and phase, respectively, of the signal harmonics, and  $PE_i$  is the PE filter gain for each harmonic.

There is no closed expression to calculate the signal excursion from (4). However, according to the central limit theorem, when the ac signal is composed of a great number of uncorrelated and random components inside a wide frequency band, e.g. an OFDM signal, it can be approximated in time domain by a normal distribution of zero mean value [21]. This can be easily proven by numeric simulations. According to this, if the BWS is increased beyond BWF, the PE method will increase the dynamic range of  $i'_{VLC}$ , even though the dynamic range of  $i_{VLC}$  is kept constant. This happens due to the PE higher gain in the signal path at frequencies attenuated by the converter, which is a clear limitation of this method.

In order to clarify the previous relations, numerical simulations were performed to obtain the maxi-

imum amplitude of  $i_{VLC}$  as a function of the ratio between BWS and BWF. In this sense, the maximum allowed amplitude of  $i_{VLC}$  is the one which assures that the duty cycle will be within its operating limits. The results are shown in Fig. 6 for different filter orders, where the maximum amplitude of  $i_{VLC}$  has been normalized with respect to its value at a very low BWS/BWF ratio. By respecting this maximum amplitude, no signal distortion will occur using the PE method, neither by high frequency attenuation, nor by signal clipping. Additionally, as can be seen in Fig. 6, there is a trade-off between amplitude and bandwidth increment: the higher the bandwidth, the lower the amplitude. Therefore, lower order filters are preferred to be used with PE method because the amplitude reduction is less intense than for higher order filters. For example, to generate a signal with 10 times bandwidth using PE,  $BWS/BWF = 10$ , a first-order filter only reduces the signal amplitude 5.9 times, while second-, third- and fourth-order filters reduce it 18.4, 54.3 and 141.3 times, respectively.

However, the limitation in the signal  $i_{VLC}$  excursion must not be considered a very negative aspect of this method when applied to VLC LED drivers. This is because small current excursions are expected in the LED, so that its efficacy is not very affected by the communication, as addressed in Section III-B.

Finally, the PE method presents an implicit coupling between harmonic components inside the bandwidth of interest and switching frequency sideband components. This comes from the fact that the PWM generation creates components in the bandwidth with respective and proportional replicas around switching frequency and its harmonics. Therefore, the increase in the useful signal intensity also increases the higher harmonic components at frequencies above half of switching frequency, which are not used for communication purposes. This unwanted harmonic content is further attenuated by the filter indeed, however they increase components current stress and LED efficacy drop.

#### E. Design of average current controller

The average current controller  $C_{AVG}(s)$  shall be specified to comply with the following two requirements: performing good reference current tracking against slow perturbations (with



$C_{AVG}(s)G_C(s)G_{LED}(s) \gg 1$  at low frequencies) and having low gain ( $C_{AVG}(s)G_C(s)G_{LED}(s) \ll 1$ ) in the VLC signal band to avoid rejecting these components. In this situation, the converter passive components dynamics ( $G_C(s)$ ) have the dominant poles, therefore defining the system bandwidth. We suggest that the requirements can be accomplished with  $C_{AVG}(s)$  as a low-pass filter (bandwidth < BWF) or an integrator, but keeping in mind that the gain and phase margin of direct path  $C_{AVG}(s)G_C(s)G_{LED}(s)$  shall be taken into account for gain tuning.

#### F. Design of the PE filter

The PE filter can be designed following the steps:

- 1) determine the linear TF of the stages that need to be compensated as presented in (2);
- 2) determine poles and zeros of this TF using PE equal to 1;
- 3) the PE filter TF is designed using poles and zeros cancellation, which is a straightforward control strategy.

A generic model for a PE filter using poles and zeros cancellation is given in (5).

$$PE(s) = \frac{\prod_{i=1}^{N_p} (1 + s/w_{SPi})}{\prod_{i=1}^{N_z} (1 + s/w_{SZi}) \prod_{i=1}^{N_p - N_z} (1 + s/w_{PPi})} \quad (5)$$

in which  $w_{SPi}$  and  $w_{SZi}$  are poles and zeros angular frequencies of (2) when PE is made equal to 1.  $N_p$  and  $N_z$  are the number of poles and zeros, respectively. Also the product of  $(1 + s/w_{PPi})$  ensures stability of the PE filter providing at least the same number of poles as the number of zeros [18]. However, it must be assured that when selecting  $w_{PPi}$  frequency, the system should not introduce any phase distortion, which can be achieved by ensuring that the phase of the system TF behaves linearly within the communication signal bandwidth. In this way, the received signal will only present a time delay, but no additional distortion.

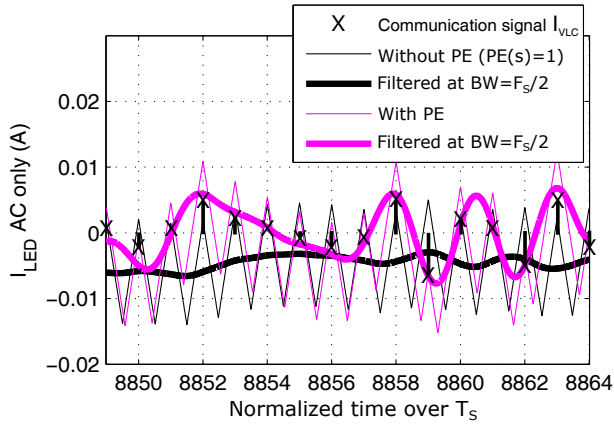
In a well tuned implementation of this filter, accordingly to (5), the product of the PE TF with the compensated system will have a flat dynamic response up to  $w_{PPi}$  rad/s, thus rendering performance similar to the shown in Fig. 3.

## IV. SIMULATION OF LINEAR SYSTEM

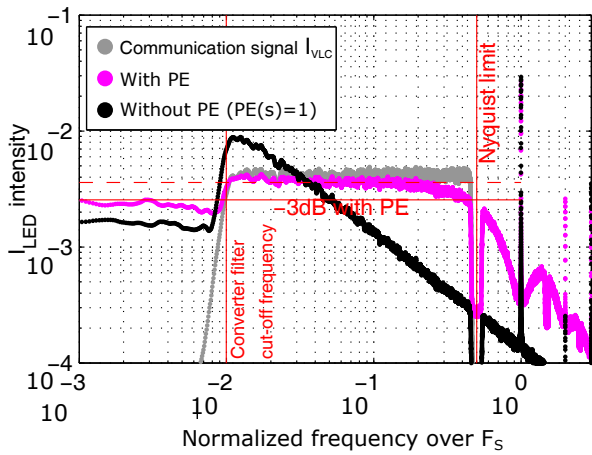
Using the control structure described, the PE method was simulated using a model of a generic power converter. A mathematical software platform was used to simulate the system with ideal switches and a linear power filter. The filter of the power converter was designed to be of first order with no zeros and the switching frequency selected was 1 MHz. The ratio  $F_S/BWF$  was selected as 100, thus ensuring an output ripple of about 15% (see Fig. 5). The design of the PE filter was performed according to the converter TF and considering the procedure described in Section III-F. In this design example, the filter and converter TFs correspond to those in Fig. 3. The pole of the converter and the zero of the PE filter were located at the same frequency of 10 kHz. Also, the additional pole was added to the PE filter in order to assure its stability. Since the communication signal bandwidth goes from 10 kHz to 450 kHz, the pole was located at a frequency one decade beyond 450 kHz. The selected frequency was 5 MHz. This design method assures no phase distortion owing to the cancellation effect around 10 kHz and because the PE filter pole at 5 MHz has no effect on the communication signal.

The test communication signal extends from  $0.01F_S$  to  $0.45F_S$  with a flat power spectral density (PSD). It is adequate to depict the performance of the system and does not exceed the Nyquist limit in  $0.5F_S$ . A small band between the signal and  $0.5F_S$  was intentionally left clear for better understanding and visual separation between the components of interest and the others in the spectrum. Moreover, that is the expected PSD of a wide-band multi-carrier scheme like an Orthogonal Frequency Division Multiplexing (OFDM) or a Discrete Multi Tone (DMT) using the whole available band. However, such approach is not restricted to those modulations, since it ensures that any scheme using this band will be generated without significant distortion.

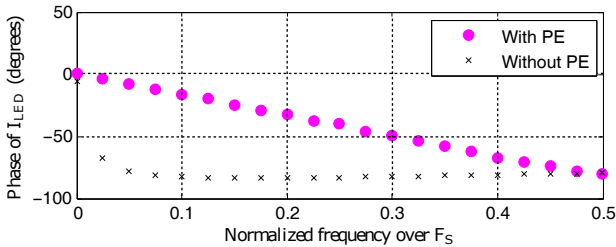
The modulated pulse train,  $S_W$  in Fig. 2b, was applied to the linear system TF. In Fig. 7a, it is possible to verify that the output current has a pronounced residual ripple. Nevertheless, the filtered version of these signals, which keeps only the components below  $0.5F_S$ , shows a good reproduction of the original communication signal. It is easy to note that the simulation with PE strategy performs much better tracking of the VLC signal than the one



(a) Transient behavior of simulated PE.



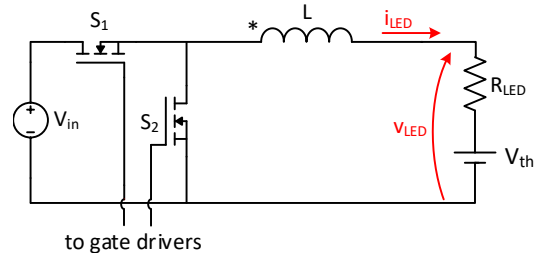
(b) Spectrum of simulated PE.



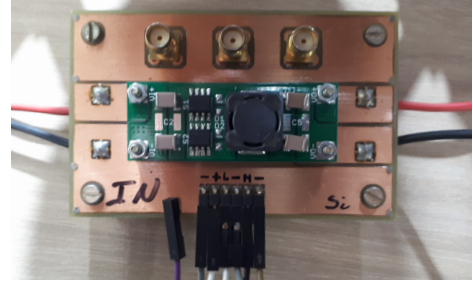
(c) Phase of simulated PE.

Fig. 7: Simulation results with and without PE strategy.

without it. That can be explained by the attenuation of a great part of the components and this effect is confirmed in the spectrum of  $I_{LED}$  shown in Fig. 7b. Additionally, Fig. 7c presents the linear phase lag using PE caused by a constant time delay, while without PE a clear phase distortion occurs. Moreover, comparing these simulated magnitude and phase results with the ones in the Bode diagram of the whole system in Fig. 3 confirms that behavior. After the compensation with PE, the frequency



(a) Synchronous buck circuit.



(b) Converter prototype.

Fig. 8: LED driver circuit used in the experimental test.

band occupied by the test signal resides inside the bandwidth of the system below a -3 dB cutoff.

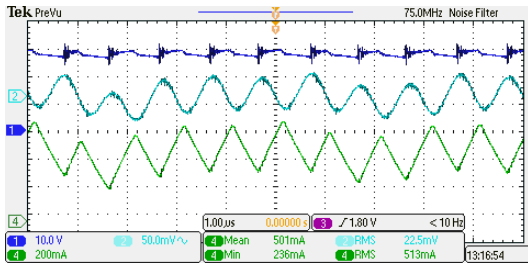
## V. EXPERIMENTAL VALIDATION

For experimental validation of the PE technique, we used a synchronous buck SMPC driving a high power LED. The values of the parameters used in experimental validation are the same as in the simulation, with the exception of the converter filter cut-off frequency that was the closest possible with available components. The converter circuit, designed with a first order filter, is depicted in Fig. 8. This SMPC is commonly used for LED drivers due to its simplicity and good efficiency in applications that do not require electrical isolation.

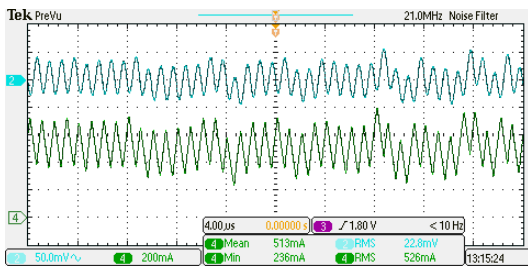
The control structure was implemented using a digital signal processor (DSP), similar to the feed-forward VLC signal with PE, and the converter design ensures duty cycle around 0.5 for the expected average LED current ( $\overline{I_{LED}}$ ). The experimental setup parameters and operating conditions are synthesized in Table I. The input voltage was defined accordingly to keep the converter operating at 0.5 duty cycle, which is the same simulated operating point. The first order filter BWF is 8.12 kHz, therefore  $F_S/BWF = 123$ , that results in the ripple factor of 18%, calculated considering (3) and without any intentional modulation. In fact, after

TABLE I: Experimental test setup parameters, components and results summary.

Parameter	Symbol	Value
Synchronous buck converter		
Switching frequency	$F_S$	1 MHz
Input voltage	$V_{in}$	63.2 V
Average output voltage	$\bar{V}_o$	28.5 V
Average output current	$I_{LED}$	0.75 A
Output power	$P_o$	21.5 W
Semiconductor switches	$S_1, S_2$	IRF7492
Semiconductor driver		MAX15019A
Digital Signal Processor		TIVA TM4C1294
Inductor	$L$	47 $\mu$ H
Average duty cycle	$\bar{D}$	0.5
LED Bridgelux Vero 18 BXRC-50C4000-F-24 [20]		
Threshold voltage	$V_{th}$	26.8 V
Dynamic series resistance	$R_{LED}$	2.4 $\Omega$
Average LED current	$I_{LED}$	0.75 A
PE filter parameters in (5)		
PE filter zero frequency	$w_{SP1}$	8.12 kHz
System dynamic		
Original system bandwidth		8.12 kHz
Increased system bandwidth		450 kHz



(a) From top to bottom: Detail of  $V_{LED}$  (ch. 1), captured light (ch. 2) and  $I_{LED}$  (ch. 4).



(b) From top to bottom: captured light signal (ch. 2) and view of the dynamic of  $I_{LED}$  (ch. 4).

Fig. 9: Measurement results on oscilloscope.

intentional modulation, the current excursion was increased up to 24%, calculated following (3). In this case, all frequency components are accounted, which includes ripple and signal.

We captured the light using a light transducer (Vishay BPW34S light sensor with an analog signal amplifier, 1.1 MHz of bandwidth) at the distance of 2 m. From the performed experiments, it is possible to confirm the effectiveness of the PE and the prototype performance is presented on the following results. Firstly, the oscilloscope plot shown in Fig. 9

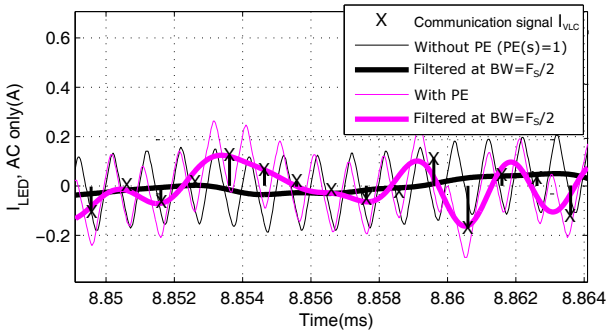
clearly depicts the dynamic in the LED current and the light captured. Either the time domain behavior (Fig. 10a) and its spectrum (Fig. 10b) match with the predicted behavior (Fig. 3) and the simulated spectrum (Fig. 7). Fig. 10c presents the phase lag of signal harmonic components which trends to a linear shift, the linear trend of the PE measurements is shown as a dashed line in this figure. Furthermore, comparing to the communication signal provided with the filtered  $I_{LED}$  in Fig. 10a, it is clear that with PE the current follows the expected shape; while without PE it is very degraded due to attenuated frequency components.

In the measurement of a 40,000 periods vector, it was verified 30.3 dB of signal-to-noise and distortion ratio between the received light and communication signal  $I_{VLC}$  at the transmitter. This comparison was performed in the signal bandwidth, in this case the signal processing performed in the receiver is responsible for ignoring ripple harmonic components above  $F_S/2$  frequency. This evidence confirms the effectiveness of the explored technique for VLC. Moreover, it showed that no significant distortion occurred to the signal although it went through PWM modulator, power stage and LED.

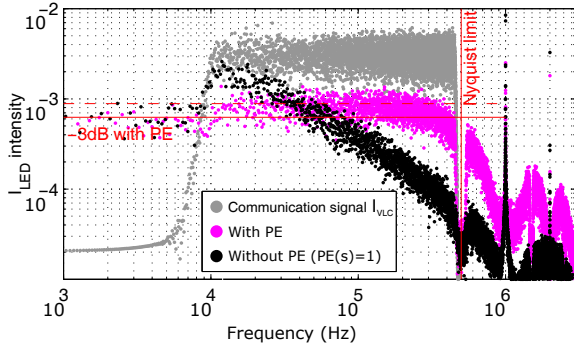
Furthermore, the LED light signal was also captured. It was verified that it presents very similar time and spectrum behaviors as those shown for the LED current in Fig. 10. Only additional attenuation was verified for components that were above the light sensor bandwidth, which are out of the interest band. Fig. 10d presents operating efficiency measurements of the proof of concept converter according to the ripple factor resulting from different modulation intensities, that in this case indicates different communication signal power levels. In this figure, it is clear to see that the converter has same efficiency with or without PE applied to the stimulus when comparing the same output signal power level.

#### A. Comparison

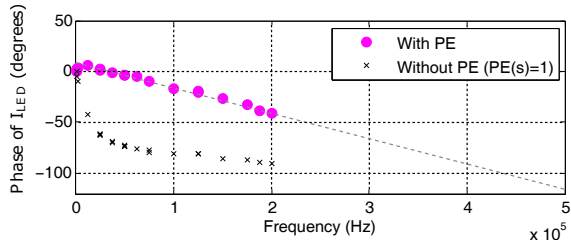
Table II presents a comparison among the current work prototype and other published solutions using SMPC-based VLC LED drivers. The modulation factor is defined as the ratio between standard deviation and average value of output current ( $\sigma_{I_o}/\bar{I}_o$ ), and it is used to compare the amplitude of the modulated signals inside the signal band. As can be



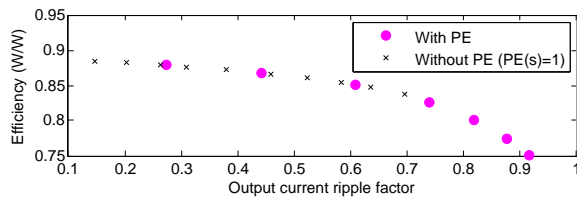
(a) Transient behavior of experimental PE test.



(b) Spectrum of experimental PE test.



(c) Phase of experimental PE test.



(d) Efficiency measurements according to the ripple factor.

Fig. 10: Measurement results with and without PE strategy.

seen, all solutions employ buck and buck-derived topologies to implement current modulation. Two-phase converters have effective double switching frequency when compared to single-phase ones. In this work, a ratio  $F_S/BWS$  of 2.2 has been achieved, which is the lowest one of the compared solutions when using average current control. Therefore, considering the limitation imposed by  $F_S$  the signal

bandwidth of this solution is among the highest in the literature. Also solutions using ripple modulation have similar performance and achieve reasonable signal amplitude [10], [11], [13], as can be seen by the modulation factor in Table II.

## VI. CONCLUSIONS

The foundations of PE technique were explored and its suitability to application in a SMPC for light modulation was explained. The analysis, simulation and experimental results showed that it performs as expected and can be implemented with no hardware changes to the power converter. It was demonstrated that the room for bandwidth improvement using this method is dependent on the switching frequency and converter filter design, thus it can be analysed with respect to the converter output ripple. Also, the analysis of the limits of this method showed that the increment in bandwidth and output communication signal excursion present a trade-off.

In the experimental test presented, without using any strategy as PE, the intentional modulation would have to be restricted on a bandwidth of about  $1/123$  of  $F_S$  (8.12 kHz) due to the allowed current ripple to avoid pronounced distortion. On the other hand, using the described PE strategy, in a, experimental proof of concept, the converter showed an increment of 55 times the original bandwidth.

Furthermore, we demonstrated from the analysis that using this strategy the signal bandwidth can reach up to  $F_S/2$  without significant distortion or intersymbol interference. That represents a significant reduction, under equal output ripple restrictions, to the  $F_S$  needed to synthesize the same VLC signal. Therefore, the PE technique has shown to be an effective method to overcome the low bandwidth issues commonly encountered in VLC applications involving SMPC.

## ACKNOWLEDGMENT

The experimental measurements would not be possible without the support provided by several colleagues of GEDRE research group. Special thanks are due to Renan Duarte, Christian Miguel Barth and João Paulo Sales Brum. This study was financed in part by the Coordenação de Aperfeiçoamento de Pessoal de Nível Superior - Brasil (CAPES) - Finance Code 001, PROEX program, PRPGP/UFMS, INCT-GD, CAPES proc

TABLE II: Comparison among VLC LED driver solutions using average and ripple modulation in SMPC.

Reference	Output power (W)	Mod. factor ( $\sigma_{I_o}/I_o$ )	Efficiency (%)	$F_S$ (MHz)	$F_S/BWS$	Modulator topology
[8] <sup>a</sup>	6.7	0.28	90	5	4.15 (8.3 °)	Two-phase buck
[9] <sup>a</sup>	1.7	1	85	0.10	10	Buck
[12] <sup>a</sup>	10.1	0.28	91.3	10	3.44 (6.9 °)	Two-phase buck <sup>d</sup>
[22] <sup>a</sup>	4.3	0.64	81	10	10	Buck
[23] <sup>a</sup>	1	-	63	0.10	10	Buck
[24] <sup>a</sup>	97.98	0.4	92	10	3.2 (6.4 °)	Two-phase buck
[10] <sup>b</sup>	22.6	0.29	91	0.1	2	Synchronous buck
[11] <sup>b</sup>	10	0.44	86	0.5	3 (6 °)	Two-phase synchronous buck
[13] <sup>b</sup>	10	0.5	96.5	0.5	8.33 (16.7 °)	Two-phase synchronous buck
This work <sup>a</sup>	21.5	0.1	89	1	2.2	Synchronous buck

<sup>a</sup> Uses average modulation.  $F_S/BWS$  is calculated from 0 up to signal bandwidth in baseband. Ripple components exist out of signal band.

<sup>b</sup> Uses ripple modulation.  $F_S/BWS$  is calculated using the signal bandwidth around switching carrier frequency, thus in passband.

<sup>c</sup> In parenthesis, it is  $F_S/BWS$  calculated using effective  $F_S$ , which is double in two-phase converters comparing with single-phase converters.

<sup>d</sup> Additional single-phase synchronous buck converter is used to process dc voltage.

23038.000776/2017-54, CNPq proc 465640/2014-1, FAPERGS proc 17/2551-0000517-1.

#### COMPLEMENTARY MEDIA

Detailed description of experiment and media that do not fit the main paper length and proposal is presented in *this online presentation (web link)*. URL: <https://gitlab.com/sr-lucasteixeira/pe-control-in-smpc-for-energy-eff-wide-bw-vlc>. Additional media file is a complementary material and it is not meant to replace the original paper content.

#### REFERENCES

- [1] I. Demirkol, D. Camps-Mur, J. Paradells, M. Combalia, W. Popoola, and H. Haas, "Powering the Internet of Things Through Light Communication," *IEEE Communications Magazine*, vol. PP, pp. 1–7, 2019.
- [2] H. Ma, A. Mostafa, L. Lampe, and S. Hranilovic, "Coordinated Beamforming for Downlink Visible Light Communication Networks," *IEEE Transactions on Communications*, vol. 66, no. 8, pp. 3571–3582, 2018.
- [3] N. Fujimoto and H. Mochizuki, "477 Mbit/s visible light transmission based on OOK-NRZ modulation using a single commercially available visible LED and a practical LED driver with a pre-emphasis circuit," *Optical Fiber Communication Conference and Exposition and the National Fiber Optic Engineers Conference (OFC/NFOEC)*, 2013, pp. 1–3, 2013.
- [4] F. M. Wu, C. T. Lin, C. C. Wei, C. W. Chen, Z. Y. Chen, H. T. Huang, and S. Chi, "Performance comparison of OFDM signal and CAP signal over high capacity RGB-LED-based WDM visible light communication," *IEEE Photonics Journal*, vol. 5, no. 4, 2013.
- [5] H. Li, X. Chen, J. Guo, Z. Gao, and H. Chen, "An analog modulator for 460 MB/S visible light data transmission based on OOK-NRS modulation," *IEEE Wireless Communications*, vol. 22, no. 2, pp. 68–73, 2015.
- [6] A. Tsiatmas, F. M. J. Willems, J. P. M. G. Linnartz, S. Baggen, and J. W. M. Bergmans, "Joint illumination and visible-Light Communication systems: Data rates and extra power consumption," *2015 IEEE International Conference on Communication Workshop, ICCW 2015*, pp. 1380–1386, 2015.
- [7] L. Teixeira, F. Loose, J. P. Brum, C. H. Barriquello, V. A. Reguera, and M. A. Dalla Costa, "On the LED Illumination and Communication Design Space for Visible Light Communication," *IEEE Transactions on Industry Applications*, vol. 55, no. 3, pp. 3264–3273, 2019.
- [8] J. Sebastian, D. G. Lamar, D. G. Aller, J. Rodriguez, and P. F. Miaja, "On the Role of Power Electronics in Visible Light Communication," *IEEE Journal of Emerging and Selected Topics in Power Electronics*, vol. 6, no. 3, pp. 1210–1223, sep 2018.
- [9] X. Deng, Y. Wu, K. Arulandu, G. Zhou, and J.-p. M. G. Linnartz, "Performance Analysis for Joint Illumination and Visible Light Communication using Buck Driver," *IEEE Transactions on Communications*, vol. 66, no. 5, pp. 2065–2078, 2018.
- [10] F. Loose, L. Teixeira, R. R. Duarte, M. A. Dala Costa, C. H. Barriquello, M. A. Costa, and C. H. Barriquello, "On the Use of the Intrinsic Ripple of a Buck Converter for Visible Light Communication in LED Drivers," *IEEE Journal of Emerging and Selected Topics in Power Electronics*, vol. 6, no. 3, pp. 1235–1245, 2018.
- [11] J. Rodriguez, D. G. Lamar, P. F. Miaja, and J. Sebastian, "Reproducing Single-Carrier Digital Modulation Schemes for VLC by Controlling the First Switching Harmonic of the DC-DC Power Converter Output Voltage Ripple," *IEEE Transactions on Power Electronics*, vol. 33, no. 9, pp. 7994–8010, 2018.
- [12] J. Rodríguez, D. G. Lamar, P. F. Miaja, D. G. Aller, and J. Sebastián, "Power Efficient VLC Transmitter Based on Pulse-Width Modulated DC-DC Converters and the Split of the Power," *IEEE Transactions on Power Electronics*, vol. 34, no. 2, pp. 1726 – 1743, 2019.
- [13] J. Rodriguez, D. G. Lamar, D. G. Aller, P. F. Miaja, and J. Sebastian, "Reproducing Multi-Carrier Modulation Schemes for Visible Light Communication with the Ripple Modulation Technique," *IEEE Transactions on Industrial Electronics*, no. Early access, 2019.
- [14] J. Kosman, O. Almer, A. V. N. Jalajakumari, S. Videv, and H. Haas, "60 Mb / s , 2 meters Visible Light Communications in 1 klx Ambient using an Unlensed CMOS SPAD Receiver," *Photonics Society Summer Topical Meeting Series (SUM)*, 2016 IEEE, vol. 1, pp. 171–172, 2016.
- [15] Z.-Y. Wu, Y.-L. Gao, J.-S. Wang, X.-Y. Liu, and J. Wang, "A Linear Current Driver for Efficient Illuminations and Visible Light Communications," *Journal of Lightwave Technology*, vol. 36, no. 18, pp. 3959–3969, 2018.
- [16] K. Modepalli and L. Parsa, "Lighting Up with a Dual-Purpose Driver," *2 IEEE Industry Applications Magazine*, no.

March/April, pp. 2–12, 2017.

- [17] M. L. G. Salmento, G. M. Soares, J. M. Alonso, and H. A. C. Braga, "A Dimmable Off-line LED Driver with OOK-M-FSK Modulation for VLC Applications," *IEEE Transactions on Industrial Electronics*, vol. 0046, no. c, pp. 1–1, 2018.
- [18] A. G. Tormo, "Bandwidth extension techniques for high-efficiency power amplifiers," Ph.D. dissertation, Technical University of Catalunya, 2011. [Online]. Available: <http://upcommons.upc.edu/handle/10803/22706>
- [19] P. S. Almeida, V. C. Bender, H. A. Braga, M. A. Dalla Costa, T. B. Marchesan, and J. M. Alonso, "Static and dynamic photoelectrothermal modeling of LED lamps including low-frequency current ripple effects," *IEEE Transactions on Power Electronics*, vol. 30, no. 7, pp. 3841–3851, 2015.
- [20] Bridgelux, "Bridgelux Vero 18 array series," Bridgelux, Tech. Rep., 2013. [Online]. Available: <https://www.bridgelux.com/resources/ds32-bridgelux-vero-18-data-sheet-gen-6>
- [21] B. P. Lathi, *Modern Digital and Analog Communications Systems*, 3rd ed., A. S. Sedra and M. R. Lightner, Eds. Nova York: Oxford University Press, 1998.
- [22] C.-S. A. Gong, Y.-C. Lee, J.-L. Lai, C.-H. Yu, L. R. Huang, and C.-Y. Yang, "The High-efficiency LED Driver for Visible Light Communication Applications," *Scientific Reports*, vol. 6, no. 1, p. 30991, 2016.
- [23] X. Deng, Y. Wu, K. Arulandu, G. Zhou, and J.-p. M. G. Linnartz, "Performance comparison for illumination and visible light communication system using buck converters," *2014 IEEE Globecom Workshops (GC Wkshps)*, pp. 547–552, 2014.
- [24] J. Sebastián, P. Fernández-Miaja, F. J. Ortega-González, M. Patiño, and M. Rodríguez, "Design of a Two-Phase Buck Converter With Fourth-Order Output Filter for Envelope Amplifiers of Limited Bandwidth," *Transactions on Power Electronics*, vol. 29, no. 11, pp. 5933–5948, 2014.



**Lucas Teixeira** (S'11) was born in Venâncio Aires, Brazil, in 1989. He received the B.S. degree in Electrical Engineering in 2012 and M.Sc. degree in Computer Science in 2015, both from the Federal University of Santa Maria (UFSM), Brazil. He is currently working towards the PhD degree in electrical engineering. His research interests include LED lighting systems, IoT and VLC systems.



**Felipe Loose** (S'17) was born in Cruz Alta, Brazil, in 1991. He received his B.S. and M.Sc. degrees in electrical engineering by the UFSM in 2016 and 2018, respectively. He is currently pursuing his Doctoral degree at the same institution. His research interests include power electronics applications, solid-state lighting systems, digital signal processing and VLC.



electronics in general.

**J. Marcos Alonso** (S'94, M'98, SM'03) received the M. Sc. Degree and Ph. D. both in electrical engineering from the University of Oviedo (UniOvi), Spain, in 1990 and 1994 respectively. Since 2007, he is a full Professor of the Electrical Engineering Department of the UniOvi. His research interests include lighting applications, dc-dc converters, power factor correction (PFC), resonant inverters, and power



for power electronics and tests of electric power transformers.

**Rafael Concatto Beltrame** (S'10–M'13) was born in Santa Maria, Brazil, in 1984. He received the B.S., M.S., and Ph.D. degrees in electrical engineering from the Federal University of Santa Maria (UFSM), Santa Maria, Brazil, in 2008, 2009 and 2012, respectively. His research interests include high-performance power converters for renewable energy sources, design of gate-driver circuits



**Carlos Henrique Barriuelo** was born in Três Passos, RS, Brazil, in 1984. He received the B.Sc., M.Sc. and Ph.D. degrees in Electrical Engineering from the UFSM in 2007, 2009 and 2012, respectively. His research interests include embedded and real time systems, wireless sensor and actuator networks, lighting systems, VLC and smart grid communication networks.



communication protocols and IoT.

**Vitalio Alfonso Reguera** received the B. Eng. degree in telecommunications and electronics engineering from the Universidad Central "Marta Abreu" de Las Villas (UCLV), Cuba. He received the M.Sc. degree in telecommunications engineering, and the Ph.D. degree in electrical engineering from the same university in 2000 and 2007, respectively. His current research interests include wireless networks,



**Marco Antônio Dalla Costa** (S'03, M'09, SM'17) was born in Santa Maria, Brazil, in 1978. He received the B.S. and M.Sc. degrees in Electrical Engineering from the UFSM, Brazil, in 2002 and 2004, respectively. His research interests include dc/dc converters, PFC, lighting systems, high-frequency electronic ballasts, renewable energy systems, solid state transformers, LED and VLC systems.



**6 MANUSCRIPT 5 - ON ENERGY EFFICIENCY OF VISIBLE LIGHT  
COMMUNICATION SYSTEMS**



# On Energy Efficiency of Visible Light Communication Systems

Lucas Teixeira, Felipe Loose, Carlos Henrique Barriquello,  
Vitalio Alfonso Reguera, Marco Antônio Dalla Costa

*Electrical Engineering Postgraduate Program Universidade Federal de Santa Maria, Santa Maria, RS, Brazil*

J. Marcos Alonso

*Electrical Engineering Department Universidad de Oviedo, Gijón, Principado de Asturias, Spain*

Corresponding author: Lucas Teixeira <teixeira@ieee.org>

**Abstract**—The reuse of the omnipresent LED lights for visible light communication (VLC) as short-range data carrier may be an environment-friendly add-on to the radio frequency-based mobile network and make several new applications feasible. However, this comes with the price of additional lighting device complexity and also of lower energy efficiency, which can be measured by its consumption factor (CF) representing the data rate to extra energy expense ratio (bits/J). This paper addresses the choice of driver circuit type and data modulation strategy in a framework based on the known VLC channel, LED and circuit models. Four applications of VLC are considered in the analysis: Li-Fi, virtual reality (VR), indoor localization (IL) and vehicular communications (VC). The main findings are that the reduced bit load and increasing bandwidth occupied by the modulation harm the efficiency of switching mode converters used as modulators, which were found to be cost-effective at low data rate applications of VLC, such as IL and VC. On the other hand, in higher data rate applications as Li-Fi and VR, linear mode modulators are surprisingly more energy efficient even when an extra step of power conversion is necessary to control average light or step down an unregulated supply voltage.

**Index Terms**—Energy conversion, light-emitting diode, visible light communication, wireless communication.

## I. INTRODUCTION

The visible light communication (VLC) uses imperceptible light intensity modulation to transfer data and simultaneously provide illumination. This technology uses the free-space optical channel, which has specific features that can be explored for different objectives. One may improve data security, increase wireless communication throughput or make new sort of applications feasible relying on light propagation behavior. VLC is not subject to limitations in the application like infrared and ultraviolet are because of health hazardous effects. However, some illumination constraints shall be taken into account because of the visual perception of the users. Although VLC can be thought as an additional feature to the lighting infrastructure, it also impacts the illumination quality and the energy efficiency of the lighting fixtures.

The term consumption factor (CF) is originally proposed as a simplification tool that allows engineers to provide a standard figure of merit to compare the energy efficiency of different cascade circuits or system implementations [1]. This can be a valuable tool for the study of VLC systems that has been proven promising for short-range and directional communication. This is especially important because

illumination systems shall comply with strict energy efficiency constraints. One of the key concepts of the CF concerns the energy efficiency factor, expressed in *bits-per-joule* [2]. The higher this ratio is, the less energy a system spends for the same communication performance. This metric is a base for communication engineers to analyze, to compare and to trade-off circuit and system design decisions [1]. In a communication link, the necessary signal power budget is dependent on the channel characteristics and on the resulting signal-to-noise ratio (SNR) at the receiver. Therefore, ultimately the analysis of the complete communication link shall be performed for the assessment of the necessary transmission signal power, which in turn affects the transmitter energy consumption.

Previous works already applied similar CF analysis in VLC application [3, 4], using models of LED, circuit drivers and different modulation schemes. In [3], the cost of a VLC system, considering only the extra energy spent in the LED at 1 Gbps data rate, showed that the CF reaches 20 Gbits/J at 2 m from the transmitter using a bandwidth of 100 MHz. Reference [4] calculated the maximum CF of 33.3 Gbits/J using two level-pulse amplitude modulation (PAM) and a class A driver converter, processing all LED forward current in a flat response VLC channel at 20 Gbps. Additionally, they compared two modulation schemes under equal conditions: for M-PAM scheme the CF was 43.5 Mbits/J and for OFDM the CF was 37.0 Mbits/J. In this sense, M-PAM is shown to be more attractive than orthogonal frequency-division multiplexing (OFDM) under an energy-constrained VLC application.

The current work aims at answering in a more comprehensive way the CF of a VLC transmitter, linking the signal power budget and the analysis of LED and driver circuit behavior. The current work method expands previous analysis from the literature using a complete photo-electro-thermal (PET) model of a commercial high power phosphor-covered white LED (PC-LED) and parameters of a real photo-diode as light sensor. We chose PC-LEDs because they are the most used for general purpose illumination, due to better efficiency-cost ratio compared to other types of LEDs. Additionally, several LED driver circuits, already proposed in the VLC literature, are modeled and compared in this study. These models use equivalent electrical component models in order to allow for a fair comparison among the analyzed circuit types. Four target applications of VLC, namely Li-Fi, virtual reality (VR), indoor

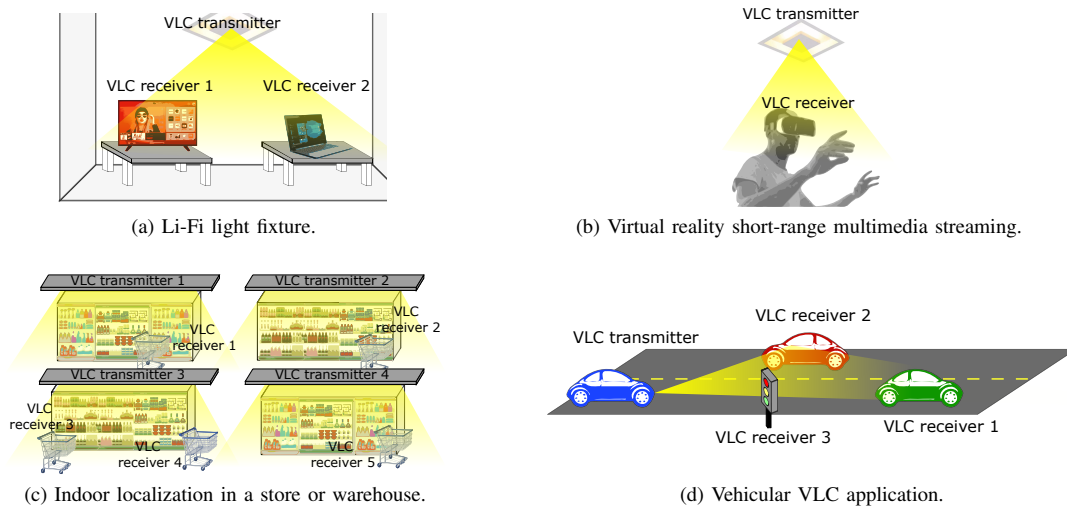


Fig. 1: VLC applications.

localization and vehicular networks, sketched in Fig. 1, were explored to point out the best design decisions on modulation circuits and modulation schemes considering the CF. These applications are characterized by light flux requirement, channel geometrical parameters and communication data rates. It should be noted that the CF here also considers the average power processing capability implicit of some converter types, which allows for a fairer comparison.

This work is organized as follows. The CF is explained in the VLC application context in Section II. After this, in Section III, the adopted models are introduced, as well as how the energy metrics were calculated in the proposed framework. The parameters of each VLC application are presented in Section IV and the main comparison charts, ruled by the CF and signal bandwidth, and analysis are shown in Section V. Section VI presents the discussion including all applications and the main findings. Finally, Section VII summarizes the conclusions of this work.

## II. SCOPE OF THE PROPOSED ENERGY-EFFICIENCY ANALYSIS FOR VLC SYSTEMS

The communication energy efficiency is expressed by its CF in the form of the ratio between the number of transmitted data bits and the energy consumed (bits/J). Moreover, it considers the power spent in the components that are on the signal path (directly processing the signal), as shown in Fig. 2, and also the power spent on ancillary functions (other system components not directly processing the signal, *off the signal path*, e.g. dc power processing, biasing, voltage regulation, etc.).

A VLC system faces simultaneously illumination constraints and also communication constraints. Regarding the first, the widespread lighting fixtures are an opportunity to the popularization of VLC. However, it also demands a high energy efficiency, because the artificial illumination consumes a significant amount of energy. For the second, the CF is a useful tool for comparing and trading-off system design decisions. It is worth noting that the energy spent for illumination purpose

shall not be considered as ancillary function. In this case, this parcel of energy is useful for other device's functionality simultaneous to the communication. Both aspects reflect either on light emitting device selection and driver circuit design and cannot be isolated from each other.

The intentional light intensity modulation for VLC may cause a drop in the global device efficacy of light emission. This happens both because of the characteristics of the irradiating device and driver circuit. Firstly, LEDs are the main light source used nowadays and they are susceptible to the so-called *droop effect* consisting in lower efficacy of emission at higher junction current densities. Therefore, as the current is varied for light intensity modulation, the stronger is the light modulation, the lower will be the luminous efficacy of the device [3, 5]. Secondly, the modulation of the current increments the effective current level that increases energy losses in the driver circuit. Thirdly, LED intentional voltage modulation requires additional voltage headroom ( $V_{HR}$ ) in some driver circuits, which ultimately reflects in complexity increase or efficiency reduction. Moreover, adding extra power processing stages aiming specifically at modulation can decrease the circuit efficiency and, therefore, the overall system efficacy. Section III-G explores deeply the CF calculation.

## III. VLC SYSTEM MODEL

The lighting and communication system model used in this study is depicted in Fig. 2. In this figure, it can be seen that the scope of this analysis is from the input bitstream to the amplified current at the receiver's analog front-end module, which includes a low noise amplifier (LNA). Although the data modulator block is not in the power path from the electrical source to the LED, it is included in the analysis because the characteristics of the signal resulting from each modulation and signaling scheme impact the system efficacy. The key measurements taken from this model to calculate the CF of the transmitter are the input power from the electrical power

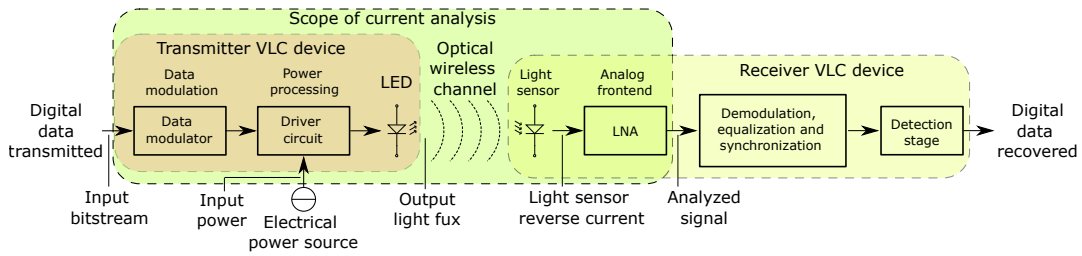


Fig. 2: VLC link model and scope of current work.

source and the light sensor amplified reverse current, at the output of the amplifier.

Finally, the illumination efficacy is calculated using the output light from the LED. The parts of this model are explored in Section III-A to Section III-G.

#### A. Modulation schemes

In this study, baseband signaling schemes as well as passband modulation schemes were considered. In baseband, the on-off-keying (OOK), pulse position modulation (PPM) and PAM are included. Those comprehend the most frequent schemes reported and used in current VLC standards. In passband, single carrier modulation schemes (SCM) and multiple carrier modulation schemes (MCM) were considered. Examples of SCM are phase-shift keying (PSK), amplitude-shift keying (ASK) and quadrature amplitude modulation (QAM). In this sense, the ripple modulation is a variation of PSK that can be implemented in switching mode modulator circuits taking advantage of the residual voltage ripple at its output, which is further explored in Section III-B2. Examples of MCM are discrete multitone and OFDM. Additionally, the passband modulation schemes are implemented using dc-offset (DCO) that is suitable for light intensity modulated communications.

OFDM has been pointed as the best scheme to be used in VLC due to the channel fading characteristic, also because of additional advantages on the implementation of symbol synchronization, channel estimation and equalization. Therefore, this scheme is considered to be included in future VLC standards [6, 7]. Flip-OFDM [8] and asymmetrically-clipped optical OFDM (ACO-OFDM) [9] are variations of OFDM modulation that are proposed in optical communications literature as alternatives to DCO-OFDM because they enable achieving higher signal variance under the restrictions of same average light. Those are considered for the VR application because of the higher data rates, which require increased bandwidth or signal power. However, in this case the average light and the signal power are not controlled independently, as is possible with DCO-OFDM, which causes higher current modulation index in the LED.

The definition of the required signal power considered the link power budget [10]. It is assumed here that the system can handle the distortion caused to the higher frequency components of the signal because of system dynamics, i. e. mainly LED low-pass behavior, as well as LED non-linear current-to-light transfer curve. This can be accomplished either by adequate carrier power distribution and bit loading at the

transmitter for MCM schemes [6] or by receiver equalization for baseband and SCM schemes [11]. In the transmitter the amplitude of ac components is adjusted aiming at achieving the minimum SNR required, which is dependent on each modulation scheme, to keep the bit-error-ratio (BER) below the forward error correction limit of  $10^{-3}$ . The required SNR is calculated from analytical expressions according to each modulation scheme [12]. However, for simplification, the effects of receiver equalization on noise components are not taken into account.

The definition of the root-mean-square modulation index ( $\alpha_{RMS}$ ) according to (1) [4] has been used in this analysis. In this equation, the overline notation  $\overline{(\cdot)}$  stands for average over time. Also, the signal bandwidth, which extends from zero to  $BW$  Hz, is controlled by the symbol rate ( $R_{SYM}$ ) according to (2). No concern is given to visible light flicker in any specific modulation scheme because there are several solutions to avoid this effect in VLC literature [13], which are out of the scope of the current work. Moreover, the frequency band that shall be avoided accounts for less than 1% of the available frequency band, which shall have little impact in the system data rate.

$$\alpha_{RMS}(X) = X_{rms}^{AC} / \overline{X} \quad (1)$$

$$R_{SYM} = \begin{cases} 2 \cdot BW, & \text{in baseband} \\ BW, & \text{in passband} \end{cases} \quad (2)$$

#### B. Driver circuit models

In this study, three types of modulators are considered, all of which have the same power processing capabilities, supplied from nominal input voltage ( $V_{IN}^N$ ). For a fair comparison, when the actual modulator circuit is not capable of efficiently dealing with high voltage step or average current control, an extra power processing stage is included to deal specifically with this role. The included circuit types are described as follows.

1) *Linear mode modulators (LMMs)*: These topologies are based on transistors operating in their linear region. Common types are class A, B, AB and C amplifiers. Thus, they operate based on a dissipative principle because there is a considerable voltage across the transistors power terminals simultaneously to the main current flow in order to keep the expected operating point. This type of circuit can be designed to have lower power consumption by minimizing the operating voltage headroom.

Besides, the limitation imposed because of the series equivalent resistance of semiconductor devices ( $R_{ON}$ ), MOSFET's used as linear amplifiers suffer from low bias voltage effects. At low source-to-drain voltage levels ( $V_{DS}^{MIN}$ ) the MOSFET's output impedance is reduced, which affects amplifier static gain performance, and the device's intrinsic capacitances are increased, harming the device's dynamic range because of slower operation.

In a practical application, an additional power processing stage is required to supply this type of converters from the nominal input voltage with optimum (minimum required) supply or with a dc current (to provide illumination bias only). Aiming at a fair comparison, for this additional power processing stage, the efficiency ( $\eta_{SD}$ ) of a synchronous buck switching mode power converter was assumed for average current control and voltage step-down. This converter has low switching frequency ( $F_{MIN}$ ) because it processes only dc power and has no modulation purpose. The use of switching mode power converter specifically as modulator is explored in the next subsection.

The linear modulator's minimum input voltage is constant, defined by design, which is enough for distortionless signal synthesis within its dynamic range. For this type of circuit, the class A and class AB amplifier are modeled. The first drains current provided to the LED from a constant voltage source, delivering simultaneously the dc and ac components of the power. For the second, a bias-T structure [4, 14] is considered to provide the dc current to the LED, therefore the amplifier provides the ac LED's current components that are coupled using a capacitor.

2) *Switching Mode Modulator (SMM)*: These converters are based on transistors operating in saturation and cut-off regions to generate a square waveform that is afterward applied to an LC band-pass filter or low-pass filter. This type of circuit is known by its high efficiency and it is commonly used in illumination purpose LED drivers. They are most frequently operated using pulse-width modulation for average output power control. The intentional modulation for communication can be performed using one of two principles:

a) *Average Current Control (ACC)*: It consists of shaping the output average voltage by modulating the duty cycle [15] to track a low-frequency reference whose harmonic content remains within the filter passband. These converters have the switching frequency ( $F_S$ ) defined accordingly to keep the modulation with a minimum ratio of  $F_S/BW$ , which is a conservative definition and it is sufficient to shape the current for VLC for small signal excursions [16]. The minimum value for this frequency is also constrained by  $F_{MIN}$ .

b) *Ripple Modulation (RM)*: It takes advantage of the converter inherent residual frequency content that remains after filtering [17, 18]. This is implemented by controlling the phase of the switches according to the information to be transmitted. Hence, the average duty cycle is kept constant and, in this case, the resulting signal shape is directly dependent on the filter bandwidth.

Therefore, the carrier frequency and signal amplitude are linked because of fixed filter parameters. The switching frequency of this converter, which is equal to the carrier fre-

quency in this case, is set at  $BW/2$  in order to accommodate most of signal components within zero to  $BW$  Hz band.

In both the above cases, the operation does not occur under dissipating principle. However, technology limitations lead to energy losses that can be estimated from operational conditions and circuit device parameters. While not claiming to be exhaustive, those conditions and parameters are switches transition time ( $t_{SW}$ ), switching frequency, root mean square currents ( $I_{RMS}$ ), series equivalent resistance of passive components ( $R_S$ ) and semiconductor devices, semiconductor blocking voltages ( $V_{BLOCK}$ ) and peak currents ( $I_{PK}$ ). In this work, the losses are calculated using (3) [19] for switching losses ( $P_{LSW}$ ) in active devices.

$$P_{LSW} = \sum_{k=\text{semiconductors}} \frac{1}{2} V_{BLOCK}^k I_{PK}^k t_{SW}^k F_S^k \quad (3)$$

The synchronous buck converter topology modeled is capable to perform simultaneous average input voltage step-down and current modulation. The design of inductance and capacitance for the passive filter followed defined magnetic current excursion ( $\Delta I$ ), which cannot be mistaken with the current ripple at the LED that is lower. Moreover, to increase the modulation bandwidth of these converters the preemphasis technique was considered to reduce switching frequency requirements [16]. Despite that, the converter is not able to keep all dynamic performance to synthesize steep zero or high current levels given to the duty cycle range restriction.

3) *Series Switch Modulator (SSM)*: This modulator is based on turning on and off the LED by using a series switch. This circuit cannot control the instantaneous current level, which is defined by input dc voltage. As an actuator, a single transistor, e.g. bipolar transistor or MOSFET, is employed. This type of modulator differs from LMM in that there is no transistor bias current to operate the transistor in linear region. On the contrary, the transistor is operated in cut-off and saturation regions, as an open and closed switch respectively. Therefore, it is only able to generate rectangular pulses, which reduces the possible signal modulation schemes; however, it is simple to implement. The energy efficiency of this converter is composed by the parcel due to semiconductor static losses and switching losses. Also in this case, a previous conversion stage, which is considered having efficiency  $\eta_{SD}$ , is necessary to step-down and regulate the required input voltage.

### C. LED photo-electro-thermal model

The LED photo-electro-thermal model includes all characterization of the photometric light emission of the device as well as the electrical behavior. All these aspects are subject to the thermal effects caused by self heating and environment temperature. The modeled LED is a Bridgelux Vero 18 array series, part number BXRC-50C4000-F-24, which has 4603 lm of nominal light flux and was already experimentally verified using a real device under extensive and comprehensive modulated current stimuli [5]. For the final light fixture special optical components can be employed to

comply with specific visual perception requirements of each application; however, for sake of simplicity, the geometrical and optical characteristics of this device were used. The power spectral emission of the LED is assumed constant, although this characteristic may change according to device junction temperature, which suffers effect of LED junction to ambient thermal resistance ( $R_T$ ) and environment temperature ( $T_{ENV}$ ). An indeep study of this effect in VLC can be found in [20]. The main thermal effects that are considered in the model of the current work are the drop of light emission according to the junction temperature ( $-0.21\%/^{\circ}C$ ) and the change in LED threshold voltage ( $-15mV/^{\circ}C$ ). Particularly, PC-LEDs exhibit a characteristic cutoff frequency around 3.8 MHz in the optical domain, which limits signal bandwidth and data rate in VLC applications [21]. In order to take advantage of the band at higher frequency range the analysis of the attenuation of each frequency component is performed, which is further explained in III-F. No higher frequency effects other than those caused by the phosphor layer were taken into account for this model.

#### D. Optical wireless channel propagation

The VLC channel is an optical wireless channel (OWC) in which the incident light depends on the transmitted light and on the VLC dc channel gain ( $H$ ) caused by several geometrical factors following (4) [4, 10, 22]. Those factors include the distance between transmitter and receiver ( $d$ ), the irradiance angle ( $\psi$ ), the incidence angle ( $\omega$ ), the order of Lambertian emission ( $m$ ) and the light sensor area ( $A$ ) [22]. The area is implicit in the sensor gain, which is presented in next subsection. This analysis includes only line-of-sight propagation.

$$H = \frac{(m+1)A}{2\pi d^2} \cos^m(\psi) \cos(\omega) \quad (4)$$

#### E. Light sensor and amplifier noise models

The analysis of the light sensor aims at calculating the photocurrent resulting from the incident light signal and the variance of the noise added to this current inside its bandwidth. The Vishay Semiconductors BPW34 PIN photodiode that was used as reference model in this study acts as a fast response light sensor in reverse-biased condition in which the responsivity to incident light is well characterized. The absolute reverse current follows a linear relationship with the incident light intensity in the range from 10 lx to 10 klx at 5  $\mu A/lx$  rate.

The noise variance is calculated from different noise effects including Shot noise and Johnson noise, the last one is also called thermal noise. Both effects have constant power spectral density [4]. Johnson noise depends on the light sensor temperature and Shot noise depends on the sensor average reverse current. The noise equivalent power (NEP) is used to calculate the input referred noise. In order to provide a realistic scenario, the noise of a commercial low-noise operational amplifier model OPA657 is also considered in the noise budget for the LNA. The NEP at the amplifier input is  $1.3fA/\sqrt{Hz}$ .

#### F. Channel capacity calculation

The SNR of the amplified light sensor photo-current is calculated according to (5) using the variance of the signal ( $\sigma_S^2$ ) at the receiver caused by the incident light and the variance of the noise ( $\sigma_N^2$ ) inside its bandwidth. The VLC receiver is affected by additive white Gaussian noise (AWGN) [4], which has constant noise power density ( $N_{PSD}$ ). Hence, the SNR expression can also be represented in terms of the total signal power ( $P_S$ ) and total noise power integrated over the entire occupied bandwidth ( $BW$ ).

$$SNR = \frac{\sigma_S^2}{\sigma_N^2} = \frac{P_S}{N_{PSD} \cdot BW} \quad (5)$$

The spectral efficiency of the modulation ( $\phi_{MOD}$ ) can be used to calculate the maximum achievable data rate ( $DR_{MS}$ ) using (6). The maximum data rate ( $DR_{MAX}$ ) expression in (7) [23] is independent of the modulation scheme; it is valid under AWGN and do not account for the positive and maximum instantaneous light power constraints. Therefore, it overestimates the actual capacity and this can be taken as an upper bound [3].

$$DR_{MS} = \phi_{MOD} \cdot BW \quad (6)$$

$$DR_{MAX} = BW \cdot \log_2(1 + SNR) \quad (7)$$

Equation (7) represents the usual bandwidth-power trade-off. Following (5) and (7), a given data rate can be achieved with different combinations of the bandwidth and signal power by means of adequate symbol rate and modulation scheme selection. It is worth noting that the bandwidth directly affects the expression (7) and also indirectly by means of SNR calculated using (5), which causes a saturation effect when increasing the bandwidth. Fig. 3 numerically exemplifies this trade-off and the LED's frequency response, which exhibits an opposite signal power to bandwidth dependence. In this sense, for a fixed data rate, the wider is the modulation bandwidth, the lower is the required signal power. Observing the LED's current, in the other hand, the lower gain of the LED, at high frequency range, requires higher current variance for same light signal power. Therefore, either improving or reducing the signal bandwidth trends to require improving LED's current variance, which is undesired to maximize LED's efficacy, because of one of these aspects. Therefore, these opposite behaviors gives no clear answer about the best choice of signal bandwidth for VLC, which will be clarified according to the applications in Section V.

#### G. Calculation of consumption factor

In this work, the input power with VLC enable ( $P_{IN}$ ) and the power provided to the LED in a non-modulated state ( $P_{LED}^{dc}$ ) are used to calculate the CF. The value of  $P_{IN}$  represents the input power of the driver circuit, performing a global device analysis, or  $P_{IN}$  represents the LED input electrical power, when focusing the analysis only on the LED performance. Therefore, the CF is calculated using (8). CF

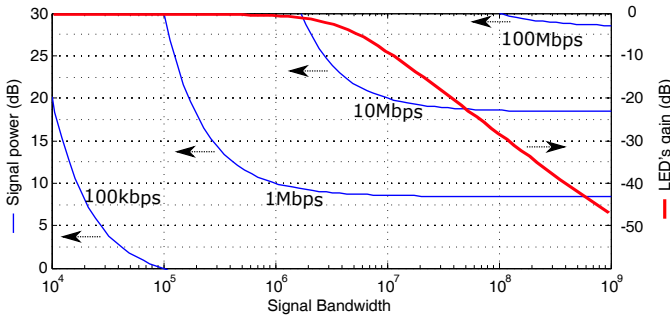


Fig. 3: Example of bandwidth-power trade-off with AWGN noise in (7) and PC-LED's frequency response.

may be independent of the modulation scheme using  $DR = DR_{MAX}$  or to an specific scheme by using  $DR = DR_{MS}$ .

$$CF = \frac{DR}{P_{IN} - P_{LED}^{dc}} [bps/W \text{ or } bits/J] \quad (8)$$

#### IV. FEATURED VLC APPLICATIONS

The parameters that characterize the four analyzed applications of VLC are described in this section, as follows.

##### A. Li-Fi capable light fixture

The Li-Fi VLC application, whose operation environment is depicted in Fig. 1a, is characterized by a data rate of 54 Mbps and mobility within a range up to 2 m from the light source, irradiance and incidence angles up to  $40^\circ$ . This is a typical office environment with expected illumination intensity of 500 lx at the desktop. To achieve the proposed data rate with a narrow bandwidth of the LED (3.8 MHz) a highly spectral efficient modulation scheme, performing at least 14.2 bps/Hz, shall be used. Otherwise, light signal distortion occurs when it is allocated in the frequency range which exceeds LEDs flat dynamic response and, therefore, some considerations described in Section III-A shall be taken into account to avoid high BER.

##### B. VR short range link

The virtual reality data link using VLC can be used to wireless stream multimedia and real time interaction stimuli in a very directional short range, as depicted in Fig. 1b. The data rate of 1 Gbps is considered, because it is sufficient for UHD video and audio real time streaming. This application has low mobility, because the light sensor lies at maximum distance of 1.5m below the light source, irradiance and incidence angles are up to  $30^\circ$ . Total light flux of 2500 lm shall be provided to generate approximately 1000 lx at the height of the receiver within the circle with radius of 1.7 m. This corresponds to 360 lx at the desktop level, approximately 2.5 m below the receiver. Most of the signal power resides in the LED attenuated band in this case because to reach the required data rate using only the flat response band would require a modulation scheme performing very high spectral efficiency (at least 263 bits/Hz), which is impracticable.

TABLE I: Simulated model parameters.

Parameter	Value
$R_{ON}$	$0.05 \Omega^a$ $0.25 \Omega^b$
$R_S$	$0.02 \Omega^a$ $0.10 \Omega^b$
$V_{DS}^{MIN}$	0.45 V
$t_{SW}$	10 ns
$\Delta I$	$0.4\bar{I}^c$
$F_S/BW$	4
$F_{MIN}$	20 kHz
$T_{ENV}$	$25^\circ C$
$R_T$	$2.5^\circ C/W$
$V_{IN}^N$	50 V
NEP	$40 fW/\sqrt{Hz}$

<sup>a</sup> Selected according to the average LED current of the indoor localization application (average 5.0 A).

<sup>b</sup> For other applications, Li-Fi, VR and vehicular.

<sup>c</sup> Default value for ACC, for RM the filter cutoff frequency is defined according to achieve the required signal power.

##### C. Indoor localization infrastructure

In this application the data rate is lower if compared to previous ones. Usually simple beacon packets are used to signal the illuminated receivers its position; therefore 100 kbps data rate is usually enough. The light sensor may be up to 6 m from the light source, in a typical store or commercial warehouse of 4m-height ceiling and the target illuminated surface at 1m height from the ground. The operating environment of this application is depicted in Fig. 1c. The irradiance and incidence angles are up to  $60^\circ$  which projects light in an area of  $84.8 m^2$  (5.2 m radius). The corresponding ground area needs 17000 lm to provide in average 200 lx at the illuminated surface.

##### D. Vehicular VLC

In a vehicular application of VLC the headlights of the car illuminate the road, the traffic signs and the other vehicles simultaneously providing data transmission, as it is depicted in Fig. 1d. The data transmitted may contain information from the vehicle, from the road or transit status, thus the required data rate is low, here defined as 100 kbps. The transmitter may head in the direction of the receiver (car-to-car communication running in same direction, receiver 1 in Fig. 1d) up to 100 m away from the light receiver. Alternatively, the receiver is slightly to the side when there are vehicles in opposite direction (receiver 2) or a traffic sign (receiver 3). In these cases the receiver lies 10 m away and near to the transmitter circulation lane within a 11.5 m-wide beam width, the irradiance and incidence angles of the light can be up to  $30^\circ$ . Total light flux of 8000 lm is expected as output of the car headlights which in this analysis requires 2 LEDs.

##### E. Simulation parameters

Table I presents a summary of all parameters used to simulate and analyze the VLC link application examples. Additionally, for each modulation scheme, the symbols are distributed with equal probability among all possibilities.

## V. RESULTS AND DISCUSSION

In this section, the results and evaluation of best design choices for the VLC applications described above are presented.

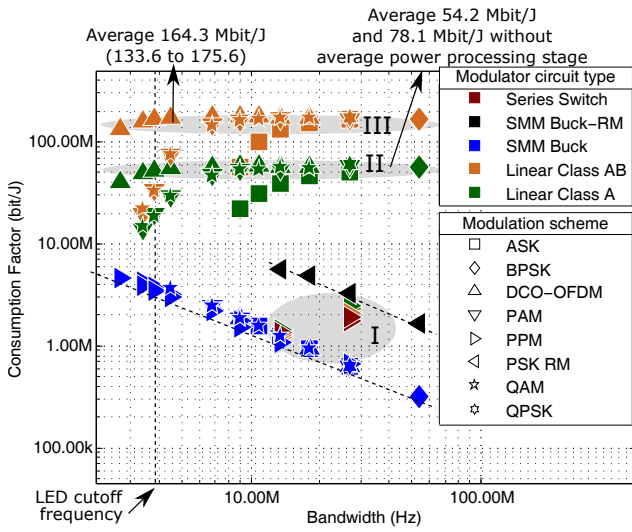


Fig. 4: CF of Li-Fi capable light fixture.

### A. Li-Fi

Fig. 4 depicts the CF of Li-Fi for fixed data rate and variable bandwidth of modulation. The solutions are classified into modulator circuit types (color of marker) and modulation schemes (shape of marker) in this figure. It shows inside the gray area I that most of the linear modulators implementing PPM have lower CF when compared to other modulation schemes. The class A modulator, solutions inside gray area II, had the average CF similar, same order of magnitude, to previously reported in [4], in which the data rate is 20Mbps and the distance is 2m, when only the modulator without average power processing stage is taken into account. This class A type of converter is directly affected by the required operating voltage headroom of 0.67 V in average, in the interval [0.59 V, 0.81 V], and the LED average current of 1.03 A which flows through the circuit. The CF achieved with switching mode modulators drops severely with the signal bandwidth, that is because the switching losses account for at least 98% of energy losses. The DCO-OFDM modulation have no significant difference in CF when compared to other SCM and baseband schemes. In this sense, it is opposed to the conclusion of [4]. Finally, the best CF was achieved with class AB linear amplifier as modulators, in average 165.4 Mbits/J, depicted in area III. In this case, the CF has little sensitivity to bandwidth because of the low average current modulation index 0.035, in the interval [0.017, 0.078], thus requiring the minimum supply voltage of 1.35 V, in the interval [1.14 V, 2.04 V], which is a critical factor for losses in class AB amplifiers. Indeed, the linear circuit supply accounts for 7% of the extra power spent and the average voltage step down processing accounts for 93% of it.

### B. VR

Fig. 5 presents CF for this application of VLC. The switching mode modulators have poor performance due to excess of switching losses in such wide bandwidth modulators. Therefore, it is clear that with the considered technology,

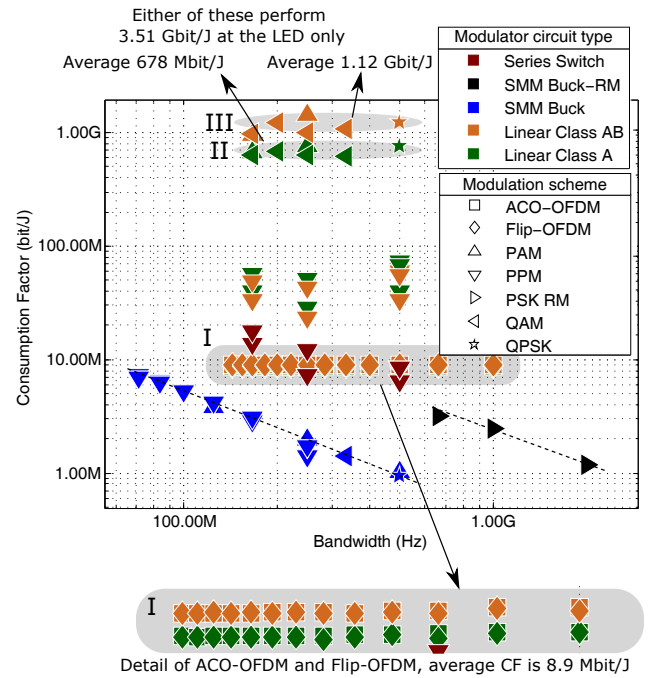


Fig. 5: CF of VLC for short VR data link.

mainly impacted by the  $t_{SW}$ , the application of switching mode modulators is not feasible. Also, the DCO-OFDM scheme is unable to achieve the required signal power with the average light flux of this application. Therefore, the ACO- and Flip-OFDM are included. These modulation schemes, in detail labeled I in the figure, achieved average CF of 8.9 Mbits/J. In this case, because of the lower LED efficacy caused by higher current modulation index ( $>1.5$ ), the LED itself performs only CF of 289.37 Mbits/J (not considering the losses in the driver circuit), also the modulator efficiency is 87.0% in average. Therefore, the many advantages of these OFDM-based modulations are severely counterweighted by the lower CF of the transmitter.

The solutions inside areas labeled II and III of Fig. 5 achieved a CF of 3.51 Gbits/J considering only the LED, in the interval [2.78 Gbits/J, 5.85 Gbits/J], that agrees with the reported for same data rate by [3], both been in the order of gigabits per joule, which considered a best case scenario in their analysis. Again the advantage of class A (see area labeled II, CF is 678 Mbits/J) and class AB (see area labeled III, CF is 1.12 Gbits/J) linear modulators is clear, when using simple modulation schemes such as 4- and 8-PAM, QPSK, 8- to 64-QAM. These modulators are able to achieve such higher performance because of lower current modulation index (0.34) and higher modulator's efficiency (93.9 % and 96.8 % for class A and AB, respectively). For these solutions in areas labeled II and III, the modulator itself spent 29.2% of the extra power and the additional stage, for voltage step down and average current control, accounts for 70.8% of the extra power.

### C. Indoor localization

Fig. 6 depicts the CF according to the modulation bandwidth. Linear class AB (58.6 kbits/J, see label I) and SMM

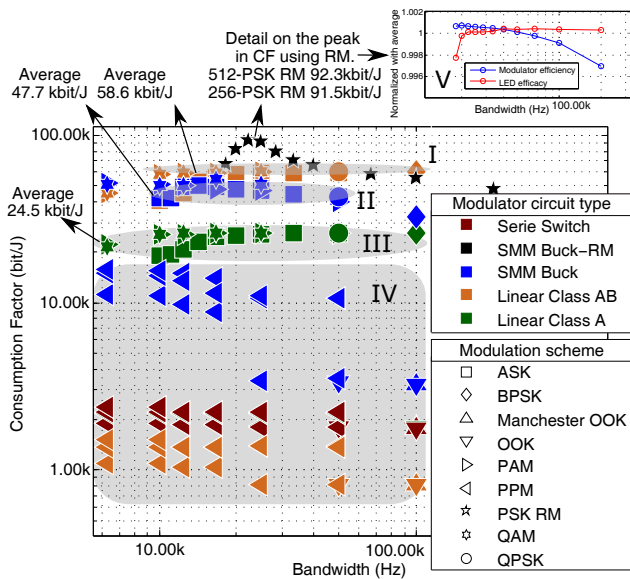


Fig. 6: CF of VLC for indoor localization.

using ACC (47.7 kbits/J, in area II) had similar CF; however, the first requires two power processing stages, which are the linear modulator itself and another converter to process the average power with high efficiency. Linear class A (24.5 kbits/J, see label III) and all OOK-based modulation schemes (OOK, Manchester-encoded OOK and PPM, see IV in Fig. 6) have significant inferior CF. The current modulation index in the cases of all DCO modulation schemes (QAM, PSK, ASK and DCO-OFDM) is reduced, in average 1.2% in the interval [0.8%, 4.8%]. No significant difference in LED's efficiency is observed among linear class modulators under different modulation schemes and bandwidth above 20 kHz. However, the bandwidth increase of switching mode drivers, using either ACC or RM, increases the required switching frequency which in turn reduces the efficiency and the CF. The best solutions considering the CF for this application are below 100 kbits/J. These solutions employ RM performing 512-PSK 92.3 kbits/J and 256-PSK 91.5 kbits/J, which is 37% higher than the average CF of linear class AB modulator. There is an optimum signal bandwidth (between 22.2 and 25.0 kHz) in which a maximum CF is achieved using RM, which is explained because of rising LED efficacy and falling modulator efficiency with increasing signal bandwidth within the studied range, see detail V in Fig. 6. In an overall analysis, for the indoor localization application of VLC and the resulting CF, the ripple modulation is pointed out as the best choice of converter because of reduced driver circuit stages.

#### D. Vehicular Communications

The CF results are summarized in Fig. 7 according to the signal bandwidth. The current modulation index required in this application is in average 7.0% (from 1.8 % to 18.5%) for the studied bandwidth range. Therefore, there is a significant difference among the CF of different modulation schemes either with SMM using ACC (see area I in Fig. 7), linear classes AB (see area II) or A (see area III). The shadowed

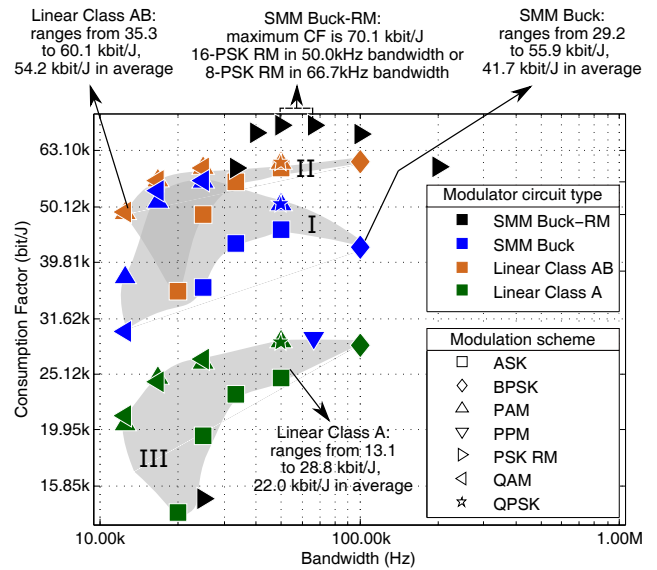


Fig. 7: CF of VLC for vehicular application.

areas highlight the wide difference of CF between M-ASK schemes, which encodes information only on the amplitude of a sinusoidal carrier, and other modulation schemes. This effect was less pronounced in the previously analyzed applications. The main finding here is that the CF of M-ASK is significantly lower than the achieved by M-QAM, M-PSK and M-PAM schemes in similar bandwidth values, e.g. with linear class AB the 32-ASK in 20.00kHz achieves only 35.4 kbits/J and 16-QAM in 25.00kHz reaches 58.7 kbits/J. This comes from the fact that M-ASK requires higher light signal modulation index at the receiver, because the pulse energy in M-ASK must be twice that in M-PSK [12], which forces the increase in current modulation index, harming the efficacy of the LED. Additionally, this modulation scheme demands higher voltage headroom in the design of linear modulators because of higher peak-to-average power ratio, finally reducing global efficacy.

In this application also RM has a maximum CF value which was already explained in Section V-C for indoor localization. Despite the better CF of SMM RM in comparison to linear class AB (+14%) and SMM using ACC (+20%), the best performance difference is less significant than the observed for the previous application scenario.

## VI. DISCUSSION

Switching mode LED drivers are the best energy-aware choice to be used as modulator circuit in low data rate VLC applications, like the indoor localization and vehicular communication. This comes from the fact that lower switching frequency allowed for reduced losses and avoids the need for two dedicated power processing stages, which is required by linear or series-switch modulators. Moreover, the use of dc-offset modulations with higher spectral efficiency improved the consumption factor of switching mode modulators because of reduced bandwidth required. It was shown that ripple modulation have the best consumption factor and it is the most indicated modulation scheme in this context.



In those applications of VLC which require wider modulation bandwidth, exceeding LED's flat response band, the switching mode modulators have very low consumption factor that results mainly from the high switching frequency required. In this case, the simultaneous average power processing and modulation for communication capabilities is disadvantageous. On the other hand, the linear power amplifiers, although working in a dissipative principle, are more suitable for the high-data rate VLC applications, such as exposed in Li-Fi and virtual-reality data link applications, because they achieve superior consumption factor, thus requiring less additional energy to perform same communication. Even when using linear modulators in these applications, the dominant energy losses were found to be related to the average power processing stage. Moreover, the most suitable modulation schemes are those with lower spectral efficiency, which require increase in bandwidth and allow for less signal excursion, thus improving linear modulators consumption factor despite the signal attenuation when using phosphor-covered white LEDs.

Additionally, all solutions using modulation schemes with at least one level at zero current, i. e. OOK-based, have always lower consumption factor in comparison with other modulation schemes. Despite the good efficiency of series switch modulator, which can realize these modulation schemes, the LED conversion efficacy drops because of higher current modulation index and it accounts for most of the extra energy spent for VLC. Therefore, in an energy-aware VLC system, the OOK-based modulation schemes and the series switch modulators shall be avoided. This conclusion is only possible, achieving the best of energy efficiency, with the analysis of the complete system that allows for the minimization of the transmitter light modulation index. In this case, the decision of simplifying the receiver (e. g. using a simple OOK-based modulation scheme) was shown to have a very high energy cost at the transmitter side. On the other hand, using linear modulators, dc-offset OFDM has similar energy expense as other baseband or dc-offset single-carrier modulation schemes. However, other optical OFDM variations, i.e. Flip-OFDM and asymmetrically-clipped optical OFDM, which allow for extra signal power under limited average light flux, have the worst energy performance because they achieved two orders of magnitude (125 times) lower consumption factor.

Finally, given the facts, it is possible to extract the following conclusions: i. the consumption factor values of the four applications of VLC are fairly constant for a wide signal bandwidth and modulation index ranges, ii. the dc-offset modulation schemes are the most energy-efficient and iii. only a small parcel of the extra power is spent in the actual modulator circuit for the best solutions. Therefore, the main loss of energy was found to be still related to the average power control targeting illumination feature, whereas the implementation of communication itself accounts for a smaller part of the extra energy consumed.

## VII. CONCLUSIONS

In this work an efficacy-driven analysis of VLC is presented including multiple aspects, i.e. LED behavior using PET

theory, driver's efficacy and several modulation schemes. The inclusion of parameters of concrete applications of VLC lead to comparison scenarios closer to the reality. Moreover, the signal power budget analysis allowed for trading off the bandwidth and modulation factor required and their effect on each combination of modulator circuit and modulation scheme. The analysis of the extra energy spent for VLC in each application lead to the find that the limitations of semiconductors affect different modulator circuits types according to the required modulation bandwidth.

The dc-offset modulation schemes are the best option considering the energy efficiency and allowing for independent average light and signal variance control. The OOK-based, ACO-OFDM and Flip-OFDM, which have no dc-offset, were shown to have a significant droop in LEDs efficacy and driver circuit efficiency, leading to lower consumption factor. The dc-offset OFDM was shown to have no significant efficacy difference in comparison with other baseband or dc-offset passband modulation schemes.

The switching mode modulators were found to be the best solutions, given the reduced number of power processing stages and higher consumption factor, indicating best use of extra energy spent for communication in application of indoor localization and vehicular communications. Both these applications are characterized by reduced data rate and signal bandwidths up to 100 kHz. In this condition the use of a single power processing and modulation stage is a clear advantage for the switching mode modulator circuits. On the other hand, in the higher data rate applications, i.e. Li-Fi and virtual reality, which require wider signal bandwidth, in the dozens of megahertz range, the linear mode modulators are clearly advantageous. In this case, including a dissipative dedicated power processing stage only for modulation purpose is the most energy efficient solution.

## REFERENCES

- [1] J. N. Murdock and T. S. Rappaport, "Consumption factor and power-efficiency factor: A theory for evaluating the energy efficiency of cascaded communication systems," *IEEE Journal on Selected Areas in Communications*, vol. 32, no. 2, pp. 221–236, 2014.
- [2] H. M. Kwon and T. G. Birdsall, "Channel Capacity in Bits Per Joule," *IEEE Journal of Oceanic Engineering*, vol. 11, no. 1, pp. 97–99, 1986.
- [3] A. Tsiatmas, F. M. J. Willems, J. P. M. G. Linnartz, S. Baggen, and J. W. M. Bergmans, "Joint illumination and visible-Light Communication systems: Data rates and extra power consumption," *2015 IEEE International Conference on Communication Workshop, ICCW 2015*, pp. 1380–1386, 2015.
- [4] X. Deng, K. Arulandu, Y. Wu, S. Mardanikorani, G. Zhou, and J. P. M. Linnartz, "Modeling and Analysis of Transmitter Performance in Visible Light Communications," *IEEE Transactions on Vehicular Technology*, vol. 68, no. 3, pp. 2316–2331, 2019.
- [5] L. Teixeira, F. Loose, J. P. Brum, C. H. Barriuello, M. Antônio, D. Costa, and V. A. Reguera, "On the LED Illumination and Communication Design Space for Visible Light Communication," *IEEE Transactions on Industry Applications*, p. (no prelo), 2019. [Online]. Available: <https://ieeexplore.ieee.org/document/8643806>
- [6] S. Mardanikorani, X. Deng, and J. P. M. Linnartz, "Sub-Carrier Loading Strategies for DCO-OFDM LED Communication," *IEEE Transactions on Communications*, vol. 68, no. 2, pp. 1101–1117, 2020.
- [7] N. Serafimovski, T. Baykas, and V. Jungnickel, "Status of IEEE 802 . 11 Light Communication TG," 2019. [Online]. Available: [http://www.ieee802.org/11/Reports/tgbb\[\\_\]update.htm](http://www.ieee802.org/11/Reports/tgbb[_]update.htm)
- [8] N. Fernando, Y. Hong, and E. Viterbo, "Flip-OFDM for unipolar communication systems," *IEEE Transactions on Communications*, vol. 60, no. 12, pp. 3726–3733, 2012.

- [9] J. Armstrong, A. Lowery, A. J., and A. Lowery, "Power efficient optical OFDM," *Electronics Letters*, vol. 42, no. 6, 2006.
- [10] B. Hussain, X. Li, F. Che, C. P. Yue, and L. Wu, "Visible Light Communication System Design and Link Budget Analysis," *Journal of Lightwave Technology*, vol. 33, no. 24, pp. 5201–5209, 2015.
- [11] M. A. Kashani and M. Kavehrad, "On the performance of single- and multi-carrier modulation schemes for indoor visible light communication systems," *2014 IEEE Global Communications Conference, GLOBECOM 2014*, pp. 2084–2089, 2014.
- [12] B. P. Lathi, *Modern Digital and Analog Communications Systems*, 3rd ed., A. S. Sedra and M. R. Lightner, Eds. Nova York: Oxford University Press, 1998.
- [13] S. H. Lee, S.-Y. Jung, and J. K. Kwon, "Modulation and coding for dimmable visible light communication," *Communications Magazine, IEEE*, vol. 53, no. 2, pp. 136–143, 2015.
- [14] H. L. Minh, D. O. Brien, G. Faulkner, L. Zeng, K. Lee, D. Jung, and Y. Oh, "80 Mbit / s Visible Light Communications Using Pre-Equalized White LED," *2008 34th European Conference on Optical Communication*, vol. 5, no. September, pp. 1–2, 2008.
- [15] J. Sebastian, D. G. Lamar, D. G. Aller, J. Rodriguez, and P. F. Miaja, "On the Role of Power Electronics in Visible Light Communication," *IEEE Journal of Emerging and Selected Topics in Power Electronics*, vol. 6, no. 3, pp. 1210–1223, sep 2018. [Online]. Available: <https://ieeexplore.ieee.org/document/8351928/>
- [16] L. Teixeira, F. Loose, J. M. Alonso, R. C. Beltrame, C. H. Barriuello, V. A. Reguera, and M. A. D. Costa, "Pre-Emphasis Control in Switched Mode Power Converter for Energy Efficient Wide Bandwidth Visible Light Communication," *IEEE Journal of Emerging and Selected Topics in Power Electronics*, pp. 1–1, 2019. [Online]. Available: <https://ieeexplore.ieee.org/document/8932532/>
- [17] J. Rodríguez, D. G. Lamar, D. G. Aller, P. F. Miaja, and J. Sebastian, "Reproducing Multi-Carrier Modulation Schemes for Visible Light Communication with the Ripple Modulation Technique," *IEEE Transactions on Industrial Electronics*, vol. 67, no. 2, pp. 1532 – 1543, 2020. [Online]. Available: <https://ieeexplore.ieee.org/document/8704307/>
- [18] F. Loose, L. Teixeira, R. R. Duarte, M. A. Dalla Costa, and C. H. Barriuello, "On the Use of the Intrinsic Ripple of a Buck Converter for Visible Light Communication in LED Drivers," *IEEE Journal of Emerging and Selected Topics in Power Electronics*, vol. 6, no. 3, pp. 1235–1245, sep 2018. [Online]. Available: <https://ieeexplore.ieee.org/stamp/stamp.jsp?tp={&}arnumber=8370626https://ieeexplore.ieee.org/document/8370626/>
- [19] R. Co, "Calculation of Power Loss ( Synchronous )," pp. 1–4, 2016. [Online]. Available: [www.rohm.com](http://www.rohm.com)
- [20] H. Chen, A. T. L. Lee, S.-c. Tan, and S. Y. Hui, "Electrical and Thermal Effects of Light-Emitting Diodes on Signal-to-Noise Ratio in Visible Light Communication," *IEEE Transactions on Industrial Electronics*, vol. 66, no. 4, pp. 2785–2794, 2019.
- [21] C. Lee, C. Shen, H. M. Oubei, M. Cantore, B. Janjua, T. K. Ng, R. M. Farrell, M. M. El-Desouki, J. S. Speck, S. Nakamura, B. S. Ooi, and S. P. DenBaars, "2 Gbit/s data transmission from an unfiltered laser-based phosphor-converted white lighting communication system," *Optics Express*, vol. 23, no. 23, p. 29779, 2015.
- [22] T. Komine and M. Nakagawa, "Performance Evaluation Of Visible-Light Wireless Communication Systems using White LED Lightining," in *Proceedings. ISCC 2004. Ninth International Symposium on Computers And Communications*, 2004, pp. 490–494.
- [23] C. Shannon, "Communication in the Presence of Noise," in *Proceedings of the IRE*, vol. 37, no. 1, jan 1949, pp. 10–21. [Online]. Available: <http://ieeexplore.ieee.org/document/1697831/>



## 7 DISCUSSION

The complete study in this thesis approaches the energy efficiency of VLC in an objective way following a bottom-up method. First, the reviewed manuscripts approached state-of-the-art technology on LED and on LED drivers for VLC application. Second, the studies on the effects of current modulation in the LED and the pre-emphasis control on switching mode modulators showed contributions on the design of a VLC transmitter. The above cited studies, together with additional modeling of the OWC and receiver noise, allowed for a comprehensive comparison among the consumption factor of different solutions of PC-LED-based VLC transmitters. This study assumed that the electronic device can be designed following the lower possible biasing voltages, the signal has its power minimized, no other illumination device causes interference and the channel response includes only direct path. Therefore, the results are best case scenarios and are meant to allow for a fair comparison with less focus in the absolute consumption factor values.

Follows the discussion of the most significant topics of this thesis that were divided in three thematic sections.

### 7.1 MODULATION SCHEMES

The study presented in Chapter 4 showed that the same drop of efficacy is observed in the LED regardless of the modulation scheme. However, the zero and maximum forward current that can be applied to the device limits the design space considering the ac signal variance for communication and the dc dimming range. In this part of the thesis, the actual required modulation depth was not studied because that study is independent of any application.

This same study also showed a strong limitation in the application of DCO-OFDM modulation for VLC. That is because the possible design space was constrained by the zero and maximum LED's forward current. In this sense, the higher is the PAPR of the signal, the smaller is this space. However, when coming to a complete analysis of the VLC link, presented in Chapter 6, it was found that the Li-Fi application suffers little or no impact because of this characteristic of DCO-OFDM when compared to other very know modulation schemes, such as PSK, QAM and baseband schemes with the exception of the OOK-based schemes. That is because in most cases a low modulation amplitude is required ( $<7\%$ ).

For the higher data rate application of virtual reality, on the other hand, DCO-OFDM could not achieve the required signal power, as shown in Chapter 6. In these cases the variants of OFDM scheme, i. e. asymmetrically-clipped optical OFDM (ACO-OFDM) and Flip-OFDM, were shown to be very energy-costly because of the drop of efficacy in the LED and lower driver circuit efficiency. In this sense, this thesis linked the modulation schemes reported in literature focused on telecommunications and pointed out the most suitable for VLC. Other aspects such as receiver equalization, channel estimation, synchronization, etc., which have to do with the selection of the modulation scheme and the implementation on the receiver, were not focused here.

## 7.2 MODULATOR CIRCUIT

A comparison among linear power amplifiers and switching mode power converters used as modulator for VLC is presented in Chapter 6. The first type is more adequate when high-bandwidth is required (i.e. Li-Fi and virtual reality). The use of linear modulator for VLC corroborates the demonstrated by (WU et al., 2018) with further grounding and a more comprehensive analysis. Also, the literature overview presented in Chapter 3 confirms the significant amount of publications using this converter type, even though, most do not follow an energy-driven approach. This analysis points out the consumption factor dependency on the chosen signal bandwidth. Moreover, this type of modulator shall be assisted by another converter for processing average power (class AB) or to tightly regulate the supply voltage (class A) for effective use in VLC. The second type, the switching mode power converters, is suitable for narrow-bandwidth applications (i.e. indoor localization and vehicular communications) performing simultaneous power control and intentional current modulation. This type of converter is in the focus of the research on VLC recently, as can be seen in Chapter 3, and suffers specially from switching losses. This matches the findings of (MÉNDEZ, 2018) about the use of switching mode power converters for VLC, who cited additional implementation aspects, which limit their implementation for wide modulation bandwidth:

The high switching frequency required for providing a bandwidth high enough for reproducing the communication signals makes the practical implementation very difficult because of the high switching losses, the difficulty of driving the MOSFETs, etc. [...] Moreover, the capability to perform very small voltage changes with a SMPC falls with switching frequency (MÉNDEZ, 2018).

In this thesis a wide range of aspects are taken into account to justify the choices of modulation schemes and modulation circuit types. One of the main findings, which leads to an objective recommendation on VLC driver design, resides in the proof that linear mode modulators are advantageous from the energy efficiency point-of-view. The option of using circuits working in a dissipative principle in an LED driver for illumination-purposed only is not endorsed considering current state of electronics technology, since the switching mode power converters are advantageous in many aspects, not only in the energy efficiency. However, when facing the requirements of wider modulation bandwidth in the order of megahertz for VLC, it was shown that the lower energy penalty is possible by using these dissipative circuits than improving the switching mode power converter-based modulation capability.

Another solution, when a dedicated modulator stage is acceptable in the power conversion, is the use of a single series switch modulator. This is frequently reported in the literature, which can be seen in Chapter 3, and allows for implementing OOK-based modulation schemes. Additionally to requiring a regulated input voltage supply, this solution causes the modulation duty cycle to affect the average light, which requires additional concern on the implementation. The results presented in Chapter 6 show that the adoption of this modulator in combination with the possible modulation schemes results in lower consumption factor when compared with the other modulator types. Although the modulator presents reasonable high efficiency, the efficacy droop of the LED determines the lower global efficacy and lower consumption factor.

When considering the low data rate applications of VLC and to allow for a single power processing stage capable of average power control and modulation, the switching mode modulators are the best option. The preemphasis technique, presented in Chapter 5, was shown to be effective for taking advantage of the maximum possible modulation bandwidth, which helps on reducing the required switching frequency when using average current modulation. This technique includes the closed-loop control of average current and open-loop injection of communication signal into the converter's operating duty cycle. Moreover, it demonstrated a flat frequency response from the point of injection of the communication signal to the LED's current. This flat range extends from a very low frequency, which could approach dc, up to 0.45 of the converter's switching frequency, in theory 0.5 is the fundamental maximum value given the Nyquist sampling theorem.

### 7.3 REVISITING THE RELATION BETWEEN VLC AND RF COMMUNICATIONS

It is worth recalling here a common discussion that brings a direct comparison between the RF communications and VLC. Although these results are not directly pointed out from the energy-aware VLC design, they deserve special attention because they help on avoiding misunderstandings about the potential use of VLC, which are common in literature. These misunderstandings concern the actual energy consumption of a VLC transmitter when compared to the RF communications and the available bandwidth for VLC.

First, the energy efficiency (concretely considering the consumption factor) of implementing VLC in the gigabits-per-second range is far lower than that of a similar communication using RF (TSIATMAS et al., 2015; RAPPAPORT; MURDOCK; GUTIERREZ, 2011). This result was a best case estimated for VLC because (TSIATMAS et al., 2015) considered the consumption factor at the LED's terminals without any concern on the driver circuit. The consumption factor analysis was revisited in Chapter 6 and the higher consumption factor values are similar as reported in the literature, although in this thesis a wider comparison among more solutions for VLC drivers was performed.

Moreover, the efficacy of VLC drops even more when considering the power losses in the driver circuit. Therefore, considering the current PC-LED and state-of-the-art electronic drivers circuits, as presented in review of Chapter 3, the VLC does not have the higher energy-efficiency in short range wireless communications when compared to RF. In the related literature, VLC is frequently called a *green technology* (ZHAO; CHI, 2018; ARNON, 2015; CHI et al., 2015; AFIFAH et al., 2018; DENG, 2018; DENG et al., 2019; REHMAN et al., 2019; MANIVANNAN; RAJA; SELVENDRAN, 2016; ALIMIM et al., 2017; KARUNATILAKA et al., 2015) having the sense of an environmentally-friendly mainly because of the lower energy consumption. Actually, on this aspect, the results from this work confirmed that VLC is less efficient than RF communications, as reported in the literature. A fairer discussion on the subject including RF and VLC for short-range data communications shall consider the adoption of VLC as an alternative for trading-off extra energy for additional data rate (mainly in downstream direction) in the situations in which the RF transmitter alone is not able to support such improvement. In this sense, this work confirms that the VLC role as a complementary channel to RF communications is much more adequate (CHOWDHURY et al., 2020; VISIBLE et al., 2018;

WU; WANG; YOUN, 2014; YU; BAXLEY; ZHOU, 2014; PATHAK et al., 2015; ELGALA; MESLEH; HAAS, 2011).

Second, the wide electromagnetic spectrum range of visible light that is highlighted as been (up to 10,000 times) wider than the spectrum of RF (SEVINCER et al., 2013; BIAN, 2019; ELGALA; MESLEH; HAAS, 2011; PATHAK et al., 2015) shall be accordingly discussed. LEDs only allow for intensity modulation with direct detection and these are the emitters used in the current technology for VLC. In this sense, the spectrum shall be differentiated from the available communication bandwidth of VLC, also called *the bandwidth of the VLC channel*, which is the frequency range in which it is possible to implement the light intensity modulation and was explored along this thesis in a wide sort of aspects. The definition of this band considers the limitations of light emitters, the light receivers, the modulator circuits, the economic aspect and energy efficiency concern. Hence, the literature shows that current technology allows for no more than hundreds of megahertz of bandwidth, or few megahertz using phosphor-covered white LED, as it is shown in the reviews of Chapter 2 and Chapter 3. On the other hand, RF systems can effectively take advantage of the whole band for communications. A fair comparison shall confront the possible bandwidth of the VLC channel and the bandwidth available in RF, which may soon allow for extra unlicensed band around 60 GHz with compatible electronics, as already demonstrated in the literature (RAPPAPORT; MURDOCK; GUTIERREZ, 2011). Therefore, the wide visible light spectrum range is not directly an advantage to be accounted for VLC over RF technology.





## 8 CONCLUSIONS

### 8.1 CONTRIBUTIONS OF THIS THESIS

The literature review and the innovative contributions, presented in Chapters 2 to 6, supported the discussion presented in this thesis, from which this short summary is drawn. The application of LED and the possible spread of VLC depends on the rational use of energy as an environmental requirement. Therefore, the careful design of a VLC transmitter accounting for illumination and communication aspects was shown to allow for great improvements in the overall lighting efficacy. This is possible by adequate modulation scheme and driver circuit type choice and a communication link analysis.

In general, the dc-offset modulation schemes proven to allow for the best consumption factor for VLC applications. However, additional practical aspects such as channel equalization, synchronization and concern on the receiver design shall be taken into account to select among the various types of dc-offset modulations. The OOK-based modulation schemes, on the other hand, have lower consumption factor, therefore, they are not indicated in the case of energy-aware VLC implementation.

The analysis of the complete communication link is the only way to get closer to the real minimum extra energy consumption in a dual-purpose VLC light fixture. This comprehensive view allowed for determining the best choices of LED drivers for VLC. The switching mode power converters, which require only a single power processing stage, are adequate to narrower bandwidth applications. The use of ripple modulation is highlighted because allows for the higher consumption factor. However, the useful signal bandwidth is constrained by the PWM switching frequency. Meanwhile, the linear mode modulators are more energy efficient when wider modulation bandwidth is required, even though they operate based in a dissipative principle.

## 8.2 PUBLICATIONS

### 8.2.1 Published contributions of the thesis

- TEIXEIRA, L. et al. **On the LED Efficacy and Modulation Design Space for Visible Light Communication.** In: IEEE Industry Applications Society Annual Meeting, 2018. Portland - OR. Proceedings. p.1–6, 2018.
- TEIXEIRA, L. et al. **Review of LED drivers for Visible Light Communication.** In: IECON 2019 - 45<sup>th</sup> Annual Conference of the IEEE Industrial Electronics Society, Lisbon. Proceedings. p.4274–4279, 2019.
- TEIXEIRA, L. et al. **On the LED Illumination and Communication Design Space for Visible Light Communication.** IEEE Transactions on Industry Applications, v.55, n.3, p.3264–3273, 2019.
- TEIXEIRA, L. et al. **An Analysis of Visible Light Communication Energy Cost.** In: IEEE Industry Applications Society Annual Meeting, 2020., Detroit. In press, 2020.
- TEIXEIRA, L. et al. **Pre-Emphasis Control in Switched Mode Power Converter for Energy Efficient Wide Bandwidth Visible Light Communication.** IEEE Journal of Emerging and Selected Topics in Power Electronics, In press. 2020.

### 8.2.2 Published contributions indirectly related to this thesis

- LOOSE, F. et al. **Ripple-based Visible Light Communication Technique for Switched LED Drivers.** 2017 IEEE Industry Applications Society Annual Meeting, p.1–6, 2017.
- LOOSE, F. et al. **Using the Inherent Ripple Waveform of a Synchronous Buck Converter for Visible Light Communication in LED Drivers.** In: Seminário de Eletrônica de Potência e Controle - SEPOC, 10. Proceedings, 2017. p.7–11, 2017.
- LOOSE, F. et al. **On the Use of the Intrinsic Ripple of a Buck Converter for Visible Light Communication in LED Drivers.** IEEE Journal of Emerging and Selected Topics in Power Electronics, [S.l.], v.6, n.3, p.1235–1245, 2018.

- LOOSE, F. et al. **Evaluation of Bit Error Ratio in Differential Phase-Shift-Keying Modulation Applied to VLC LED Drivers**. In: IEEE Industry Applications Society Annual Meeting, 2019. Proceedings. p.1–6, 2019.

### 8.3 FUTURE WORK

The research lines listed bellow may be followed continuing the study presented in this thesis:

**Design space considering the use of LASER diodes for VLC** LASER diodes are suggested as suitable for application in VLC because of the wider modulation bandwidth capability and because recently more device models for illumination are commercially available. Moreover, the different current-to-light behavior and resulting efficacy of these devices requires a new paradigm on the selection of modulation scheme and dimming method. The design space analysis was presented in this thesis for PC-LEDs, using a LASER diode model and the same design space method may bring interesting findings on possible advantages of these devices for VLC.

**Expanding the consumption factor analysis** There are some switching mode circuit topologies that are specially promising for improving the energy efficiency of switching mode power converters when used as modulators for VLC. First, the use of the strategy called split of the power and buck-derived converters (RODRIGUEZ et al., 2018; RODRÍGUEZ et al., 2019). Second, switching mode LED drivers including a linear modulator circuit or hybrid switching mode modulator assisted by linear circuit can also be efficient solutions for several implementation aspects of VLC. Therefore, modeling of such circuit types can be included for a wider comparison considering the consumption factor.



## REFERENCES

- AFIFAH, S. et al. Energy efficient transmitter for guided indoor navigation using visible light. **IOP Conference Series: Materials Science and Engineering**, [S.l.], v.434, p.012213, dec 2018.
- AGARWAL, A.; SAINI, G. SNR Analysis for Visible Light Communication Systems. **International Journal of Engineering Research & Technology (IJERT)**, [S.l.], v.3, n.10, p.520–524, 2014.
- AL-KINANI, A. et al. Optical wireless communication channel measurements and models. **IEEE Communications Surveys and Tutorials**, [S.l.], v.20, n.3, p.1939–1962, 2018.
- ALIMI, I. et al. Challenges and Opportunities of Optical Wireless Communication Technologies. In: **Optical Communication Technology**. [S.l.]: InTech, 2017. p.135–152.
- ARNON, S. (Ed.). **Visible Light Communication**. Cambridge: Cambridge University Press, 2015.
- BAI, R. et al. Iterative receiver for ADO-OFDM with near-optimal optical power allocation. **Optics Communications**, [S.l.], v.387, n.November 2016, p.350–356, 2017.
- BAY, C. W.; CITY, E. A 160 m visible light communication link using hybrid undersampled phase-frequency shift on-off keying and CMOS image sensor. **Optics Express**, [S.l.], v.27, n.3, p.2478–2487, 2019.
- BIAN, R. **Practical Implementation of Multiple-input Multiple-output Visible Light Communication Systems**. 2019. Tese (Doutorado em Ciência da Computação) — .
- BISPO, F. R. **Using an LED as a Sensor and Visible Light Communication device in a Smart Illumination System**. 2015. Tese (Doutorado em Ciência da Computação) — Universidade Nova de Lisboa.
- CHE, F. et al. Design and implementation of IEEE 802.15.7 VLC PHY-I transceiver. In: IEEE 12TH INTERNATIONAL CONFERENCE ON SOLID-STATE AND INTEGRATED CIRCUIT TECHNOLOGY, ICSICT 2014, 2014. **Proceedings...** [S.l.: s.n.], 2014. p.5–8.

CHEN, C.; ZHONG, W.-D. Performance Comparison of Different Types of Receivers in Indoor MIMO-VLC Systems. In: INTERNATIONAL CONFERENCE ON COMPUTER NETWORKS AND COMMUNICATION TECHNOLOGY (CNCT 2016), Paris, France. **Proceedings...** Atlantis Press, 2017.

CHEN, H. et al. Electrical and Thermal Effects of Light-Emitting Diodes on Signal-to-Noise Ratio in Visible Light Communication. **IEEE Transactions on Industrial Electronics**, [S.l.], v.66, n.4, p.2785–2794, 2019.

CHI, N. et al. Visible light communications: demand factors, benefits and opportunities [guest editorial]. **IEEE Wireless Communications**, [S.l.], v.22, n.2, p.5–7, 2015.

CHOWDHURY, M. Z. et al. Optical Wireless Hybrid Networks: trends, opportunities, challenges, and research directions. **IEEE Communications Surveys & Tutorials**, [S.l.], v.22, n.2, p.930–966, 2020.

CHUN, H. et al. OPEN A Wide-Area Coverage 35 Gb / s Visible Light Communications Link for Indoor Wireless Applications. **Nature Scientific Reports**, [S.l.], p.4–11, 2019.

DEMIRKOL, I. et al. Powering the Internet of Things Through Light Communication. **IEEE Communications Magazine**, [S.l.], v.PP, p.1–7, 2019.

DENG, X. **Throughput, power consumption and interference considerations in visible light communication Throughput , Power Consumption and Interference Considerations in Visible Light Communication**. [S.l.: s.n.], 2018. 198p. n.2018.

DENG, X. et al. Performance comparison for illumination and visible light communication system using buck converters. **2014 IEEE Globecom Workshops (GC Wkshps)**, [S.l.], p.547–552, 2014.

DENG, X. et al. Effect of buck driver ripple on BER performance in visible light communication using LED. **2015 IEEE International Conference on Communication Workshop, ICCW 2015**, [S.l.], n.2, p.1368–1373, 2015.

DENG, X. et al. LED power consumption in joint illumination and communication system. **Optics Express**, [S.l.], v.25, n.16, p.18990, 2017.

DENG, X. et al. Mitigating LED Nonlinearity to Enhance Visible Light Communications. **IEEE Transactions on Communications**, [S.l.], v.PP, n.c, p.1–1, 2018.

DENG, X. et al. Performance Analysis for Joint Illumination and Visible Light Communication using Buck Driver. **IEEE Transactions on Communications**, [S.l.], v.66, n.5, p.2065–2078, 2018.

DENG, X. et al. Modeling and Analysis of Transmitter Performance in Visible Light Communications. **IEEE Transactions on Vehicular Technology**, [S.l.], v.68, n.3, p.2316–2331, 2019.

DONG, Z. et al. An integrated transmitter for LED-based visible light communication and positioning system in a 180nm BCD technology. In: IEEE BIPOLAR/BICMOS CIRCUITS AND TECHNOLOGY MEETING (BCTM), 2014. **Proceedings...** IEEE, 2014. p.84–87.

ELECTROPAEDIA. **Electromagnetic Radiation and Radio Waves**. 2019. 1–7p.

ELGALA, H.; MESLEH, R.; HAAS, H. Indoor optical wireless communication: potential and state-of-the-art. **IEEE Communications Magazine**, [S.l.], v.49, n.9, p.56–62, 2011.

FUJIMOTO, N.; MOCHIZUKI, H. 477 Mbit/s visible light transmission based on OOK-NRZ modulation using a single commercially available visible LED and a practical LED driver with a pre-emphasis circuit. **Optical Fiber Communication Conference and Exposition and the National Fiber Optic Engineers Conference (OFC/NFOEC), 2013**, [S.l.], p.1–3, 2013.

GONG, C.-S. A. et al. The High-efficiency LED Driver for Visible Light Communication Applications. **Scientific Reports**, [S.l.], v.6, n.1, p.30991, nov 2016.

HAAS, H. et al. What is LiFi? **Journal of Lightwave Technology**, [S.l.], v.34, n.6, p.1533–1544, 2016.

HUI, S. Y.; QIN, Y. X. A general photo-electro-thermal theory for light emitting diode (LED) systems. **IEEE Transactions on Power Electronics**, [S.l.], v.24, n.8, p.1967–1976, 2009.

HUSSAIN, B. et al. A fully integrated IEEE 802.15.7 visible light communication transmitter with on-chip 8-W 85% efficiency boost LED driver. In: SYMPOSIUM ON VLSI CIRCUITS (VLSI CIRCUITS), 2015. **Proceedings...** IEEE, 2015. v.34, n.10, p.C216–C217.

HUSSAIN, B. et al. Visible Light Communication System Design and Link Budget Analysis. **Journal of Lightwave Technology**, [S.l.], v.33, n.24, p.5201–5209, 2015.



IEEE Power Electronics Society. IEEE Recommended Practices for Modulating Current in High-Brightness LEDs for Mitigating Health Risks to Viewers. **IEEE Std 1789-2015**, [S.l.], p.1–80, 2015.

INC, N. C. **Energy Savings Forecast of Solid-State Lighting in General Illumination Applications**. [S.l.]: U.S. Department of Energy, 2014. (August).

International Commission on Illumination. **ISO/CIE 11664-1:2019 colorimetry — part 1: cie standard colorimetric observers**. 2019. 34p.

International Energy Agency. **Lighting**. [S.l.: s.n.], 2020. (June).

International Telecommunication Union. **ITU-R: managing the radio-frequency spectrum for the world**. 2019.

JALAJAKUMARI, A. V. N. et al. An Energy Efficient High-Speed Digital LED Driver for Visible Light Communications. In: IEEE ICC 2015 CONFERENCE PROCEEDINGS. **Proceedings...** [S.l.: s.n.], 2015. p.5054–5059.

JENQ, F. L.; LIU, T. J.; LEU, F. Y. An AC LED smart lighting system with visible light time-division multiplexing free space optical communication. **Proceedings - 2011 5th International Conference on Innovative Mobile and Internet Services in Ubiquitous Computing, IMIS 2011**, [S.l.], p.589–593, 2011.

KARUNATILAKA, D. et al. LED Based Indoor Visible Light Communications: state of the art. **IEEE Communications Surveys & Tutorials**, [S.l.], v.17, n.3, p.1649–1678, 2015.

KHALIGHI, M. A. et al. Survey on Free Space Optical Communication: a communication theory perspective. **IEEE Communications Surveys & Tutorials**, [S.l.], v.16, n.4, p.2231–2258, 2014.

KISHI, T. et al. A high-speed LED driver that sweeps out the remaining carriers for visible light communications. **Journal of Lightwave Technology**, [S.l.], v.32, n.2, p.239–249, 2014.

KOMINE, T.; NAKAGAWA, M. Fundamental analysis for visible-light communication system using LED lights. **IEEE Transactions on Consumer Electronics**, [S.l.], v.50, n.1, p.100–107, 2004.

KOSMAN, J. et al. 60 Mb / s , 2 meters Visible Light Communications in 1 klx Ambient using an Unlensed CMOS SPAD Receiver. **Photonics Society Summer Topical Meeting Series (SUM), 2016 IEEE**, [S.l.], v.1, p.171–172, 2016.

KOURKOUMELIS, N.; TZAPHLIDOU, M. Eye safety related to near infrared radiation exposure to biometric devices. **TheScientificWorldJournal**, [S.l.], v.11, n.March 2011, p.520–528, 2011.

LEE, C. et al. 2 Gbit/s data transmission from an unfiltered laser-based phosphor-converted white lighting communication system. **Optics Express**, [S.l.], v.23, n.23, p.29779, 2015.

LI, H. et al. An analog modulator for 460 MB/S visible light data transmission based on OOK-NRS modulation. **IEEE Wireless Communications**, [S.l.], v.22, n.2, p.68–73, 2015.

LI, S. et al. A Survey, Classification, and Critical Review of Light-Emitting Diode Drivers. **IEEE Transactions on Power Electronics**, [S.l.], v.31, n.2, p.1503–1516, 2016.

LIU, Y. et al. Visible Light Communication Using Receivers of Camera Image Sensor and Solar Cell. **IEEE Photonics Journal**, [S.l.], v.8, n.1, p.1–7, 2016.

LOOSE, F. et al. Ripple-based visible light communication technique for switched LED drivers. In: IEEE INDUSTRY APPLICATIONS SOCIETY ANNUAL MEETING, IAS 2017, 2017., Cincinnati. **Proceedings...** IEEE Industry Applications Society, 2017. v.2017-Janua, p.1–6.

LOOSE, F. et al. On the Use of the Intrinsic Ripple of a Buck Converter for Visible Light Communication in LED Drivers. **IEEE Journal of Emerging and Selected Topics in Power Electronics**, [S.l.], v.6, n.3, p.1235–1245, 2018.

MANIVANNAN, K.; RAJA, A. S.; SELVENDRAN, S. Performance Investigation of Visible Light Communication System Using Optisystem Simulation Tool Performance Investigation of Visible Light Communication System Using Optisystem Simulation Tool. **INTERNATIONAL JOURNAL OF MICROWAVE AND OPTICAL TECHNOLOGY**, [S.l.], n.September, 2016.

MARCHESAN, T. B. **Integração de conversores estáticos aplicados a sistemas de iluminação pública**. 2007. Tese (Doutorado em Ciência da Computação) — .

MARTÍNEZ-CIRO, R. A. et al. Design and Implementation of a Multi-Colour Visible Light Communication System Based on a Light-to-Frequency Receiver. **Photonics**, [S.l.], v.6, n.2, p.42, 2019.

MCKENDRY, J. D. et al. 1.5 Gbit/s Multi-Channel Visible Light Communications Using CMOS-Controlled GaN-Based LEDs. **Journal of Lightwave Technology**, [S.l.], 2013.

MÉNDEZ, J. R. **Switching-mode Power Converters for Visible Light Communication**. 2018. Tese (Doutorado em Ciência da Computação) — . (December).

MINH, H. L. et al. 80 Mbit / s Visible Light Communications Using Pre-Equalized White LED. **2008 34th European Conference on Optical Communication**, [S.l.], v.5, n.September, p.1–2, 2008.

MINH, H. L. et al. High-Speed Visible Light Communications Using Multiple-Resonant Equalization. **IEEE Photonics Technology Letters**, [S.l.], v.20, n.14, p.1243–1245, 2008.

MIRVAKILI, A.; KOOMSON, V. J. High efficiency LED driver design for concurrent data transmission and PWM dimming control for indoor visible light communication. **2012 IEEE Photonics Society Summer Topical Meeting Series, PSST 2012**, [S.l.], v.2, p.132–133, 2012.

MODEPALLI, K.; PARSA, L. Dual-purpose offline LED driver for illumination and visible light communication. **IEEE Transactions on Industry Applications**, [S.l.], v.51, n.1, p.406–419, 2015.

MODEPALLI, K.; PARSA, L. Lighting Up with a Dual-Purpose Driver. **2 IEEE Industry Applications Magazine**, [S.l.], n.March/April, p.2–12, 2017.

NAVIN, K.; NUNO, L. **Led-Based Visible Light Communication System: a brief survey and investigation.pdf**. 2010. 296–308p.

PANDEY, O. J.; SHARAN, R.; HEGDE, R. M. Localization in Wireless Sensor Networks Using Visible Light in Non-Line of Sight Conditions. **Wireless Personal Communications**, [S.l.], 2017.

PATHAK, P. H. et al. Visible Light Communication, Networking, and Sensing: a survey, potential and challenges. **IEEE Communications Surveys & Tutorials**, [S.l.], v.17, n.4, p.2047–2077, 2015.

Pure Lifi. **Pure LiFi website**. 2020.

RAPPAPORT, T. S.; MURDOCK, J. N.; GUTIERREZ, F. State of the Art in 60-GHz Integrated Circuits and Systems for Wireless Communications. **Proceedings of the IEEE**, [S.l.], v.99, n.8, p.1390–1436, aug 2011.

REHMAN, S. U. et al. Visible light communication: a system perspective—overview and challenges. **Sensors (Switzerland)**, [S.l.], v.19, n.5, p.1–22, 2019.

RODRIGUEZ, J. et al. Taking advantage of the output voltage ripple of a two-phase buck converter to perform quadrature amplitude modulation for visible light communication. In: IEEE APPLIED POWER ELECTRONICS CONFERENCE AND EXPOSITION (APEC), 2017. **Proceedings...** IEEE, 2017. p.2116–2123.

RODRÍGUEZ, J. et al. Efficient Visible Light Communication Transmitters Based on Switching-Mode dc-dc Converters. **Sensors**, [S.l.], v.18, p.1–18, 2018.

RODRÍGUEZ, J. et al. Reproducing Single-Carrier Digital Modulation Schemes for VLC by Controlling the First Switching Harmonic of the DC-DC Power Converter Output Voltage Ripple. **IEEE Transactions on Power Electronics**, [S.l.], v.33, n.9, p.7994–8010, 2018.

RODRIGUEZ, J. et al. Performance evaluation of a VLC transmitter based on the split of the power. In: IEEE APPLIED POWER ELECTRONICS CONFERENCE AND EXPOSITION (APEC), 2018. **Proceedings...** IEEE, 2018. p.1179–1186.

RODRÍGUEZ, J. et al. Power Efficient VLC Transmitter Based on Pulse-Width Modulated DC-DC Converters and the Split of the Power. **IEEE Transactions on Power Electronics**, [S.l.], v.34, n.2, p.1726 – 1743, 2019.

Rodriguez Mendez, J. et al. Reproducing Multicarrier Modulation Schemes for Visible Light Communication With the Ripple Modulation Technique. **IEEE Transactions on Industrial Electronics**, [S.l.], v.67, n.2, p.1532–1543, feb 2020.

SAADI, M. et al. Visible Light Communication : opportunities , challenges and channel models. **International Journal of Electronics & Informatics (IJEI)**, [S.l.], v.2, n.1, p.1–11, 2013.

SALMENTO, M. L. G. **Comunicação de Dados por Luz Visível Aplicada a Sistemas Modernos de Iluminação - Componentes, Conversores e Proposta de Técnica de Modulação**. 2019. 1–3p. Tese (Doutorado em Ciência da Computação) — . (81).

SALMENTO, M. L. G. et al. A Dimmable Offline LED Driver With OOK-M-FSK Modulation for VLC Applications. **IEEE Transactions on Industrial Electronics**, [S.l.], v.66, n.7, p.5220–5230, jul 2019.

SCHMID, S. et al. Linux light bulbs: enabling internet protocol connectivity for light bulb networks. **VLCS 2015 - Proceedings of the 2nd International Workshop on Visible Light Communications Systems, co-located with MobiCom 2015**, [S.l.], p.3–8, 2015.

SCHOLAND, M. **Fast Learning Curves – LED Lighting ’ s Rapid Reduction in Price**. [S.l.]: CLASP Europe, 2016. (August).

SEBASTIÁN, J. et al. Design of a Two-Phase Buck Converter With Fourth-Order Output Filter for Envelope Amplifiers of Limited Bandwidth. **Transactions on Power Electronics**, [S.l.], v.29, n.11, p.5933–5948, 2014.

SEBASTIAN, J. et al. On the Role of Power Electronics in Visible Light Communication. **IEEE Journal of Emerging and Selected Topics in Power Electronics**, [S.l.], v.6, n.3, p.1210–1223, sep 2018.

SEVINCER, A. et al. LIGHTNETs: smart lighting and mobile optical wireless networks - a survey. **IEEE Communications Surveys and Tutorials**, [S.l.], v.15, n.4, p.1620–1641, 2013.

TANAKA, H.; UMEDA, Y.; TAKYU, O. High-speed LED driver for visible light communications with drawing-out of remaining carrier. In: **IEEE RADIO AND WIRELESS SYMPOSIUM, 2011. Proceedings...** IEEE, 2011. p.295–298.

TEIXEIRA, L. et al. Review of LED drivers for Visible Light Communication. In: **ANNUAL CONFERENCE OF THE IEEE INDUSTRIAL ELECTRONICS SOCIETY, 45.**, Lisbon. **Proceedings...** [S.l.: s.n.], 2019.

TEIXEIRA, L. et al. On the LED Illumination and Communication Design Space for Visible Light Communication. **IEEE Transactions on Industry Applications**, [S.l.], v.55, n.3, p.3264–3273, 2019.

TEIXEIRA, L. et al. Pre-Emphasis Control in Switched Mode Power Converter for Energy Efficient Wide Bandwidth Visible Light Communication. **IEEE Journal of Emerging and Selected Topics in Power Electronics**, [S.l.], p.1–1, 2020.

TEIXEIRA, L. et al. An Analysis of Visible Light Communication Energy Cost. In: IEEE INDUSTRY APPLICATIONS SOCIETY ANNUAL MEETING, 2020., Detroit. **Proceedings...** In press, 2020.

TEIXEIRA, L.; LOOSE, F. On the LED Efficacy and Modulation Design Space for Visible Light Communication. In: IEEE INDUSTRY APPLICATIONS SOCIETY ANNUAL MEETING, 2018., Portland - OR. **Proceedings...** [S.l.: s.n.], 2018. p.6.

TSIATMAS, A. et al. An illumination perspective on visible light communications. **IEEE Communications Magazine**, [S.l.], v.52, n.7, p.64–71, 2014.

TSIATMAS, A. et al. Joint illumination and visible-Light Communication systems: data rates and extra power consumption. **2015 IEEE International Conference on Communication Workshop, ICCW 2015**, [S.l.], p.1380–1386, 2015.

U.S. Department of Energy. **How LEDs are Different**. [S.l.]: Office of Energy Efficiency & Renewable Energy, 2020.

U.S. Department of Energy. **2019 Lighting R & D Opportunities**. [S.l.: s.n.], 2020. (January).

VISIBLE, I. M.-c. M. et al. Light Communications. **Journal of Lightwave Technology**, [S.l.], v.36, n.10, p.1944–1951, 2018.

VUCIC, J. et al. 125 Mbit/s over 5 m wireless distance by use of OOK-Modulated phosphorescent white LEDs. In: EUROPEAN CONFERENCE ON OPTICAL COMMUNICATION, 2009. **Proceedings...** [S.l.: s.n.], 2009. n.1, p.9–10.

VUCIC, J. et al. 513 Mbit/s visible light communications link based on DMT-modulation of a white LED. **Journal of Lightwave Technology**, [S.l.], v.28, n.24, p.3512–3518, 2010.

WANG, Z. et al. On the Design of a Solar-Panel Receiver for Optical Wireless Communications With Simultaneous Energy Harvesting. **IEEE Journal on Selected Areas in Communications**, [S.l.], v.33, n.8, p.1–12, 2015.

WU, S.; WANG, H.; YOUN, C.-h. Visible light communications for 5G wireless networking systems: from fixed to mobile communications. **Network, IEEE**, [S.l.], n.December, p.41–45, 2014.

WU, Z.-Y. et al. A Linear Current Driver for Efficient Illuminations and Visible Light Communications. **Journal of Lightwave Technology**, [S.l.], v.36, n.18, p.3959–3969, 2018.

YEH, C.-h. H.; CHOW, C.-w. W.; WEI, L.-y. Y. 1250 Mbit/s OOK Wireless White-Light VLC Transmission Based on Phosphor Laser Diode. **IEEE Photonics Journal**, [S.l.], v.11, n.3, p.1–5, 2019.

YU, Z.; BAXLEY, R. J.; ZHOU, G. T. Distributions of upper PAPR and lower PAPR of OFDM signals in visible light communications. **ICASSP, IEEE International Conference on Acoustics, Speech and Signal Processing - Proceedings**, [S.l.], n.1, p.355–359, 2014.

ZAFAR, F.; BAKAUL, M.; PARTHIBAN, R. Laser-Diode-Based Visible Light Communication: toward gigabit class communication. **IEEE Communications Magazine**, [S.l.], v.55, n.2, p.144–151, 2017.

ZHAO, J.; CHI, N. A novel illumination-efficient dimming control scheme based on reversed unipolar return-to-zero coding and circular (7, 1) modulation in high-speed visible light communication. **Microwave and Optical Technology Letters**, [S.l.], v.60, n.4, p.806–812, apr 2018.

ZHAO, S.; XU, J.; TRESCASES, O. A dimmable LED driver for Visible Light Communication (VLC) based on LLC resonant DC-DC converter operating in burst mode. In: TWENTY-EIGHTH ANNUAL IEEE APPLIED POWER ELECTRONICS CONFERENCE AND EXPOSITION, 2013. **Proceedings...** [S.l.: s.n.], 2013. p.2144–2150.

ZHAO, S.; XU, J.; TRESCASES, O. Burst-Mode Resonant LLC Converter for an LED Luminaire With Integrated Visible Light Communication for Smart Buildings. **IEEE Transactions on Power Electronics**, [S.l.], v.29, n.8, p.4392–4402, 2014.

ZHUANG, Y. et al. A survey of positioning systems using visible LED lights. **IEEE Communications Surveys and Tutorials**, [S.l.], v.20, n.3, p.1963–1988, 2018.

ZONG, S.; WU, J.; HE, X. A novel method for illumination and communication using white LED lights. In: IET INTERNATIONAL CONFERENCE ON POWER ELECTRONICS, MACHINES AND DRIVES (PEMD 2012), 6. **Proceedings...** IET, 2012. p.P70–P70.